

#### **GOVERNMENT OF INDIA**

# MINISTRY OF WATER RESOURCES, RIVER DEVELOPMENT AND GANGA REJUVINATION CENTRAL WATER & POWER RESEARCH STATION, PUNE-24

(http://cwprs.gov.in)



TECHNICAL MEMORANDUM ON

# GUIDELINES FOR HYDRAULIC DESIGN OF ORIFICE SPILLWAY by

Dr. (Mrs.) V. V. Bhosekar, Scientist E Dr. (Mrs.) P. P. Gadge, Scientist B



DR. M K Sinha, Director

May 2017



# GOVERNMENT OF INDIA MINISTRY OF WATER RESOURCES, RIVER DEVELOPMENT AND GANGA REJUVINATION CENTRAL WATER & POWER RESEARCH STATION, PUNE-24

(http://cwprs.gov.in)

# TECHNICAL MEMORANDUM ON

# GUIDELINES FOR HYDRAULIC DESIGN OF ORIFICE SPILLWAY by

Dr. (Mrs.) V. V. Bhosekar, Scientist E Dr. (Mrs.) P. P. Gadge, Scientist B

DR. M K Sinha, Director

May 2017

#### **PREFACE**

Overflow spillways have been in use for many years in high head storage dams of peninsular India. All the major sites in this part of the country having been exploited, the focus has shifted to the North and North Eastern Himalayan region to tap the perennial discharges for hydro power generation. Orifice spillways are commonly used in this region, as the high head overflow spillways are unable to flush the sediments. During last decade, CWPRS has made significant contributions to more than 35 projects in evolving hydraulically safe and efficient designs of orifice spillways. A Technical Memorandum titled 'Research into Factors Which Influence Hydraulic Design of Breast Wall / Sluice Spillways' was published in 2008 covering the design considerations and selected case studies. However, guidelines could not be developed as the studies were site specific for each case. Though several large dams have been constructed all over the world with orifice spillway, no systematic guidelines have been provided to design an orifice spillway.

Central Water and Power Research Station, which is the premier hydraulic research organization in India has always been in the forefront to evolve new designs. Hence, a basic research work has been taken up at the research station to develop guidelines for the hydraulic design of orifice spillways in terms of various hydraulic parameters such as water and pressure profiles, coefficient of discharge etc. using both physical and numerical model studies. A basic research set up was established at CWPRS under the funding of Plan Scheme from MoWR, RD & GR.

The investigation started from the basic form of sharp edged large orifice. The equation of the bottom profile was finalised from these experiments and need for the solid bottom profile was identified. After fixing the bottom profile, further studies were carried out for evolving the equation of roof profile. This roof profile was fixed to form a complete set up of orifice spillway and basic guidelines for hydraulic design were formulated in terms of coefficient of discharge, water profiles and pressures on bottom & roof profiles.

The present guidelines are the outcome of very comprehensive research at CWPRS to study the orifice spillways using both physical and numerical modelling techniques. The publication is expected to serve very useful purpose for the designers.

-- May 2017 Pune.

> Dr. M. K. Sinha Director, CWPRS

#### **EXECUTIVE SUMMARY**

Dams, reservoirs and canal networks are some of the important hydraulic structures used to reduce the problem of spatial and temporal water availability. One of the most important and primary component of a dam is surplus spillways. They are used to pass the flood safely from upstream to downstream. Overflow spillways are commonly used and studied much throughout the globe. Sedimentation of reservoirs is a serious problem, especially in the mountainous region, which reduces the capacity of reservoirs and damages the hydropower plants. Thus, apart from safe disposal of flood from upstream to downstream of dams, the sediments entering into the reservoir should also be flushed to the downstream. Attention is focused on developing run-of-the-river schemes in cascades with suitable sediment disposal arrangement, in order to minimize the deposition of silt in the reservoir.

In order to have safe disposal of flood as well as to flush the sediments, orifice spillway in the form of breastwall/sluice are thus evolved over the last few years. The voluminous and systematic data on physical model studies of about 22 orifice spillways studied in CWPRS was a big asset to develop guidelines and evolve the preliminary design of orifice spillway. However, the same could not be done as the studies are site specific for each case and not basic research studies. Though several large dams have been constructed all over the world with orifice spillway, no systematic guidelines have been provided to design an orifice spillway. Hence, the major objective of the present research work is to develop an equation for the design of roof and bottom profile of an orifice spillway. It is also aimed to provide guidelines for design in terms of various hydraulic parameters such as water and pressure profiles, coefficient of discharge etc. using physical and numerical model studies.

Physical model studies are being used extensively to understand the complexity of spillway flows. Though physical models are indispensable, they are expensive and time consuming. Today, with the help of high-performance computers and more efficient Computational fluid dynamics (CFD) codes, the behaviour of hydraulic structures can be investigated numerically in reasonable time and cost. However, the numerical model is required to be validated using the data from physical model. Several alternative designs can be studied on the numerical model and most suitable design can finally be studied on the physical model. Spillway flows have been investigated numerically for overflow spillways. However, scanty literature is available on numerical modelling of orifice spillway. In the present study, the CFD software FLUENT version 6.3.26 was used to simulate the flow through orifice spillway.

United States Bureau of Reclamation and U. S. Army Corps of Engineers have conducted extensive research on overflow spillway to determine its profiles and other hydraulic parameters by investigating the flow over sharp edged weir. In the present study, as a basic step, an attempt has been made to develop basic equation for design of the bottom and

roof profile of an orifice spillway by investigating the flow through sharp edged large orifice using physical and numerical models (set up-1). Total 60 numbers of studies were carried out on physical and numerical models. The numerical model was verified in respect of grid convergence and turbulence models by comparing the results with physical model. The grid size of 0.004 m and RNG k- $\epsilon$  turbulence model with modified high resolution interface capturing (HRIC) scheme was found suitable for modelling the flow through sharp edged large orifice. The flow through large orifice was analysed in terms of coefficient of discharge, coefficient of velocity and lower & upper nappe profiles. The results obtained from physical and numerical models were compared with the available literature. Based on the comparison, the spillway bottom profile confirming to an equation  $x^2 = kh_dy$  with value of k as 4 was finalized for the initial design. The study also indicated that there is a need to provide solid spillway bottom profile to design the roof profile of an orifice spillway.

In the next attempt (set up-2) the solid spillway bottom profile in the form of an equation  $x^2 = 4h_{dy}$  (finalised from set up-1) was fixed at the downstream of orifice opening. Total 67 numbers of experiments and simulations were carried out for various combinations of design heads, operating heads and heights of orifices. Based on grid convergence study and checking sensitivity of turbulence models, grid size of 0.004 m and Realizable k-ε turbulence model were found suitable to represent the flow in CFD model. The main aim in this set up was to derive an equation for design of roof profile of an orifice spillway from resulted water surface profiles. However, before deriving an equation, the design of bottom profile finalised from set up-1 was checked by calculating pressures and corresponding cavitation indices. Positive pressures were observed on the spillway surface for all the combinations of design heads, operating heads and heights of orifice. Based on the results, it is concluded that the bottom profile of an orifice spillway having an equation  $x^2 = 4h_dy$  (finalised from set up-1) can be adopted for further studies. The coefficient of discharge was obtained in the range of 0.647 to 0.681, which was quite less than the range of coefficient of discharge observed on most of the real life orifice spillway projects i.e. 0.72 to 0.95 (Bhosekar et al., 2014). Hence, the present study indicated a need for further work to calculate discharging capacity of an orifice spillway by providing solid roof profile. Based on the results of upper nappe water surface profile, an equation was developed for the design of roof profile considering design head (h<sub>d</sub>) and height of orifice (d) as important hydraulic parameters. The studies indicated insignificant effect of height of spillway (P) on design of roof profile. The developed roof profile equation has been verified with the upper nappe profile obtained from the numerical model that had not been used in derivation of equation.

In order to verify the adoptability of the proposed roof profile equation, solid roof profile designed with the proposed equation was fixed on the roof of previous experimental set up. In this set up-3, total 99 numbers of experiments and simulations were carried on physical and numerical models. The studies were carried out to check the performance of orifice spillway for various combinations of design heads, heights of orifice and different spillway operating conditions. The grid size of 0.004 m and Realizable k- $\epsilon$  turbulence model was found to be suitable for modelling the flow through orifice spillway for present problem. In this set up, main aim was to provide design guidelines of orifice spillway in terms of

different hydraulic parameters. The performance of bottom and roof profiles designed from present research work was assessed in respect of coefficient of discharge, pressure distribution on roof & bottom profile and water surface profile along centre line of spillway. The coefficient of discharge was obtained in the range of 0.831 to 0.942. Hence, the discharging capacity of orifice spillway was found to be adequate. Based on the results, an equation was developed to estimate coefficient of discharge considering all practical design heads (h<sub>d</sub>) and heights of orifice (d). The equation was validated with data of real life orifice spillway projects. The C<sub>d</sub> value with proposed equation of roof profile was found to be better than the one obtained by trial and error method in model studies of various projects. This is because the equation in the present study was developed after finalizing design of spillway bottom and roof profile for a particular head over the crest and height of orifice. Non dimensional plots have been developed in respect of pressures over spillway bottom and roof profiles and water surface profile along centreline of spillway for various configurations of orifice spillway. These plots would be helpful to the engineers at the initial stage of design of an orifice spillway.

The performance of orifice spillway was assessed for variation of width of orifice, height of spillway, factor k in design of bottom profile and b/d ratio, which were kept constant during basic research study. To check the general adoptability, the developed equations of bottom and roof profile was also validated with the existing real life orifice spillway. Based on the results, it is concluded that the design of orifice spillway propsed in present research work would be helpful to the engineers at initial design stage to make the structure hydraulically and economically safe.

## **CONTENTS**

DESIGN GUIDELINES FOR ORIFICE SPILLWAY	Error! Bookmark not defined.
Contents	v
List of Figures	viii
List of Tables	xii
Abbreviations and Acronyms	xiii
Chapter 1 Introduction	11
<ul> <li>1.1 General</li> <li>1.2 Overflow Spillways</li> <li>1.3 Need of Orifice Spillway</li> <li>1.4 Orifice Spillways</li> <li>1.5 Physical Model Studies-A Traditional Technique</li> <li>1.6 Numerical Model Studies- A Recent Technique</li> <li>1.7 Motivation of the Present Study</li> </ul>	11 12 12 13 14 15
<ul><li>1.8 Scope of the Present study</li><li>1.9 Objectives of the Present Study</li></ul>	17 17
Chapter 2 Orifice Spillway: Design Considerations, Theor	
Modelling and Dimensional Analysis	18
<ul> <li>2.1 General</li> <li>2.2 Design Consideration of Orifice Spillway</li> <li>2.2.1 Discharging capacity of spillway</li> <li>2.2.2 Spillway bottom profile</li> <li>2.2.3 Roof profile of an orifice spillway</li> <li>2.2.4 Size and dimensions of orifice spillway</li> <li>2.2.5 Structural design considerations</li> <li>2.2.6 Special design consideration for design of energy design of Orifice</li> <li>2.4 Methods of Dimensional Analysis</li> <li>2.5 Dimensional Analysis of Orifice Spillway Geometry</li> <li>2.6 Necessity of Physical Modelling and Similitude</li> <li>2.6.1 Scale effects in physical modelling</li> <li>2.6.2 Construction methodology of physical model</li> <li>2.7 Need of CFD Modelling</li> <li>2.8 Theoretical Background of Computational Fluid Dynam</li> <li>2.8.1 Continuity equation</li> <li>2.8.2 Momentum equation</li> </ul>	26 29 30 33 35 36 37 nics 37 38
<ul> <li>2.9 Numerical Methods</li> <li>2.10 Boundary Conditions/Initial conditions/Operating conditions/Initial conditions/Operating c</li></ul>	41

2.16 Post Processing	48
Chapter 3 Contribution of CWPRS in evolving the design of orifice spillway	49
<ul> <li>3.1 General</li> <li>3.2 Analysis of Data from CWPRS in respect of Discharging Capacity</li> <li>3.3 Analysis of roof profile</li> <li>3.4 Case studies</li> <li>3.4.1 Chamera H.E. Project, stage – I, Himachal Pradesh</li> <li>3.4.2 Tala H. E. Project, Bhutan</li> <li>3.4.3 Punatsanghchhu H.E.Project, Bhutan</li> </ul>	49 53 56 57 57 61 67
Chapter 4 Basic Research Study	71
4.1 General 4.2 Physical model set up 1 4.3 Numerical model set up 1 4.3.1 Grid size and boundary conditions 4.3.2 Set up in FLUENT 4.3.3 Grid convergence study 4.4 Results from set up 1 4.4.1 Coefficient of discharge (C <sub>d</sub> ) and coefficient of velocity (C <sub>v</sub> ) 4.4.2 Lower nappe profile 4.4.3 Upper nappe profile 4.5 Physical and numerical model set up 2 4.6 Effect of Height of Orifice Spillway (P) 4.6.1 Discharge through orifice 4.6.2 Upper nappe water surface profile 4.7 Effect of Design Head on Upper Nappe Profiles 4.8 Effect of Operating Head on Upper Nappe Profiles 4.9 Effect of Height of Orifice on Upper Nappe Profiles 4.10 Development of an Equation for Roof Profile of an Orifice Spillway 4.11 Verification of the Proposed Equation 4.12 Validation of the Proposed Equation 4.12.1 Comparison of roof profiles 4.12.2 Flow conditions 4.12.3 Comparison of pressures on roof profile 4.12.4 Comparison of pressures on spillway bottom profile 4.12.5 Comparison of discharge 4.13 Application of the Proposed Equation	71 74 75 75 77 77 80 81 83 85 87 92 92 94 97 97 98 100 102 103 104 105 106 108 110
Chapter 5 Design guidelines and non dimensional plots	112
5.1 Introduction 5.2 Experimental Set Up 3 5.2.1 Studies carried out on physical model 5.2.2 Measurement set up 5.3 Numerical Model 5.3.1 Grid size and boundary conditions 5.3.2 Studies carried out on numerical model 5.3.3 Validation of numerical model 5.4 Analysis of Results and Discussions 5.4.1 Discharging capacity of orifice spillway	112 113 116 117 118 118 120 121 127 128

5.4.2 Effect of non-dimensional parameters on coefficient of discharge	131
5.4.3 Derivation of an equation to estimate $C_d$ of an orifice spillway	132
5.4.4 Validation of proposed equation with the results reported in literature	135
5.4.5 Pressures on spillway bottom profile and corresponding cavitation index	137
5.4.6 Pressures on spillway roof profile and corresponding cavitation index	146
5.4.7 Hydrodynamic pressures on spillway roof profile	154
5.4.7.1 Impact of vibration on roof profile (Resonance study)	160
5.4.8 Water surface profiles along centreline of spillway	161
Chapter 6 Studies for Assessing the Effect of Various Hydraulic Parameters on Orifi	ice
Spillway using Numerical Model Studies	164
6.1 Introduction	164
6.2 Effect of Height of Crest of Spillway from the Bed of the Upstream Reservoir (P)	165
6.3 Effect of Width of Orifice (w)	167
6.4 Effect of factor 'k' while designing spillway bottom profile	169
6.5 Effect of b/d Ratio while Designing Roof Profile	172
6.6 Performance of Orifice Spillway at Gated Condition	174
Chapter 7 Summary and Conclusions	179
7.1 Summary	179
7.1 Summary 7.2 Conclusions	181
7.2.1 Conclusion from physical and numerical model studies of sharp edged large or	
(set up1)	181
7.2.2 Conclusion from physical and numerical model studies with solid spillway bott	
profile without roof profile (set up 2)	182
7.2.3 Conclusion from physical and numerical model studies with solid spillway bott	tom
and roof profiles (set up 3)	183
7.3 Limitation of the Present Study	186
7.4 Research Contributions from the Present Studies	187
7.5 Scope for Further Studies	187
References	189

## LIST OF FIGURES

Fig. 2.1 Typical definition sketch for calculation of discharging capacity	19
Fig. 2.2 Typical roof profile of orifice spillway	21
Fig. 2.3 Details of construction joint in orifice spillway	23
Fig. 1.4 Concrete apron downstream of the end sill	24
Fig. 1.5 Few spans at higher level	25
Fig. 1.6 Typical sketch for free discharging jet through an orifice (Bansal, 2010)	27
Fig.3.1 Scatter plot of C <sub>d</sub> Vs h <sub>cl</sub> / d (Bhosekar et al., 2014)	54
Fig. 3.2 Scatter plot of C <sub>d</sub> Vs h <sub>cl</sub> / h <sub>d</sub> (Bhosekar et al., 2014)	54
Fig. 3.3 Observed Vs Estimated C <sub>d</sub> (Bhosekar et al., 2014)	55
Fig. 3.4 Typical comparisons between observed and estimated C <sub>d</sub> curves (Bhosekar et al.,	
2014)	55
Fig. 3.5 Non-dimensional plot of a/d Vs h <sub>d</sub> /d (Deolalikar et al., 2008)	56
Fig. 3.6 Non-dimensional plot of b/d Vs h <sub>d</sub> /d (Deolalikar et al., 2008)	57
Fig. 3.7 Longitudinal section of the spillway	59
Fig. 3.8 Discharging apacity curves for various alternatives of breastwall profiles and orifo	ce
openings	60
Fig. 3.9 Plan, upstream elevation and section of the spillway	62
Fig. 3.10 View of sectional model	63
Fig. 3.11 Alternative top profiles of sluice	64
Fig. 3.12 Pressures for roof profile – Alternative 1	64
Fig. 3.13 Pressures for roof profile – Alternative 2	65
Fig. 3.14 Pressures for roof profile – Alternative 3	65
Fig. 3.15 Upstream elevation	67
Fig. 3.16 Flow conditions in the vicinity of roof profile for original and modified design	69
Fig. 4.1 Methodology adopted for basic research study	72
Fig. 4.2 Plan and section for physical/numerical model	73
Fig. 4.3 Flow conditions through orifice in physical model	74
Fig. 4.4 Grid generation and boundary conditions	76
Fig. 4.5 Effect of grid size on lower nappe profile	78
Fig. 4.6 Effect of grid size on upper nappe profile	79
Fig. 4.7 Flow conditions for grid size 0.07 m	79
Fig. 4.8 Flow conditions for grid size 0.004 m	80
Fig. 4.9 Comparison of lower nappe profile for $d = 0.26 \text{ m}$	83
Fig. 4.10 Comparison of lower nappe profiles for $d = 0.40 \text{ m}$	84
Fig. 4.11 Comparison of upper nappe profile for $d = 0.26$ m	86
Fig. 4.12 Comparison of upper nappe profile for $d = 0.40 \text{ m}$	86
Fig. 4.13 Plan and section for physical/numerical model set up 2	88
Fig. 4.14 Flow conditions in physical model	91
Fig. 4.15 Flow conditions in numerical model	91
Fig. 4.16 Effect of P on discharging capacity	93
Fig. 4.17 Effect of P on upper nappe profiles for $h_e/h_d = 0.8$	95
Fig. 4.18 Effect of P on upper nappe profiles for $h_e/h_d = 1$	95
Fig. 4.19 Effect of P on upper nappe profiles for $h_e/h_d = 1.33$	96
Fig. 4.20 Effect of design head on the upper nappe profiles	97
Fig. 4.21 Effect of operating head on the upper nappe profiles	98
Fig. 4.22 Effect of height of orifice on the upper nappe profiles	99

Fig.4.23Closer view of the roof profile	100
Fig. 4.24 Plot for coefficients 'A' and 'B' and 'm'	101
Fig. 4.25 Computed and estimated values of upper nappe profiles for $h_e/h_d = 0.8$	102
Fig. 4.26 Computed and estimated values of upper nappe profiles for $h_e/h_d = 1.33$	103
Fig. 4.27 Comparison of roof profile of propsed equation with modified roof profile	
suggested by CWPRS for specific case study	104
Fig. 4.28 Flow condition in the vicinity of original and modified design of roof profile f	or
case study - 3	105
Fig. 4.29 Simulation of flow in the vicinity of modified roof profile for case study - 3	106
Fig. 4.30 Validation of proposed equation in respect of pressures on roof	•
profile of orifice spillway for case study - 1	107
Fig. 4.31 Validation of proposed equation in respect of pressures on roof p	rofile
of orifice spillway for case study - 2	107
Fig. 4.32 Validation of proposed equation in respect of pressures	on
roof profile of orifice spillway for case study - 3	108
Fig. 4.33 Validation of proposed equation in respect of pressures on spillway bottom pr	
of orifice spillway for case study- 1	109
Fig. 4.34 Validation of proposed equation in respect of pressures on spillway bottom pr	
of orifice spillway for case study - 2	109
Fig. 4.35 Validation of proposed equation in respect of pressures on spillway bottom pr	
of orifice spillway for case study - 3	110
Fig. 5.1 Plan and section of physical model set up 3	114
Fig. 5.2 Side view of physical model showing bottom and roof profile for experimental	
3	114
Fig. 5.3 Upstream view of physical model	115
Fig. 5.4 Close up view of roof profile for experimental set up 3  Error! Bookma	rk not
defined.	
<b>defined.</b> Fig. 5.5 Arrangement of the transducers on roof profile of orifice spillway in physical n	nodel
<b>defined.</b> Fig. 5.5 Arrangement of the transducers on roof profile of orifice spillway in physical n (set up 3)	nodel 118
defined.  Fig. 5.5 Arrangement of the transducers on roof profile of orifice spillway in physical n (set up 3)  Fig. 5.6 Grid generation and boundary conditions of domain	nodel 118 119
defined.  Fig. 5.5 Arrangement of the transducers on roof profile of orifice spillway in physical n (set up 3)  Fig. 5.6 Grid generation and boundary conditions of domain  Fig. 5.7 Closer view showing grid generation in the vicinity of roof profile	nodel 118 119 119
defined.  Fig. 5.5 Arrangement of the transducers on roof profile of orifice spillway in physical n (set up 3)  Fig. 5.6 Grid generation and boundary conditions of domain  Fig. 5.7 Closer view showing grid generation in the vicinity of roof profile  Fig. 5.8 Comparison of pressures on spillway roof profile between physical and p	nodel 118 119 119 nd
defined.  Fig. 5.5 Arrangement of the transducers on roof profile of orifice spillway in physical m (set up 3)  Fig. 5.6 Grid generation and boundary conditions of domain  Fig. 5.7 Closer view showing grid generation in the vicinity of roof profile  Fig. 5.8 Comparison of pressures on spillway roof profile between physical armamerical model studies	nodel 118 119 119 nd 122
defined.  Fig. 5.5 Arrangement of the transducers on roof profile of orifice spillway in physical m (set up 3)  Fig. 5.6 Grid generation and boundary conditions of domain  Fig. 5.7 Closer view showing grid generation in the vicinity of roof profile  Fig. 5.8 Comparison of pressures on spillway roof profile between physical and numerical model studies  Fig. 5.9 Comparison of pressures on spillway bottom profile between physical and numerical model studies	nodel 118 119 119 nd 122 erical
defined.  Fig. 5.5 Arrangement of the transducers on roof profile of orifice spillway in physical m (set up 3)  Fig. 5.6 Grid generation and boundary conditions of domain  Fig. 5.7 Closer view showing grid generation in the vicinity of roof profile  Fig. 5.8 Comparison of pressures on spillway roof profile between physical and numerical model studies  Fig. 5.9 Comparison of pressures on spillway bottom profile between physical and numerical model studies	nodel 118 119 119 nd 122 erical 122
defined.  Fig. 5.5 Arrangement of the transducers on roof profile of orifice spillway in physical m (set up 3)  Fig. 5.6 Grid generation and boundary conditions of domain  Fig. 5.7 Closer view showing grid generation in the vicinity of roof profile  Fig. 5.8 Comparison of pressures on spillway roof profile between physical an numerical model studies  Fig. 5.9 Comparison of pressures on spillway bottom profile between physical and num model studies  Fig. 5.10 Comparison of water surface profile between physical and numerical model	nodel 118 119 119 ad 122 erical 122 123
defined.  Fig. 5.5 Arrangement of the transducers on roof profile of orifice spillway in physical m (set up 3)  Fig. 5.6 Grid generation and boundary conditions of domain  Fig. 5.7 Closer view showing grid generation in the vicinity of roof profile  Fig. 5.8 Comparison of pressures on spillway roof profile between physical and numerical model studies  Fig. 5.9 Comparison of pressures on spillway bottom profile between physical and numerical model studies  Fig. 5.10 Comparison of water surface profile between physical and numerical model  Fig. 5.11 Flow conditions through orifice spillway in physical model	nodel 118 119 119 ad 122 erical 122 123 125
defined.  Fig. 5.5 Arrangement of the transducers on roof profile of orifice spillway in physical m (set up 3)  Fig. 5.6 Grid generation and boundary conditions of domain  Fig. 5.7 Closer view showing grid generation in the vicinity of roof profile  Fig. 5.8 Comparison of pressures on spillway roof profile between physical an numerical model studies  Fig. 5.9 Comparison of pressures on spillway bottom profile between physical and nummodel studies  Fig. 5.10 Comparison of water surface profile between physical and numerical model  Fig. 5.11 Flow conditions through orifice spillway in physical model  Fig. 5.12 Flow conditions through orifice spillway in numerical model	nodel 118 119 119 ad 122 erical 123 125 126
defined.  Fig. 5.5 Arrangement of the transducers on roof profile of orifice spillway in physical m (set up 3)  Fig. 5.6 Grid generation and boundary conditions of domain  Fig. 5.7 Closer view showing grid generation in the vicinity of roof profile  Fig. 5.8 Comparison of pressures on spillway roof profile between physical an numerical model studies  Fig. 5.9 Comparison of pressures on spillway bottom profile between physical and nummodel studies  Fig. 5.10 Comparison of water surface profile between physical and numerical model  Fig. 5.11 Flow conditions through orifice spillway in physical model  Fig. 5.12 Flow conditions through orifice spillway in numerical model  Fig. 5.13 Closer view showing flow conditions in the vicinity of roof profile in physical	nodel 118 119 119 ad 122 erical 122 123 125
defined.  Fig. 5.5 Arrangement of the transducers on roof profile of orifice spillway in physical m (set up 3)  Fig. 5.6 Grid generation and boundary conditions of domain  Fig. 5.7 Closer view showing grid generation in the vicinity of roof profile  Fig. 5.8 Comparison of pressures on spillway roof profile between physical and numerical model studies  Fig. 5.9 Comparison of pressures on spillway bottom profile between physical and nummodel studies  Fig. 5.10 Comparison of water surface profile between physical and numerical model  Fig. 5.11 Flow conditions through orifice spillway in physical model  Fig. 5.12 Flow conditions through orifice spillway in numerical model  Fig. 5.13 Closer view showing flow conditions in the vicinity of roof profile in physical model	nodel 118 119 119 ad 122 erical 123 125 126
defined.  Fig. 5.5 Arrangement of the transducers on roof profile of orifice spillway in physical m (set up 3)  Fig. 5.6 Grid generation and boundary conditions of domain  Fig. 5.7 Closer view showing grid generation in the vicinity of roof profile  Fig. 5.8 Comparison of pressures on spillway roof profile between physical and numerical model studies  Fig. 5.9 Comparison of pressures on spillway bottom profile between physical and numerical studies  Fig. 5.10 Comparison of water surface profile between physical and numerical model  Fig. 5.11 Flow conditions through orifice spillway in physical model  Fig. 5.12 Flow conditions through orifice spillway in numerical model  Fig. 5.13 Closer view showing flow conditions in the vicinity of roof profile in physical model  Fig. 5.14 Closer view showing flow conditions in the vicinity of roof profile in numerical	nodel 118 119 119 ad 122 erical 123 125 126 126
defined.  Fig. 5.5 Arrangement of the transducers on roof profile of orifice spillway in physical m (set up 3)  Fig. 5.6 Grid generation and boundary conditions of domain  Fig. 5.7 Closer view showing grid generation in the vicinity of roof profile  Fig. 5.8 Comparison of pressures on spillway roof profile between physical an numerical model studies  Fig. 5.9 Comparison of pressures on spillway bottom profile between physical and nummodel studies  Fig. 5.10 Comparison of water surface profile between physical and numerical model  Fig. 5.11 Flow conditions through orifice spillway in physical model  Fig. 5.12 Flow conditions through orifice spillway in numerical model  Fig. 5.13 Closer view showing flow conditions in the vicinity of roof profile in physical model  Fig. 5.14 Closer view showing flow conditions in the vicinity of roof profile in numerical model	nodel 118 119 119 110 122 erical 123 125 126 126 al
defined.  Fig. 5.5 Arrangement of the transducers on roof profile of orifice spillway in physical m (set up 3)  Fig. 5.6 Grid generation and boundary conditions of domain  Fig. 5.7 Closer view showing grid generation in the vicinity of roof profile  Fig. 5.8 Comparison of pressures on spillway roof profile between physical and numerical model studies  Fig. 5.9 Comparison of pressures on spillway bottom profile between physical and numerical model studies  Fig. 5.10 Comparison of water surface profile between physical and numerical model  Fig. 5.12 Flow conditions through orifice spillway in physical model  Fig. 5.13 Closer view showing flow conditions in the vicinity of roof profile in physical model  Fig. 5.14 Closer view showing flow conditions in the vicinity of roof profile in numerical model  Fig. 5.15 A typical non-dimensional plot of C <sub>d</sub> Vs h <sub>cl</sub> /h <sub>d</sub>	nodel 118 119 119 119 110 122 erical 122 123 125 126 126 127 131
defined.  Fig. 5.5 Arrangement of the transducers on roof profile of orifice spillway in physical m (set up 3)  Fig. 5.6 Grid generation and boundary conditions of domain  Fig. 5.7 Closer view showing grid generation in the vicinity of roof profile  Fig. 5.8 Comparison of pressures on spillway roof profile between physical an numerical model studies  Fig. 5.9 Comparison of pressures on spillway bottom profile between physical and nummodel studies  Fig. 5.10 Comparison of water surface profile between physical and numerical model  Fig. 5.11 Flow conditions through orifice spillway in physical model  Fig. 5.12 Flow conditions through orifice spillway in numerical model  Fig. 5.13 Closer view showing flow conditions in the vicinity of roof profile in physical model  Fig. 5.14 Closer view showing flow conditions in the vicinity of roof profile in numerical model  Fig. 5.15 A typical non-dimensional plot of C <sub>d</sub> Vs h <sub>cl</sub> /h <sub>d</sub> Fig. 5.16 A typical non-dimensional plot of C <sub>d</sub> Vs h <sub>cl</sub> /d	nodel 118 119 119 110 122 erical 123 125 126 126 al
defined.  Fig. 5.5 Arrangement of the transducers on roof profile of orifice spillway in physical necessary (set up 3)  Fig. 5.6 Grid generation and boundary conditions of domain  Fig. 5.7 Closer view showing grid generation in the vicinity of roof profile  Fig. 5.8 Comparison of pressures on spillway roof profile between physical and numerical model studies  Fig. 5.9 Comparison of pressures on spillway bottom profile between physical and numerical studies  Fig. 5.10 Comparison of water surface profile between physical and numerical model  Fig. 5.11 Flow conditions through orifice spillway in physical model  Fig. 5.12 Flow conditions through orifice spillway in numerical model  Fig. 5.13 Closer view showing flow conditions in the vicinity of roof profile in physical model  Fig. 5.14 Closer view showing flow conditions in the vicinity of roof profile in numerical model  Fig. 5.15 A typical non-dimensional plot of C <sub>d</sub> Vs h <sub>cl</sub> /h <sub>d</sub> Fig. 5.16 A typical non-dimensional plot of C <sub>d</sub> Vs h <sub>cl</sub> /d  Fig. 5.17 Comparison of estimated and computed C <sub>d</sub> for	nodel 118 119 119 119 110 122 123 125 126 126 127 131 132
defined.  Fig. 5.5 Arrangement of the transducers on roof profile of orifice spillway in physical m (set up 3)  Fig. 5.6 Grid generation and boundary conditions of domain  Fig. 5.7 Closer view showing grid generation in the vicinity of roof profile  Fig. 5.8 Comparison of pressures on spillway roof profile between physical an numerical model studies  Fig. 5.9 Comparison of pressures on spillway bottom profile between physical and nummodel studies  Fig. 5.10 Comparison of water surface profile between physical and numerical model  Fig. 5.11 Flow conditions through orifice spillway in physical model  Fig. 5.12 Flow conditions through orifice spillway in numerical model  Fig. 5.13 Closer view showing flow conditions in the vicinity of roof profile in physical model  Fig. 5.14 Closer view showing flow conditions in the vicinity of roof profile in numerical model  Fig. 5.15 A typical non-dimensional plot of C <sub>d</sub> Vs h <sub>cl</sub> /h <sub>d</sub> Fig. 5.16 A typical non-dimensional plot of C <sub>d</sub> Vs h <sub>cl</sub> /d  Fig. 5.17 Comparison of estimated and computed C <sub>d</sub> for  Fig. 5.18 Comparison of estimated and computed C <sub>d</sub> for	nodel 118 119 119 119 110 122 erical 122 123 125 126 126 127 131 132 134 134
defined.  Fig. 5.5 Arrangement of the transducers on roof profile of orifice spillway in physical necessary (set up 3)  Fig. 5.6 Grid generation and boundary conditions of domain  Fig. 5.7 Closer view showing grid generation in the vicinity of roof profile  Fig. 5.8 Comparison of pressures on spillway roof profile between physical and numerical model studies  Fig. 5.9 Comparison of pressures on spillway bottom profile between physical and numerical studies  Fig. 5.10 Comparison of water surface profile between physical and numerical model  Fig. 5.11 Flow conditions through orifice spillway in physical model  Fig. 5.12 Flow conditions through orifice spillway in numerical model  Fig. 5.13 Closer view showing flow conditions in the vicinity of roof profile in physical model  Fig. 5.14 Closer view showing flow conditions in the vicinity of roof profile in numerical model  Fig. 5.15 A typical non-dimensional plot of C <sub>d</sub> Vs h <sub>cl</sub> /h <sub>d</sub> Fig. 5.16 A typical non-dimensional plot of C <sub>d</sub> Vs h <sub>cl</sub> /d  Fig. 5.17 Comparison of estimated and computed C <sub>d</sub> for	nodel 118 119 119 119 110 122 erical 122 123 125 126 126 127 131 132 134 134
defined.  Fig. 5.5 Arrangement of the transducers on roof profile of orifice spillway in physical necessary (set up 3)  Fig. 5.6 Grid generation and boundary conditions of domain  Fig. 5.7 Closer view showing grid generation in the vicinity of roof profile  Fig. 5.8 Comparison of pressures on spillway roof profile between physical and numerical model studies  Fig. 5.9 Comparison of pressures on spillway bottom profile between physical and numerical model studies  Fig. 5.10 Comparison of water surface profile between physical and numerical model  Fig. 5.11 Flow conditions through orifice spillway in physical model  Fig. 5.12 Flow conditions through orifice spillway in numerical model  Fig. 5.13 Closer view showing flow conditions in the vicinity of roof profile in physical model  Fig. 5.14 Closer view showing flow conditions in the vicinity of roof profile in numerical model  Fig. 5.15 A typical non-dimensional plot of C <sub>d</sub> Vs h <sub>cl</sub> /h <sub>d</sub> Fig. 5.16 A typical non-dimensional plot of C <sub>d</sub> Vs h <sub>cl</sub> /d  Fig. 5.17 Comparison of estimated and computed C <sub>d</sub> for  Fig. 5.18 Comparison of estimated and computed C <sub>d</sub> for  Fig. 5.19 Non dimensional plots for pressures and corresponding cavitation index for sp	nodel 118 119 119 110 110 111 122 123 125 126 126 127 131 132 134 134 134 131 132 134 134 134

Fig. 5.21 Non dimensional plots for pressures and corresponding cavitation index or bottom profiles designed for the heads 0.6 m and 0.8 m for he/	
Fig. 5.22 Non dimensional plots for pressures and corresponding cavitation index or bottom profiles designed for the heads 1 m and 1.4 m for $h_e/h_d = 1$	
Fig. 5.23 Non dimensional plots for pressures and corresponding cavitation index or	
bottom profiles designed for the heads 0.6 m and 0.8 m for h <sub>e</sub> /	$h_d = 1.33$ 143
Fig. 5.24 Non dimensional plots for pressures and corresponding cavitation index or	
bottom profiles designed for the heads 1 m and 1.4 m for h	144
Fig. 5.25 Non dimensional plots for pressures and corresponding cavitation index or roof profiles designed for the heads 0.6 m and 0.8 m for $h_e/h_d = 0.8$	n spillway 147
Fig. 5.26 Non dimensional plots for pressures and corresponding cavitation index or roof profiles designed for the heads 1 m and 1.4 m for $h_e/h_d = 0.8$	n spillway 148
Fig. 5.27 Non dimensional plots for pressures and corresponding cavitation index of	n spillway
roof profiles designed for the heads 0.6 m and 0.8 m for h <sub>e</sub> /h	d = 1  149
Fig. 5.28 Non dimensional plots for pressures and corresponding cavitation index or	ı spillway
roof profiles designed for the heads 1 m and 1.4 m for $h_e/h_d = 1$	150
Fig. 5.29 Non dimensional plots for pressures and corresponding cavitation index or	-
roof profiles designed for the heads $0.6$ m and $0.8$ m for $h_e/h_d = 1.33$	151
Fig. 5.30 Non dimensional plots for pressures and corresponding cavitation index or	
roof profiles designed for the heads 1 m and 1.4 m for 1.33	$h_e/h_d = 152$
Fig. 5.31 Location of transducers along spillway roof profile in the physical model	156
Fig. 5.32 Time series plot of pressure variation at point b <sub>1</sub> on roof profile	156
Fig. 5.33 Time series plot of pressure variation at point b <sub>2</sub> on roof profile	157
Fig. 5.34 Time series plot of pressure variation at point b <sub>3</sub> on roof profile	157
Fig. 5.35 Time series plot of pressure variation at point b <sub>4</sub> on roof profile	158
Fig. 5.36 Time series plot of pressure variation at point b <sub>5</sub> on roof profile	158
Fig. 5.37 Cumulative probability distribution of pressure at point b <sub>1</sub> with respect to o	occurance
in % of time	159
Fig. 5.38 Typical plot for power spectral density	160
Fig. 5.39 Non dimensional plots for water surface profiles along	orifice
spillway bottom profile designed for head 0.6 m	161
Fig. 5.40 Non dimensional plots for water surface profiles along orifice spillway bot	
profile designed for head 0.8 m	162
Fig. 5.41 Non dimensional plots for water surface profiles along spillway bottom pro	
designed for head 1 m	162
Fig. 5.42 Non dimensional plots for water surface profiles along spillway bottom pro	
designed for head 1.4 m	163
Fig. 6.1 Effect of 'P' on the pressures on spillway roof profile	165
Fig. 6.2 Effect of 'P' on the pressures on spillway roof profile	166
Fig. 6.3 Effect of 'P' on the water surface profile	166
Fig. 6.4 Effect of 'w' on the pressures on spillway roof profile	167 168
Fig. 6.5 Effect of 'w' on the pressures on spillway bottom profile Fig. 6.6 Effect of 'w' on the water surface profile along centerline of spillway	168
Fig. 6.6 Effect of 'k' on the pressures on spillway roof profile for $d = 0.24 \text{ m}$ , $h_d = 1 \text{ m}$	
11g.o. / Effect of K on the pressures on spinway foot profileror u = 0.24 III, IId = IIII	$\frac{170}{170}$
Fig. 6.8 Effect of 'k' on the pressures on spillway roof profile	170
Fig. 6.9 Effect of 'k' on the pressures on spillway bottom profile	170

Fig. 6.10 Effect of 'k' on the water surface profile along centerline of the spillway	171
Fig. 6.11 Effect of b/d ratio on the pressures on spillway roof profile	173
Fig. 6.12 Effect of b/d ratio on the pressures on spillway bottom profile	173
Fig. 6.13 Effect of b/d ratio on the water surface profile	174
Fig. 6.14 Pressures on roof profile for gated and ungated operation of orifi	ce
spillway	175
Fig. 6.15 Pressures on bottom profile for gated and ungated operation of orifice spillway	175
Fig. 6.16 Simulation of flow for 75 % gated operation of orifice spillway	176
Fig. 6.17 Contour plot showing pressures in the vicinity of roof profile for	75
% gated operation of orifice spillway	177
Fig. 6.18 Velocity vectors in the vicinity of roof profile for	
75 % gated operation of orifice spillway	177

## LIST OF TABLES

Table 3.1 Details of orifice spillway (Bhosekar et al., 2014)	50
Table 3.2 Cavitation index for alternative roof profiles of sluice	66
Table 4.1 List of experiments/simulations carried out on physical and numerical model	75
Table 4.2 Effect of grid size on discharge of flow through sharp edged large orifice	78
Table 4.3 Values for coefficient of discharge, coeffcient of velocity and factor k observe	d on
physical model	82
Table 4.4 List of experiments/simulations carried out using physical and numerical mode	el set
up 2	89
Table 4.5 Effect of P on discharging capacity	93
Table 4.6 Comparison of discharge and coefficient of discharge calculated for different of	ease
studies	111
Table 5.1 List of experiments conducted on physical model	116
Table 5.2 List of simulations carried out on numerical model set up 3	120
Table 5.3 Comparison of discharges between physical and	121
Table 5.4 Calculation of R <sup>2</sup> , RMSE and average % error for validation of numerical model.	del
	124
Table 5.5 Discharges and corresponding C <sub>d</sub> for design head of 0.6 m	128
Table 5.6 Discharges and corresponding C <sub>d</sub> for design head of 0.8 m	129
Table 5.7 Discharges and corresponding C <sub>d</sub> for design head of 1 m	129
Table 5.8 Discharges and corresponding C <sub>d</sub> for design head of 1.4 m	130
Table 5.9 Regression coefficients for estimating	133
Table 5.10 Observed and estimated C <sub>d</sub> of orifice spillways	136
Table 5.11 Static pressures in pipe, pressures using DAS set up and voltage generated du	ıring
calibration of pressure transducers	155
Table 5.12 Statistics of pressures on roof profile measured using transducers	159

### ABBREVIATIONS AND ACRONYMS

A, B = semi-major and semi-minor axis of upstream profile of an overflow spillway

A = area of orifice in m<sup>2</sup>

A = cell surface area

 $A_r$  = area scale ratio

 $A_r$  = acceleration scale ratio

a = length of roof profile of orifice spillway, m

b = height of roof profile curve, m

 $C_d$  = coefficient of discharge

 $C_v = coefficient of velocity$ 

D = height of orifice at the entrance of roof profile curve, m

d = height of orifice opening at the exit of roof profile curve, m

Eu = Euler number

F = vector of fluxes

Fg = gravity force

Fi = inertia force

Fp = pressure force

Fr =Froude number

Fv = friction or viscous force

 $F_S$  = surface tension force

Fe = elastic force

 $G_0$  = vertical opening from gate seat to the lip of the gate, m

g = acceleration due to gravity, m/s<sup>2</sup>

h = the water elevation above the center of the orifice, m

H<sub>d</sub>= design head for overflow spillway, m

h<sub>d</sub>= design head for orifice spillway, m

h<sub>cl</sub>= head over centre line of orifice, m

 $H_{e}$  = operating head for overflow spillway, m

h<sub>e</sub>= operating head for orifice spillway, m

 $h_p$  = hydrostatic pressures on spillway bottom profile, m

 $h_{p1}$  = hydrostatic pressures on spillway roof profile, m

K= factor affecting spillway bottom profile of an overflow spillway

k = factor affecting spillway bottom profile of an orifice spillway

k = turbulent kinetic energy

k = factor affecting spillway bottom profile of an orifice spillway

L = width of span, m

M = mass

l,  $l_1$ , = characteristic lengths, m

 $L_r$  = length scale ratio

M= Mach number

n = variable

P = height of spillway crest from upstream river bed, m

 $P_0$  = reference pressure head in m of water,

 $P_{v}$  = vapour pressure of water

 $P_r$  = pressure scale ratio

 $p = \text{density}, \text{Kg/m}^3$ 

 $Q = discharge, m^3/sec$ 

 $Q_r$  = discharge scale ratio

Re =Reynolds number

 $R_i$  = equation residual at an element vertex

 $T_r$  = time scale ratio

t = time, seconds

u = velocity, m/s

 $\mu = \text{dynamic viscosity}, \text{N.s/m}^2$ 

 $\mu_t$ = eddy viscosity

V = cell volume

V, v = velocity of flow, m/s

 $v_o$ = reference velocity, m/s

 $V_r$  = volume scale ratio

 $V_r$  = velocity scale ratio

w = width of orifice opening/span width, m

 $\omega$  = specific dissipation rate

We = Weber no

 $W_i$  = weight factor

x = horizontal coordinates of bottom profile of an orifice spillway, m

y = vertical coordinates of bottom profile of an orifice spillway, m

 $x_1$ = horizontal coordinates of roof profile of an orifice spillway, m

y<sub>1</sub>= vertical coordinates of roof profile of an orifice spillway, m

 $X_1$ ,  $Y_1$  = horizontal and vertical coordinates of the upstream profile of overflow spillway, m

 $X_2$ ,  $Y_2$  = horizontal and vertical coordinates of the bottom profile of overflow spillway, m

 $\sigma$  = surface tension, N/m

 $\sigma$  = cavitation index

n = Manning's constant

 $\alpha_{\rm w}$ = volume fraction of water

 $\alpha_a$ = volume fraction of air

 $\Delta p$ =pressure difference number between atmospheric pressure & pressure under jet, Pascal

 $\mathcal{E}$  = rate of dissipation of turbulent kinetic energy

 $\vec{\tau}$  = stress tensor

APD-IAHR = Asia and pacific division -international association of hydraulic research ASME = American Society of Mechanical Engineers

BIS = Bureauof Indian Standard

CFD =Computational Fluid Dynamics

CWPRS = Central Water and Power Research Station

DES = Detached Eddy Simulation

DNS = Direct Numerical Simulation

FVM = Finite Volume Method

FEM = Finite Element Method

FDM = Finite Difference Method

GCI = Grid Convergence Index

HRIC = High Resolution Interface Capturing Scheme

LES = Large Eddy Simulation

RANS= Reynolds-Averaged Navier-Stokes

RMSE = Root mean square error

RNG = Renormalization-group

RSM = Reynolds Stress Model

SST = Shear-Stress Transport

STM = Statistical Turbulence Modelling

USBR = United State Bureau of Reclamation

USACE = U.S. Army Corps of Engineers

WES = Waterways experiment station

VOF = Volume of Fluid

# Chapter 1 Introduction

#### 1.1 General

There is no life on earth without water; it is one of the most important resources required next to air. Even though water is available abundant on earth, its spatial and temporal distribution on earth makes it as one of the most vulnerable resources (Gunter et al., 2007). The most widely used water management strategy to reduce the problem of spatial and temporal water availability is through dams, reservoirs and canal networks. Thousands of dams have been constructed worldwide and new dams continue to add to this total (Senturk, 1994). One of the most important components of a dam is surplus spillway. Spillways are to be designed as transition structures for smooth passage of surplus water from upstream to downstream of a storage reservoir without causing any damage to the structure or endangering the river system. The aspects such as hydrology and hydraulics, topography and geology, utility and operational aspects, constructional and structural aspects are involved in design of spillways. Appropriate design, proper construction, and reliable operation of spillways are critical to the safety of a dam (USBR, 1987).

Spillways can be broadly classified into overflow and orifice spillways depending on the position of the outlet. The type of spillway to be adopted for a particular situation is largely governed by the type of dam, hydrology, purpose of dam, operating conditions and safety consideration consistent with economy. The spillway design has to be accomplished in a manner that would minimize pressures acting on the crest boundary, acceptable velocities and flow characteristics (USACE, 1990). This complication initiated several studies on spillways that are very much important for the safety of the dam. In case of overflow spillways, the flow over a control section i.e. spillway crest is free surface flow. The most commonly implemented overflow spillway includes free overfall spillway, ogee shaped spillway, chute spillway, stepped spillway, side channel spillway etc. In case of orifice spillways, the orifice opening is set well below full supply level and has pressurized flow over a significant part of their length. Orifice spillway in the form of breastwall/sluice is one of the most important types of submerged spillway. United States Bureau of Reclamation (USBR) and U.S. Army Corps of Engineers (USACE) have conducted extensive research on overflow spillways. Nowadays, orifice spillways are being adopted on most of hydroelectric projects due to its dual purpose of passing the flood and flushing of sediments from the reservoir. However, the studies reported on orifice spillways are very much less than the studies for overflow spillways. Hence, there is a need to carry out basic research on the orifice spillway to evolve design guidelines.

## 1.2 Overflow Spillways

The ogee-crested spillway is one of the most studied hydraulic structures of overflow spillways. The two important characteristics of spillways are profiles (shapes) of spillway and coefficient of discharge. The shape of the ogee-shaped spillway depends upon a number of factors such as head over the crest, height of the spillway above the stream bed or the bed of the entrance channel and the inclination of the upstream face of the spillway. USBR conducted extensive experiments to obtain the profile of the overflow spillways with respect to various hydraulic parameters. The U.S. Army Corps of Engineers developed several standard shapes of the crests of overflow spillways on the basis of U.S.B.R. data. The shapes are known as the W.E.S. standard spillway shapes, because they were developed at Waterways Experiment Station at Vicksberg (W.E.S.), USA. The shape of ogee spillway ordinarily conforms closely to the profile of lower nappe of a ventilated sheet falling from sharp-crested weir. For discharges at design head, the flow glides over the crest and attains maximum discharge efficiency (USBR, 1987).

The design of a spillway requires utmost attention. Many failures of dams occurred in the past due to improperly designed spillways or by spillways of inadequate capacity. Estimation of coefficient of discharge of the spillway is an important step while designing, since, the discharging capacity of spillway depends on it. The coefficient of discharge for overflow spillway depends on various factors such as height of spillway crest above the stream bed, ratio of actual total head to the design total head, slope of the upstream face of spillway, extent of the downstream submergence of crest and downstream apron (USACE, 1990). USACE has developed the guidelines to determine the coefficient of discharge of an overflow type of spillway.

In the past, overflow spillways were being used on most of the dams. However, due to sedimentation of dams especially in Himalayan region, the design of overflow spillway is modified to orifice spillway which can carry out dual function of passing the flood and flushing the sediment out of the reservoir. A need of orifice spillway and its advantages has been discussed in following sections.

## 1.3 Need of Orifice Spillway

In situations where large amount of sediment enters the reservoir, the flood disposal capacity of the spillway can be utilized effectively to dispose off sediment from the reservoir. This combination is possible, particularly in run-of-the river schemes on mountainous streams with narrow and steep gorges. For example, the river systems of Himalayas are perennial as they are fed by the melting of snow and glaciers in summer and are rain-fed during other seasons. High mountains, narrow gorges, fragile geology, high level of seismicity are a few of the characteristics of the Himalayan terrain (Bhosekar et al., 2014). So also, the enormous

sediment loads especially during monsoon months are characteristics of the Himalayan Rivers. The highly abrasive silt particles cause erosion followed by cavitation of the underwater parts of the water conductor system. In case of hydropower plants, the main problems faced because of sediments are frequent chocking of strainers, damage of turbine blades and seals, sealing problems in hydro mechanical gates etc. In addition to this, considerable damage is caused to different valves in high head water conductor system. Several projects like Baira-Siul, Maneri Bhali-1, Chilla and Salal have been affected because of high sediment load. Removal of sediment in the vicinity of power intakes becomes essential to overcome the problems caused due to sediment (Deolalikar et al., 2008).

The most efficient way of flushing out the sediment is to provide low-level bottom outlets or spillways and to affect drawdown conditions by opening them fully during floods. Flushing used to be carried out previously by providing small sluices of the size 3 m x 4 m or so at very low level. However, it was realized that these sluices were effective only locally. Also, there was a tendency of choking of sluices within a short period. Recent trends in designing the spillways is by modifying the low level sluices with due consideration for flushing. Orifice spillways in the form of breastwall/sluice are thus evolved over the last few years to cater for both flood disposal and flushing of sediments. The current trend in design of orifice spillway is keeping the crest as low and near the river bed as possible from consideration of flushing of sediment from the reservoir. The main advantages of orifice spillway are:

- Can be accommodated in a narrow valley
- Reduction in height of spillway gates
- Reduction in number of spillway spans
- Ease of regulating flood and storage
- Reduction in cost of gates and operating mechanism
- Can be used for diversion of flows during construction of project
- Can also be used for flushing of sediments

Though the provision of orifice spillway has many advantages, there is no specific design procedure for its configurations. Thus, design of orifice spillway is need of the hour.

## 1.4 Orifice Spillways

The characteristics of orifice spillway are entirely different from overflow type of spillway. The hydraulics of orifice spillway changes with varying reservoir level. The flow is free flow for reservoir water levels below the roof of the sluice, for higher water levels the flow is orifice flow (BIS 6934: 2010). The crest of orifice spillway is kept as near the river bed as possible for flushing of the sediments from reservoir. The range of design heads for the orifice spillways adopted on most of the project varies from 30-60 m (CWPRS Technical Reports (2000, 2005)). Due to large design discharges the orifice sizes varies between 8-20 m (w) x

12-22 m (d). This results in high velocities of the order of 20-25 m/s over the spillway crest corresponding to discharge intensity of the order of 200-300 m<sup>3</sup>/s/m (Deolalikar et al., 2008). The bottom profile of orifice spillway is flatter as compared to the overflow crest profile to avoid flow separation and negative pressures on the crest for small partial gate openings. The upper quadrant of the crest is usually designed as quarter of an ellipse similar to the ogee profile of free overflow spillway.

In orifice spillway, the coefficient of discharge is influenced by many parameters such as shape of spillway, head over the spillway crest, upstream depth of spillway crest from river bed, river slope, width of piers, shape of pier nose, aspect ratio of orifice opening, approach flow conditions etc. Thus, assessment of the coefficient of discharge is difficult due to a wide variation of these parameters from site to site. In addition to the upstream and downstream spillway bottom profile, roof profile is also an important parameter of an orifice spillway because it affects the discharging capacity of the spillway. Literature shows that the flow through orifice does not follow the elliptical roof profile recommended by United state Bureau of Reclamation for sluice flow (USBR, 1987), which results in reducing the discharging capacity of orifice spillway. Unlike overflow spillway, the roof profile of orifice spillway has not been designed considering various hydraulic parameters. Therefore, the hydraulic design of each orifice spillway has been finalised based on model studies for case to case (CWPRS Technical Reports, (1991, 2005, 2014)). Thus, there is a need to conduct basic research to optimise the design of an orifice spillway especially in respect of bottom and roof profiles and provide guidelines in respect of different hydraulic parameters such as discharge, pressures over spillway bottom & roof profile and water surface profile.

## 1.5 Physical Model Studies-A Traditional Technique

Physical model study is an indispensable tool to optimize various components of reservoir and appurtenant structures. Many of the hydraulic design problems are unique and complex due to their site specific conditions. The hydraulic design of various components of a river valley project involves two types of problems viz. site specific problems and problem connected with complex hydraulic flow phenomena. At present, these problems cannot be solved analytically and therefore they have to be tackled by conducting the studies on physical models of these structures (USBR, 1980). An advantage of a physical model is its potential capacity to replicate many features of a complicated flow situation.

The basis of all physical modelling is the idea that the model behaves in a manner similar to the prototype it is intended to emulate. The model study includes systematic examination of each feature of the proposed prototype and examines the necessity of any modification from consideration of operational improvement, possible reduction in cost of construction and reduction in maintenance cost. Thus, a properly validated physical model can be used to predict the behaviour of prototype under a specified set of conditions. However, there is a possibility that physical model results may not be exactly indicative of

prototype behaviour due to scale effects or laboratory effects. The role of the modeller is to minimize scale effects by understanding and applying proper similitude relationships, and to minimize laboratory effects through careful model operation (Steven et al., 2008). Inspite of several guidelines available, specific model study may still become necessary because of some uniqueness in design, layout and operational aspect. However, basic guidelines help to reduce the number of trials to be made through a physical model. A proper basic guideline derived through physical model for hydraulic design of an orifice spillway is need of the hour.

## 1.6 Numerical Model Studies- A Recent Technique

In the past, the characteristics behaviour and hydraulics of spillway has been understood mainly based on physical models. Today, with the help of high-performance computers and more efficient Computational Fluid Dynamics (CFD) codes, the behaviour of hydraulic structures can be investigated numerically in reasonable time and cost. CFD is a branch of science, which deals with replacing the differential equations governing the fluid flow into a set of algebraic equations. These algebraic equations are solved with the help of digital computers. A key advantage of CFD is that it is very compelling, non-intrusive and virtual modelling technique with powerful visualization capabilities. One of the most important steps in CFD is that, the numerical model should be well calibrated and validated. Validation of CFD model is carried out by comparing the results of CFD model with that of physical model studies. Calibration and validation are the primary methods for building and quantifying the confidence of CFD modelling. Hence, one must be very careful in calibration of numerical model.

This technique has been used in a wide range of industrial and non-industrial application areas. It has an ability to provide a large amount of data more cost effectively with more flexibility and more rapidly than with experimental procedures. It uses numerical methods to solve the fundamental nonlinear differential equations that describe fluid flow for predefined geometries and boundary conditions. It is able to overcome many difficulties of physical models especially measuring the flow quantities in inaccessible flow regions and which could not be measured due to disturbances caused by the instrument (Unami et al. (1999), Savage and Johnson (2001), Dargahi (2006), Mao et al. (2006), Bhosekar (2011), Jothiprakash et al. (2015)).

## 1.7 Motivation of the Present Study

Orifice spillways in the form of sluice or breastwall are becoming more popular in large dams that are subjected to heavy siltation. Orifice spillways apart from safe disposal of flood from upstream to downstream of dams, also pass the sediments entering into the

reservoir to the downstream. Orifice spillways help in reducing the number of spillway spans and height of the spillway gates, overall cost of gates and operating mechanism.

Unlike an overflow spillway, an orifice spillway has additional design features to be determined and examined before construction. Some of the important parameters required to be determined while designing an orifice spillway are:

- Bottom profile of the spillway crest including the upstream and downstream quadrants
- Roof profile of the orifice spillway
- Estimating of discharge characteristics of spillway
- Size and dimensions of the orifice opening
- Protection of the spillway surface to resist abrasion
- Choice of energy dissipator

The main aim of finding appropriate parameter is to increase the discharging capacity so that maximum flood is passed through the spillway. The coefficient of discharge of an orifice spillway is influenced by number of hydraulic and structural parameters. The first step in getting the maximum discharge capacity is to first standardize the design of profiles of spillway i.e. bottom and roof profile in case of orifice spillway. However, no systematic literature has been reported especially on design of roof profile of an orifice spillway. Thus, there is a strong need to standardize the design of roof profile with respect to all the parameters affecting the discharging capacity of spillway.

To understand the hydraulics of flow through orifice spillway, there is a need to minimize the physical model studies and develop a strong mathematical model. The main attraction in using CFD is its ability to investigate physical fluid systems and provide a large amount of data where it is difficult to measure the same in physical model. CFD models can be developed cost effectively with more flexibility and more rapidly than physical models. Numerical simulation has become a viable complementary tool to physical modelling of spillways (Chen et al. (2002), Ho et al. (2003), Bhajantri (2007), Chanel and Doering (2007), Jothiprakash et al. (2015)). Literature search of numerical modelling of spillways has revealed that it began as an investigative tool at research institutions (Kjellesrig 1996, Savage and Johnson 2001) and was gradually being accepted by the hydraulic dam engineering community (Higgs (1997), Yang and Johansson (1998), Cederstrom et al. (2000)). Though many orifice spillways have been designed and implemented worldwide, hydraulic model studies for individual project has remained the principal tool for estimating the coefficient of discharge and pressures over the roof profile (Deolalikar et al., 2008). The literature available on physical and numerical modelling of profiles of orifice spillway is scanty. Unlike overflow spillway, the design of orifice spillway has not been standardized with respect to the spillway bottom and roof profiles. Nevertheless, designers have realized the advantage of an orifice spillway. Thus, the motivation of the present study is to investigate bottom and roof profiles of orifice spillway so as to achieve maximum discharging capacity. In general, the motivation

is to help the designer with the guidelines for design of orifice spillway derived through physical and numerical model studies.

## 1.8 Scope of the Present study

Fairly large numbers of studies have been carried out on overflow spillway and the design has been standardized. Most of the investigations reported in literature have been carried out through experimental and numerical models. Nowadays, orifice spillways are becoming more popular due to its dual purpose of flushing of sediment and flood disposal. Estimation of coefficient of discharge for design of orifice spillways is very important for a designer as the discharging capacity of the spillway is the most important aspect. The study of bottom and roof profiles of an orifice spillway is important as it governs the coefficient of discharge of the spillway. Even though, the theory on hydraulics of fluid flow through orifice is available, the fluid flow characteristics through orifice spillway need to be studied. Hence, there is a scope to study fluid flow characteristics through orifice spillway in physical model. Nowadays, with the use of high performance computer and more efficient computational fluid dynamics software, it is possible to investigate the flow through spillway numerically. Hence, there is a scope to study the bottom and roof profiles of an orifice spillway through physical model as well as developing a 3-D numerical model using Computational Fluid Dynamic technique.

## 1.9 Objectives of the Present Study

Based on the above motivation and scope, the major objective of the present study is to investigate the flow through an orifice spillway using physical and numerical models. The specific objectives are as follows:

- 1. To investigate the bottom and roof profiles of an orifice spillway for various hydraulic parameters using physical and numerical models
- 2. To derive an equation for designing the roof profile of an orifice spillway
- 3. To derive an equation for estimating the coefficient of discharge of an orifice spillway
- 4. To derive non dimensional plots for the hydraulic design of roof and bottom profile of an orifice spillway
- 5. To validate the proposed research with existing model studies of real life orifice spillway projects

## Chapter 2

# Orifice Spillway: Design Considerations, Theoretical Background of Modelling and Dimensional Analysis

#### 2.1 General

Orifice spillway in the form of breastwall/sluice is a recent development in spillway design. It is widely adopted spillway because of its dual purpose of passing the flood and flushing of sediment from the reservoir. However, its basic design has not been evolved as that of overflow spillways. Almost the design of all the orifice spillway profiles is finalized based on trial and error process through physical modelling. Various hydraulic design aspects such as discharging capacity, pressures, water surface profiles and energy dissipation arrangement are considered to evolve hydraulically efficient design of spillway. This chapter discusses about hydraulic and structural design considerations of orifice spillway. Dimensional analysis carried out to determine non-dimensional parameters affecting the flow through spillway is also reported. Physical model studies are indispensable tools to optimize various components of reservoir and appurtenant structures. In the past, the study of the spillway was mainly based on physical models. The recent development in computer software has advanced the use of Computational Fluid Dynamics (CFD) in analysing flow over spillways. Physical and numerical modelling techniques for modelling the flow through spillways are also discussed in the present chapter.

## 2.2 Design Consideration of Orifice Spillway

Orifice type of spillway has advantage of lesser number of spillway spans, reduction in height of the spillway gates, the overall cost of gates and operating mechanism. The U.S. Army Corps of Engineers (USACE, 1990) have provided guidelines for design of overflow spillway. Unlike overflow spillway, the design of orifice spillway has not been evolved with respect to its different hydraulic parameters. Some of the important aspect required to be determined while designing an orifice spillway are:

- Discharging capacity of spillway
- Spillway bottom profile
- Spillway roof profile

- Size and dimensions of orifice spillway
- Structural design considerations
- Energy dissipator

#### 2.2.1 Discharging capacity of spillway

The discharging characteristic of spillway is the main considerations while designing the orifice spillway. The assessment of coefficient of discharge is essential for the preliminary design of the spillway in order to provide sufficient waterway and to pass the PMF at the maximum reservoir water level. The coefficient of discharge for orifice flow is influenced by the entrance profile-composed of the roof profile of orifice opening, spillway crest profile, side wall profiles if provided. Figure 2.1 shows the definition sketch for calculation of discharging capacity.

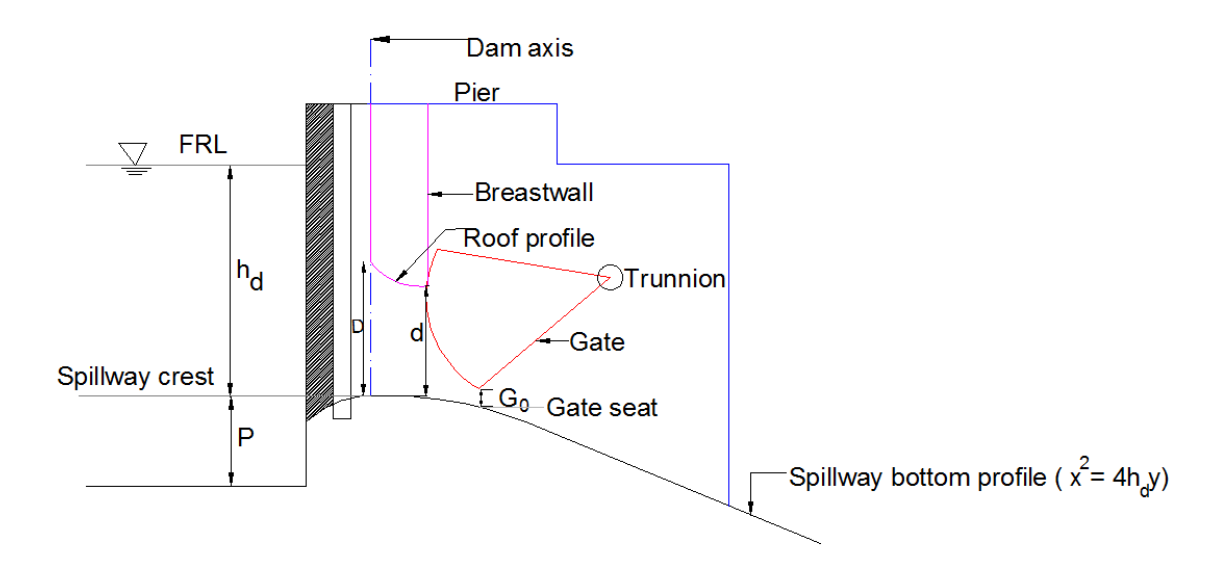


Fig. 2.1 Typical definition sketch for calculation of discharging capacity

Figure 2.1 shows all the important components to be considered in design of an orifice spillway. In orifice spillway, hydraulics of flow changes with varying reservoir water levels. The flow is free flow for reservoir water levels below the roof profile. For higher water levels the flow is orifice flow. Generally, the orifice flow condition requires head over the crest in excess of about 1.5 to 1.7 D, where D is the height of the orifice opening at the entrance of orifice. For free flow conditions the discharge is given by

$$Q = \frac{2}{3} * \sqrt{2g} * C_d * L * h_e^{3/2}$$
 (2.1)

Where,  $Q = \text{discharge in m}^3/\text{s}$   $C_d = \text{coefficient of discharge}$  L = width of spillway in m (no. of span x width of span)  $h_e = \text{head over the crest in m}$ 

The discharging capacity for ungated and gated operation of orifice spillway is calculated using equations 2.2 and 2.3 respectively.

For ungated operation of orifice spillway (BIS 6934: 2010)

$$Q = C_d * n * A * \sqrt{2g(h_d - d/2)}$$
(2.2)

For gated operation of orifice spillway (BIS 6934: 2010)

$$Q = C_d * n * w * G_0 * \sqrt{2g(h_d - G_0/2)}$$
(2.3)

Where,  $Q = \text{discharge in m}^3/\text{s}$ 

 $C_d$  = coefficient of discharge

n = number of spans

w =width of orifice/span in m

A =area of orifice in  $m^2 = w \times d$ 

 $h_d - d/2$  = head over the center line of orifice in m

 $G_0$  = vertical opening from gate seat to the lip of the gate in m

It was experienced from model studies of orifice spillway conducted in CWPRS (2000, 2014) that in addition to height of orifice (d) and design head (h<sub>d</sub>), roof profile also affects the discharging capacity of orifice spillway. However, design of orifice spillway has not been standardized for roof as well as bottom profiles in respect of discharging capacity. Bureau of Indian Standard has given some guidelines for design of profiles. However, these profiles have not been standardized for various combinations of design heads, heights of orifice and different spillway operating conditions. Hence, there is a need to evolve the design of bottom and roof profile for making the structure hydraulically efficient. The guidelines given by BIS 6934: 2010 are discussed below.

### 2.2.2 Spillway bottom profile

Bottom profile of an orifice spillway consisted of two quadrants i.e. upstream and downstream quadrant. As per BIS 6934: 2010, the upper quadrant of the crest may conform to the ellipse similar to ogee profile of free overflow spillway. The downstream spillway crest profile is flatter as compared to the overflow crest profile to avoid flow separation and negative pressures on the crest for small partial gate openings. The crest profile generally

follows the equation  $x^2 = 4h_{cl}y$ , where  $h_{cl}$  is the head over the centreline of the orifice opening. The details of profile are shown in Figure 2.1.

### 2.2.3 Roof profile of an orifice spillway

The shape of roof profile plays a significant role in deciding the discharging capacity of spillway as it guides the flow out of the spillway opening. Figure 2.2 shows a typical roof profile of orifice spillway. Usually, a profile in the form of full or part of an ellipse, adopted from the inlet profile of sluice (USBR, 1987) is provided bearing the following equation

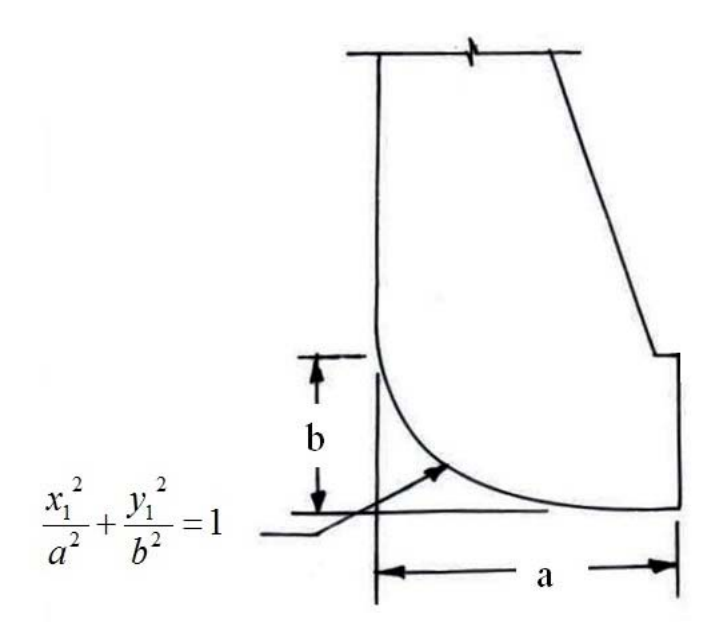
$$\frac{{x_1}^2}{a^2} + \frac{{y_1}^2}{b^2} = 1 \tag{2.4}$$

Where,  $x_1$  = horizontal coordinates of roof profile in m

 $y_I$ = vertical coordinates of roof profile in m

a =length of roof profile in m

b =height of curve which governs the steepness of the profile in m



In most of the cases of orifice spillway, flow through orifice does not follow the elliptical roof profile. The flow separation takes place on the roof profile resulting in inadequate discharging

capacity. Hence, it is essential to evolve suitable roof profile based on hydraulic consideration for improving the discharging capacity of spillway.

#### 2.2.4 Size and dimensions of orifice spillway

In the past, flushing of sediments from reservoir are used to be carried out by providing small sluices (of the size of 3 m x 4 m or so) at very low level. However, it was realized that these sluices were effective only locally. Also, there was a tendency of choking of sluices within a short period. Recent trends in designing the spillways is by modifying the low level sluices with due consideration for flushing. In this design of spillway large openings of the size of 6 -15 m (w) x 10 - 21 m (d) are required to be located 30-60 m below the full reservoir water level and as near the river bed as possible for flushing of the reservoir (Deolalikar et al., 2008). The spillway would allow the setting of its crest at significantly lower elevation, yet retaining the choice of a high dam for creating head for power generation. A relatively smaller size of radial gate results in overall economy. Greater depth of flow over the crest offers large margin for locating the power intake allowing large submergence for vortex free operation, at the same time keeping the intake as high above the river bed as possible to keep it free of sediments.

## 2.2.5 Structural design considerations

The vertical wall which creates an orifice (opening) over the crest to pass the design flood and maintain head (water level above crest) at upstream of spillway crest is known as breastwall. Breastwall in orifice spillway is an important part from structural point of view. Hence it necessitates some special design considerations. Breastwalls in orifice spillway has to bear the upstream water head with beams or slabs spanning between two piers. As such, the breastwall and both the piers have to be constructed as a single structural unit. The construction joint is, therefore, provided at the centre of each pier, except the end piers. Thus, a single pier is virtually a combination of two full piers separated by a construction joint, and a typical spillway monolith is composed of two piers and breastwall as shown in Figure 2.3.

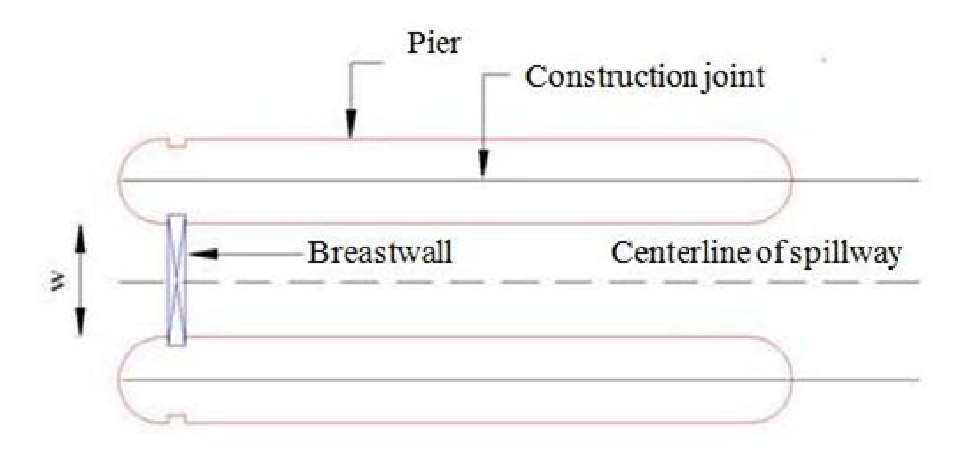


Fig. 2.3 Details of construction joint in orifice spillway

Special care is also required in respect of the seal of the radial gate for ensuring water tightness. The larger velocities associated with the high heads may increase the potential for cavitation and erosion damage to the structure. Adequate protection measures should be taken during the construction of the sluice barrel and breast wall spillway, to withstand the erosive power of the silt laden water while flushing the reservoir and flood routing, by way of special type of concreting (poly impregnated concrete) or providing steel lining along the discharge channel of the spillway (Khatsuria, 2004).

#### 2.2.6 Special design consideration for design of energy dissipators

Special considerations are required for design of suitable energy dissipator, since the spillway has to surpass both the flood and the sediment. Steep bed slopes of the rivers in the hilly regions result in low tail water depth permitting two choice of energy dissipator. Skijump bucket is found to be the most suitable as energy dissipator because of its obvious advantage during flushing operation. The sediment passes down the spillway with supercritical flow without deposition and churning in the bucket. In many projects like Nathpa Jhakri, Tala, Chamera - I, Dhauliganga and Ranganadi, ski-jump bucket has been provided as energy dissipator.

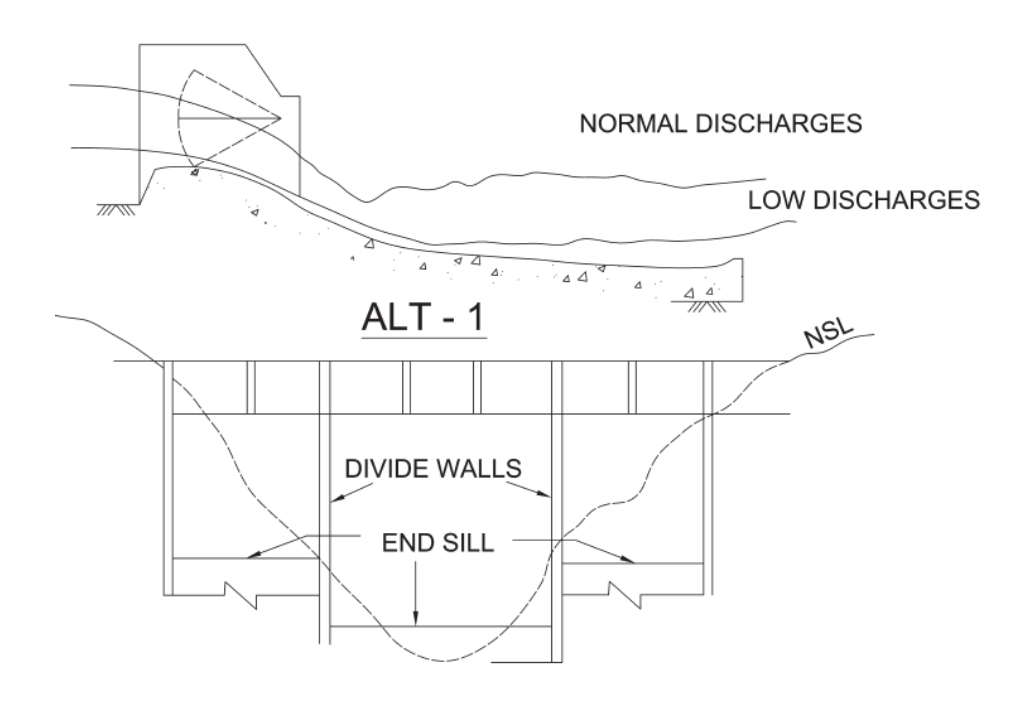
#### 2.2.6.1 Stilling basin

A hydraulic jump stilling basin may have to be adopted where geological conditions are not favourable. The high unit discharge passing down a low head during flushing, results in a low Froude number condition. The stilling basin for the Froude number in the range of 2.5 - 4.5 are rather difficult to design to ensure satisfactory performance for the entire range of discharge. Because of the requirement of passing high sediment flows, use of energy

dissipating appurtenances like chute and baffle blocks is not advisable. As a result the stilling basin becomes excessively long and often deep-seated below the general river bed, making it vulnerable to deposition of silt during flushing operation. Experience with stilling basin of Chamera - II project shows that a trade-off is desirable between the hydraulic efficiency of energy dissipation and the self-cleansing potential of the stilling basin during flushing operation. Cylindrical end sills are generally preferred for easy movement of sediment out of the basin. Provision of roller bucket is generally avoided as an energy dissipator due to likelihood of abrasion damage of the bucket due to churning of sediment.

#### 2.2.6.2 Ski-jump bucket

In some cases, head-discharge-tail water combinations for the full operating range of a structure do not result in a design, which is exclusively a flip bucket or hydraulic jump stilling basin. In such a situation, a composite type of energy dissipator with a horizontal apron terminating with a low circular upturned end sill is found to be quite satisfactory. A concrete apron downstream of the end sill as shown in Figure 2.4 is required to protect the spillway against undermining due to scour during transition from hydraulic jump to flip action and vice versa. Another alternative would be to isolate a few spans of the spillway on the flanks with apron at higher level for flushing out sediment (Figure 2.5). These spans would function with hydraulic jump under sweep out condition, for small discharges of the order of average annual flow, during flushing operation. The central spans would cater to the normal discharges. Such arrangement has been provided for Chukha dam spillway, Bhutan.



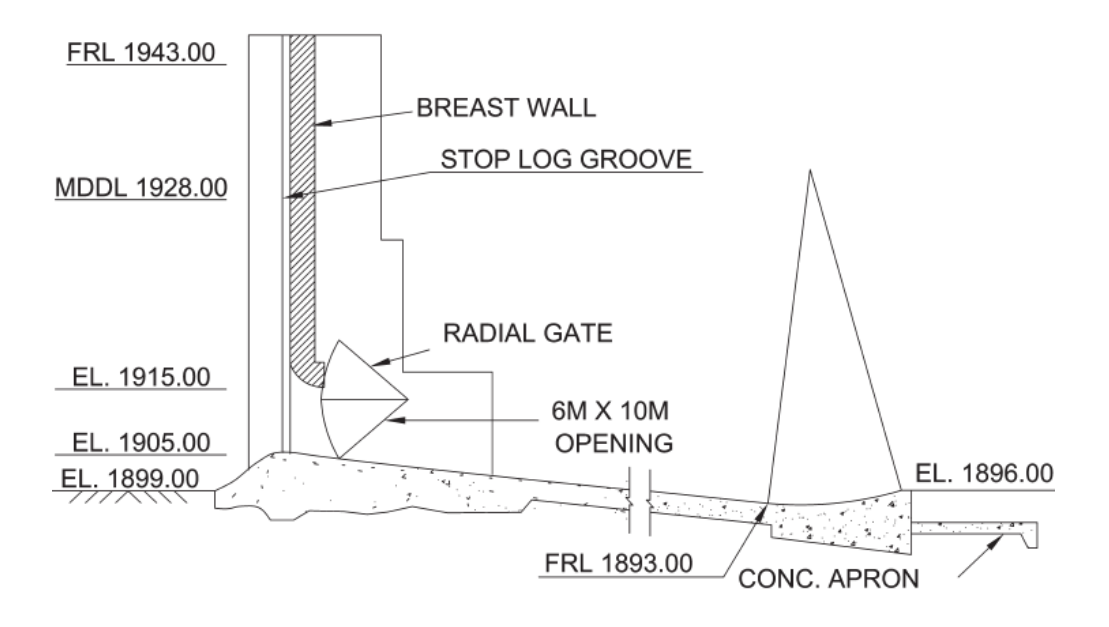


Fig. 2.5 Few spans at higher level

#### 2.2.6.3 Protection of flow surfaces

The flow surfaces of spillway and stilling basins suffer abrasion damage due to passing of high sediment laden flow. At Chukha project, Bhutan, the spillway glacis has been protected against damage due to boulders, by embedding 50 pound rails at 30 cm center to center. For stilling basin, rich concrete of M 250 grade with 20 m size aggregate has been provided for a thickness of 50 cm. It is reported that the above protection has stood well after the spillway came into operation in 1984.

In case of Nathpa Jhakri sluice spillway, steel lining consists of 20 mm thick steel plate forming the top and 25 mm thick plate forming the bottom and side walls of the sluice. In order to stabilize the liner and anchor it in to the surrounding concrete, stiffeners in the form of 700 mm deep and 20 mm thick web with 300 mm wide and 30 mm thick flanges have been provided around the sluice opening at a spacing of 700 mm c/c. Steel rails @ 175 mm center to center have been provided on the spillway glacis downstream of sluices and the space in between is filled with high strength silica fume concrete.

The guidelines given above would be useful in preparing a preliminary design of orifice type of spillway. However, the final design should be evolved on the basis of studies on a physical model. The construction of dams involves huge capital cost and recurring expenditure of maintenance. The dam hydraulics should be optimized functionally and economically before the execution of construction work. Physical modelling is a design technique used by engineers to optimize the structure design, to ensure the safe operation of

the structure and/or to facilitate the decision-making process. The rapidly varied spillway flows with complex geometry, supercritical velocities due to high heads leading to cavitation damages, intense turbulence causing hydrodynamic forces on the spillway structure are normally investigated by physical models.

USBR (1987) and USACE (1952) have conducted extensive research to determine the profiles and other hydraulic parameters of overflow type of spillway by investigating the flow over sharp edged weir. Though several large dams have been constructed all over the world with orifice spillway, guidelines for the hydraulic design of orifice spillway are not readily available. In the present study, an attempt has been made to optimise the bottom and roof profile of an orifice spillway by investigating the flow through sharp edged orifice. It is also aimed to derive non dimensional plots that help designers to ascertain basic profile and assess the performance of spillway in respect of discharging capacity, pressure distribution on spillway surfaces and water surface profiles. To understand the hydraulics of the orifice spillway, the basic theory of orifice needs to be studied first. The basic theory of flow through orifice is discussed in following section.

## 2.3 Theory of Orifice

This section describes the theory of flow through an orifice. The theory was used for further investigating the bottom and roof profiles of an orifice spillway. Orifice is an opening of any cross-section (such as circular, triangular, rectangular etc.) on the side or at the bottom of a tank, through which a fluid is flowing. The orifices are classified on the basis of their size, shape, nature of discharge and shape of the upstream edge. They are as follows:

#### a. According to size:

Small orifice: Head of the liquid from the centre of orifice is more than 5 times the

depth of orifice.

Large orifice: Head of the liquid from the centre of orifice is less than 5 times the

depth of orifice.

#### b. According to shape:

Circular orifice

Rectangular orifice

Triangular orifice

#### c. According to shape of upstream edge:

Sharp-edged

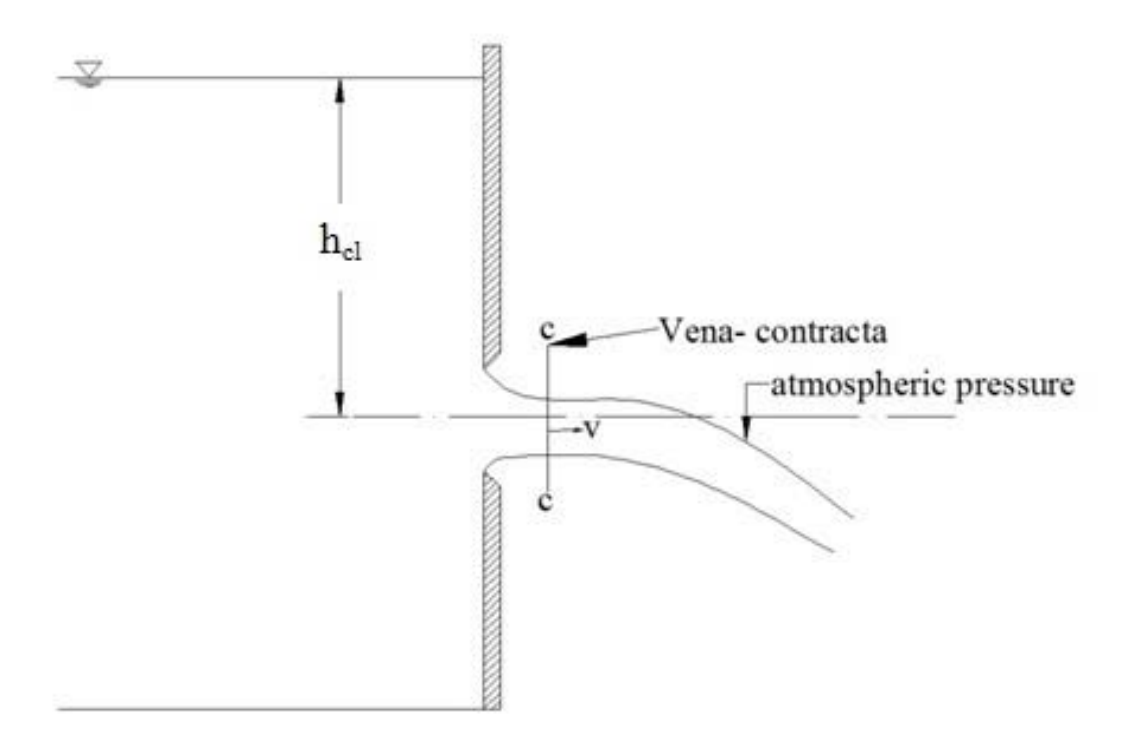
Bell-mouth

#### d. According to nature of discharge:

Fully submerged orifice

Partially submerged orifice

The flow of water through an orifice is illustrated in Figure 2.6. Water approaches the orifice with a relatively low velocity and issues from the orifice as a contracted jet. If the orifice discharges free into the air, there is modular flow and the orifice is said to have free discharge; if the orifice discharges under water it is known as a submerged orifice. If the orifice is not too close to the bottom, sides, or water surface of the approach channel, the water particles approach the orifice along uniformly converging streamlines from all directions. Since these particles cannot abruptly change their direction of flow upon leaving the orifice, they cause the jet to contract. The area of the jet of fluid goes on decreasing. At this section, the streamlines are straight and parallel to each other. This section is called venacontracta (section c-c). Beyond this section, the jet diverges and is attracted in the downstream direction by the gravity.



The steady state Bernoulli equation predicts that the horizontal jet velocity leaving the orifice at the vena contracta is:

$$u = \sqrt{2gh_{cl}} \tag{2.5}$$

Where, g is the gravitational acceleration and  $h_{cl}$  is the water elevation above the center of the orifice. With energy losses present, the discharge velocity is modified by a velocity coefficient  $C_v$ :

$$u = C_v \sqrt{2gh_{cl}} \tag{2.6}$$

If the jet drops as a body in free fall, elementary mechanics tells us that the jet will travel a horizontal distance

$$x = ut (2.7)$$

at time t, and will over that time have fallen a vertical distance

$$y = \frac{1}{2}gt^2 {(2.8)}$$

Hence the trajectory is a parabola. Substituting Equation 2.6 for u and eliminating t, from equation 2.7, an equation for  $C_v$  is arrived in the form

(2.9)

Where, x and y are the horizontal and vertical coordinates of jet profile from orifice,  $C_v = \text{coefficient of velocity}$  and  $h_{cl} = \text{centreline head}$ .

Large orifices of rectangular shapes are generally used in dams to pass surplus water from upstream to downstream. The coefficient of discharge, coefficient of velocity and coefficient of contraction are the three important hydraulic coefficients to be considered in analysis of flow through orifice. Most of the literature reported the value of the coefficient of velocity as 0.98 to 0.99. Judd and King (1908) conducted the experiments to determine  $C_v$  and obtained the value more than 0.99995. Their experimental setup was very small (maximum head up to 30 m and the orifice diameter was varying from 0.075 to 2.5 inches). However, the size of orifice on most of the orifice spillway projects varies from 8 m to 22 m and the maximum head goes up to 60 m. Due to this high variation, it is necessary to calculate the coefficient of velocity for various combinations of heads and size of a large sharp edged orifice.

Lienhard (V) and Lienhard (IV) (1984) calculated velocity coefficients for free jets from sharp-edged orifice. Gill (1987) studied flow through short square side orifice in two conditions i.e. open channel and pressure flow. Montes (1997) and Shammaa et al. (2005) adopted potential flow theory to investigate the flow patterns behind sluice gates and orifices. Chanson et al. (2002) investigated the unsteady flow pattern upstream of orifices and discharge capacity of a large rectangular orifice using an experimental study. Bryant et al. (2008) investigated the flow upstream of orifices. The discharge characteristics of sharp crested circular and rectangular side orifices have been identified using analytical and experimental by Hussain et al. (2010) and Hussain et al. (2011). Several attempts have been made to study coefficient of discharge, coefficient of velocity and flow upstream of orifices. However, little efforts have been made to study the lower as well as upper nappe profiles of jet through large orifices to use it as spillway.

The bottom profile of the orifice spillway is expressed in the form of  $x^2=kh_{cl}y$  (Khatsuria, 2004), where k is the important factor in fixing the bottom profile of the spillway.

From equation 2.9, it can be seen that the k value is directly related to the coefficient of velocity i.e.  $k = 4C_v^2$ . In general, the  $C_v$  was considered as 1 and hence the equation becomes  $x^2$ =4h<sub>cl</sub>y is being used for estimating the trajectory of the jet issuing from the orifice. One of the major objectives in the present research is to find out the value of the parameter k corresponding to the coefficient of velocity calculated for different heads and heights of orifice openings and fix the bottom profile of an orifice spillway. The basic theory of orifice has been used to finalise the bottom profile of an orifice spillway. Dimensional analysis has been carried out for determining the significance of the parameters considered in the design of an orifice spillway.

# 2.4 Methods of Dimensional Analysis

Dimensional analysis is a mathematical technique in which dimensions of a physical quantity are expressed in terms of fundamental dimensions mass (M), length (L) and time (T). It provides some basic information about the investigated phenomenon on the assumption that it can be expressed by a dimensionally correct equation containing the variables influencing it(Tropea et al., 2007). Two conventional and related methods of dimensional analysis are of the greatest importance in hydraulics-Rayleigh's method and Buckingham's method (Π theorem) (Novak et al., 2010).

The Rayleigh's method becomes more laborious if the numbers of variables in physical phenomena are more than the number of fundamental dimensions. This difficulty is overcome by using Buckingham's  $\Pi$  method, which states that "If there are 'n' variables (independent and dependent variables) in a physical phenomenon and if these variables contains 'm' fundamental dimensions, then the variables are arranged into (n-m) dimensionless terms. Each term is called  $\Pi$  term".

Let  $A_1$ ,  $A_2$ ,  $A_3$ ... $A_n$  be the quantities involved, such as pressure, viscosity, velocity, etc. All the quantities are known to be essential to the solution, and hence some functional relation must exist:

$$f(A_1, A_2, A_3...A_n) = 0$$
 (2.10)

If  $\Pi_1$ ,  $\Pi_2$ ,  $\Pi_3$ ,.... $\Pi_n$  represent dimensionless groupings of the quantities  $A_1$ ,  $A_2$ ,  $A_3$ ... $A_n$ , then with m dimensions involved, an equation of the form exists:

$$f(\Pi_1, \Pi_2, \Pi_3 \dots \Pi_{n-m}) = 0$$
 (2.11)

The method of determining the number of  $\Pi$  parameters is to select m of the A quantities, with different dimensions, that contain among them the m dimensions, and to use them as repeating variables together with one of the other A quantities for each  $\Pi$ .

For example, let  $A_1$ ,  $A_2$ ,  $A_3$  contain M, L and T, not necessarily in each one, but collectively. Then the  $\Pi$  parameter is defined as

$$\Pi_1 = A_1^{a_1} A_2^{b_1} A_3^{c_1} A_4 \tag{2.12}$$

$$\Pi_2 = A_1^{a_2} A_2^{b_2} A_3^{c_2} A_5 \tag{2.13}$$

$$\Pi_{n-m} = A_1^{a_{n-m}} A_2^{b_{n-m}} A_3^{c_{n-m}} A_n \tag{2.14}$$

In these equations the exponents are to be determined so that each  $\Pi$  is dimensionless. The dimensions of the A quantities are substituted, and the exponents of M, L, and T are set equal to zero respectively. These produce three equations in three unknowns for each  $\Pi$  parameter, so that a, b, c exponents can be determined and hence the  $\Pi$  parameter. The Buckingham  $\Pi$  theorem has been adopted in the present study to understand the dimensional analysis of the orifice spillway flows.

# 2.5 Dimensional Analysis of Orifice Spillway Geometry

The Buckingham  $\Pi$  theorem has been adopted in the present study to understand the dimensional analysis of the spillway flows. The basic relevant parameters needed for any dimensional analysis may be grouped into the following categories (Chanson, 1999).

- (a) Fluid properties and physical constants
- (b) Channel (or flow) geometry
- (c) Flow properties

The flow through an orifice spillway is characterized by various hydraulic parameters such as density  $\rho$  (Kg/m³), dynamic viscosity  $\mu$  (N.s/m²), surface tension  $\sigma$  (N/m), acceleration due to gravity g (m/s²), velocity of flow V (m/s), head over the crest  $h_d$  (m) or depth of flow I (m), horizontal coordinates of the spillway bottom profile x(m), vertical coordinates of the spillway bottom profile from crest of orifice y (m), height of orifice opening d (m), width of orifice opening w (m), horizontal coordinates of the roof profile  $x_I$  (m) and vertical coordinates of the roof profile from the top of orifice opening  $y_I$  (m). Taking into account all the above parameters, the dimensional analysis yields

$$f(V, g, \mu, \rho, \sigma, h_d, x, y, d, w, x_l, y_l) = 0$$
 (2.15)

As there are three dimensions involved, three repeating variables V,  $\rho$  and l are selected. As per Buckingham  $\Pi$  theorem, this leads to ten  $\Pi$  parameters as listed below.

$$\prod_{1} = V^{a_{1}}, h_{d}^{b_{1}}, \rho^{a_{1}}, g \tag{2.16}$$

$$\prod_{2} = V^{\nu_{2}}, h_{d}^{\nu_{2}}, \rho^{\rho_{2}}, \mu \tag{2.17}$$

$$\Pi_{\underline{j}} = V^{i_{3}}, h_{\underline{i}}^{b_{3}}, \rho^{c_{3}}, \sigma \tag{2.18}$$

$$\Pi_{\underline{A}} = V^{a_{\underline{A}}} h_{\underline{A}}^{b_{\underline{A}}} \rho^{c_{\underline{A}}}, x \tag{2.19}$$

$$\Pi_{\varsigma} = V^{u_{\varsigma}}, h_d^{b_{\varsigma}}, \rho^{c_{\varsigma}}, y \tag{2.20}$$

$$\Pi_{6} = V^{a_{7}}, h_{d}^{b_{7}}, \rho^{c_{7}}, d \tag{2.21}$$

$$\Pi_{7} = V^{a_{8}}, h_{d}^{b_{8}}, \rho^{c_{8}}, w \tag{2.22}$$

$$\Pi_{o} = V^{a_{0}}, h_{d}^{b_{0}}, \rho^{c_{0}}, x_{1} \tag{2.23}$$

$$\Pi_{0} = V^{a_{10}}, h_{d}^{b_{10}}, \rho^{a_{10}}, y_{1} \tag{2.24}$$

From the detailed Buckingham  $\Pi$  theorem analysis, it is found that the values are:

$$\Pi_1 = \frac{gl}{V^2} \tag{2.25}$$

$$\Pi_2 = \frac{\mu}{\rho V h_s} \tag{2.26}$$

$$\Pi_3 = \frac{\sigma}{\rho V^2 h_d} \tag{2.27}$$

$$\Pi_4 = \frac{h_d}{x} \tag{2.28}$$

$$\Pi_{5} = \frac{h_{s}}{v} \tag{2.29}$$

$$\Pi_6 = \frac{h_d}{d} \tag{2.30}$$

$$\Pi_7 = \frac{h_d}{w} \tag{2.31}$$

$$\Pi_8 = \frac{h_d}{x_1} \tag{2.32}$$

$$\Pi_9 = \frac{h_d}{y_1} \tag{2.33}$$

Rearranging all the parameters, the following equation has been obtained as a result of dimensionanalysis is of orifice spillway flows:

$$f\left(\frac{gl}{V^{2}}, \frac{\mu}{\rho Vl}, \frac{\sigma}{\rho V^{2}l}, \frac{h_{d}}{x}, \frac{h_{d}}{y}, \frac{h_{d}}{d}, \frac{h_{d}}{w}, \frac{h_{d}}{x_{1}}, \frac{h_{d}}{y_{1}}\right) = 0$$
 (2.34)

In the analysis,  $h_d$  and l denote the same meaning i.e. the depth of flow, but at different locations. Here,  $h_d$  is the depth of flow above the crest i.e. design head and l is the depth of flow at any section of spillway flow.

Based on the above analysis following dimensionless numbers have been found important:

• Froude number, 
$$Fr = \frac{V^2}{gl}$$
, (2.35)

• Reynolds number, 
$$Re = \frac{\rho Vl}{\mu}$$
, (2.36)

• Weber number, 
$$We = \frac{\rho V^2 l}{\sigma}$$
 (2.37)

It is convenient to invert some of the parameters and to take some square roots. This yields the following results of dimensional analysis of orifice spillway flows.

Hence 
$$f\left(Fr, \text{Re}, We, \frac{x}{h_d}, \frac{y}{h_d}, \frac{d}{h_d}, \frac{w}{h_d}, \frac{x_1}{h_d}, \frac{y_1}{h_d}\right) = 0$$
 (2.38)

However, in overflow type of spillway, width (w) of orifice, & height of the orifice (d), length of roof profile  $(x_I)$  and height of roof profile  $(y_I)$  are not considered. Hence, dimensional analysis for geometry of overflow spillway without breastwall yields:

$$f\left(Fr, \text{Re}, We, \frac{x}{h_d}, \frac{y}{h_d}, \frac{w}{h_d}\right) = 0$$
(2.39)

The above equations indicate that orifice spillway flow is governed by few more hydraulic parameters than the overflow spillway. Due to more parameters involved, the hydraulics of orifice spillway become complex in case of orifice spillway.

The coefficient of discharge is an important hydraulic parameter in determining the discharging capacity of any type of spillway. Dimensional analysis has been also carried out to investigate the effect of various hydraulic parameters on  $C_d$  of an orifice spillway. The Buckhingham  $\Pi$  theorem was adopted to understand the dimensional analysis of the orifice flows (Chanson, 1999). The  $C_d$  of an orifice spillway is influenced by density  $\rho$  (kg/m³), dynamic viscosity  $\mu$  (N.s/m²), acceleration due to gravity g (m/s²), velocity of flow V (m/s), width of span b (m), height of orifice d (m), centerline head over the crest  $h_{cl}$  (m), design head  $h_d$  (m) and height of spillway crest from upstream reservoir bed P (m). The functional relationship for  $C_d$  may be written as:

$$C_d = f_1(\rho, \mu, g, V, b, d, h_{cl}, h_{d}, P)$$
(2.40)

Taking  $\rho$ , V and  $h_{cl}$  as the repeating variables, the functional relationship for  $C_d$  in terms of non-dimensional parameters may thus be written as

$$C_d = f_2\left(\frac{h_{cl}}{h_d}, \frac{h_{cl}}{d}, \frac{h_{cl}}{p}, \frac{h_{cl}}{b}, \frac{\rho V d}{\mu}, \frac{V}{\sqrt{gd}}\right)$$
(2.41)

Where 
$$Re = \frac{\rho V d}{\mu}$$
 and  $Fr = \frac{V}{\sqrt{g d}}$  
$$C_d = \left(\frac{h_{cl}}{h_d}, \frac{h_{cl}}{d}, \frac{h_{cl}}{P}, \frac{h_{cl}}{b}, Re, Fr\right)$$
(2.42)

However, to study the effect of all these parameters and also to study their interaction physical model studies are necessary. The following section describes about the physical modelling and its similitude.

# 2.6 Necessity of Physical Modelling and Similitude

Physical modelling is widely used to investigate design and operational issues in hydraulic engineering. The model is a scaled replica of the actual structure. The actual structure is called prototype. An advantage of physical models is its potential capacity to replicate many features of a complicated flow situation. Physical model simulates actual complex prototype situations to provide specific information for design use or in a retrospective study of failures. The tests performed on the models can be utilized for obtaining, in advance, useful information about the performance of the prototypes if a complete similarity exists between the model and the prototype (USBR, 1980). Principle of similitude forms the basis of designing a model so that the model results can be converted to prototypes. The following three types of similarities have to be established between the model and the prototype.

#### Geometric similarity

Geometric similarity exists between the model and the prototype if the ratios of corresponding length dimensions in the model and prototype are equal. Such a ratio is defined as the scale ratio as follows (USBR, 1980):

Length scale ratio = 
$$L_r = \frac{L_p}{L_m}$$
 (2.43)

Area scale ratio = 
$$A_r = \frac{A_p}{A_m} = L_r^2$$
 (2.44)

Volume scale ratio = 
$$V_r = \frac{V_p}{V_m} = L_r^3$$
 (2.45)

In which subscript m and p correspond to model and prototype respectively.

#### Kinematic similarity

Kinematic similarity exists between the model and the prototype if the ratios of the velocity and acceleration at the corresponding points in the model and prototype are the same (USBR, 1980).

Time scale ratio = 
$$T_r = \frac{T_p}{T_m}$$
 (2.46)

Velocity scale ratio = 
$$V_r = \frac{V_p}{V_m} = \frac{L_r}{T_r}$$
 (2.47)

Acceleration scale ratio = 
$$A_r = \frac{A_p}{A_m} = \frac{L_r}{T_r^2}$$
 (2.48)

Discharge scale ratio = 
$$Q_r = \frac{Q_p}{Q_m} = \frac{L_r^3}{T_r}$$
 (2.49)

#### **Dynamic similarity**

Dynamic similarity exists between the model and the prototype if the ratios of all the forces acting at the corresponding points are equal (Warnock, 1950). In fluid flows, the forces acting may be one or a combination of (i) Inertia force Fi, (ii) Friction or viscous force Fv, (iii) Gravity force Fg, (iv) Pressure force Fp,(v) Elastic force Fe and (vi) Surface tension force Fs.

If complete similitude does not exist there will be some discrepancy between the results obtained from the model tests and those which will be indicated by prototype after its construction. This discrepancy or disturbing influence is called scale effects. Often it may not be possible to correctly simulate all the conditions in the model as that of the prototype.

Gravitational force is predominant in spillway flows. Similarity of geometric form and equality of Froude number are two mandatory requirements to produce a good approximation to dynamic similitude.

The Froude number is the ratio of inertia and gravity force and can be expressed as:

$$Fr = \frac{V^2}{gl} = \frac{V}{\sqrt{gd}} \tag{2.50}$$

Where V is the velocity, d is the depth of flow at the orifice and g is the acceleration due to gravity. Various model scales based on Froudian law are as follows (USBR, 1980):

Length, 
$$Lr = \frac{L_p}{L_m}$$
 (2.51)

Velocity, 
$$V_m = \frac{V_p}{\sqrt{L_r}}$$
 (2.52)

Pressure in metre of water head, 
$$P_r = \frac{L_p}{L_m}$$
 (2.53)

Discharge, 
$$Q_m = \frac{Q_p}{L_r^{2.5}}$$
 (2.54)

Time, 
$$T_m = \frac{T_p}{\sqrt{L_r}}$$
 (2.55)

Manning's 
$$n_m = \frac{n_p}{L_{...}^{1/6}}$$
 (2.56)

The Froude number is used generally for scaling free surface flows, open channels and hydraulic structures. The Froude law represents the condition of dynamic similarity for flow in the model and prototype governed by gravity and inertia force (Pfister and Hager, 2014). Other forces such as the frictional resistance of a viscous liquid, capillary forces and the forces of volumetric elasticity, either don't affect the flow or their effect may be neglected.

## 2.6.1 Scale effects in physical modelling

The first and most important step in the design is careful selection of a model scale. Small models may be used (scale 1:50 to 1:100) to study the approach flow conditions, discharging capacity, pressures over the crest profile of spillway, water profiles for assessing the height of training and divide walls, performance of energy dissipator, downstream flow conditions etc. Very small Froudian models should be avoided to ensure that viscous and surface tension forces do not distort the Froudian similarity. Scale effects arise due to forces which are more dominant in the model than in its prototype. This results in deviations between the up-scaled model and prototype observations. Scale effects can potentially result in an inappropriate design and failure of the prototype. Gravity is the predominant force in free surface flows such as flow over spillways, weirs, sluices, channels etc. Therefore, spillway models are based on Froude scaling. Care should be taken in selection of scale of model in such a way that Reynolds number should be sufficiently large to be in the fully turbulent flow regime (USBR, 1980, Pfister and Chanson, 2014). Since air-water flow and air discharges are not of much relevance, the effect of Weber number is taken care of by reproducing large enough model so that the flow depths over the crest are at least 75 mm for the design normal operating head, thus minimizing surface tension and viscous effect (USBR,1980).

Design head  $(h_d)$  and height of orifice opening (d) adopted on most of the orifice spillway projects constructed so far are in the range of 30 m to 70 m and 10 m to 20 m respectively. In the present study, the physical model was constructed with a scale of 1:50 to cover the entire range of  $h_d$  and d.

## 2.6.2 Construction methodology of physical model

A model need not be made of the same material as the prototype. If surfaces over which water flows are reproduced in geometrically similar shape and the roughness of the surface is approximately to scale, the model will usually be satisfactory. The spillway surface can be constructed in masonry with neat plaster and painted or may be fabricated in Perspex. Spillway piers in teak wood/ PVC sheets/ fibre reinforced plastic, radial gates in sheet metal. Sometimes the entire model is fabricated in transparent Perspex to observe the flow conditions, which is the most important parameter. Close tolerance, particularly in critical areas such as spillway crest profile are essential. Greatest accuracy should be maintained where there is rapid changes in direction of flow and very high velocities. Piezometers are embedded in the spillway surface to observe the hydrostatic pressures.

Spillway models can be classified either as two dimensional sectional model built in a glass sided flume or three dimensional comprehensive model constructed in a model tray incorporating entire spillway, non-overflow dam, part of reservoir and river downstream including other structures such as power intakes etc. The sectional model usually built to a large size and incorporating fewer spans to analyse spillway flows. A 1:50 scale model for the orifice spillway incorporating one full span is built in a flume at CWPRS, Pune for the present study.

Once the model is ready for experimentation, the operating program of the model is carefully planned to evaluate the performance of the proposed design. The operating program can be divided into two phases:

- 1. Adjustment phase
- 2. Experimental phase

The adjustment phase includes preliminary trials to identify model defects and inadequacies. The need for partial redesign, revision or shifting of measuring instruments is often indicated by these trials. Making the model leak proof which operates under high head and discharge is a job in itself and needs time and patience.

The experimental phase includes regular model studies after removing all the defects observed during the adjustment phase. The discharge on the physical models of spillways is measured on the Rehbock weir using hook gauge of 0.1 mm least count in a stilling well. The accuracy of the discharge measurement would be around  $\pm 2\%$ . Reservoir Water levels are measured using pointer gauges fitted with a vernier scale having a least count of 0.1 mm. Reservoir water levels are measured at least 10 times upstream from the crest axis of the spillway to ensure that they are not affected by the draw down effect. Piezometers of 4 mm internal diameter are provided on the spillway surface along the centre of span for measurement of hydrostatic pressures. Pressures are measured using the piezometer board with plastic tube vented to the atmosphere.

Traditionally, reduced scale physical spillway models are used to study spillway hydraulic performance. In recent years, numerical modelling is extensively being used to investigate hydraulic performance of spillways. Need of CFD modelling is discussed in following section.

# 2.7 Need of CFD Modelling

Physical modelling is the proven standard or tool for modelling hydraulic structures and has successfully been used for decades. The drawback of physical model studies of spillways are cost of construction, delayin time for fabrication and construction of model parts, conducting the experiments and difficulties in changing structural details of various components of spillway while doing parametric studies. From the 1960s onwards the aerospace industry has integrated CFD techniques into the design, R &D and manufacture of aircraft and jet engines. Nowadays, this technique has been used in various hydraulic applications. The technique is very powerful and spans a wide range of industrial and non-industrial application areas. There are several unique advantages of CFD over the experiment-based approaches to fluid system design.

- Substantial reduction of lead times and costs of new designs and modification of the existing design
- Ability to study systems where controlled experiments are difficult or impossible to perform (e.g. very large systems)
- Ability to study systems under hazardous conditions at and beyond their normal performance limits (e.g. safety study and accident scenarios)
- Practically unlimited level of detail of results

Composite modelling is defined as the integrated use of physical and numerical models for the design and rehabilitation of hydraulic structures. It may be used to enhance the design and analysis process. Composite modelling is extremely valuable because both physical modelling and numerical modelling each have limitations that can restrict their use independently. In the present study, composite modelling (physical and numerical modelling) was used to analyse the orifice flow.

# 2.8 Theoretical Background of Computational Fluid Dynamics

Computational Fluid Dynamics or CFD uses numerical methods and algorithms to solve and analyze problems that involve fluid flows. The foundation on which CFD is built is the Navier-Stokes equations, the set of partial differential equations that describe fluid flow. With CFD, the area of interest is subdivided into a large number of cells or control volumes. In each of these cells, the Navier-Stokes partial differential equations can be rewritten as

algebraic equations that relate the velocity, temperature and pressure. The resulting set of equations can then be solved iteratively, yielding a complete description of the flow throughout the domain. By solving the fundamental equations governing fluid flow processes, CFD provides information on important flow characteristics such as pressure loss, flow distribution and mixing rates. The basic equations for fluid flow are based on the law of mass, momentum and energy. The equations for conservation of mass (continuity) equation and momentum equations are described in following sections.

## 2.8.1 Continuity equation

The equation for conservation of mass, or continuity equation, can be written as follows:

$$\frac{\partial \rho}{\partial t} + \nabla \cdot \left( \rho \vec{v} \right) = S_m \tag{2.57}$$

Equation 2.57 is the general form of the mass conservation equation and is valid for incompressible as well as compressible flows. The source  $S_m$  is mass added to the continuous phase from the dispersed second phase and any user-defined sources,  $\rho$  is the fluid density and v is the fluid velocity.

## 2.8.2 Momentum equation

Conservation of momentum in an inertial (non-accelerating) reference frame is described as:

$$\frac{\partial}{\partial t}(\rho \vec{v}) + \nabla \cdot (\rho \vec{v} \vec{v}) = -\nabla p + \nabla \cdot (\vec{\tau}) + \rho \vec{g} + \vec{F}$$
(2.58)

Where p is the static pressure,  $\vec{\tau}$  is the stress tensor and  $\rho \vec{g}$  and  $\vec{F}$  are the gravitational body force and external body forces (e.g. that arise from interaction with the dispersed phase), respectively. The stress tensor  $\vec{\tau}$  is given by

$$\vec{\tau} = \mu \left[ \left( \nabla \vec{v} + \nabla \vec{v}^T \right) - \frac{2}{3} \nabla \vec{v} \vec{I} \right]$$
(2.59)

Where  $\mu$  is the molecular viscosity, I is the unit tensor and the second term on the right hand side is the effect of volume dilation.

There are various numerical methods which are used in Computational Fluid Dynamics analysis. The following sections gives the brief summary of the important terms used in CFD such as numerical methods, boundary conditions, turbulence models ,volume of fluid model for air and water two phase flow, verification and validation, grid convergence. CFD software FLUENT used in the study is discussed in detail.

## 2.9 Numerical Methods

There are three distinct streams of numerical solution techniques finite difference, finite element and finite volume methods. The numerical methods that form the basis of the solver perform the following steps (Versteeg and Malalasekera, 1995):

- Approximation of the unknown flow variables by means of simple functions.
- Discretization by substitution of the approximations into the governing flow equations and subsequent mathematical manipulations.
- Solution of the algebraic equations.

The main differences between the three separate streams are associated with the way in which the flow variables are approximated and with the discretization processes. Various codes of CFD uses a control-volume-based technique to convert the governing equations to algebraic equations that can be solved numerically. This control volume technique consists of integrating the governing equations abouteach control volume, yielding discrete equations that conserve each quantity on a control-volume basis. Discretization of the governing equations can be illustrated as follows:

$$\frac{\partial}{\partial t} \int_{\mathcal{V}} \rho \emptyset dV + \oint_{A} \rho \emptyset V. dA = \oint_{A} \Gamma_{\phi} \nabla_{\emptyset}. dA + \int_{V} s_{\emptyset} dV$$
 (2.60)

Where,

 $\rho$  = density

v = velocity vector

A = surface area vector

 $\Gamma_{\varphi}$  = diffusion coefficient for  $\emptyset$ 

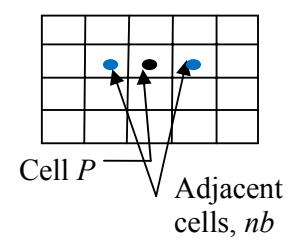
 $\nabla_{\omega}$  = gradient of  $\emptyset$ 

 $S_{\omega}$  = source of Ø per unit volume

Equation 2.60 is applied to each control volume, or cell, in the computational domain. Each transport equation is discretized into algebraic form. For corresponding figure, the equation is written as

$$\frac{(\rho\phi_p)^{t+\Delta t} - (\rho\phi_p)^t}{\Delta t} \Delta V + \sum_{faces} \rho_f \, \emptyset_f V_f A_f = \sum_{faces} \Gamma_f (\nabla \emptyset)_n \, A_f + s_\emptyset \Delta V \tag{2.61}$$

 $N_{faces}$ = number of faces enclosing cell  $\emptyset_f$  = value of  $\emptyset$  convected through face  $\rho_f V_f A_f$  = mass flux through the face  $A_f$  = area of face ( $\nabla \phi$ )n = magnitude of  $\nabla \phi$  normal to face V = cell volume



FLUENT stores discrete values of the scalar  $\varphi$  at the cell centers. However face values  $\varphi_{\text{f}}$  are required for convection terms in equation 2.61 and must be interpolated from the cell centervalues. This is accomplished using an upwind scheme. Unwinding means that the face value  $\varphi_{f}$  is derived from quantities in the cell upstream or "upwind," relative to the direction of the normal velocity in Equation 2.61. FLUENT allows you to choose from several upwind schemes: first-order upwind, second-order upwind, power law, and QUICK. The diffusion terms in Equation 2.61 are central-differenced and are always second-order accurate. For simulations using the VOF multiphase model, upwind schemes are generally unsuitable for interface tracking because of their overly diffusive nature. Central differencing schemes, while generally able to retain the sharpness of the interface, are unbounded and often give unphysical results. In order to overcome these deficiencies, FLUENT uses a modified version of the High Resolution Interface Capturing (HRIC) scheme. The modified HRIC scheme is a composite NVD scheme that consists of a non-linear blend of upwind and downwind differencing. In the present study, modified HRIC scheme is used for the simulation. Interpolation schemes for calculating cell - face pressures using segregated solver in FLUENT are i) Standard, ii) Presto, iii) Linear, iv) Second order and v) Body force weighted. In the present study 'Body force weighted scheme' is used as gravity force is predominant in the spillway flows. However, 'Simple' scheme is used for pressure velocity coupling.

The discretized scalar transport equation (Equation 2.61) contains the unknown scalar variable  $\varphi$  at the cell center as well as the unknown values in surrounding neighbour cells. This equation will, in general, be non-linear with respect to these variables. A linearized form of Equation 2.61 can be written as

$$a_n \emptyset = \sum_{nh} a_{nh} \emptyset_{nh} + b \tag{2.62}$$

Where, the subscript nb refers to neighbour cells, and  $a_p$  and  $a_{nb}$  are the linearized coefficients for  $\varphi$  and  $\varphi_{nb}$ .

The number of neighbours for each cell depends on the grid topology, but will typically equal the number of faces enclosing the cell (boundary cells being the exception). Similar equations can be written for each cell in the grid. This results in a set of algebraic equations with a sparse coefficient matrix. For scalar equations, FLUENT solves this linear system using a

point implicit (Gauss-Seidel) linear equation solver in conjunction with an algebraic multigrid (AMG) method (FLUENT, 2006).

# 2.10 Boundary Conditions/Initial conditions/Operating conditions

An important initial concept for CFD analysis is that of boundary conditions. Each of the dependent variable equations requires meaningful values at the boundary of the calculation domain in order for the calculations to generate meaningful values throughout the domain. These values are known as boundary conditions and can be specified in a number of ways. All CFD problems are defined in terms of initial and boundary conditions. When solving the Navier-Stokes equation and continuity equation, appropriate initial and boundary conditions need to be applied. The main boundary conditions in the discretized equations of the finite volume method are inlet, outlet, wall, prescribed pressure, symmetry and periodicity or cyclic boundary condition. Before starting the solution, an initial guess has to be provided for the solution flow field. An accurately assumed velocity and free surface profile will accelerate the convergence of the computations. Following information is required for initializing the calculation:

- 1. Geometrical information of all the grid points was specified as gauge pressure and all the three velocity components as zero.
- 2. Initial upstream reservoir water level
- 3. Patch values or functions for selected flow variables in selected cell zones. In the present case the water phase from reservoir bottom to the required level for which simulation is required to be run was patched. The x, y and z coordinates of the two diagonal points in the reservoir viz. bottom level and reservoir water levels were defined
- 4. Number of time steps of 5000 was input with a time step size of 0.001 seconds, until steady state solution is reached. Maximum iterations per time step were 30.

Operating pressure was defined as 101325 Pascal i.e. the atmospheric pressure. The option of gravity was chosen as the flow was open channel flow. The gravitational acceleration was input as  $9.81 \text{ m/s}^2$  in y direction. The operating density was specified as  $1.223 \text{ m}^3/\text{s}$ , as air was the primary phase.

# 2.11 Turbulence Modelling

A turbulence model is computational procedure to close the system of mean flow equations (continuity, Reynolds equations and scalar transport equations) so that a more or less wide

variety of flow problems can be calculated. Whenever turbulence is present in a certain flow it appears to be the dominant over all other flow phenomena. That is why successful modelling of turbulence greatly increases the quality of numerical simulations. One of the main characteristics of turbulent flow is fluctuating velocity fields. These fluctuations cause mixing of transported quantities like momentum, energy and species concentration and thereby also fluctuations in the transported quantities. Because of the small scales and high frequencies of the fluctuations they are too computationally expensive to simulate directly in practical engineering situations. Instead, the instantaneous governing equations are time-averaged to remove the small scales and the result is a set of less expensive equations containing additional unknown variables. These unknown (turbulence) variables are determined in terms of modelled variables in turbulence models. For turbulent flow, the range of length scales and complexity of phenomena makes most approaches impossible. The chief difficulty in modelling turbulent flows comes from the wide range of length and time scales associated with turbulent flow. The more turbulent scales that are resolved, the finer the resolution of the simulation, and therefore the higher the computational cost. There are three major approaches topredict turbulent flows, viz. Statistical Turbulence Modelling (STM), Large Eddy Simulation (LES) and Direct Numerical Simulation (DNS). Statistical turbulence models based on the Reynolds-Averaged Navier-Stokes (RANS) equations represent transport equations for themean flow quantities only, with all the scales of the turbulence being modelled. There are many turbulence models available in CFD software FLUENT as listed below:

- Spalart- Allmaras
- $k-\varepsilon$  model (Standard, Renormalization-group (RNG) model & Realizable)
- *k*-ω models (Standard, Shear-Stress Transport (SST))
- $v^2$ -f model
- Reynolds Stress model (RSM)
- Detached eddy simulation
- Large eddy simulations

Qian et al. (2009) used various turbulence models such as Realizable k- $\varepsilon$ , SST k- $\omega$ ,  $v^2$ -f and LES modelto analyse the flow overthe stepped spillway in respect of different hydraulic aspects. However, Realizable k- $\varepsilon$  was found more efficient in simulating the flow over the spillway. Tadayon and Ramamurthy (2009) made comparative study of three different turbulence models (RSM, RNG k- $\varepsilon$  and standard k- $\varepsilon$ ) to analyse the characteristics of the flow over circular spillways. However, RSM simulation results agree well with the experimental data in respect of water surface profiles and velocity and pressure distribution at the crest. Various researchers such as Olsen and Kjellesvig (1998), Chen et al. (2002), Deng et al. (2005), Cheng et al. (2006), Bhosekar (2011), Jothiprakash et al. (2015) used different k -  $\varepsilon$  turbulence models for modelling the spillways flows and found satisfactory results. There is no specific guideline available for selection of turbulence model.

In the present study, a sensitivity analysis of the turbulence model has been carried out for modelling the flow through orifice. The k- $\varepsilon$  (Standard, Renormalization group (RNG) and Realizable) and k- $\omega$  turbulence models were used for flow simulation as these are more sophisticated and widely used models in various applications (Mao et al., 2006, Cheng et al., 2006).

## 2.12 Volume of Fluid Model for Air-water Two-Phase Flow

Free surface flows are more complex than closed conduit flows. The reason is that the freesurface is a dependent variable so that various streamline curvatures can create widely variable pressure distributions over the cross section. Rapidly varied flow such as flow overspillway having large streamline curves exerts non-hydrostatic pressure distribution over thesection. It is important to track the free surface accurately to solve the flow numerically overthe spillway. Tracking involves, locating the surface, defining the surface as a sharp interfacebetween the water and air and applying the boundary condition at the interface. There are different means for tracking the free-surface boundary condition. Volume of Fluid (VOF) isone of them and used in the present study. The volume of fluid (VOF) model was proposed by Hirt and Nichols (1981). It was designed for two or more immiscible fluids where the position of the interface between the fluids is of interest. The VOF model is based upon multiphase flow theory. But it is not a multi-fluid model, and the simple single fluid model is introduced in the VOF model. Therefore, as for the gas and water flow field, a single set of momentum equations is shared by gas and water, and the volume fraction of each of the fluids in each computational cell is tracked throughout the domain. In each cell, the sum of the volume fractions of air and water is unity. The tracking of the interface between air and water is accomplished by the solution of the continuity equation with the following form:

$$\frac{\partial \alpha_w}{\partial t} + u_i \frac{\partial \alpha_w}{\partial x_i} = 0 \tag{2.63}$$

The value of  $\alpha_w$  in a cell represents the fractional volume of the cell occupied by water. In particular, a unit value of  $\alpha_w$  will correspond to a cell full of water, while  $\alpha_w = 0$  will indicate that the cell is full of air. Cells with  $\alpha_w$  values between 0 and 1 must contain a free surface. Thus, the coarse interface information can be known according to the value of  $\alpha_w$ . In the VOF model, because water and air phases share the same velocity and pressure field, the single set of equations can describe the flow field of the air-water two-phase flow such as a single-phase flow. If  $\alpha_w$  denotes the volume fraction of water, then the volume fraction of air  $\alpha_a$  can be given as

$$\alpha_a = 1 - \alpha_w \tag{2.64}$$

As long as the volume fraction of air and water is known at each location, the fields for all variables and properties are shared by air and water and represent volume-averaged values. Thus, the variables and properties in any given cell are either purely representative of water or air, or representative of a mixture of them, depending upon the volume fraction values.

## 2.13 Verification and Validation of CFD Models

Verification and validation are the primary steps for building and quantifying the confidence between modelling and simulation. Verification is the assessment of the accuracy of the solution to a computational model. Validation is the assessment of the accuracy of a computational simulation by comparison with experimental data. Validation is defined as the process of determining the degree to which a model is an accurate representation of the real world from the perspective of the intended uses of the model. Validation of CFD code is an essential element of the code development process. Validation of the entire code is not possible. It is possible for a specific range of applications for which there is experimental data. The strategy is to identify and quantify error and uncertainty through comparison of simulation results with experimental data. The experiment data sets themselves will contain bias errors and random errors which must be properly quantified and documented as part of the data set. Validation Assessment Process involves:

- 1. Examine Iterative Convergence
- 2. Examine Consistency
- 3. Examine Spatial (Grid) Convergence
- 4. Examine Temporal Convergence
- 5. Compare CFD Results to Experimental Data
- 6. Examine Model Uncertainties

Experimental data is the observation of the "real world" in some controlled manner. Validation procedure does not imply that the experimental data is always correct. Experimental uncertainty estimates may be very large and unknown bias errors can exist in the experimental data. This is usually related to the complexity of the experiment. Hence, the results of numerical model sometimes does not compare well with experimental data. The physical models in the CFD code contain uncertainties due to a lack of complete understanding or knowledge of the physical processes. One of the models with the most uncertainty is the turbulence models. The uncertainty can be examined by running a number of simulations with various turbulence models and examine the aspect of the results.

The grid convergence study is an important step in conducting CFD analysis. It is carried out by reducing the grid spacing and examines its effect on the predicted outcome. It is

usual to find that as the cell size is reduced the results converge. Thus, further reducing the cell size has virtually no effect on the results produced and the result are known as grid-independent result. The guidelines for grid convergence study given by the American Society of Mechanical Engineers (ASME) editorial policy statement (Freitas, 1993) are discussed below.

# 2.14 Grid Convergence

Systematic grid-convergence studies are the most common; most straightforward and arguably constitute the most reliable technique for the quantification of numerical uncertainty (Roache, 1997). The GCI (Grid Convergence Index) method used herein is the most widely used and universally accepted & recommended method that has been evaluated over several hundred CFD cases (Richardson and Gaunt, 1927, Roache, 1993, Broadhead et al., 2004, Eçaet al., 2007, Ferziger and Peric, 1996). The GCI was originally proposed by Roache (1994, 1997, and 1998) as a general method for reporting the sensitivity of model solutions to numerical discretization. Roache defined the GCI as a scale to evaluate how far the solution is from the asymptotic value and highlighted that a small value of GCI is an indication that the numerical uncertainty due to the discretization error is negligible. This method is based on the generalized Richardson Extrapolation involving comparison of discrete solutions. In order to perform the GCI test, three different grids spacing,  $h_1$ ,  $h_2$ , and  $h_3$  yielding three solutions  $f_1$ ,  $f_2$ , and  $f_3$  for the fine, medium and coarse mesh resolutions are required. A fine-grid Richardson error estimator approximates the error in a fine-grid solution  $f_1$ , by comparing this solution to that of coarse grid  $f_2$ , and is defined as

$$E_1^{Fine} = \frac{\varphi}{\left(1 - r^p\right)} \tag{2.66}$$

Where,  $\varphi = f_2 - f_1$ ,  $f_2$  is a coarse-grid numerical solution obtained with grid spacing  $h_2$ ,  $f_1$  is a fine-grid numerical solution obtained with grid spacing  $h_1$ , r is a refinement factor between the coarse and fine grid and p is order of accuracy. Practical experience (Roache, 1998) has shown that grid refinement ratios need only be greater than 1.1 e.g.  $r = h_2/h_1 > 1.1$  to obtain good results using GCI.

If the grid refinement is performed with constant r, then the order can be extracted directly from three grid solutions.

$$p = \frac{\ln(\phi_{32} / \phi_{21})}{\ln(r)} \tag{2.67}$$

But, if r is not restricted to constant, the order can be calculated using the expression

$$p = \frac{1}{\ln(r_{21})} \ln \left| \frac{\phi_{32}}{\phi_{21}} + q(p) \right|$$
 (2.68)

(2.69)

where  $\phi_{21}=f_2$  -  $f_1$ ,  $\phi_{32}=f_3$  -  $f_2$ ,  $r_{21}=h_2/h_1$ ,  $r_{32}=h_3/h_2$  and s=1.sign ( $\phi_{32}/\phi_{21}$ ), with subscript 1 indicating finest grid in present notations. The approximate relative error can be calculated as

$$e_{21} = \left| \frac{f_1 - f_2}{f_1} \right| \tag{2.70}$$

The GCI is defined with a safety factor for fine and coarse grids as

$$GCI_{I}^{Fine} = F_{s} |E_{I}| \tag{2.71}$$

 $GC1_2^{Coarse} = F_s |E_2| \tag{2.72}$ 

Where  $F_s$  is a safety factor.

However, for performed grid convergence studies using three or more grid solutions, a modest value of Fs= 1.25 was recommended (Roache, 1997). The relative grid convergence index with a safety factor defined by (Roache, 1994) is as follows:

$$GCI_{fine} = \frac{1.25e_{21}}{r^{p} - 1} \tag{2.73}$$

Roache (1994) suggests a grid convergence index GCI to provide a consistent manner in reporting the results of grid convergence studies and perhaps provide an error band on the grid convergence of the solution. The GCI can be computed using two levels of grid; however, three levels are recommended in order to accurately estimate the order of convergence and to check that the solutions are within the asymptotic range of convergence. It indicates an error band on how far the solution is from the asymptotic value. It indicates how much the solution would change with a further refinement of the grid. A small value of GCI indicates that the computation is within the asymptotic range.

After this grid independence study, exercise can be conducted for varying time step forthe same cell size. There is usually a maximum allowable time-step  $\Delta t$  max beyond which thenumerical scheme is unstable. If  $\Delta t \geq \Delta t$  max, the numerical errors will grow exponentially intime, causing the solution to diverge from the steady-state result. A time step below which the solution does not change can be defined as time convergence. This may vary from case to case, depending on the type of problem under consideration. No specific recommendation is reported in the literature in this regard.

# 2.15 Computational Fluid Dynamic Software FLUENT

There are various codes are available in CFD software. Few of them are STAR CD, FLOW 3D and FLUENT. In the present study, a CFD code FLUENT was used for numerical simulation. FLUENT is multi-purpose computer software for modelling fluid flow, heat transfer and chemical reaction, which enables a rapid analysis of complex flows. FLUENT applies computer simulation methods to analyse and solve practical design problems based on fundamental principles of Computational Fluid Dynamics (CFD) such as the conservation of mass, momentum and energy. It has the advantage over conventional physical modelling approach to ensuring that both Froude and Reynolds similarities can be met. FLUENT is the world leading CFD code for a wide range of flow modelling applications. It has an extensive range of physical modelling and multi-physics capabilities. FLUENT also allows refining or coarsening the grid based on the flow solution. FLUENT is written in the 'C' computer language and makes full use of the flexibility and power offered by the language. It solves the conservative form of the Navier-Stokes equations using the finite volume method on an unstructured, non-orthogonal, curvilinear coordinate grid system. Turbulent flows can be simulated in FLUENT using the Spalart- All-maras model, k-ε model, k-ω model, v<sup>2</sup>f model, Reynolds stress model (RSM), Detached eddy simulation (DES) model and Large eddy simulation model (LES). The solver has a multiple choice of discretization and pressurevelocity coupling methods. The model solves free-surface problems using a VOF method for two fluids. The code has been verified on a variety of applications from aerospace, mechanical, and chemical engineering. A large selection of boundary conditions is also available to properly model each specific application.

Gambit is the pre-processor provided in the CFD software package, FLUENT, for building geometries and generating meshes. The GAMBIT software package is designed to help analysts and designers to build and mesh models for computational fluid dynamics (CFD) and other scientific applications. GAMBIT receives user input primarily by means of its graphical user interface (GUI). The GAMBIT GUI makes the basic steps of building and meshing a model simple and intuitive, yet it is versatile enough to accommodate a wide range of modelling applications. GAMBIT has a single interface for geometry creation and meshing that brings together all FLUENT pre-processing technologies in one environment for parametric studies. Gambit's mesh options include both structured and unstructured meshes in two and three dimensions, as well as tools for checking the mesh quality. Once the grid is generated in Gambit software, it is then exported to FLUENT solver. The procedure adopted in FLUENT software is:

- Create the model geometry and grid
- Start the appropriate solver for 2D or 3D modelling
- Import the grid
- Check the grid

- Select the solver formulation
- Choose the basic equations to be solved
- Specify material properties
- Specify the boundary conditions
- Adjust the solution control parameters.
- Initialize the flow field
- Calculate a solution
- Examine the result
- Save the results

If necessary, refine the grid or consider revisions to the numerical or physical model. Post processing was then carried out for extracting information in different forms from the solution.

# 2.16 Post Processing

Post processing is an important step in CFD for extracting information in different forms from the solution. It pertains to examining the following aspects:

- Visualization tools such as phase diagrams, velocity and pressure contours were used to findout:
  - The overall flow pattern
  - Separation if any
  - Checking for key flow features being resolved
- Numerical reporting tools were used to calculate the following quantitative results:
  - Display grid, rotate and view it
  - Creating Iso surfaces
  - Contours of different quantities such as pressure, velocity and phases
  - Velocity Vectors
  - XY Plots were used for displaying the pressure, water surface and velocityprofile

# Chapter 3 Contribution of CWPRS in evolving the design of orifice spillway

## 3.1 General

United State Bureau of Reclamation (USBR) and U. S. Army Corps of Engineers (USACE) have standardized the design of overflow spillway with respect to various parameters. The characteristics of orifice spillway are entirely different than those of the overflow spillway. Many of the dams in India are constructed with the orifice type spillway. These spillways have been designed for heads (h<sub>d</sub>) in the range of 20 m to 65 m for height of orifice (d) ranging from 8 m to 22 m. The width of orifice/span is in the range of 6 m to 15 m. The recent trend in design of orifice spillway is keeping the crest as lower and near the river bed as possible from the consideration of flushing of sediment from reservoir. Central Water and Power Research Station (CWPRS), Pune, India has contributed to evolve the innovative designs of orifice spillway and carried out the hydraulic model studies for number of projects. Feedbacks from the prototype performance from these structures were also valued and were used in improving the subsequent designs. Table 3.1 shows details of orifice spillway projects studied at CWPRS, Pune, India. Data of model studies at CWPRS was analyzed in respect of discharging capacity, pressures over spillway bottom profile and roof profiles by developing non dimensional plots.

Model studies indicated that in most of the orifice spillway projects, the water surface profile passed through orifice does not follow the path of elliptical roof profile. During the regime of flow with high heads, flow separation takes place on the orifice roof profile resulting in reduced discharging capacity. It is found that there is no specific method available for its design with respect to the upstream head as well as other parameters. Extensive model studies were carried out at CWPRS for Tala, Punatsanghchhu-I, Pare, Kishanganga, Teesta, Mangdechhu etc. for studying this aspect. The design was finalized based on trial and error methods carried out on physical model. Hence, design of roof profile is also found to be an important aspect in achieving the maximum discharging capacity of orifice spillway. Based on this experience, a need was identified to evolve the design of bottom and roof profile for efficient use and operation orifice spillway.

Table 3.1 Details of orifice spillway (Bhosekar et al., 2014)

Sr. No.	Name of Project	Spillway Profiles			D	d	h <sub>d</sub>	P	Span		Design	C
		Upstream	Downstream	Roof Profile	( <b>m</b> )	( <b>m</b> )	( <b>m</b> )	( <b>m</b> )	Nos.	Width (m)	Discharge (m <sup>3</sup> /s)	$C_d$
1	Chamera – I	Combination of circular arcs of R=5.2 m and 13 m	$x^2 = 102y$	$\frac{x^2}{10^2} + \frac{y^2}{5^2} = 1$	17.8	12.8	32.5	110	8	10	20376	0.84
2	Chamera – III	Circular arcs of radius 26.27 m	$x^2 = 122 y$	$\frac{x^2}{7^2} + \frac{y^2}{3.5^2} = 1$	20	16.5	37	20	3	12.5	11400	0.78
3	Dhauliganga	Circular arcs of radius 6 m 1:1 slope reverse arc R = 4.8 m	$x^2 = 132 y$	$\frac{x^2}{4.5^2} + \frac{y^2}{2^2} = 1$	14	10	41.5	12	2	6	2560	0.80
4	Kurichu	$\frac{x^2}{4.5^2} + \frac{y^2}{2.5^2} = 1$	$x^2 = 80 y$	$\frac{x^2}{5.5^2} + \frac{y^2}{2^2} = 1$	16	14	28	26	5	10.5	12200	0.83
5	Nathpa Jhakri	Flat	$x^2 = 126 y$	$\frac{x^2}{8.5^2} + \frac{y^2}{2.833^2} = 1$	11.3	8.5	37.5	23	5	7.5	5660	0.88
6	Nimoo bazgo	$\frac{x^2}{5^2} + \frac{y^2}{2^2} = 1$	$x^2 = 100y$	$\frac{x^2}{5.6^2} + \frac{y^2}{2^2} = 1$	11	9	23.5	28	5	7	4500	0.84

Table 3.1 Contd...

7	Pandoh	Flat	$x^2 = 42735 y$	$\frac{x^2}{39.37^2} + \frac{y^2}{13.1^2} = 1$	16	13.5	21.64	20	5	12	9939	0.71
8	Parbati - II	$\frac{x^2}{7.38^2} + \frac{y^2}{5.344^2} = 1$	$x^2 = 101y$	$\frac{x^2}{5^2} + \frac{y^2}{2^2} = 1$	11	9	33	36	3	6	1850	0.77
9	Parbati - III	$\frac{x^2}{9.86^2} + \frac{y^2}{5.344^2} = 1$	$x^2 = 100 y$	$x^2 = 0.158 \ y^{2.4}$	17.64	14	32	10	2	7.2	3300	0.74
10	Ranganadi	Bipse	$x^2 = 92 y$	Circular arc R=5 m width 5 m	14	12	23	29	7	10	9100	0.65
11	Sewa - II	$\frac{x^2}{8.059^2} + \frac{y^2}{4.152^2} = 1$	$x^2 = 96.4 y$	$\frac{x^2}{3.6^2} + \frac{y^2}{2^2} = 1$	14.95	10.8	29.5	9.7	4	7	4020	0.76
12	Lower Subansiri	$\frac{x^2}{5^2} + \frac{y^2}{2^2} = 1$	$x^2 = 195 y$	$\frac{x^2}{6^2} + \frac{y^2}{2.5^2} = 1$	17.2	14.7	63.25	51	9	11.5	35000	0.80
13	Tala	Flat	$x^2 = 111 \ y$	$\frac{x^2}{13.15^2} + \frac{y^2}{6.58^2} = 1$	19.73	13.15	43	46	5	6.5	10490	0.89
14	Teesta - III	$\frac{x^2}{3.4^2} + \frac{y^2}{10^2} = 1$	$x^2 = 126 y$	$\frac{x^2}{6^2} + \frac{y^2}{3^2} = 1$	18	14	25	1	7	14	10430	0.62
15	Teesta - IV	$\frac{x^2}{6^2} + \frac{y^2}{3.5^2} = 1$	$x^2 = 67 y$	$\frac{x^2}{4.25^2} + \frac{y^2}{2^2} = 1$	22.1	17	25.25	6	7	11	15400	0.70
16	Teesta - V	$\frac{x^2}{6^2} + \frac{y^2}{3.5^2} = 1$	$x^{1.85} = 45 y$	$\frac{x^2}{6^2} + \frac{y^2}{2^2} = 1$	17.5	12	40.72	25	5	9	9500	0.76

Table 3.1 Contd...

17	Uri-II	$\frac{x^2}{5.4^2} + \frac{y^2}{125^2} = 1$	$x^2 = 80 \ y$	$\frac{x^2}{4.8^2} + \frac{y^2}{2^2} = 1$	14.65	11.4	24	20	4	9	4850	0.81
18	Myntdu	Flat	$x^2 = 80 \ y$	$\frac{x^2}{12^2} + \frac{y^2}{8^2} = 1$	20	12	30.5	24	7	8	10440	0.78
19	Kotlibhel -1A	$\frac{x^2}{12^2} + \frac{y^2}{7^2} = 1$	$x^2 = 130 y$	$\frac{x^2}{6^2} + \frac{y^2}{3^2} = 1$	21.5	18.5	32.5	41.5	5	11	13500	0.63
20	Kotlibhel -1B	$\frac{x^2}{14.164^2} + \frac{y^2}{8.038^2} = 1$	$x^2 = 164 \ y$	$\frac{x}{4} = \left(\frac{y}{4}\right)^{2.4}$	25.2	21.2	42	27.5	6	15	33500	0.71
21	Kotlibhel - II	$\frac{x^2}{13.934^2} + \frac{y^2}{8.286^2} = 1$	$x^2 = 144 \ y$	$\frac{x}{4} = \left(\frac{y}{3}\right)^{2.4}$	25	22	36	47.5	8	15.3	39750	0.77
22	Pare	$\frac{x^2}{5.0^2} + \frac{y^2}{2.0^2} = 1$	$x^2 = 100 y$	$\frac{x^2}{10^2} + \frac{y^2}{5^2} = 1$	18.47	14	29.15	16	3	10.4	5000	0.80
23	Punatsangchhu -	$\frac{x^2}{9^2} + \frac{y^2}{4.5^2} = 1$	$x^2 = 200 y$	$\frac{x^2}{40^2} + \frac{y^2}{8^2} = 1$	19.97	15	36	14	7	8	15800	0.80

# 3.2 Analysis of Data in respect of Discharging Capacity

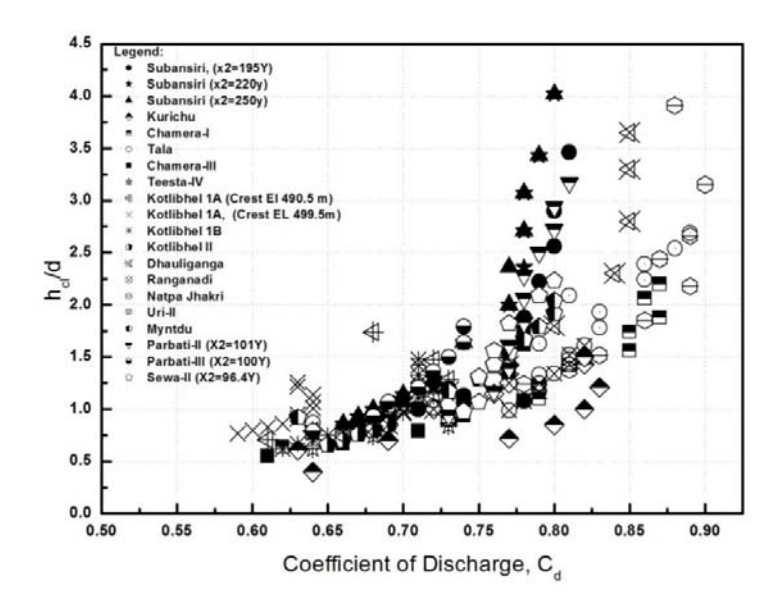
Estimation of coefficient of discharge is a key parameter for calculation of the capacity of a spillway. Non-dimensional ratios  $h_{cl}/h_d$  and  $h_{cl}/d$  were chosen to study the effects of variation in head over the spillway with reference to design head and reservoir water level with reference to the height of orifice opening. The  $h_{cl}$  is the head from centerline of orifice opening up to reservoir water level,  $h_d$  is the design head and d is the orifice opening. The non-dimensional plots arrived from those large numbers of physical model studies are shown in Figure 3.1 and 3.2. Figure 3.1 shows scatter plot of  $C_d$  Vs  $h_{cl}/d$ . Figure 3.2 shows scatter plot of  $C_d$  Vs  $h_{cl}/h_d$ .

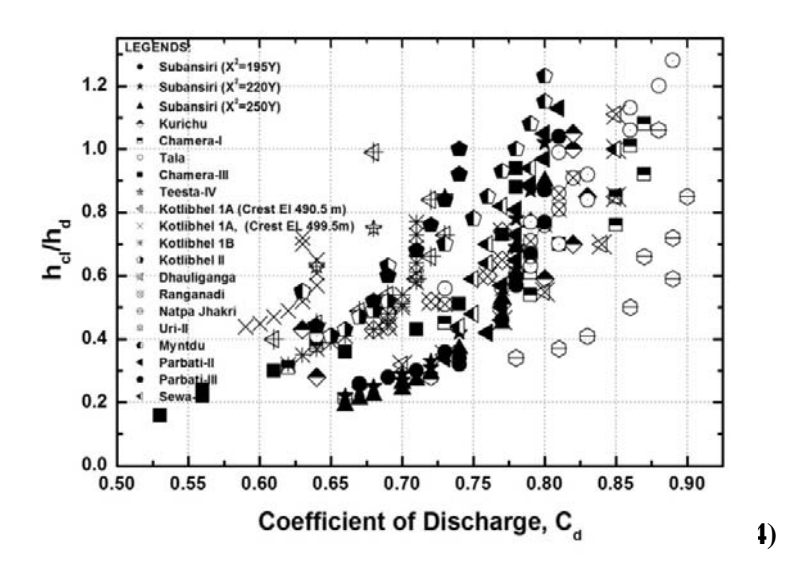
Though the data was seen to follow a simple power law in terms of  $h_{cl}$  for each individual case, there was wide scattering in the data from case to case. This scattering can be attributed to possible significant dependence of  $C_d$  on several other parameters like spillway bottom and roof profiles, head over the spillway crest, location of spillway with respect to deep river channel, width of piers, shape of pier nose, aspect ratio of orifice opening, approach flow conditions etc. Assessment of the coefficient of discharge was therefore not a simple task due to complicated dependence on the governing parameters. Based on the analysis; following conclusions were reported by (Bhosekar et al., 2014):

- 1. The  $C_d$  for Nathpa Jhakri Project was the maximum reaching up to 0.9 due to large transitions in plan and section leading to smooth entry of flow. Similar is the case for Tala project. In both the cases, the length of roof profile was more (8 and 13 m) than the usual thickness of 6-7 m. Thus, larger and steeper roof profile is favourable for generating higher  $C_d$ .
- 2. The coefficient of discharge C<sub>d</sub> was seen to be minimum for Chamera-III project, as the orifice opening is excessively large i.e. 16.5 m. The upstream profile of Chamera-III is flat resembling broad crested weir from structural considerations. Hence, C<sub>d</sub> was affected and is in the range of 0.67 to 0.78, which was less as compared to the other projects.
- 3. For Subansiri project, three alternative spillway profiles viz.  $x^2 = 195y$ ,  $x^2 = 220$  y,  $x^2 = 250$  y were studied. The  $C_d$  was seen to be more for steeper profile of spillway ( $x^2 = 195$  y). The other two profiles generated almost the same co-efficient of discharge i.e.  $C_d = 0.8$  as the spillway profile becomes flatter.
- 4. It is generally observed that the upstream depth of spillway with respect to river bed (P/h<sub>d</sub>) influence the C<sub>d</sub> only in the free flow regime (WES Design Charts, 1987) and for the orifice flow regime the effect of this parameter is negligible due to high head over the orifice centreline.

Still, an empirical equation was derived by CWPRS considering the important factors such as centre line head  $h_{cl}$ , design head  $h_d$ , clear width of spillway span wand width including side transitions L, orifice height d and orifice height including bottom and top transitions D, using multiple regression analysis as follows (Bhosekar et al., 2014):

(3.1)





Equation (3.1) shows that  $C_d$  depends strongly on ratio of centerline head to design head  $h_{cl}/h_d$  as also in the case of overflow spillway. The influence of transitions of the orifice in plan and elevation are also strong. The observed and estimated  $C_d$  was plotted in Figure 3.3. The  $C_d$  values estimated are almost near the  $C_d$  observed on physical model with a maximum variation of  $\pm$  10%. The equation was also applied to estimate  $C_d$  for several projects. Typical curves for the observed versus estimated  $C_d$  were plotted in Figure. 3.4 for Pare and Lower Siang projects, which shows good match between the observed and estimated values. Thus, the empirical relationship of eqn. (3.1) can be used for predicting  $C_d$  for the initial designs. However it can be further improved by optimizing the design of bottom and roof profile, which are found to be the important parameters in determining the discharging capacity of orifice spillway.

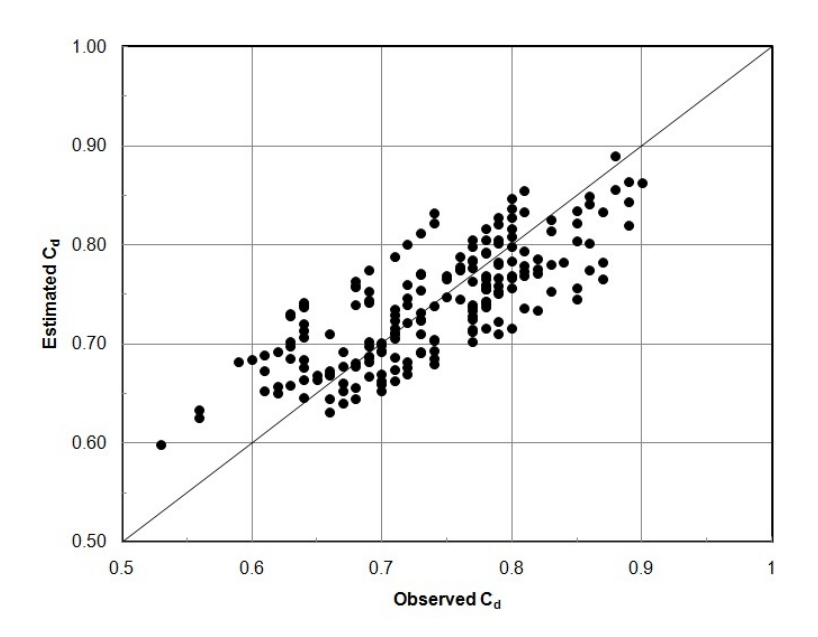


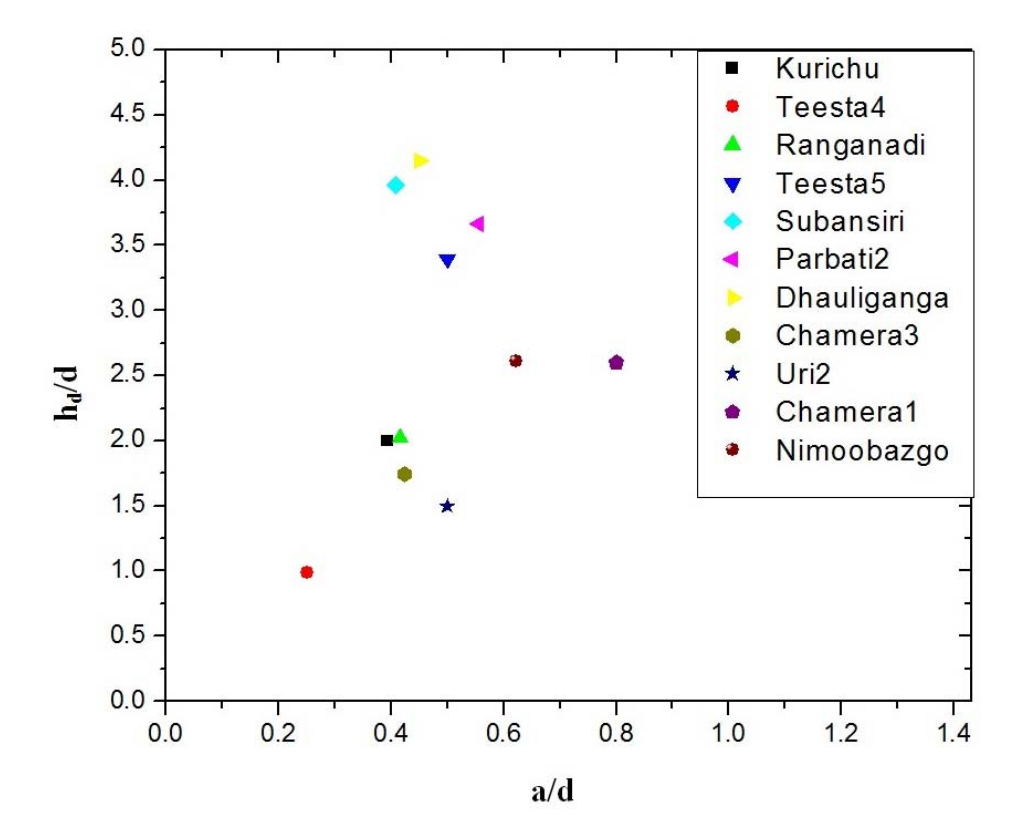
Fig. 3.3 Observed Vs Estimated C<sub>d</sub> (Bhosekar et al., 2014)

Fig. 3.4 Typical comparisons between observed and estimated  $C_d$  curves (Bhosekar et al., 2014)

The equation 3.1 can however be used as guideline for assessing the  $C_d$  for initial design stage of new projects. The study also indicates the need for comprehensive investigations for the designs of roof profile(breast wall profile) and upstream and downstream spillway profiles linked with the coefficient of discharge (Bhosekar et al., 2014). Data of model studies for the above projects was also analyzed in respect of pressure by developing non dimensional plots. The plots were not indicated any specific trend due to large variation in hydraulic parameters from project to project.

# 3.3 Analysis of roof profile

The data in respect of roof profile for the existing spillways were analysed and non-dimensional plots were developed. The length of roof profile 'a', height of curve 'b' and opening of the orifice 'd' are plotted against the ratio of head 'h<sub>d</sub>' with respect to the opening of the orifice 'd'. The plots are shown in Figures 3.5 and 3.6. Figure 3.5 shows non dimensional plot of a/dVs  $h_d$ /d. Figure 3.6 shows non dimensional plot of b/d Vs  $h_d$ /d.



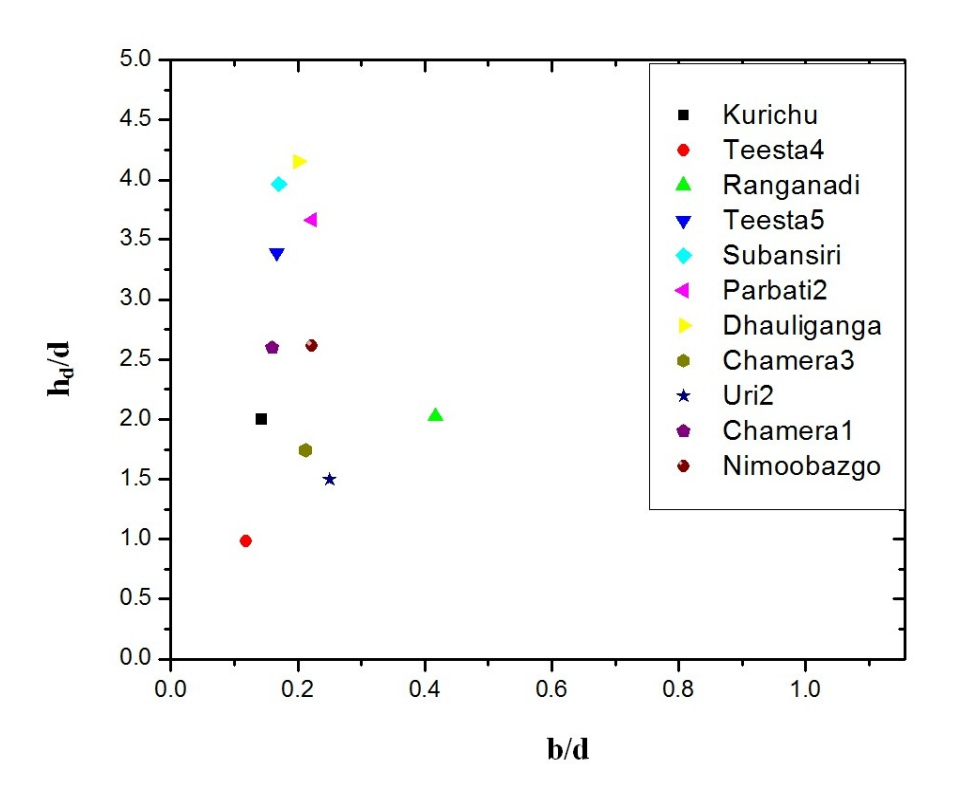


Fig. 3.6 Non-dimensional plot of b/d Vs h<sub>d</sub>/d (Deolalikar et al., 2008)

Deolalikar et al. (2008) has reported that the ratio of a/d lies between 0.3 and 0.7, whereas the b/d ratio lies between 0.1 and 0.4. The above Figures give the limit for fixing the length of roof profile i.e 'a' and height of curve, 'b' for corresponding height of orifice and design head. However, a and b varies from project to project. Hence, systematic research is required to fix length of roof profile and height of curve for various combinations of heads and heights of orifice.

## 3.4 Case studies

For some typical cases the findings of the model studies at CWPRS, important design features and the prototype experience are described in the following paragraphs:

## 3.4.1 Chamera H. E. Project, Stage - I, Himachal Pradesh

The Chamera H.E. Project, Stage - I is the downstream most project in the cascades on the river Ravi. It is a 125 m high concrete gravity dam with breast wall spillway at the center. Figures 3.7, 3.8 and 3.9 show the plan, upstream elevation and section of the spillway respectively. The spillway is designed to pass a maximum discharge of 22,000 m<sup>3</sup>/s. The spillway is provided with openings at 32.5 m below FRL El. 762.5 m with breast walls and a

ski-jump bucket is provided for energy dissipation. The Chamera dam has been provided with four under sluice gates of size 4 m x 5.5 m with their crest 90 m below the FRL. The invert of the intake is 27 m below the FRL.

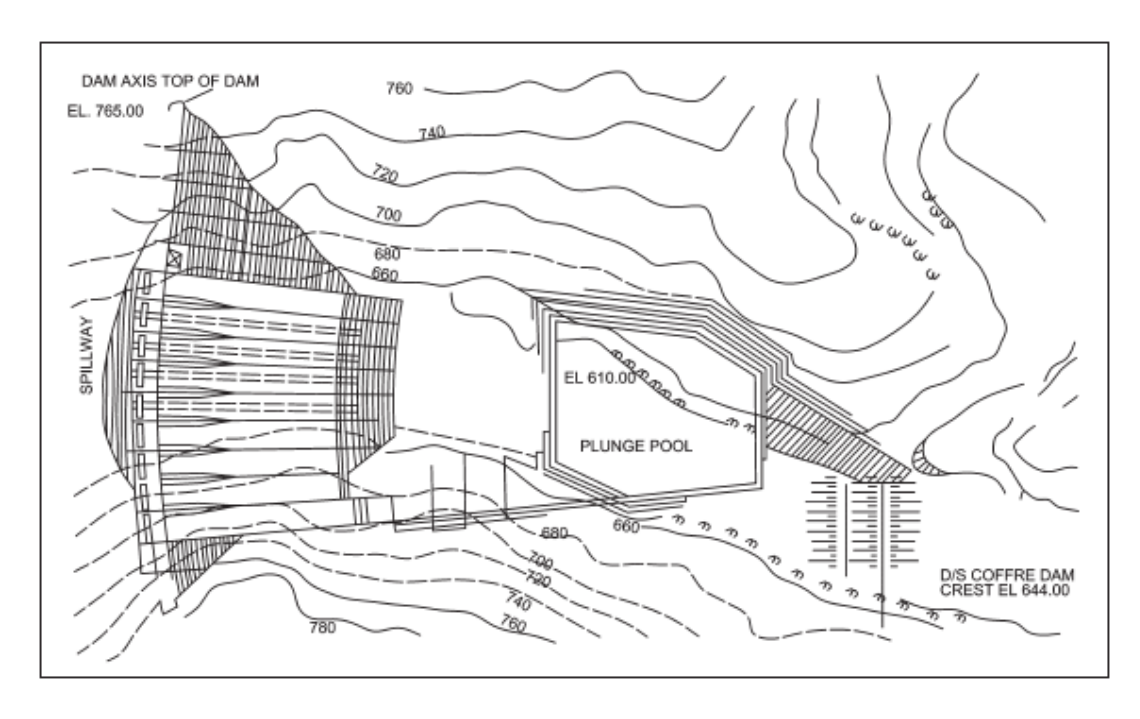


Fig. 3.7 General layout plan of the original design of spillway

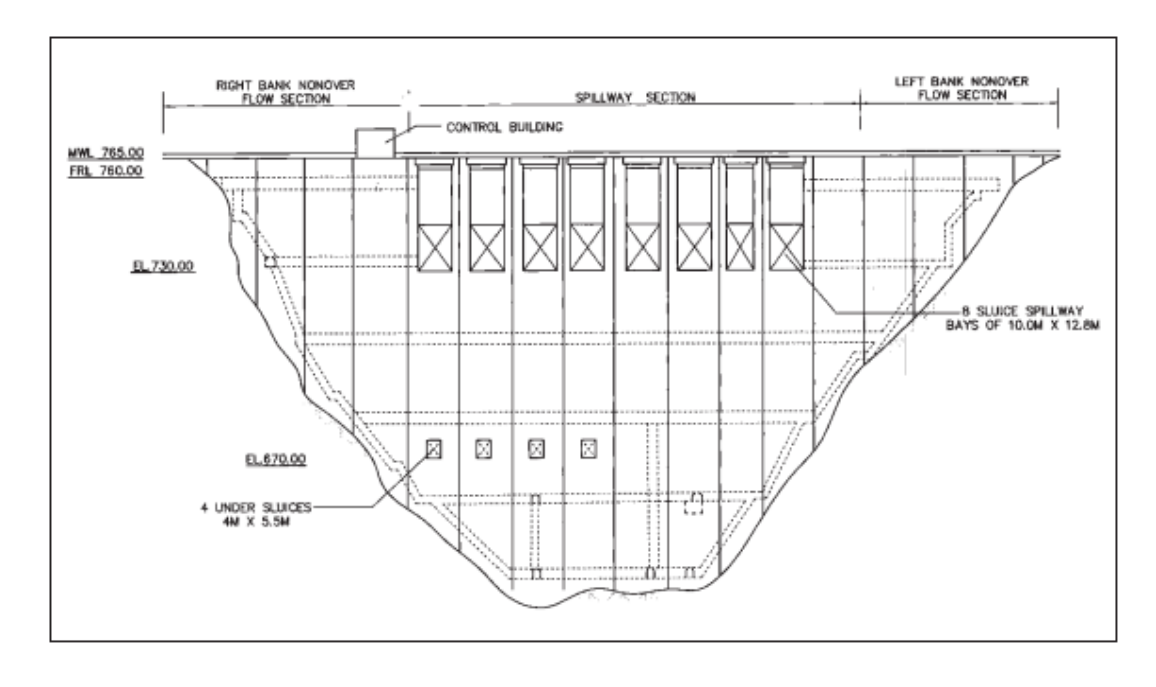


Fig. 3.8 Upstream elevation of the spillway

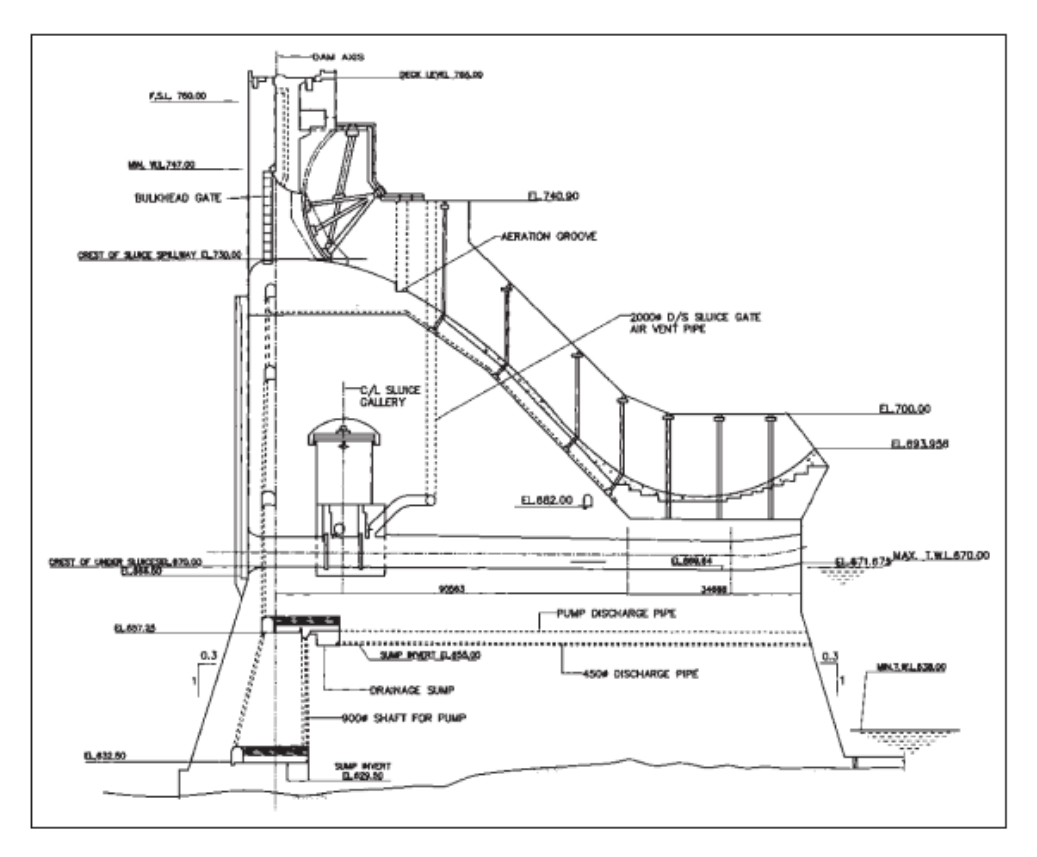


Fig. 3.7 Longitudinal section of the spillway

Four different orifice alternatives of size 10 m (w) x 12.5 m (H), 12.8 (m) (H), 13 m (H) and 13.5 m (H) were studied. In addition two different bottom profiles viz.  $\frac{x^2}{10^2} + \frac{y^2}{5^2} = 1$  &  $\frac{x^2}{4^2} + \frac{y^2}{2^2} = 1$ , were studied to optimise the coefficient of discharge and limit the negative pressures on the breast wall profile. The studies indicated that the maximum discharge of 22,000 cumec could be passed with higher MWL El. 765 m with orifice opening of 10 m x 12.8 m and modified breast wall profile  $\frac{x^2}{10^2} + \frac{y^2}{5^2} = 1$ . Figure 3.10 shows the discharging capacity curve for the two alternatives of breast wall profiles and four orifice openings. The variation of coefficient of discharge and the discharging capacity curves for the four alternatives of orifice sizes with the profile of the breast wall  $\frac{x^2}{4^2} + \frac{y^2}{2^2} = 1$ , when studied for pressure, indicated that negative pressure of -2 m of water head was prevalent along the profile. For the modified profile of the breast wall,  $\frac{x^2}{10^2} + \frac{y^2}{5^2} = 1$ , which was made sharper for increasing the coefficient of discharge, the negative pressure increased up to -3.5 m of water head. This profile was also checked for assessing the cavitation potential. It was observed that even for the maximum negative pressure of - 3.5 m, the cavitation index was much above the critical cavitation index of 0.2. Also, width of breast wall was very small and the bottom profile would be aerated from the downstream side. Therefore, there was no possibility of the beast wall being subjected to cavitation. The breast wall was provided with steel lining so as

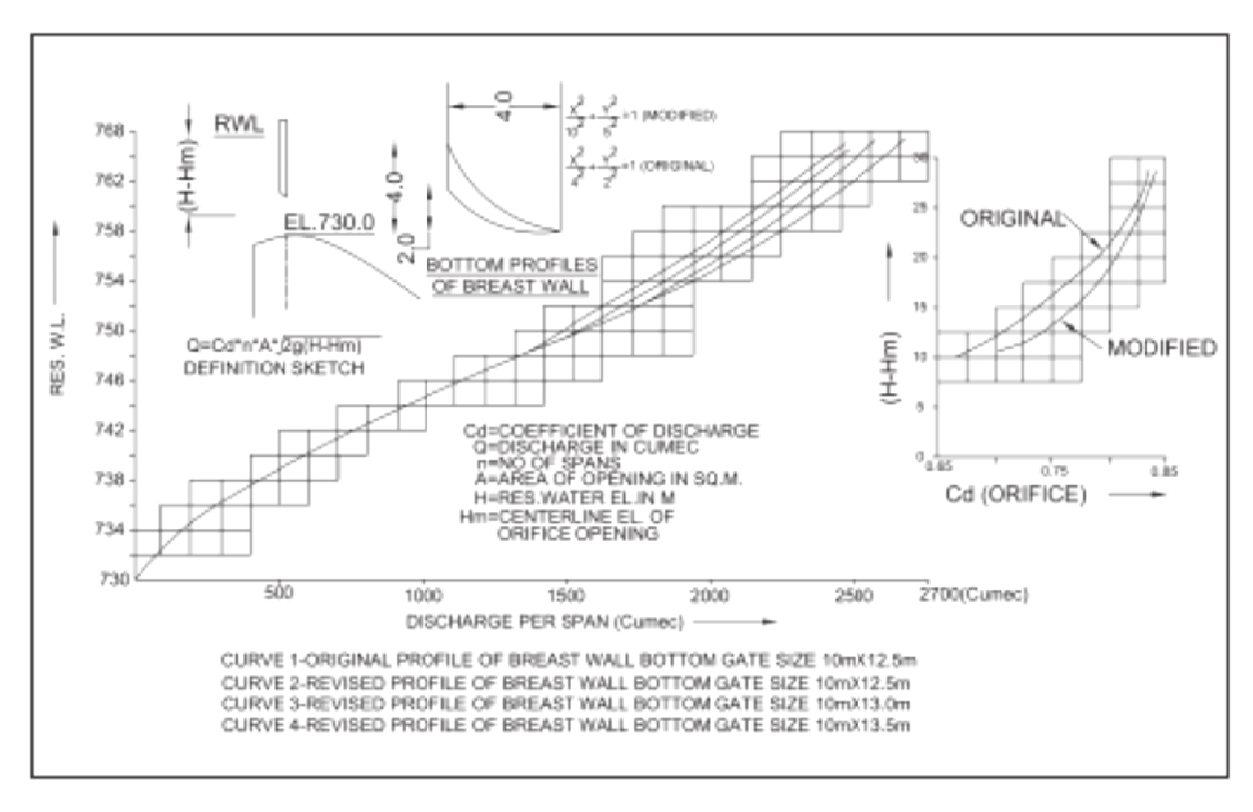


Fig. 3.8 Discharging apacity curves for various alternatives of breastwall profiles and orifce openings

to increase the overall stiffness and to protect the bottom profile from abrasion damage due to floating materials. This would additionally provide safety against cavitation. Another alternative for reducing the negative pressure on the breast wall was considered. This necessitated increasing the thickness of the breast wall from 4 m to 6 m. However, this alternative was considered to be costly and even the spillway piers were required to be redesigned. As such, the modified design of the breast wall with orifice opening of 12.8 m with profile — was accepted. This is one of the model studies for breast wall spillways carried out during the early eighties which amply demonstrated the contribution of breast wall profile in the discharging capacity of the spillway.

## 3.4.2 Tala H. E. Project, Bhutan

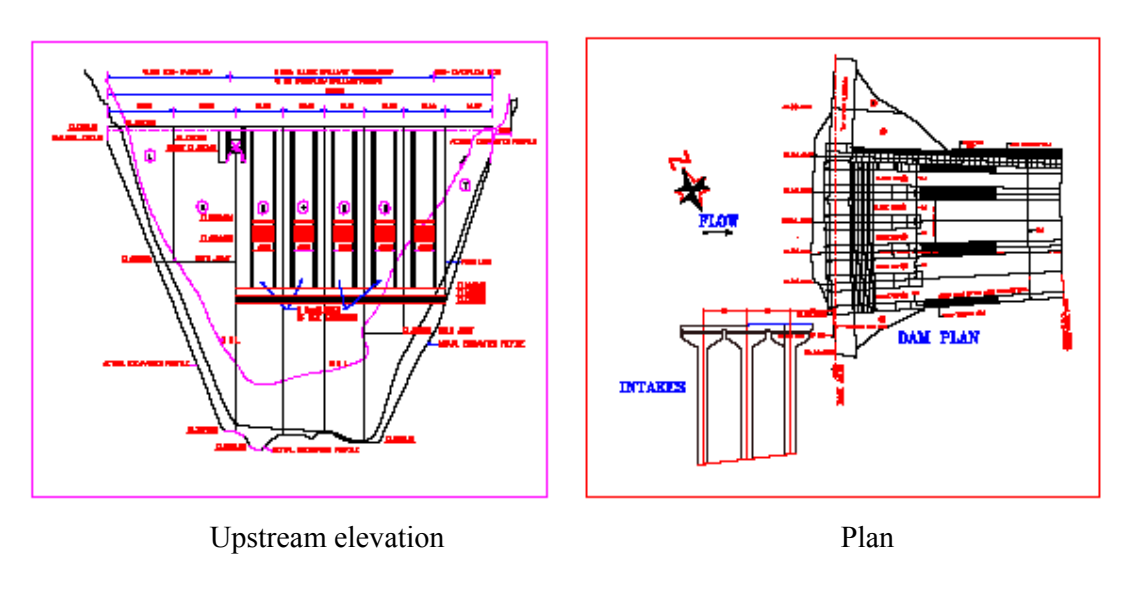
The Tala H.E. Project, Bhutan is a 91 m high concrete gravity dam across river Wangchu near Honka and an underground power house near Tala having head of 900m and installed capacity of 1020 MW (6 x 170 MW). The spillway in the form of a battery of low-level sluices has been provided in the central portion of the dam with ski-jump bucket for energy dissipation. The spillway has been designed to pass SPF of 8575 m³/s at FRL El. 1363 m and PMF with peak outflow of 10,600 m³/s at RWL El. 1365 m.

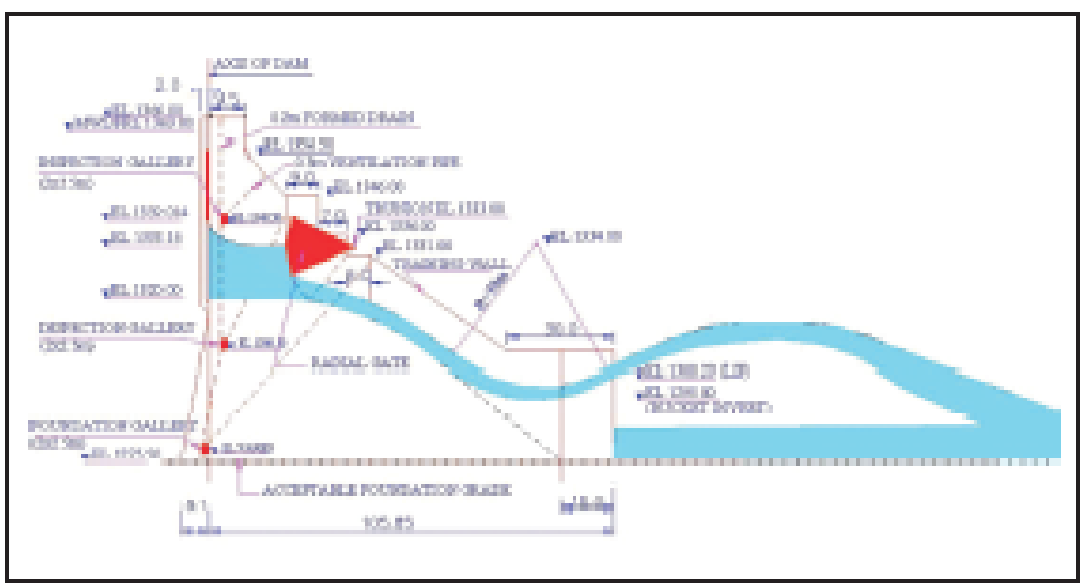
The original design of spillway comprised four sluices of size 8 m wide x 13.15 m high with invert at El. 1320 m and one span of overflow portion of size 8 m wide x 11 m high at El. 1352 m on left. Due to the large head of the order of 45 m over the spillway crest, the spillway has been designed as a sluice spillway instead of a breast wall spillway. Hydraulic model studies were conducted at CWPRS for assessing the performance of the spillway in respect of discharging capacity, flow conditions and pressures on spillway and breast wall profiles. The studies indicated that the discharging capacity of spillway was adequate. The piezometric pressures observed along the bottom and sides of the spillway were acceptable. However, the pressures along the top profile of the sluices were negative when the sluices were operated under fully open condition for discharges of 9000 m³/s and above. Negative pressure of -13.5 m was observed for the PMF discharge of 10,600 m³/s under free flow conditions. The spillway is located in a narrow gorge. Excavation of the right bank was necessary in order to have clear waterway. The flow conditions in the vicinity of the impingement of jet were violent and with a potential to cause substantial damage along both the banks endangering their safety.

In view of the above observations, the design of the spillway was revised after studying large number of alternatives. The axis of dam was given 110 curvature with radius of 670.35 m to reduce the width of ski-jump jet. Also, considering the thrust on the trunnion of radial gate and the operation of the spillway, five sluice bays of 6.5 m x 13.5 m were proposed as against four sluices bays of 8 m x 13.15 m. Figure 3.9 shows the modified plan, upstream elevation and section of the spillway. The studies for discharging capacity revealed that the five sluices were able to discharge 10,210 m³/s at FRL El. 1363 m and 10,490 m³/s at RWL El. 1365 m as against 10,049 m³/s and 10,363 m³/s respectively for the original layout. The coefficient of discharge remained the same, in the neighborhood of 0.893 for both the designs.

Piezometric pressures were observed along the bottom, top and sides of sluices and the bottom profile of the overflow spillway. A maximum negative pressure of -2 m was observed on the bottom profile of the sluice for discharges less than 4000 m<sup>3</sup>/s passed under partial gate operation with FRL El. 1365 m. Cavitation index corresponding to this negative pressure is 0.22, which is more than the critical cavitation index of 0.2. Therefore, the negative pressures observed on the bottom profile of the sluices were acceptable. The pressures on the top profile of the sluices were positive when the discharges up to SPF of 8,575 m<sup>3</sup>/s were passed with partial gate operation. It was observed that a maximum negative pressure of -13.5 m occurred

along the top profile of the sluice when the PMF of 10,600 m<sup>3</sup>/s was passed through the sluices with gates fully open.





Longitudinal section

Fig. 3.9 Plan, upstream elevation and section of the spillway

In order to reduce the negative pressures along the top profile of the sluice spillway, a 1:40 scale 2-D sectional model as shown in Figure 3.10 was constructed and three different profiles as shown in Figure 3.11 were studied. It was observed that the angle of the tangent of the profile with the vertical at the upstream face plays a significant role. Figures 3.12 (a) to (c) show the pressure profiles for the three alternatives studied on the model. It was found that a  $45^{\circ}$  circular curve reduced the pressure to -3 m and was found acceptable. Table - II gives cavitation indices at the location of maximum negative pressure for various discharges. The cavitation indices calculated from the pressures observed are higher than critical cavitation index of 0.2. As such, alternative 3 profile was considered to be suitable and was recommended.

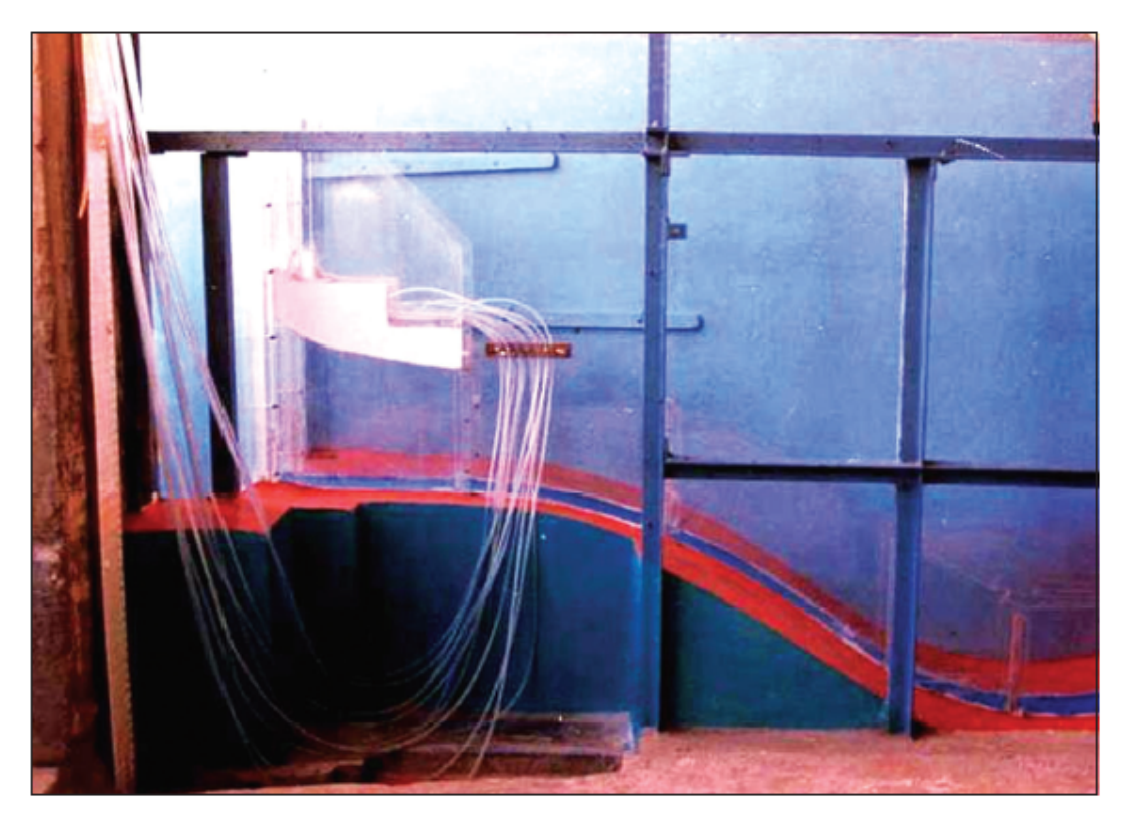


Fig. 3.10 View of sectional model

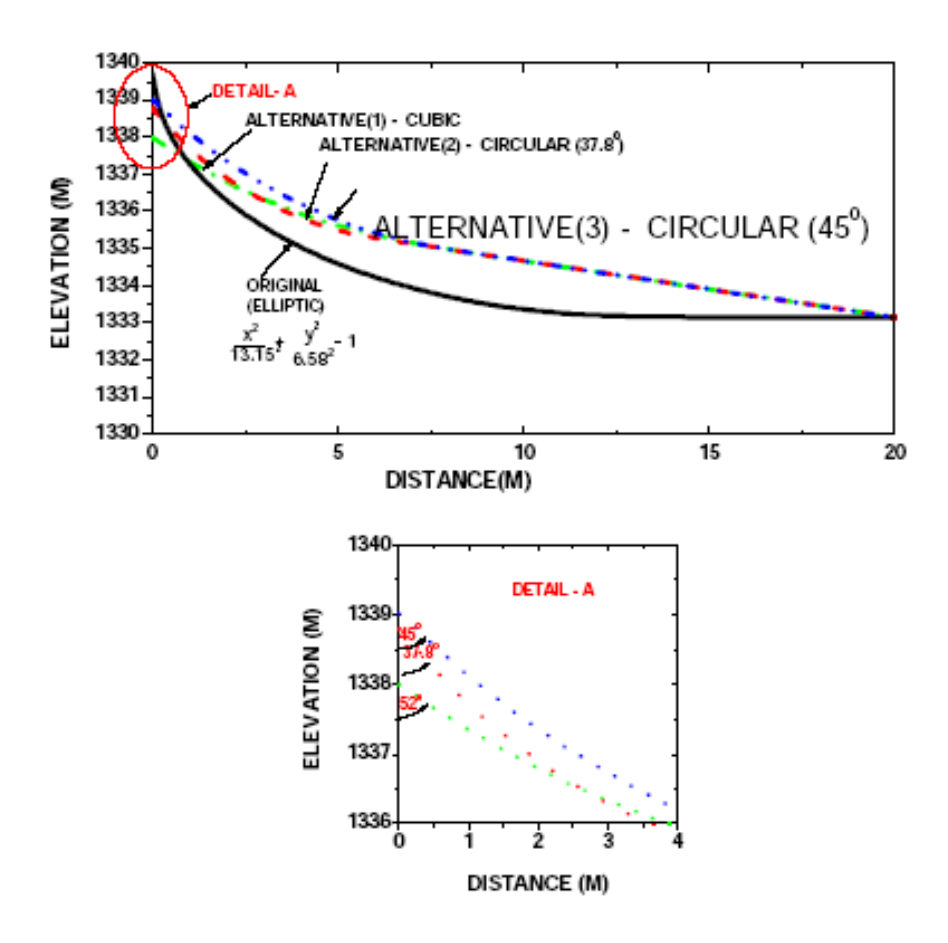


Fig. 3.11 Alternative top profiles of sluice

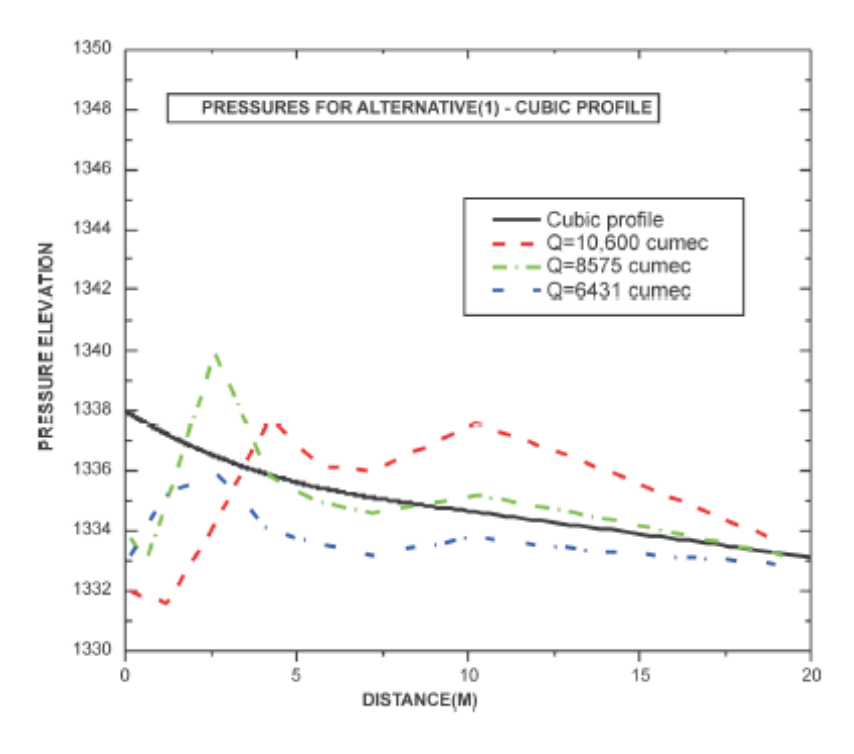


Fig. 3.12 Pressures for roof profile - Alternative 1

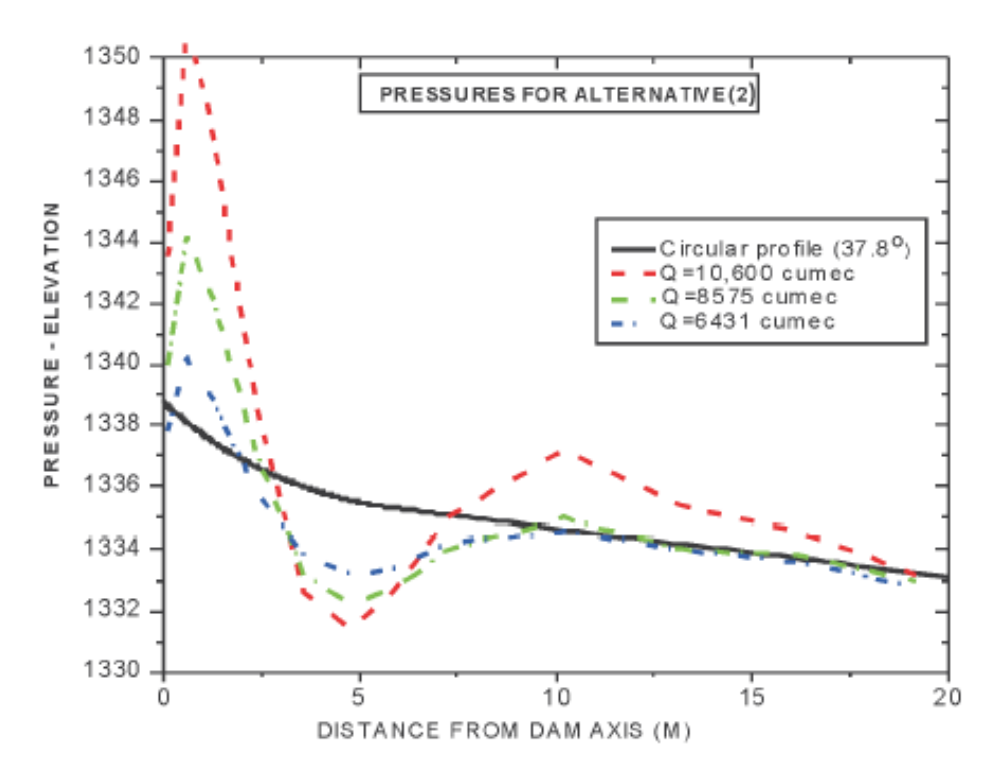


Fig. 3.13 Pressures for roof profile - Alternative 2

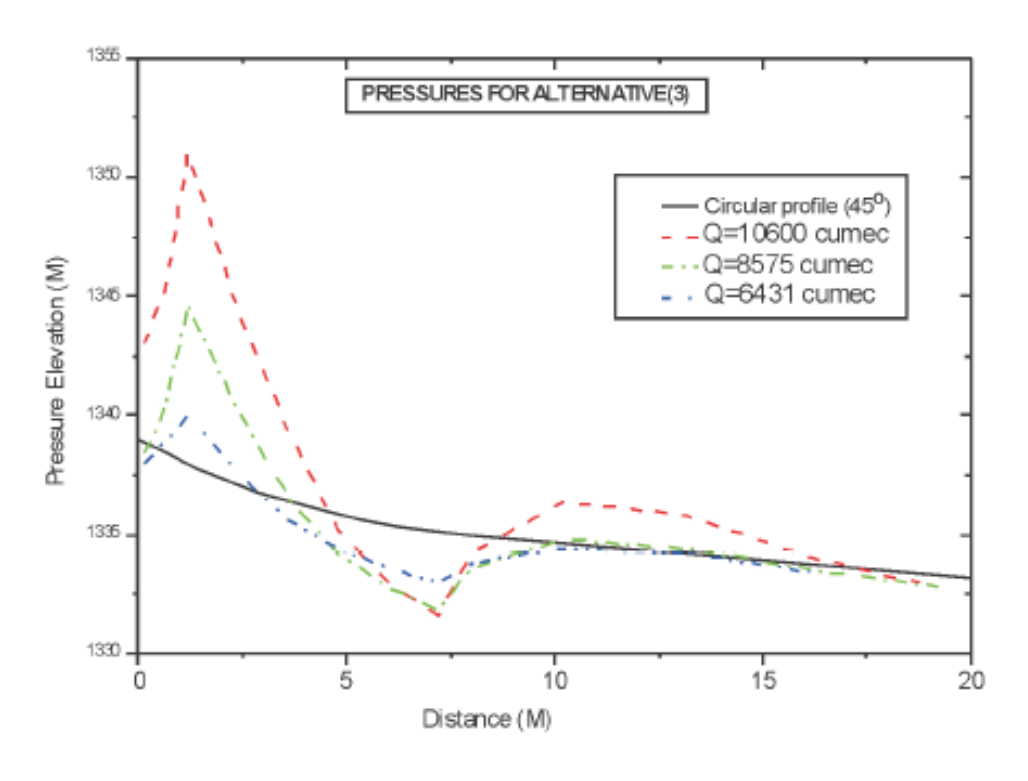


Fig. 3.14 Pressures for roof profile - Alternative 3

Table 3.2 Cavitation index for alternative roof profiles of sluice

Discharge In cumec	Profile	RWL	Max. Negative Pressure (m)	Piezometric Elevation (m)	Velocity (m/s)	Velocity Head (m)	Cavitation Index
	Original	1365.20	-13.5	1333.90	24.80 23.46 (Av.)	31.30 28.10	
40.000	Alt1 Cubic	1365.23	- 5.90	1337.90	23.20 18.2 (Av.)	27.33 16.90	0.15 0.24
10,600	Alt2 Circular 54.7°	1365.87	- 4.14	1335.54	24.39 20.98 (Av.)	30.33 22.45	0.19 0.26
	Alt3 Circular 45°	1364.87	- 3.56	1335.16	24.14 21.51 (Av.)	29.71 23.58	0.22 0.27
	Original	1355.00	-9.60	1333.90	20.35 18.98 (Av.)	21.10 18.36	0.019 0.021
8,575	Alt1 Cubic	1353.93	- 4.20	1337.60	17.90 15.0 (Av.)	6.33 11.50	0.36 0.51
0,575	Alt2 Circular 54.7º	1353.37	-2.80	1336.00	18.46 16.50 (Av.)	17.37 13.90	0.41 0.50
	Alt -3 Circular 45°	1353.01	-3.36	1335.16	18.71 17.40 (Av.)	17.85 15.43	0.37 0.43
	Original	1345.10	-3.70	1333.30	15.21 14.90 (Av.)	11.80 11.30	0.53 0.56
6 424	Alt1 Cubic	1345.43	- 4.90	1337.90	12.20 11.0 (Av.)	7.53 6.20	0.68 0.80
6,431	Alt2 Circular 54.7°	1345.43	-2.34	1335.54	12.90 12.70 (Av.)	8.53 8.30	0.90 0.92
	Alt3 Circular 45°	1344.57	- 2.16	1335.16	13.60 13.05 (Av.)	9.41 8.68	0.83 0.90

#### 3.4.3 Punatsangchhu H. E. Project, Bhutan

The Punatsangchhu - I H.E. Project is under construction as a run-of-river scheme on the Punatsangchhu river in Wangdue Phodrang district of western Bhutan. The project envisages construction of a 136 m high and 279 m long concrete gravity diversion dam with top El. 205 m. The sluice spillway has been provided to pass a flood discharge (PMF) of 11,500 m³/s along with Glacial Lake Outburst Flood (GLOF) of 4,300 m³/s through 7 orifice openings of size 8 m wide x 15 m high with crest level at El. 1166 m. The FRL/MWL has been fixed at El. 1202 m and MDDL at El. 1195 m. Radial gates have been provided at the downstream face of breastwall for controlling the outflow discharge. The ski-jump bucket with pre-formed plunge pool is provided for energy dissipation. Besides sluice spillway, an auxiliary spillway bay has been provided with crest El. 1198 m for passing floating debris. Figures 3.15,3.16 and 3.17 show upstream elevation, layout plan and section of of spillway.

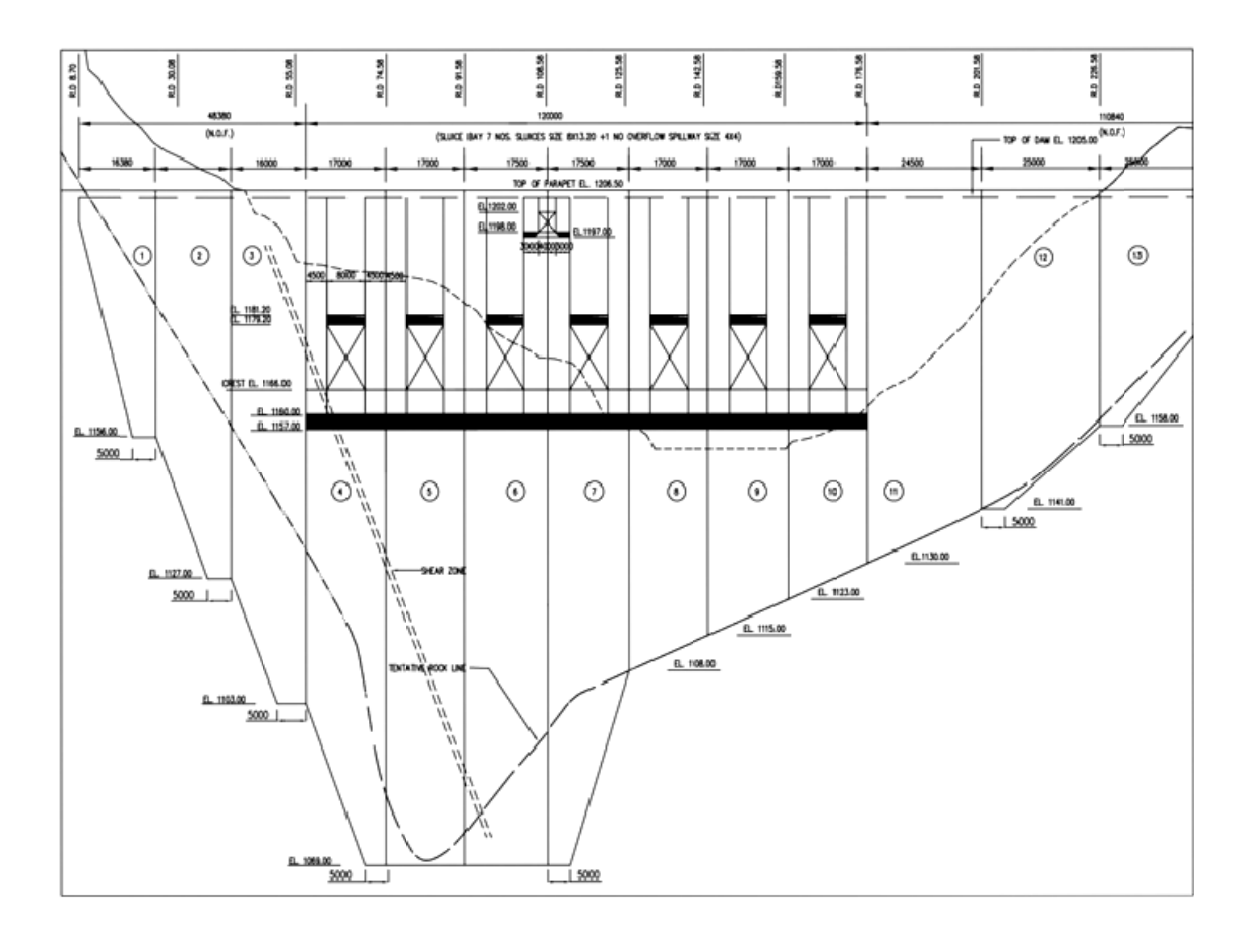


Fig. 3.15 Upstream elevation

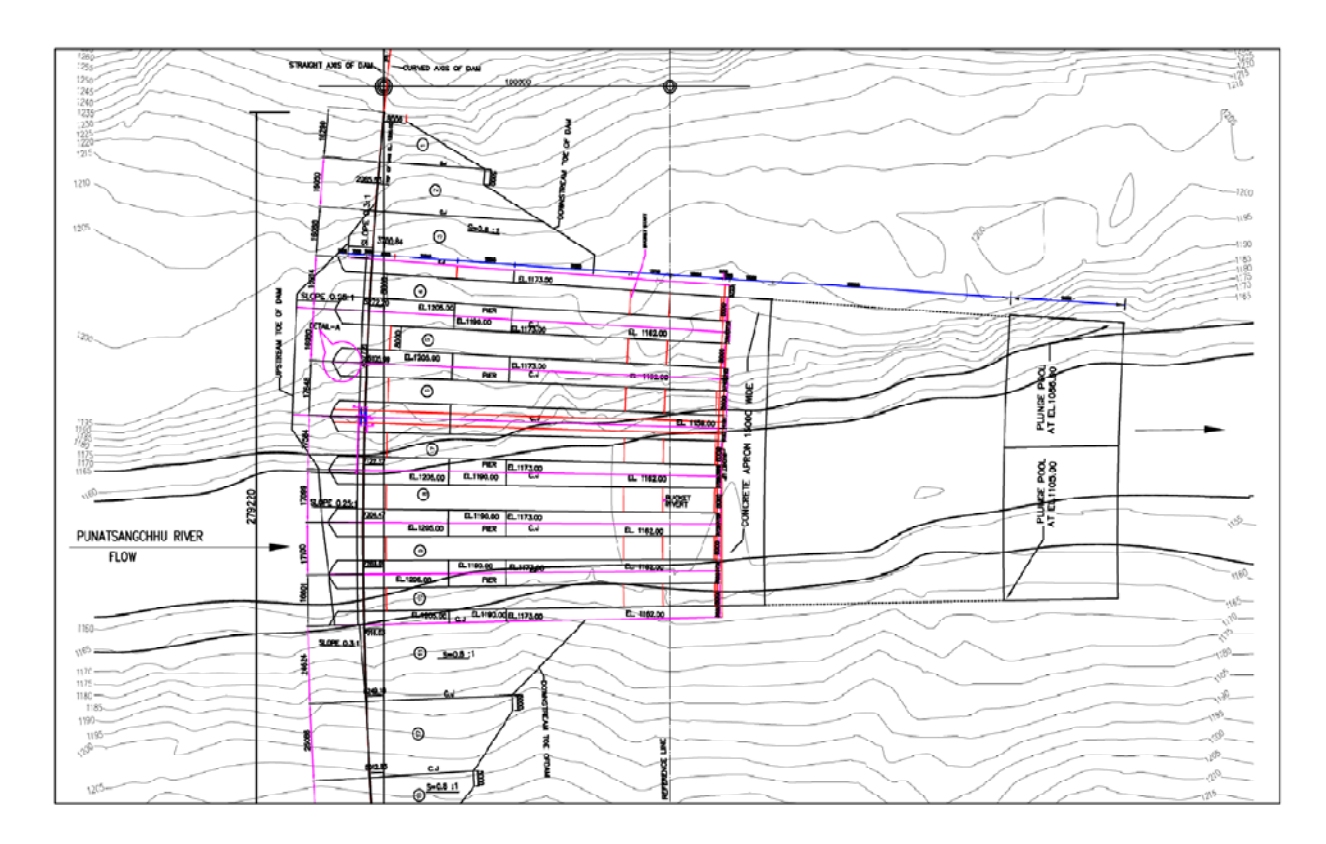


Fig. 3.16 General layout plan

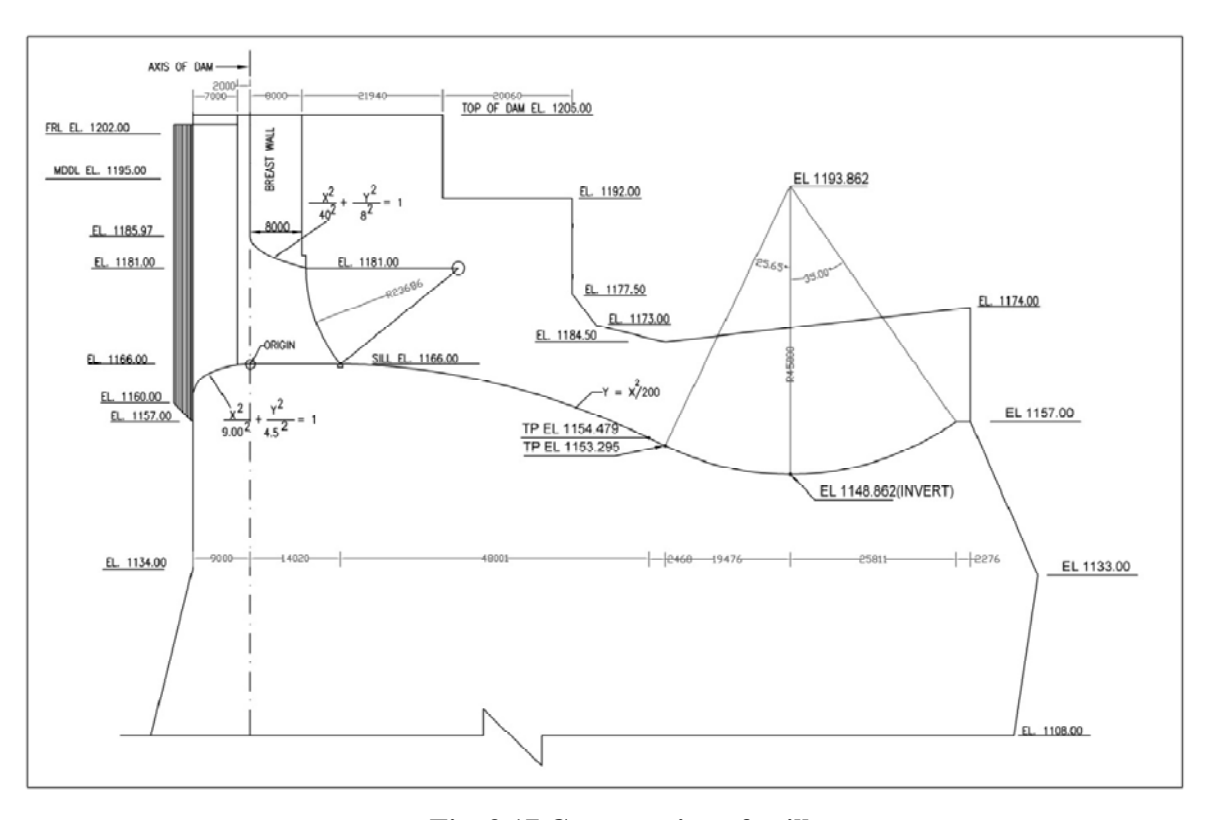
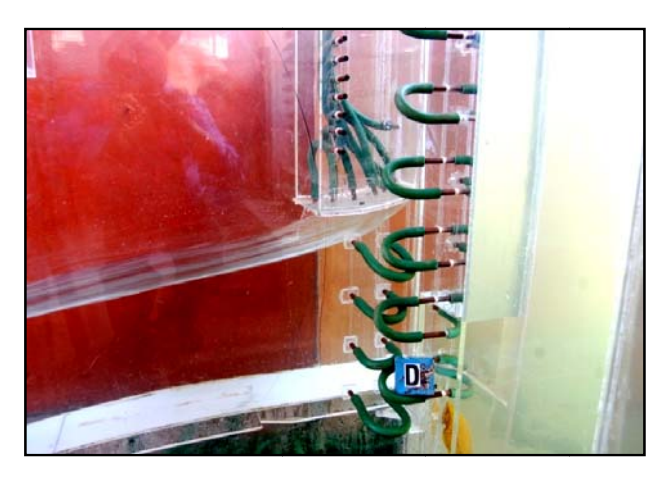


Fig. 3.17 Cross section of spillway

Preliminary studies were conducted for assessing the discharging capacity of spillway for the breastwall profile equation  $\frac{X^2}{8.66^2} + \frac{Y^2}{2^2} = 1$ . The studies indicated that the discharge of 13,426 m<sup>3</sup>/s could be passed at FRL El. 1202 m with all 7 spans operating fully open. This is 15% less as compared to the design discharge of 15,800 m<sup>3</sup>/s (PMF+GLOF). It was also observed that for FRL El. 1202 m condition the water surface was not following the breastwall bottom profile as shown in Figure 3.18 a. The whole opening of orifice was not effective resulting in reduced capacity to pass the flow. It was, therefore, necessary to modify the bottom profile of breastwall. In this regard, three alternative designs of breastwall were tested. Figure 3.18 shows the flow condition in the vicinity of roof profile for original and modified design of breastwall bottom profile.

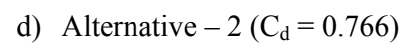




a) Original design

b) Alternative – 1 ( $C_d = 0.763$ )







c) Alternative -3 ( $C_d = 0.75$ )

Fig. 3.16 Flow conditions in the vicinity of roof profile for original and modified design

In Alternative-I, breastwall bottom profile conforming to equation  $\frac{X^2}{8.66^2} + \frac{Y^2}{4.6^2} = 1$  was incorporated keeping the same gate height opening of 15 m. The spillway could able to pass the discharge of 15,169 m³/s at FRL El. 1202 m, which is 4% less than the design discharge and the water surface follows only half upstream width of breastwall bottom profile. In Alternative –II, breastwall bottom profile conforming to equation  $\frac{X^2}{40^2} + \frac{Y^2}{8^2} = 1$  was incorporated keeping the same gate height opening of 15 m. It was observed that a discharge of 15,554 m³/s could be passed at FRL El. 1202 m, with all 7 spans operating fully open and the water surface follows the full width of breastwall bottom profile. This is also 1.0 % less than the design discharge. In Alternative-III, breastwall bottom profile was kept same as in Alternative-II. The gate height was increased from 15 to 16 m. The discharges of 15,736 m³/s and 16,706 m³/s could be passed at FRL El. 1202 m and dam top El. 1205 m respectively. As such discharging capacity is just adequate to pass the design discharge of 15,800 m³/s through 7 spans. After discussion with the design engineers, the breastwall bottom profile of Alternative - II has been adopted for further studies on 2-D sectional and 3-D comprehensive models.

The voluminous and systematic data on physical model studies of about 23 orifice spillways as shown in Table 3.1 was a big asset to develop guidelines to evolve the preliminary design of orifice spillway. However, the same could not be done as the studies are site specific for each case and not basic research studies. The standard design of providing of an ellipse for the roof profile of the sluice/breast wall did not work in case of most of the sluice spillways. Model studies indicated that this profile experiences high negative pressure as the flow passage cannot be constricted downstream, as in the case of sluice barrels. Extensive model studies carried out at CWPRS could be helpful in finalizing the design of roof profile so as to make the structure hydraulically efficient. Based on the detailed study for more than 23 projects, a need of basic research was identified to evolve the design of roof profile for improving the performance of orifice spillway.

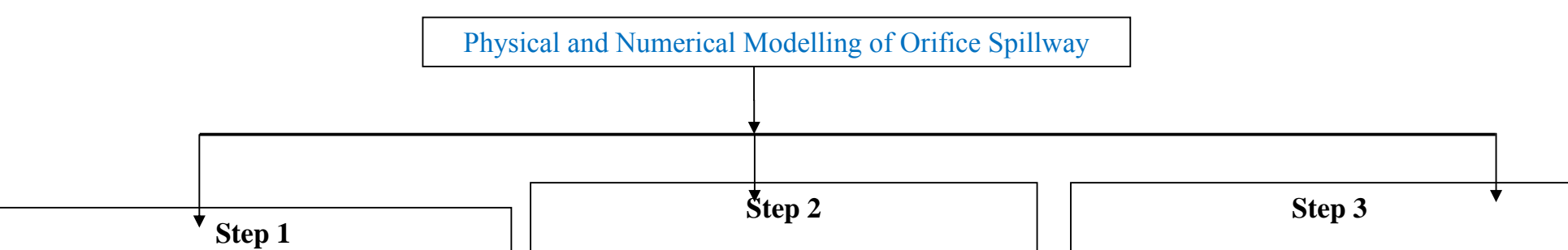
# **Chapter 4**

# **Basic Research Study**

#### 4.1 General

Large orifices are generally used in the dam to pass the surplus water from upstream to downstream as well as for flushing of sediments from the reservoirs. The structure with large orifice in a dam is known as orifice spillway. Several dams in India and Bhutan have been constructed with orifice type of spillway due to it's dual advantages. However, no systematic guidelines have been reported for design of an orifice spillway. The discharging capacity, pressure distribution on spillway bottom profile, pressure distribution on spillway roof profile and water surface profile along spillway profile are some of the essential parameters to be studied while assessing the performance of orifice spillway. Hence, utmost care should be taken in design of bottom as well as roof profile, as it affects the performance of orifice spillway. CWPRS has contributed in evolving the design of orifice spillway by conducting hydraulic model studies for more than 25 orifice spillway. Orifice spillways were studied for heads (h<sub>d</sub>) in the range of 20 m to 65 m and height of orifice (d) 8 m to 22 m. Similarly, height of spillway crest from upstream reservoir (P) bed also varies from project to project. Model studies indicated that as the flow passes through orifice, it does not follow the path of roof profile. This resulted in reducing the discharging capacity which is one of the important hydraulic aspects in assessing the performance of orifice spillway. The design of roof profile was finalised by trial and error method carried out on physical model. This increased the cost of fabrication, conducting the experiments (water and electric charges) duration of work, manpower etc. Hence, it is felt necessary to conduct the basic research to evolve especially the design of roof profile. Basic research studies have been taken to develop the design guidelines for bottom and roof profile of orifice spillway using physical and numerical model. Research work was started with a basic theory of sharp edged orifice. The studies were extended with the provision of bottom and roof profile for providing the design guidelines. Methodology adopted for basic research study has been given in detail in Figure 4.1. The studies have been carried out on following three set ups:

- 1. Physical and numerical model studies on flow through sharp edged large orifice (Set up1): **60 Nos.**
- 2. Physical and numerical model studies on flow through orifice with the solid spillway bottom profile (Set up- 2): 67 Nos.
- **3.** Physical and numerical model studies onflow through orifice with solid spillway bottom and roof profile (Set up -3): **99 Nos.**

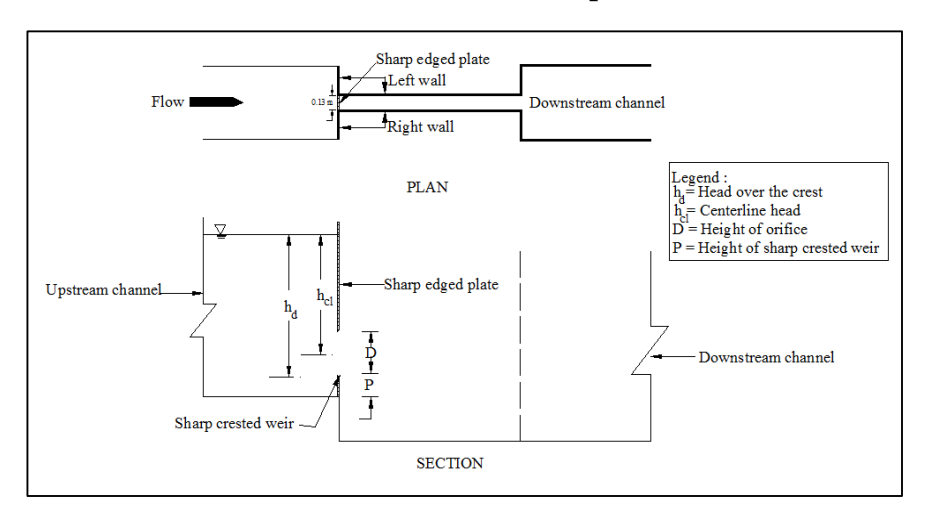


- 1. Physical and numerical model studies of flow through sharp edged large orifice.
- 2. Experiments/simulations for various combinations of heads and heights of orifice.
- 3. Verification and validation of numerical model
- 4. To study the different coefficients and parameter affecting the design of lower and upper nappe profile.
- 1. Physical and numerical model studies of flow through sharp edged large orifice with **solid spillway bottom** profile.
- 2. Experiments/simulations for various combinations of heads and heights of orifice.
- 3. Verification and validation of numerical model.
- 4. To study the effect of different hydraulic parameters to be considered in design of roof profile.
- 5. To derive an equation to design roof profile of orifice spillway.
- 6. Verification and validation of the proposed equation with real life orifice spillway projects.

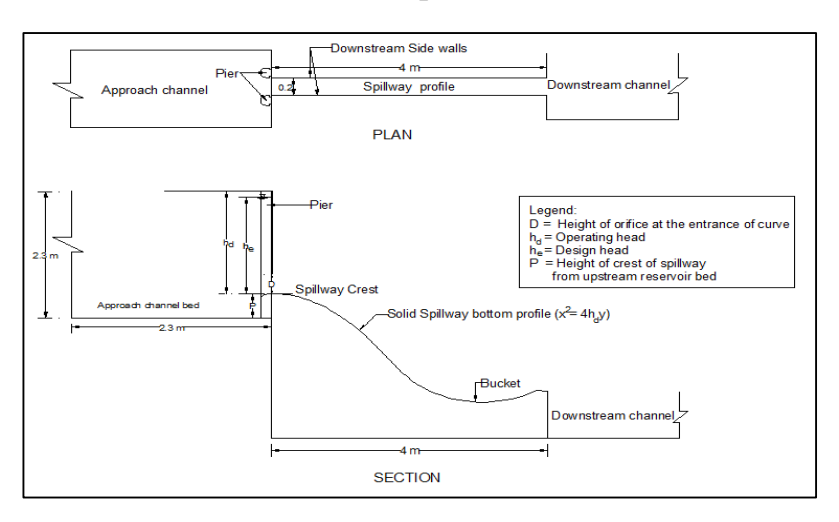
- 1. Physical and numerical model studies of flow through sharp edged large orifice with solid spillway bottom and roof profile.
- 2. Experiments/simulations for various combinations of heads and heights of orifice.
- 3. Verification and validation of numerical model.
- 4. To assess the performance of orifice spillway in respect of different hydraulic parameters.
- 5. To derive an equation to estimate coefficient of discharge of an orifice spillway.
- 6. Verification and validation of the proposed equation with real life orifice spillway projects.
- 7. To develop non dimensional plots in respect of discharging capacity, pressures on bottom and roof profile and water surface profiles.

Fig. 4.1 Methodology adopted for basic research study

#### a) Set up 1



## b) Set up 2



## c) Set up 3

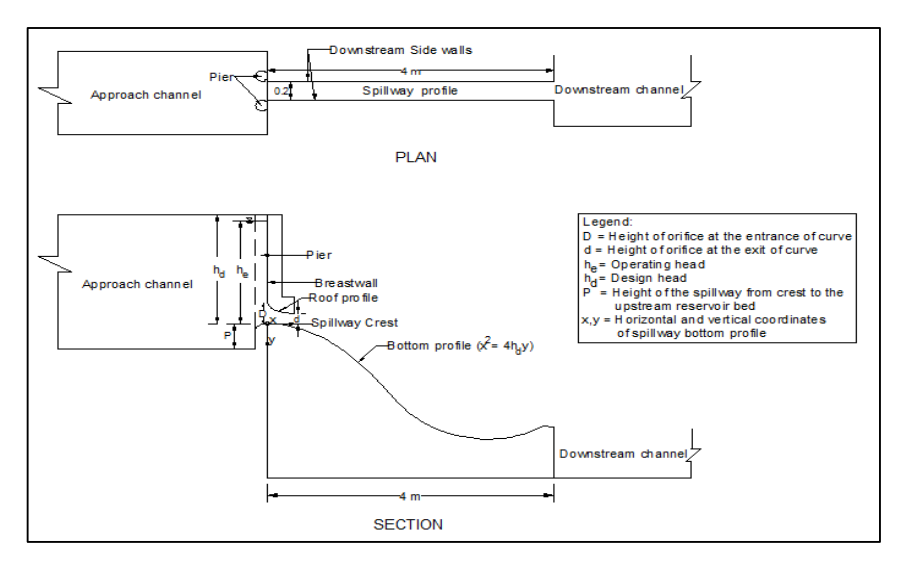


Fig. 4.2 Plan and section for physical/numerical model

#### 4.2 Physical model set up -1

To study the profiles of an orifice spillway, the basic experiments on flow through sharp edged large orifice have been conducted. The physical model was constructed in a 1 m wide and 10 m long flume at Central Water and Power Research Station (CWPRS), Pune, India. The sharp edged weir of width 0.13 m and height (P) 0.2 m was fixed at the bottom of the channel. A vertical sharp edged plate of height 1 m was placed above the sharp edged weir. The plate was kept movable to change the height of the orifice opening so created. The model was constructed in 12 and 15 mm thick transparent Perspex sheet to visualize the flow conditions. The height of the weir (P) was kept constant for all the experiments i.e. 0.2 m. The height of orifice (D) was varied from 0.2 m to 0.4 m and head in the range of 0.5 m to 0.8 m. The Reynolds number calculated for the corresponding dimensions was 9 x10<sup>5</sup> which was found quite above the value suggested (Re  $> 10^{5}$ ) by many researchers to ensure turbulent flow conditions in the model (USBR, 1980; Pfister and Chanson, 2014). The downstream side walls were kept in line with orifice, which will act as a divide wall for further study. Figure 4.2 a shows plan and section of experimental set up-1. Experiments were carried out for different heads and heights of orifice as shown in Table 4.1. The water levels corresponding to particular head were maintained in the upstream channel and water was allowed to flow freely from the sharp edged orifice in the downstream channel. Experiments were carried to measure the discharge flowing through the orifice openings and to determine lower and upper profiles of the jet issuing from sharp edged large orifice opening. The discharge flowing through the orifice opening was measured using a Rehbock plate. The lower and upper nappe profiles of the jet through orifice were marked on the transparent Perspex sheet provided on either side of the orifice jet. The profiles were then measured using a point gauges throughout the length of jet. Figure 4.3 shows the flow condition through orifice in physical model.

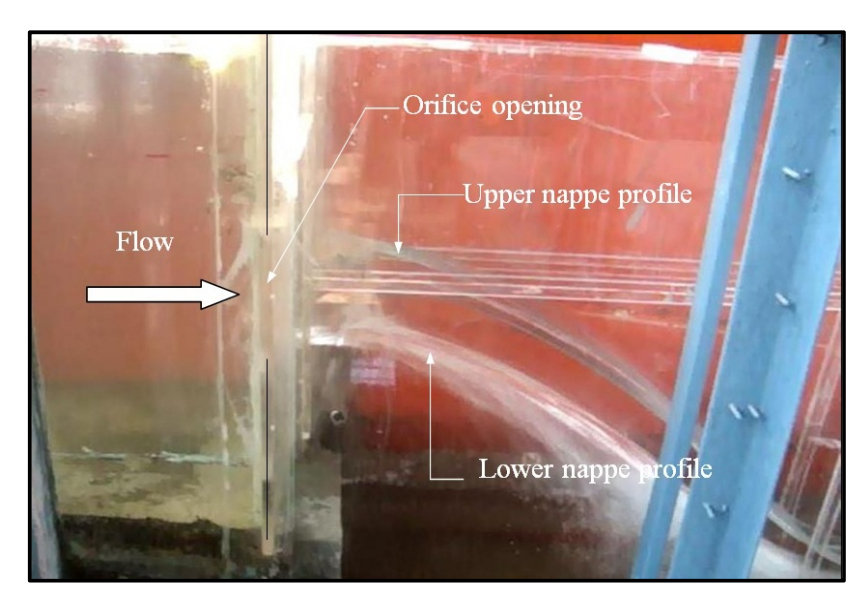


Fig. 4.3 Flow conditions through orifice in physical model

## 4.3 Numerical model set up-1

The Computational Fluid Dynamics module of the FLUENT version 6.3.26 (FLUENT, 2006) has been used for the numerical simulation. The geometry of the model was created in GAMBIT software. The geometry of the model consisted of an upstream tank, a sharp edged orifice and a downstream channel, same as the one studied on physical model setup 1. Generation of geometry was carried out by creating points, edges, faces and volumes of the geometry in three dimensions. The domain extended 2 m upstream and downstream of the orifice to capture the path of the jet after leaving the sharp edged orifice opening. The domain height above the water surface was considered as 0.2 m to capture the air-water interface phenomena. The numerical model has been studied for height of orifice opening of 0.26 m and 0.4 m. However, the ranges of design heads are varied from 0.6 m to 1.2 m. Table 4.1 shows the list of the experiments and simulations carried out using physical and numerical model set up 1.

Table 4.1 List of experiments/simulations carried out on physical and numerical model

Physical model studies									
G. N	D (m)	Design head, h <sub>d</sub> (m)							
Sr. No		0.5	0.6	0.7	0.8	1.2			
1	0.20	$\sqrt{}$	V	V	V	X			
2	0.24	$\sqrt{}$	V	V	V	X			
3	0.26	$\sqrt{}$	V	V	V	V			
4	0.28			V	V	X			
5	0.30			V	V	X			
6	0.32		V	V	V	X			
7	0.36		V	V	V	X			
8	0.40		V	V	V	V			
Numerical model studies									
1	0.26	X	<b>√</b>	V	V	V			
2	0.40	Х		<b>√</b>		V			

#### 4.3.1 Grid size and boundary conditions

In a CFD numerical model, a mesh is a subdivision of the flow domain into relatively small regions called cells (grid), in which numerical values such as velocity and pressure are computed. Determining the appropriate mesh domain along with a suitable grid size is a critical part of any numerical model simulation. Grid size can affect both the accuracy of the results and the simulation time. Hexahedral mesh was used in entire domain. The boundary

conditions were selected carefully, since poorly defined boundary conditions can have a significant impact on the solution. Pressure inlet boundary condition with turbulence intensity and viscosity ratio 1% was used at the domain inlet through which the water enters in the tank. The turbulence intensity was considered as 1%, since the flow was supposed to enter the reservoir with minimum turbulence as expected in a large reservoir. The upstream head in the tank was maintained at the domain inlet. The top of the tank was defined as the pressure inlet boundary condition. The wall boundary with no slip condition was applied to the bottom and sides of the upstream tank and downstream channel. Pressure outlet boundary condition with turbulence intensity and viscosity ratio of 10% was defined at domain outlet. A set of 'backflow' conditions is also specified to be used if the flow reverses direction at the pressure outlet boundary during the solution process. The default value of this field is Normal to Boundary, and requires no further input. Figure 4.4 shows the grid generation and the boundary conditions applied at various faces of the entire domain.

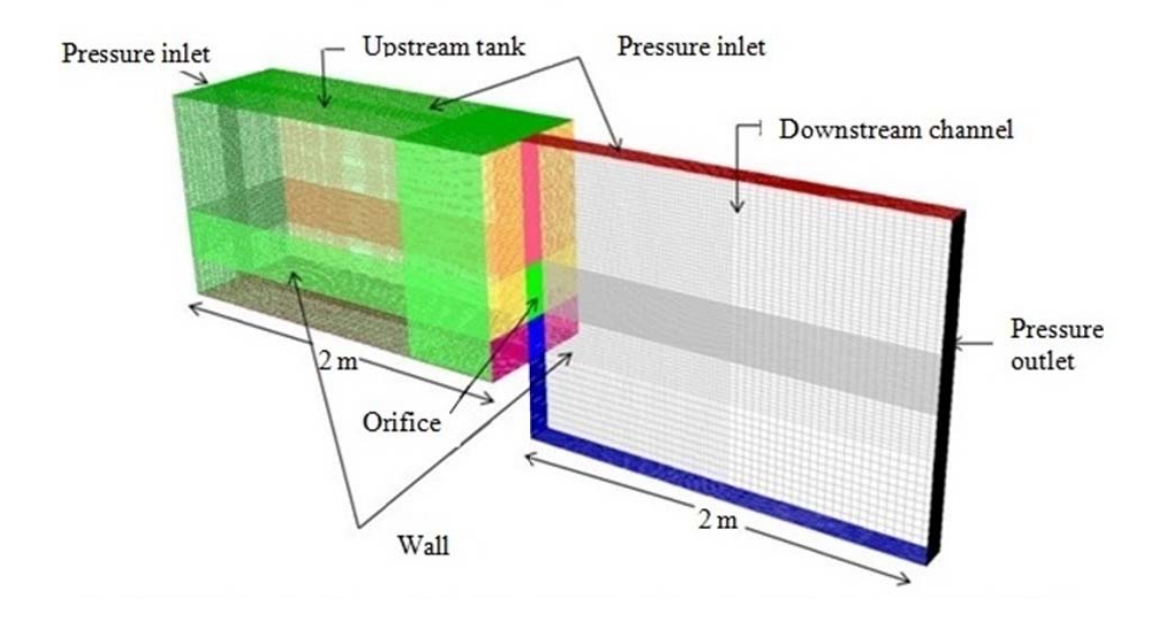


Fig. 4.4 Grid generation and boundary conditions

It is important to minimize the amount of cells while including enough resolution to capture the important features of the geometry as well as sufficient flow detail. An effective way to determine the critical grid size is to start with a relatively large grid and then progressively reduce the grid size until the desired output no longer changes significantly with any further reductions in grid size. In the present study, coarse grid of size of 0.07 m and finer grid size of 0.004 m with the mesh count of 11,370 and 26, 07,660 respectively were used for the simulation. The results obtained from grid convergence study are discussed in following sections.

#### 4.3.2 Set up in FLUENT

Once the grid and boundary conditions are defined, the geometry is exported into FLUENT software. In the present study, the most widely adopted solver namely segregated pressure based solver has been used. The absolute velocity formulation is preferred in applications where the flow in most of the domain is not rotating and hence used for the present application. The implicit method was opted to solve the equations simultaneously to arrive at unknown quantities. The flow through orifice has been considered as unsteady flow. The rate of change of flow characteristics has been studied until equilibrium is reached.

The atmospheric pressure is taken 101325 Pascal and acceleration due to gravity is taken as  $9.81 \text{ m/s}^2$ . In addition, the density and the dynamic viscosity of the water were taken as  $998.2 \text{ kg/m}^3$  and 0.001003 kg/m-s, respectively. The density and dynamic viscosity of air is considered as  $1.225 \text{ kg/m}^3$  and  $1.7894 \times 10^{-05} \text{ kg/m/s}$ , respectively. Various turbulence models are available in FLUENT. The numerical model was verified in terms of turbulence models by comparing results with physical model. The turbulence models k- $\epsilon$  and k- $\omega$  were used in the simulation. However, RNG turbulence model was found to be suitable in analysing the flow through sharp edged large orifice.

The Volume of fluids (VOF) method (Hirt and Nichols, 1981) with modified High Resolution Interface Capturing (HRIC) scheme was used to capture air-water interface phenomena. This method is less expensive computationally. The method is designed for two or more immiscible fluids where the position of the interface between the fluids is of interest. In the VOF model, a single set of momentum equations is shared by the fluids, and the volume fraction of each of the fluids in each computational cell is tracked throughout the domain. In each cell, the sum of the volume fractions of air and water is unity. Before starting CFD solution, FLUENT needs a value with an initial 'guess' for the solution field. In the present simulation, solution was initialized with patch values for the water zone in the reservoir up to a selected reservoir water level.

The simulation was started with an initial time step of 0.001 second and continued till flow convergence was reached. The simulations were performed on a desktop computer with Intel core 3.29 GHz i7 CPU and 8 GB of RAM. During the simulations, convergence of residuals and volume flow rate at the orifice opening were monitored. Once the convergence is reached, data was extracted in the form of discharge and water surface profiles.

## 4.3.3 Grid convergence study

The grid convergence study was carried out to finalise the grid size for present problem. Table 4.2 shows the effect of grid size on discharge of flow through sharp edged

orifice. Figures 4.5 and 4.6 show the effect of grid size on lower as well as upper nappe profile. Similarly, Figures 4.7 and 4.8 shows flow condition for coarse and fine grid size respectively. From the figures, it can be concluded that grid size is an important parameter for getting accuracy of results. The results are found to be more accurate for the fine grid than the coarser grid size. The results computed with grid size 0.004 m was found to be closer to the results obtained in physical model. Numerical model was also verified in terms of grid convergence index based on ASME guidelines. Based on the results, grid size 0.004 m was used for further simulations.

Table 4.2 Effect of grid size on discharge of flow through sharp edged large orifice

Grid Size		Discharg			
(m)	Mesh Count	Numerical model	Physical model	% error	
0.07	11,370	0.091		5.8	
0.05	28,080	0.091	0.086	5.8	
0.03	1,32,990	0.089		3.5	
0.02	4,76,000	0.088		2.3	
0.01	14,27,368	0.087	0.080	1.2	
0.007	21,17,010	0.086		0	
0.005	24,60,750	0.086	]	0	
0.004	26,07,660	0.086		0	

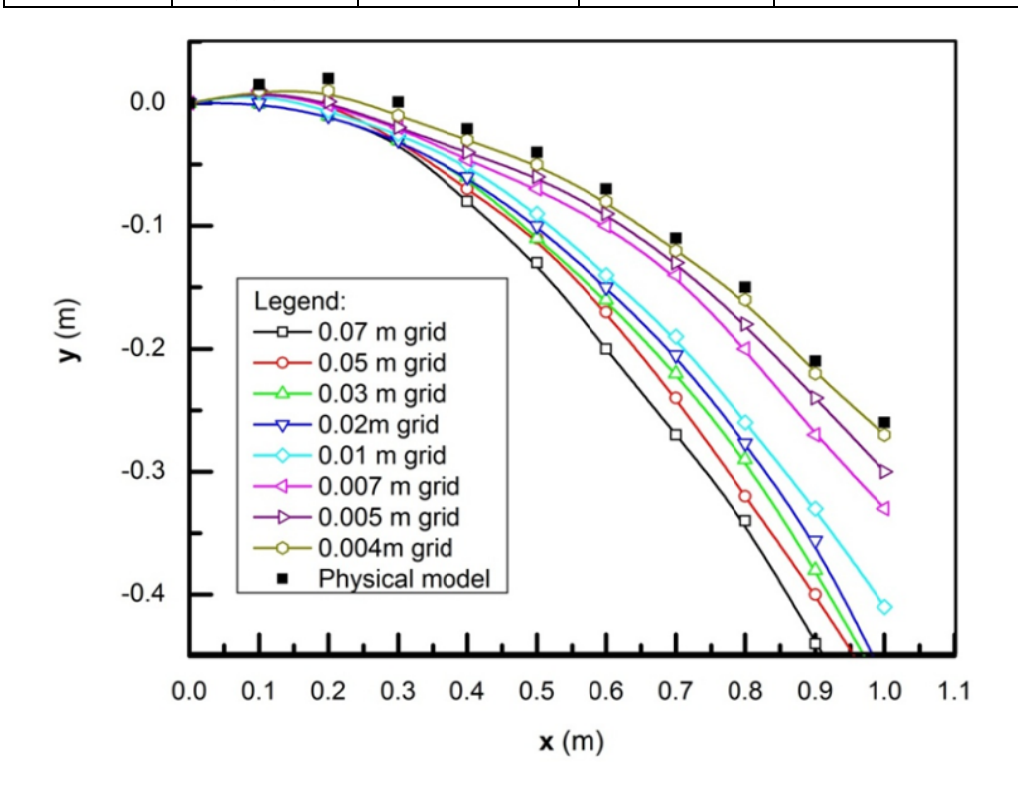


Fig. 4.5 Effect of grid size on lower nappe profile

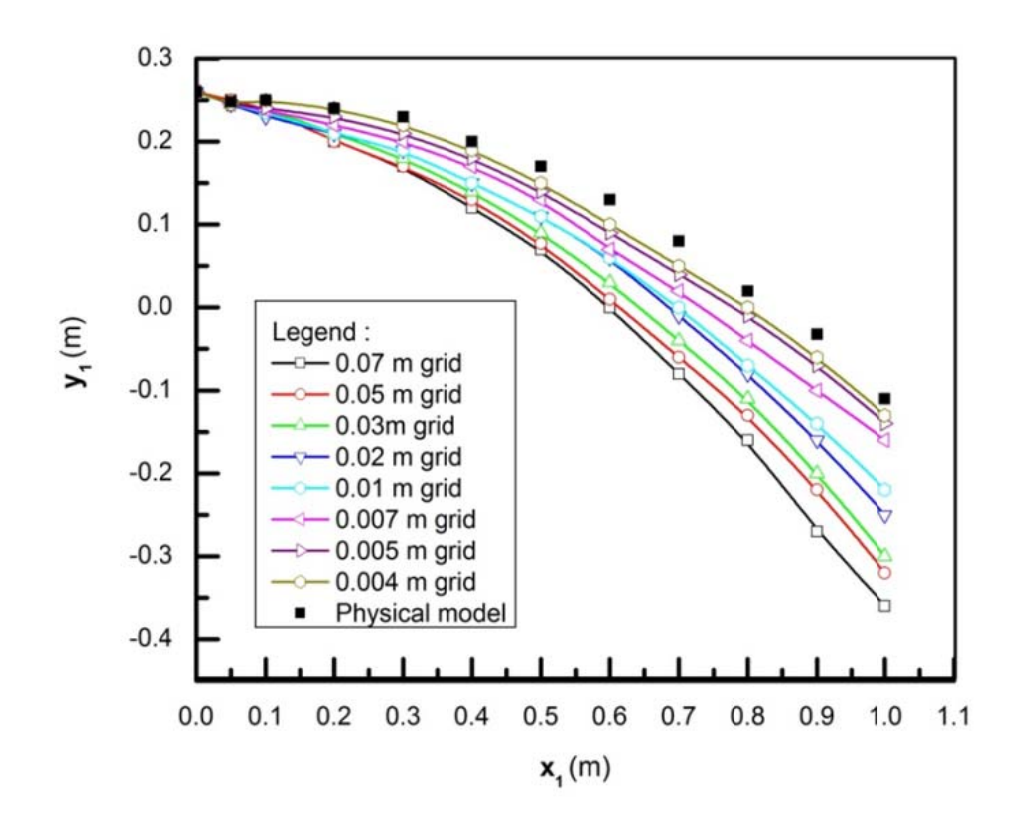


Fig. 4.6 Effect of grid size on upper nappe profile

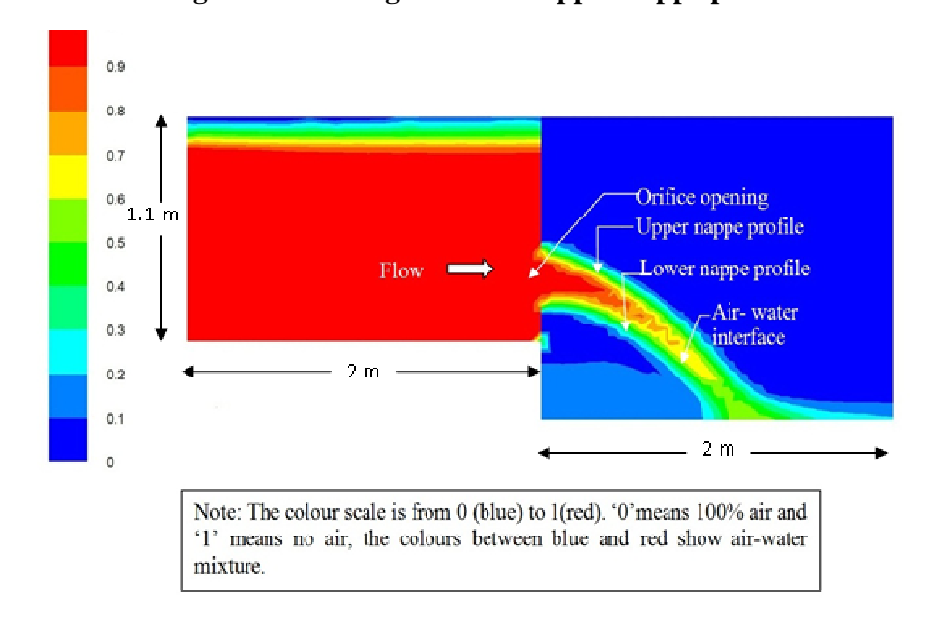


Fig. 4.7 Flow conditions for grid size 0.07 m

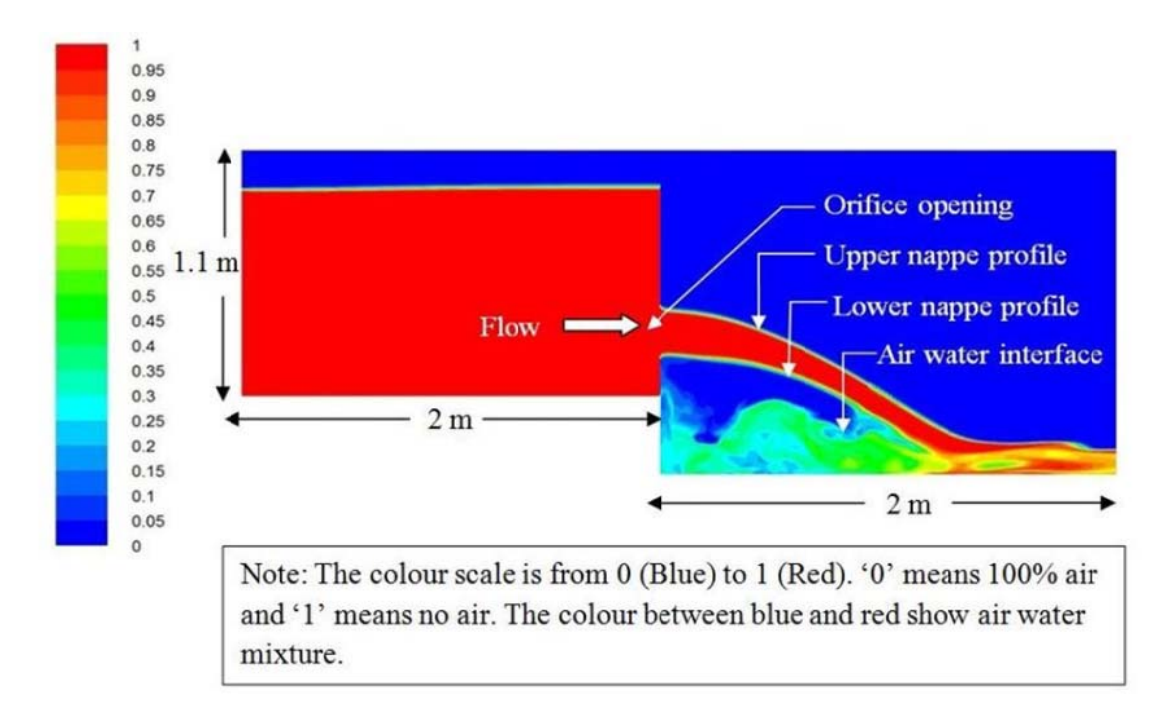


Fig. 4.8 Flow conditions for grid size 0.004 m

It is concluded from the above study that numerical model developed for grid size 0.004 m could capture the flow conditions and compute the discharge and wter surface profile same as that observed in physical model. Based on this, the physical and numerical model results were combined and used for further analysis.

# 4.4 Results from set up-1

Numbers of physical and numerical model studies were carried out for various orifice heights and operating heads to investigate the flow through sharp edged large orifice. The results were analysed in the form of important hydraulic coefficients affecting the flow through orifice such as coefficient of velocity and coefficient of discharge and lower and upper nappe profiles of the jet issuing from sharp edged orifice. The main aim in this experimental set up was to finalize the bottom and roof profile of an orifice spillway from the results of lower and upper nappe profile of sharp edged orifice respectively obtained in physical and numerical model. In view this, the results obtained from physical and numerical model was combined and compared with the data of the available literature. Based on the comparison, the bottom profile of the orifice spillway was finalized from the results of lower nappe profile. However, a further need was identified in respect of investigation of upper nappe profile for evolving the equation of roof profile of orifice spillway.

#### 4.4.1 Coefficient of discharge $(C_d)$ and coefficient of velocity $(C_v)$

Coefficient of discharge and coefficient of velocity are two important hydraulic coefficients in analysing the flow through sharp edged large orifice. Coefficient of discharge is an indicator of the efficiency of the orifice. The  $C_d$  was calculated by using following discharge formula:

$$Q = C_d A \sqrt{2gh_{cl}} \tag{4.1}$$

Where, Q is the discharge passing through sharp edged orifice, 'A' is area of orifice and h<sub>cl</sub> is the centreline head.

Coefficient of velocity was calculated by using the following formula which represents the physics of the flow through sharp edged orifice.

$$C_v^2 = \frac{x^2}{4vh_{cl}} \tag{4.2}$$

In the above formula x and y are the horizontal and vertical distance of the jet,  $h_{cl}$  is the centerline head and  $C_v$  is the coefficient of velocity. The coordinates of x and y measured at the horizontal distance of about 0.9 m downstream of the vena contracta section were considered to determine the value of  $C_v$ .

Table 4.7 shows the values of  $C_d$  and  $C_v$  calculated in physical model. It was found that for a particular height of orifice, the value of  $C_d$  increases with increase in the head. The value of coefficient of discharge was varying in the range of 0.60 to 0.66 which was found to be very close to the values of 0.61 to 0.66 reported in the literature of sharp edged large orifice (Som and Biswas (2004), Bansal (2010)). Hence, the results of physical and numerical model studies carried out confirm the coefficient of discharge of large orifice available in literature. In the present study, coefficient of velocity ( $C_v$ ) is found to be in the range of 0.89 to 1 as the orifice is large. The values for coefficient of velocity were further used to finalise the bottom profile of an orifice spillway.

Table 4.3 Values for coefficient of discharge, coeffcient of velocity and factor k observed on physical model

D(m)	h <sub>d</sub> (m)	$C_d$	$\mathbf{C}_{\mathbf{v}}$	k
	0.5	0.62	0.93	3.46
0.20	0.6	0.63	0.95	3.60
0.20	0.7	0.64	0.96	3.80
	0.8	0.60	0.99	3.94
	0.5	0.61	0.91	3.31
0.24	0.6	0.61	0.91	3.33
0.24	0.7	0.62	0.92	3.35
	0.8	0.62	0.93	3.46
	0.5	0.62	0.89	3.17
0.26	0.6	0.62	0.90	3.24
0.26	0.7	0.63	0.95	3.93
	0.8	0.63	0.98	3.87
	0.5	0.62	0.99	3.89
0.20	0.6	0.63	0.99	3.92
0.28	0.7	0.64	0.99	3.92
	0.8	0.64	1.00	4.00
	0.5	0.60	0.91	3.31
0.32	0.6	0.61	0.92	3.41
0.52	0.7	0.63	0.94	3.51
	0.8	0.64	0.96	3.65
	0.5	0.62	0.92	3.40
0.26	0.6	0.63	0.94	3.54
0.36	0.7	0.64	0.95	3.64
	0.8	0.65	0.97	3.76
	0.5	0.62	0.92	3.39
0.40	0.6	0.63	0.93	3.47
0.40	0.7	0.64	0.95	3.60
	0.8	0.65	0.97	3.75

#### 4.4.2 Lower nappe profile

The lower and upper nappe profiles obtained from physical model for height of orifice of 0.26 m and 0.4 m were compared with numerical model results, the profiles proposed by Hu et al. (1990) and parabolic profile of orifice spillway i.e.  $x^2 = 4h_{cl}y$  (BIS 6934: 1998). The lower nappe profile measured after vena contracta section was considered for comparison as it may be useful in designing bottom profile of an orifice spillway. The comparison was made to develop a guideline for fixing the spillway bottom profile. The results were plotted in terms of dimensionless parameters x/D and y/D, where, x and y are the horizontal and vertical distance of the jet in meter from sharp edged large orifice and y is height of large orifice opening. Figure 4.9 show the comparison of lower nappe profile of height of orifice of 0.26 m for the heads of 0.6 m, 0.7 m, 0.8 m and 1.2 m. Figure 4.10 show the comparison of lower nappe profile of height of orifice of 0.4 m for the heads of 0.6 m, 0.7 m, 0.8 m and 1.2 m. All the profiles were plotted considering origin (0, 0) at the bottom of sharp edged orifice opening.

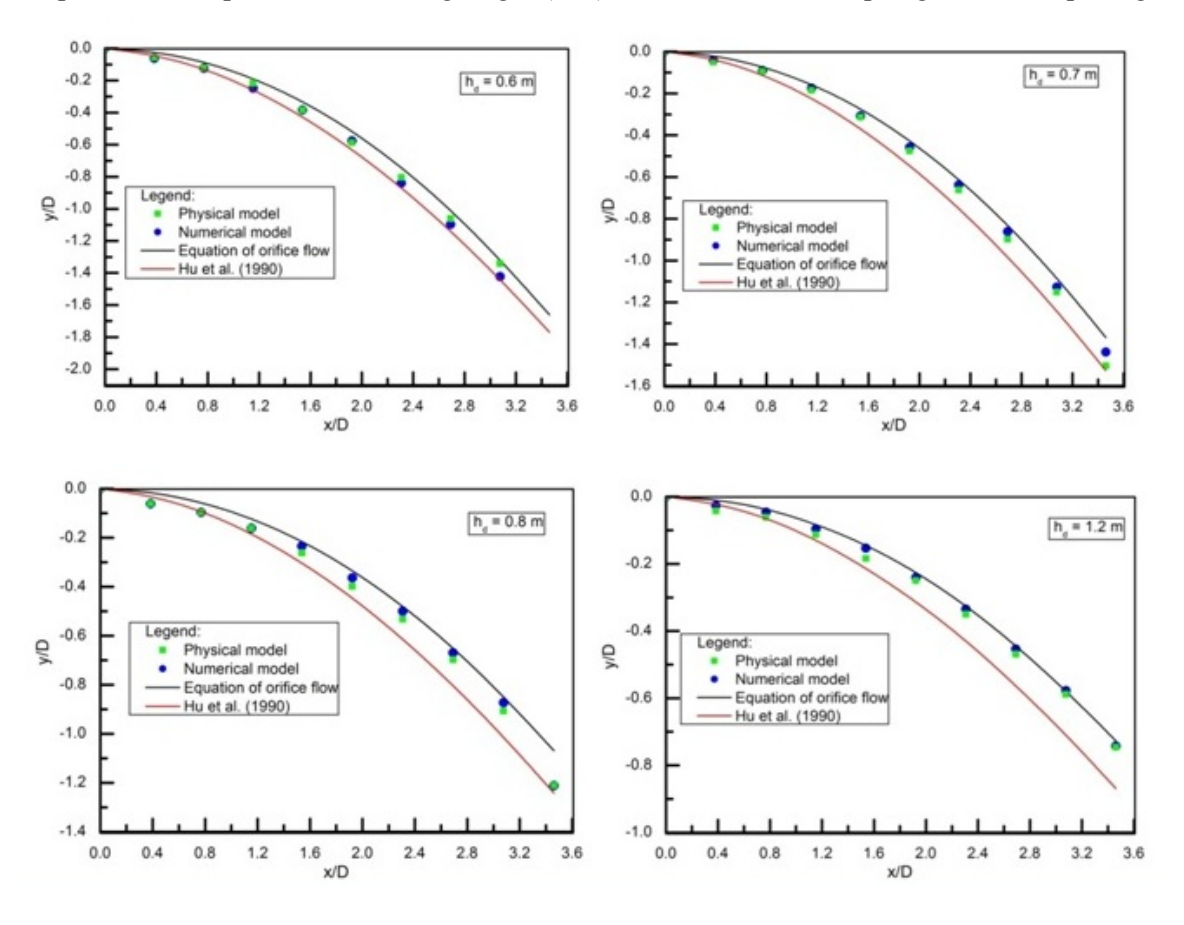


Fig. 4.9 Comparison of lower nappe profile for d = 0.26 m

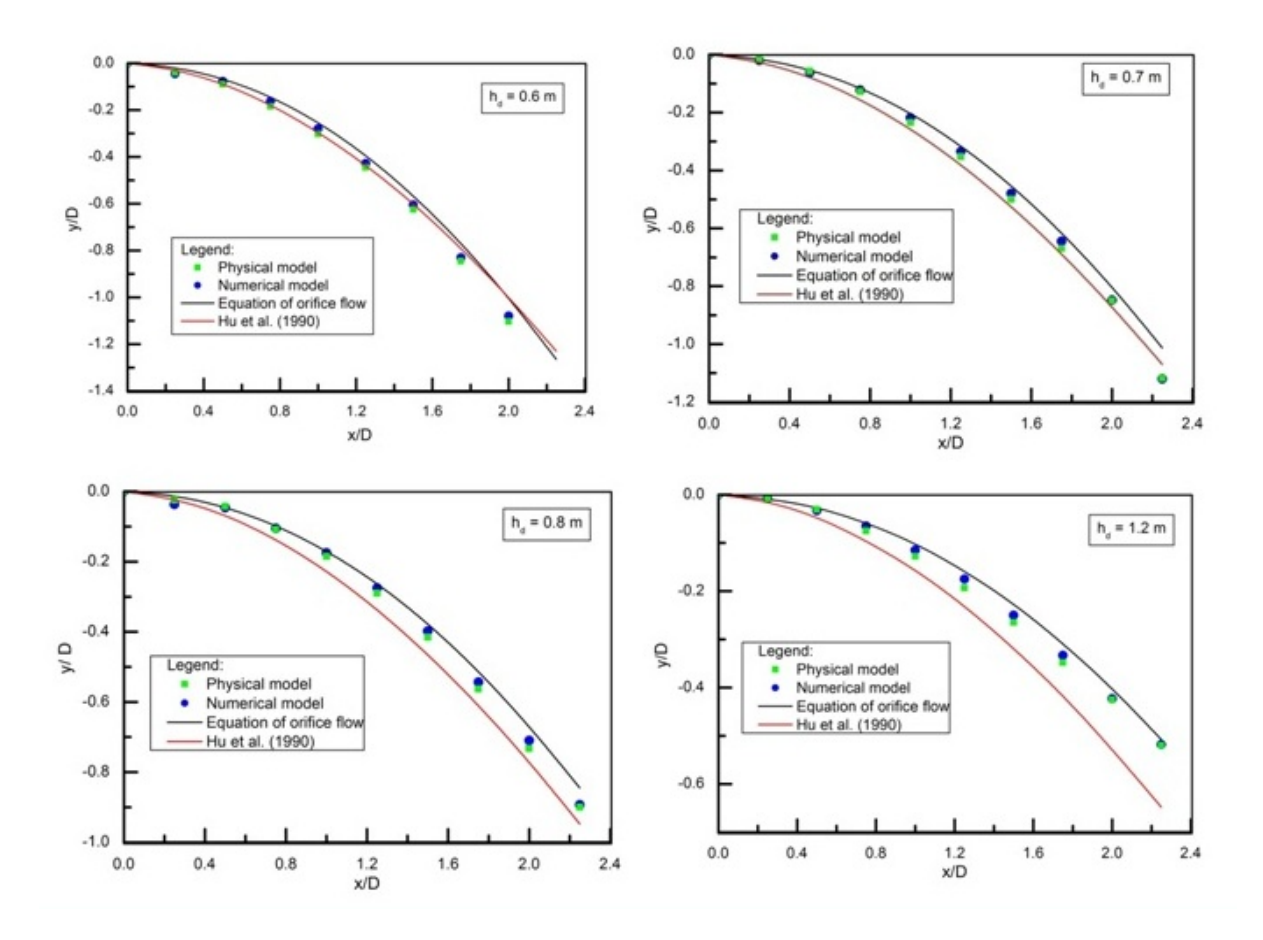


Fig. 4.10 Comparison of lower nappe profiles for d = 0.40 m

From Figures 4.9 and 4.10, it is found that the lower nappe profiles generated using numerical simulation were close to the results of physical model studies. The comparison shows that the profiles computed from the equations proposed by Hu et al. (1990) are steeper than the ones computed in the present study for entire range of design heads and heights of orifice. The difference in values increases with increasing head and height of the orifice. This difference can be due to the small range of heights of orifice i.e. 0.12 m to 0.24 m and design heads i.e. 0.36 m to 0.72 m studied by Hu et al. (1990). Most of the dams in India are planned for heads higher than 0.8 m (40 m in prototype). Due to high design discharge the height of orifice is also increasing from 0.6 to 1.4 m (30 to 70 m in prototype). Thus, there is a need to study the bottom profile of orifice spillway for large heads and larger orifice openings.

There was a small variation in the results obtained in present study from the equation of orifice flow i.e.  $x^2 = 4h_{cl}y$ . In orifice spillway, the parabolic profile having an equation  $x^2 = kh_{cl}y$  is generally provided as a bottom profile of orifice spillway. Most of the available literature on flow through sharp edged orifice reports the value of coefficient of velocity as 1 or nearly equal to one (Judd and King (1908), Lienhard V and Lienhard IV (1984)). Hence, the equation of spillway bottom profile of an orifice spillway becomes  $x^2 = 4h_{cl}y$  (BIS 6934:

2010). However, in the present study, coefficient of velocity (C<sub>v</sub>) is found to be in the range of 0.894 to 1. The changes in  $C_v$  will result in change in k value (where  $k = 4C_v^2$ ) and will affect the bottom profile of spillway. The data in respect of variation of k value for varying heads and orifice heights also could not be found explicitly in the available literature. In the present study, k values corresponding to C<sub>v</sub> were calculated for various range of heads and orifice height as shown in the Table 4.7. The value of factor k is not exactly 4 as normally used to compute the orifice profile, but rather varies between 3 and 4. The curve becomes steeper with k value of 3 than 4. The results also indicated that bottom profile of orifice with k value of 3 and 4 are flatter than the equation used for the ogee profile ( $x^{1.85} = kh_a^{0.85}y$ ) with the k value of 2 for the vertical upstream face of an overflow spillway. The steep profile increases the coefficient of discharge, but at the same time there may be a possibility of sub atmospheric pressures prevailing on the spillway surface. Hence, the equation of the ogee profile recommended by USBR cannot be used directly for the orifice spillway. However, the k value calculated in the range of 3 to 4 from sharp edged large orifice may be useful for designing spillway bottom profile of an orifice spillway in the form of an equation  $x^2 = kh_{cl}v$ or  $x^2 = kh_dy$ .

#### 4.4.3 Upper nappe profile

Similar to the lower nappe profile, the upper nappe profile was also plotted in non-dimensional form with respect to height of orifice D. Figure 4.11 show the comparison of upper nappe profile of height of orifice of 0.26 m for the heads of 0.6 m, 0.7 m, 0.8 m and 1.2 m. Similarly, Figure 4.12 show the comparison of upper nappe profile of height of orifice of 0.4 m for the heads of 0.6 m, 0.7 m, 0.8 m and 1.2 m. In these Figures,  $x_1$  and  $y_1$  are the horizontal and vertical distances of jet in m by considering the origin at the top of the orifice opening. The comparison of the results were made between physical model, numerical model and available equations in the literature proposed by Hu et al. (1990) and USBR (1987). The elliptical profile suggested by USBR (1987) for pressurized sluice flows was generally adopted to design the roof profile of an orifice spillway. It may be mentioned here that USBR profile is in the form of quarter of an ellipse and not related with variation of head. Hence, only one profile could be plotted in case of USBR.

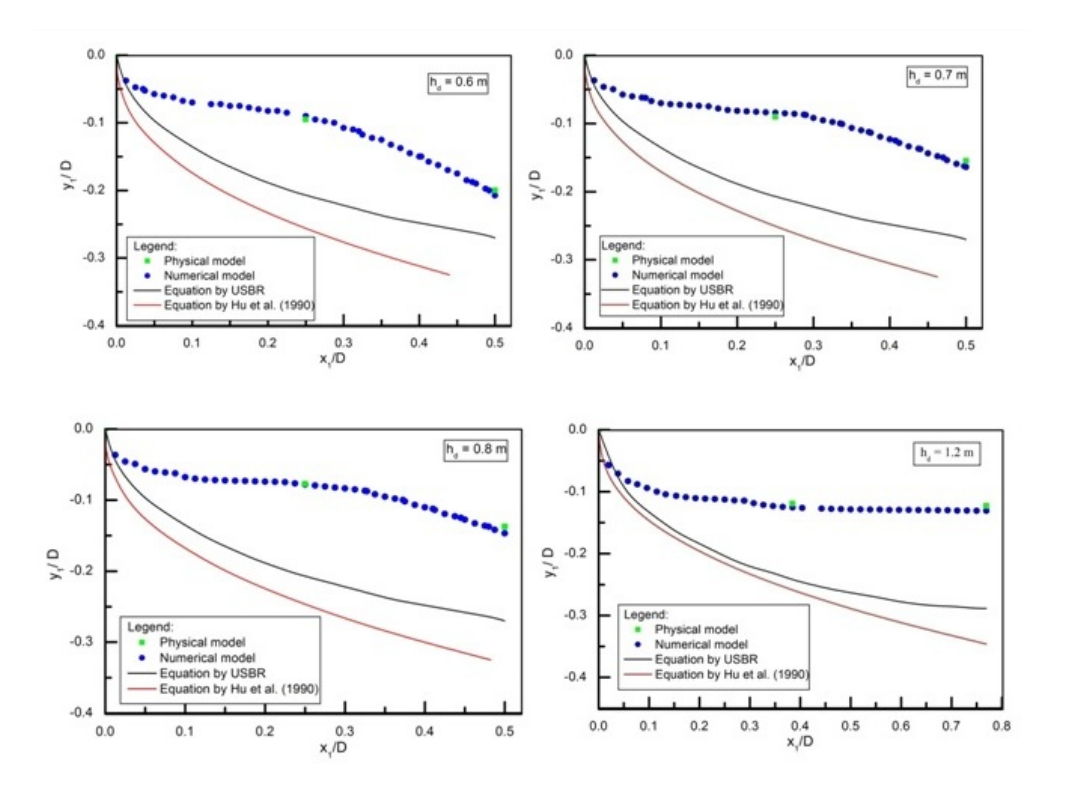


Fig. 4.11 Comparison of upper nappe profile for d = 0.26 m

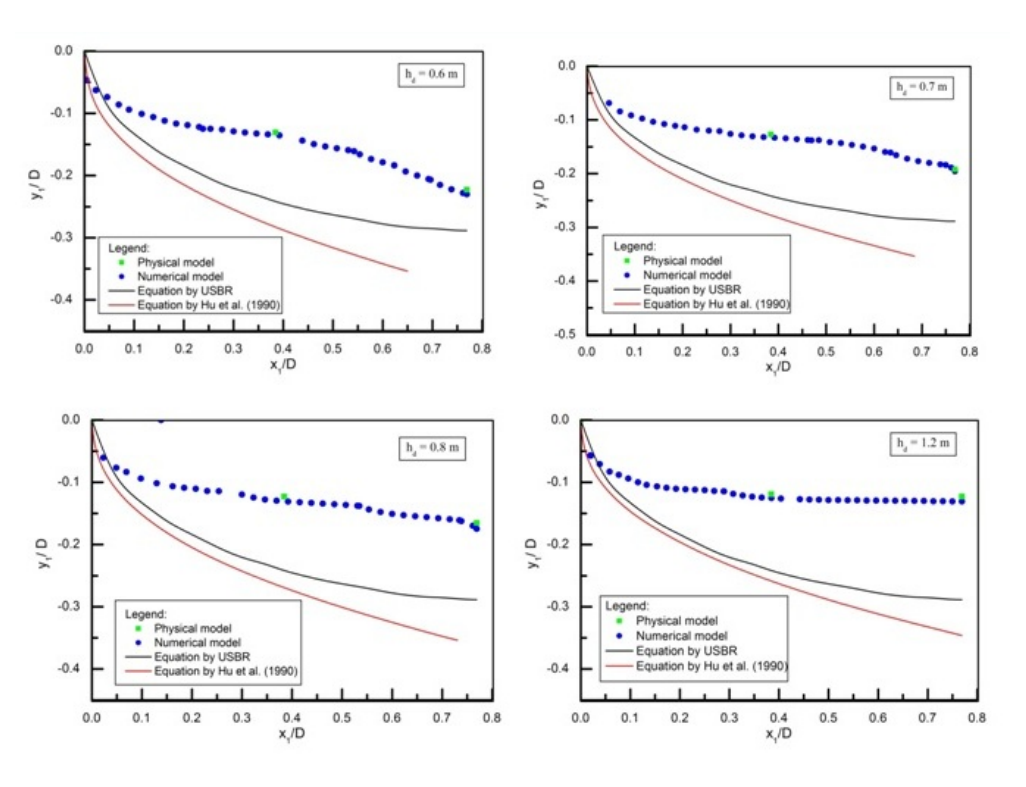


Fig. 4.12 Comparison of upper nappe profile for  $d=0.40\ m$ 

Figures 4.11 to 4.12 indicate that there is close agreement in the values of upper nappe profile obtained from physical and numerical model studies for all the combinations. Hence, CFD model can be used as a complementary tool for modelling flow through sharp edged large orifice. However, there is a large deviation in the profiles obtained from the present research and values proposed by Hu et al. (1990) and USBR (1987). This is because the profiles are developed by considering the bottom profile of the spillway as a solid boundary. However, in the present study the profiles are calculated through sharp crested orifice without fixing the solid bottom spillway profile. Due to large difference in the values obtained from the present study and available literature, the upper nappe profiles computed from the study cannot be used directly to fix the roof profile of an orifice spillway. However, it is necessary to study the orifice flow with a solid bottom profile to develop guidelines for the design of the roof profile. Hence, further studies have been taken up in set up 2 with solid bottom profile conforming to the equation  $x^2 = 4h_dy$  (k = 4) using physical and numerical model for various combinations of heads and height of orifice opening. Physical and numerical model set up and the results obtained from the studies have been discussed in following sections.

# 4.5 Physical and numerical model set up-2

In this set up-2, the studies through orifice were carried out by providing the solid spillway bottom profile at the downstream of sharp edged orifice opening, upstream curve in the form of an ellipse and semi-circular shaped pier. A sharp edged plate of width 0.2 m was fixed at a height (P) of 0.4 m from the bottom of the channel. A vertical sharp edged plate of height 1.5 m was placed above the sharp edged weir. The plate was kept movable to change the height of the orifice opening. The width of span was kept as 0.2 m. Bottom profile of spillway is in the form of  $x^2 = 4h_d y$ , where,  $h_d$  is the design head and x and y are horizontal and vertical coordinates of the spillway profile considering origin (0,0) at spillway crest. The curve is followed by straight line and circular ski jump bucket to lift the flow to the downstream channel. The roof profile of orifice spillway was not introduced while conducting the experiments. The side walls were provided at the downstream of sharp edged orifice on both the sides, which will represent pier and training wall in prototype structure. Hence, an effect of side walls has been considered in analysing the flow.

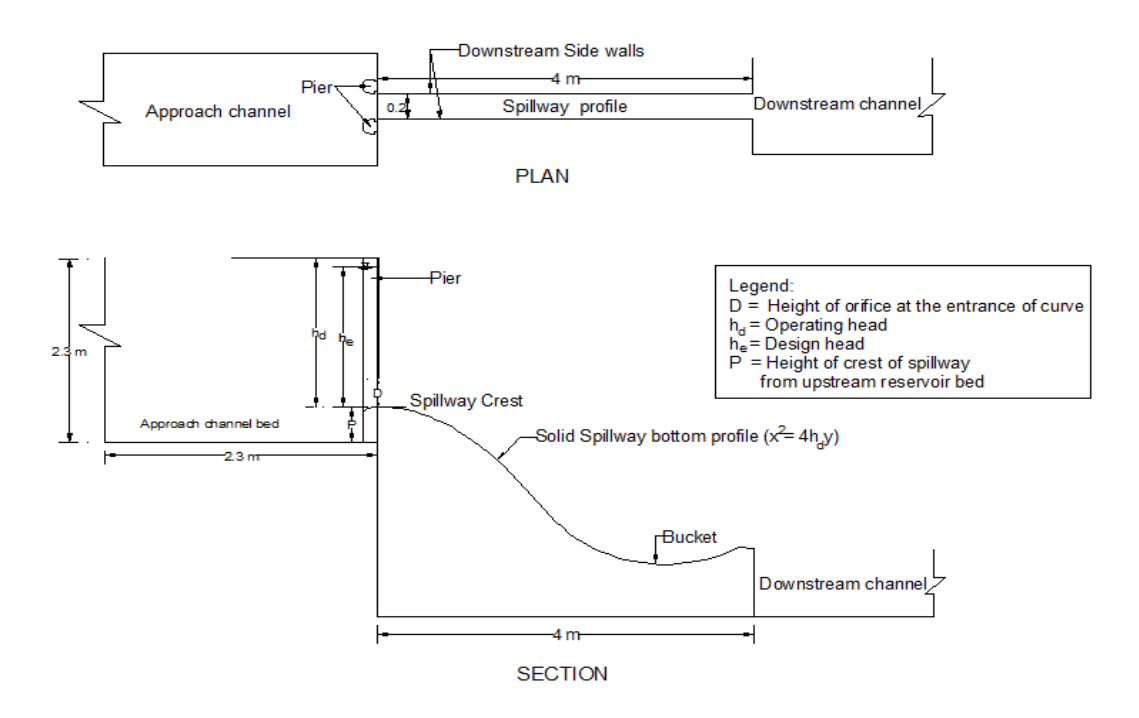


Fig. 4.13 Plan and section for physical/numerical model set up 2

An upstream channel of height 2.3 m and width 1.4 m was constructed in 15 mm thick Perspex sheet to visualize the approach flow conditions. The approach channel was connected to a 7 m (L) x 8 m (W) x 2.3 m (H) steel tank as shown in Figure 4.13. Two pumps of capacity 10 ft<sup>3</sup>/s were connected to the steel tank for supply of water. The spillway was fitted to one of the sides of the tank. The flume of the spillway channel was also constructed in 15 mm thick transparent Perspex sheet to visualize the flow conditions throughout the length of the spillway. The downstream channel of width 1 m was constructed in brick masonry at the end of the spillway channel. Figure 4.13 shows a plan and section of physical/numerical model for set up 2.

The main aim of the present experimental set up i.e. Set up 2 is to develop an equation for design of roof profile of an orifice spillway. It is aimed to cover all possible ranges of design heads ( $h_d$ ) and heights of orifice (D) generally adopted on most of the orifice spillway projects. In view of this, physical and numerical model studies were carried out for various combinations of heads and heights of orifice opening. Flow through orifice spillway was analysed for the spillway bottom profiles designed for head i.e.  $h_d$  of 0.6 m, 0.8 m, 1.0 m and 1.4 m at different spillway operating conditions i.e.  $h_e/h_d=0.8$ , 1 and 1.33. Heights of orifice opening were selected as 0.2 m, 0.28 m and 0.32 m for the study. Table 4.4 shows list of experiments/simulations carried out using physical and numerical models.

In Table 4.4, 'h<sub>d</sub>' is design head, 'h<sub>e</sub>' is operating head, 'D' is height of orifice at the orifice entrance and 'P' is height of spillway crest from upstream reservoir bed. As indicated in Table 4.4, experiments on the physical model were conducted for the design heads 0.6 m and 0.8 m and height of orifice openings of 0.2 m, 0.28 m and 0.32 m. However, numerical

simulations were carried out for the design heads 0.6 m, 1.0 m and 1.4 m and height of orifice openings of 0.2 m, 0.28 m and 0.32 m. Computational Fluid Dynamics software FLUENT version 6.3.26 was used for the numerical simulation.

Table 4.4 List of experiments/simulations carried out using physical and numerical model set up-2

Physical Model					Numerical Model					
Experiment No.	h <sub>d</sub> (m)	<b>D</b> (m)	h <sub>e</sub> /h <sub>d</sub>	P (m)		Simulation No.	$\mathbf{h}_{\mathrm{d}}\left(\mathbf{m}\right)$	<b>D</b> (m)	h <sub>e</sub> /h <sub>d</sub>	<b>P</b> (m)
1	0.6	0.2	0.8	0.4		1	0.6	0.2	0.8	0.4
2	0.6	0.2	1	0.4		2	0.6	0.2	1	0.4
3	0.6	0.2	1.33	0.4		3	0.6	0.2	1.33	0.4
4	0.6	0.28	0.8	0.4		4	0.6	0.28	0.8	0.4
5	0.6	0.28	1	0.4		5	0.6	0.28	1	0.4
6	0.6	0.28	1.33	0.4		6	0.6	0.28	1.33	0.4
7	0.6	0.32	0.8	0.4		7	0.6	0.32	0.8	0.4
8	0.6	0.32	1	0.4		8	0.6	0.32	1	0.4
9	0.6	0.32	1.33	0.4		9	0.6	0.32	1.33	0.4
10	0.6	0.2	0.8	0.2		10	1	0.2	0.8	0.2
11	0.6	0.2	1	0.2		11	1	0.2	1	0.2
12	0.6	0.2	1.33	0.2		12	1	0.2	1.33	0.2
13	0.6	0.28	0.8	0.2		13	1	0.28	0.8	0.2
14	0.6	0.28	1	0.2		14	1	0.28	1	0.2
15	0.6	0.28	1.33	0.2		15	1	0.28	1.33	0.2
16	0.6	0.32	0.8	0.2		16	1	0.32	0.8	0.2
17	0.6	0.32	1	0.2		17	1	0.32	1	0.2
18	0.6	0.32	1.33	0.2		18	1	0.32	1.33	0.2
19	0.8	0.2	0.8	0.2		19	1.4	0.2	0.8	0.2
20	0.8	0.2	1	0.2		20	1.4	0.2	1	0.2
21	0.8	0.2	1.33	0.2		21	1.4	0.2	1.33	0.2
22	0.8	0.28	0.8	0.2		22	1.4	0.28	0.8	0.2
23	0.8	0.28	1	0.2		23	1.4	0.28	1	0.2
24	0.8	0.28	1.33	0.2		24	1.4	0.28	1.33	0.2
25	0.8	0.32	0.8	0.2		25	1.4	0.32	0.8	0.2
26	0.8	0.32	1	0.2		26	1.4	0.32	1	0.2
27	0.8	0.32	1.33	0.2		27	1.4	0.32	1.33	0.2
	Total number of studies = 54									

Experiments were carried out to analyse the flow through the spillway in terms of discharge and velocity at the orifice opening, upper nappe water surface profile and pressure distribution on the spillway surface. The pressure taps were located at the centre of spillway width for measuring the pressures over the spillway bottom surface. Pressures were measured using the piezometer board with plastic tube vented to the atmosphere. The accuracy of measurement was about 1mm. Water surface measurements were taken using pointer gauge along spillway profile. Velocity at the orifice opening was measured by using L-shaped Pitot tube. Special arrangement for holding the Pitot tube was also made. In physical model set up 2, the crest of the spillway (P) was kept at 0.4 m from the bed of the upstream approach channel for design head of 0.6 m at initial stage of experiments. The results obtained for P = 0.4 m were used for verification of numerical model. After completing the studies, the height of spillway was changed from 0.4 m to 0.2 m and experiments were repeated. This is done to investigate the effect of 'P' in determining the design of roof profile. The results obtained with variation of 'P' are discussed in subsequent sections.

Numerical model was verified only for one case i.e. spillway bottom profile designed for head (h<sub>d</sub>) of 0.6 m, height of orifice (D) of 0.2 m and h<sub>e</sub>/h<sub>d</sub> =0.8. However, numerical model was validated for the configurations other than the one used for verification in terms of turbulence model. The spillway profile designed for head of 0.6 m with the heights of orifice (D) 0.2 m, 0.28 m and 0.32 m and all spillway operating conditions were used for the study. Total 9 numbers of simulations with different D and h<sub>e</sub>/h<sub>d</sub> were used for validation. The results in terms of discharge, velocity, pressure over spillway bottom surface and water surface profiles computed using numerical model were compared with the results obtained using physical model. The results were found in good agreement. The physical models in the CFD code contain uncertainties due to a lack of complete understanding or knowledge of the physical processes. One of the models with the most uncertainty is the turbulence models. The uncertainty can be examined by running a number of simulations using different turbulence models and examine the effect on the results. The numerical model for the present set has been verified in terms of k-\varepsilon (Standard, Renormalization group (RNG) and Realizable) and k-ω turbulence models and using different volume of fraction (VOF)schemes. Based on the above comparison, Realizable k-ɛ turbulence model with Modified High Resolution Interface Capturing (HRIC) scheme was found to be suitable in analysing the flow over the spillway in respect all the parameters. Hence, it is used to run all the simulations mentioned in Table 4.4. The results obtained seem promising for an application of numerical models to the analysis of hydraulic behaviour of these structures. Hence, it can be concluded that numerical modelling or CFD can be used as a complementary tool along with the physical modelling for modelling the flow through orifice spillway. In view of this, numerical simulations were carried out for all the combinations of spillway bottom profiles designed for different heads, heights of orifice and spillway operating conditions mentioned in Table 4.4 for further studies. Figures 4.14 and 4.15 show flow conditions in physical and numerical model.

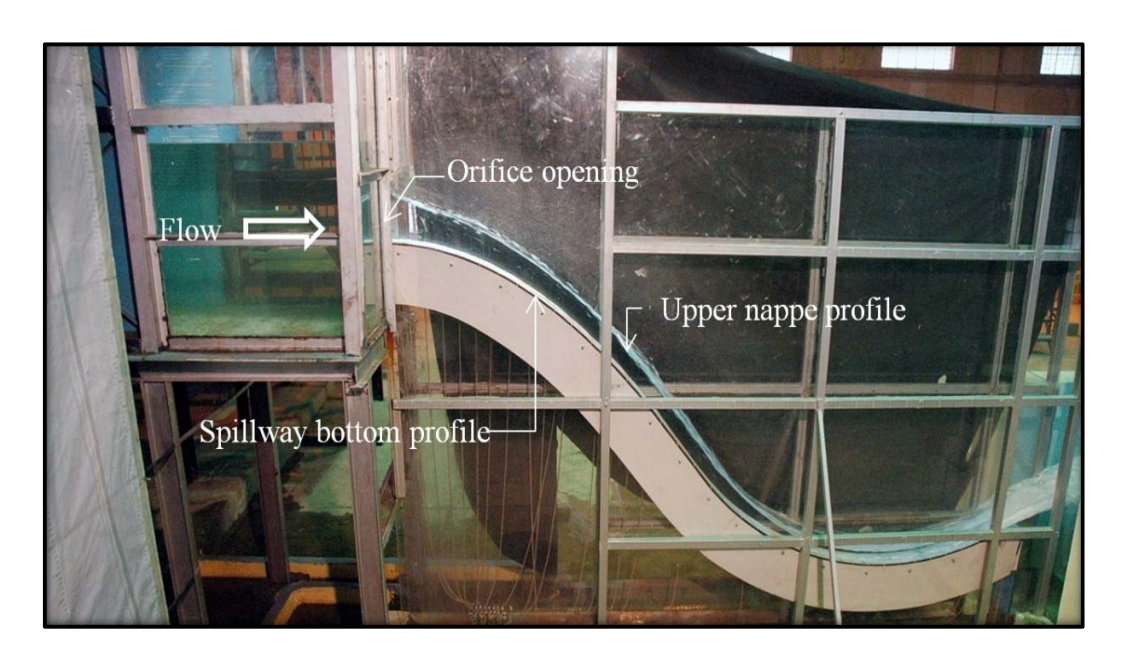


Fig. 4.14 Flow conditions in physical model

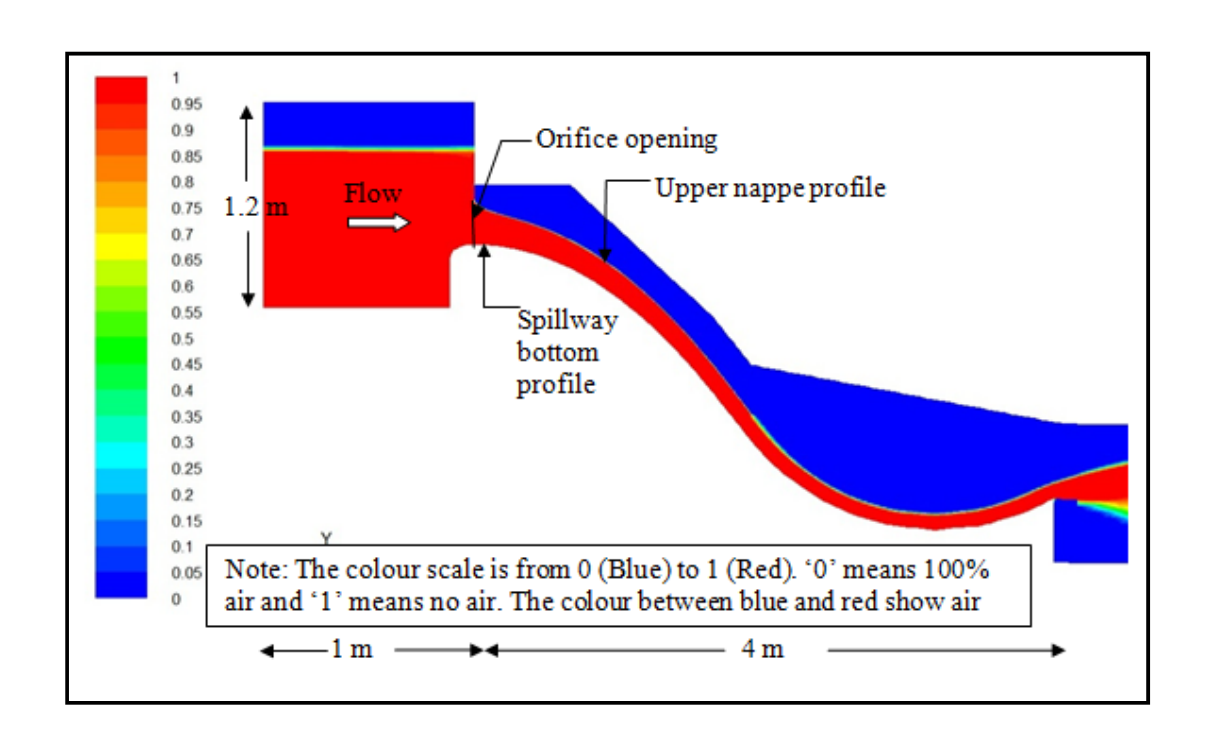


Fig. 4.15 Flow conditions in numerical model

## 4.6 Effect of Height of Orifice Spillway (P)

In an orifice spillway, height of spillway 'P' is one of the most important parameter to be considered for effective flushing of sediments. However, no specific work has been reported about the effect of 'P' in an orifice spillway. Hence, it is felt necessary to identify a need of parameter 'P' in design of an orifice spillway before carry out further studies. Experiments on physical model were conducted for P of 0.2 m (10 m in prototype) and 0.4 m (20 m in prototype) for the spillway bottom profile designed for head of 0.6 m (refer Table 4.4). However, numerical simulations were carried out for an additional P of 0.8 m (40 m in prototype, considering a model scale of 50) to cover minimum and maximum range of P adopted in most of the orifice spillway projects. Numerical model was developed for heights of orifice 0.2 m, 0.28 m and 0.32 at spillway operated for design head i.e.  $h_e/h_d = 1.0$  condition. Results obtained from physical and numerical model were used to study the effect of P on discharge through orifice and upper nappe water surface profile.

#### 4.6.1 Discharge through orifice

Discharging capacity is one of the most important parameter in design of any type of spillway. Discharges through orifice were calculated for different design heads (h<sub>d</sub>) and heights of orifice opening (D) as shown in Table 4.4. Coefficient of discharge was calculated using the following formula:

$$Q = C_d * A * \sqrt{(2gh_{cl})} \tag{4.3}$$

Where Q is the discharge through orifice in  $m^3/s$ , A is area of orifice in  $m^2$ , g is acceleration due to gravity in  $m/s^2$  and  $h_{cl}$  is centreline head  $(h_d - D/2)$ .

In case of an overflow spillway, the height of spillway above the stream bed (P) affects the discharge coefficient because the velocity of approach depends upon this height. With an increase in the height P, the velocity of approach deceases but the coefficient of discharge  $C_d$  increases. In the present work, an attempt has been made to study the effect of 'P' on discharge and  $C_d$  value of orifice spillway. Table 4.5 shows the comparison of discharges calculated at the orifice opening for  $h_e/h_d$  ratio 0.8, 1.0 and 1.33 and for height of orifice opening of 0.2 m, 0.28 m and 0.32 m. Table 4.5 indicates that there is increase in discharge with increase in height of orifice and head over the crest. However, little change was found in discharge and  $C_d$  values with change in height of spillway P for most of the cases.

Table 4.5 Effect of P on discharging capacity

	h <sub>e</sub> /h <sub>d</sub>	F	Physica	Numerical Model				
D (m)		$\mathbf{P} = 0.4$	m	$\mathbf{P} = 0.2$	2 m	P = 0.8  m		
		$Q (m^3/s)$	$C_d$	$Q (m^3/s)$	$C_d$	$Q (m^3/s)$	$C_d$	
	0.8	0.072	0.66	0.072	0.66	-	-	
0.2	1	0.078	0.64	0.081	0.64	0.082	0.65	
	1.33	0.098	0.67	0.099	0.67	ı	-	
	0.8	0.095	0.66	0.095	0.66	ı	1	
0.28	1	0.108	0.64	0.108	0.64	0.11	0.65	
	1.33	0.135	0.68	0.133	0.68	-	-	
0.32	0.8	0.102	0.64	0.102	0.64	ı	1	
	1	0.126	0.67	0.123	0.67	0.123	0.65	
	1.33	0.157	0.70	0.158	0.70	-	-	

In addition to the above, the discharges were also calculated at various upstream water levels ( $h_e$ ) above the crest up to the level of 1.2 m ( $h_e/h_d=2$ ) for different height of orifice openings. This range covers the free as well as orifice flow regime of an orifice spillway. Figure 4.16 shows the discharging capacity curve in respect of height of orifice opening and height of spillway.

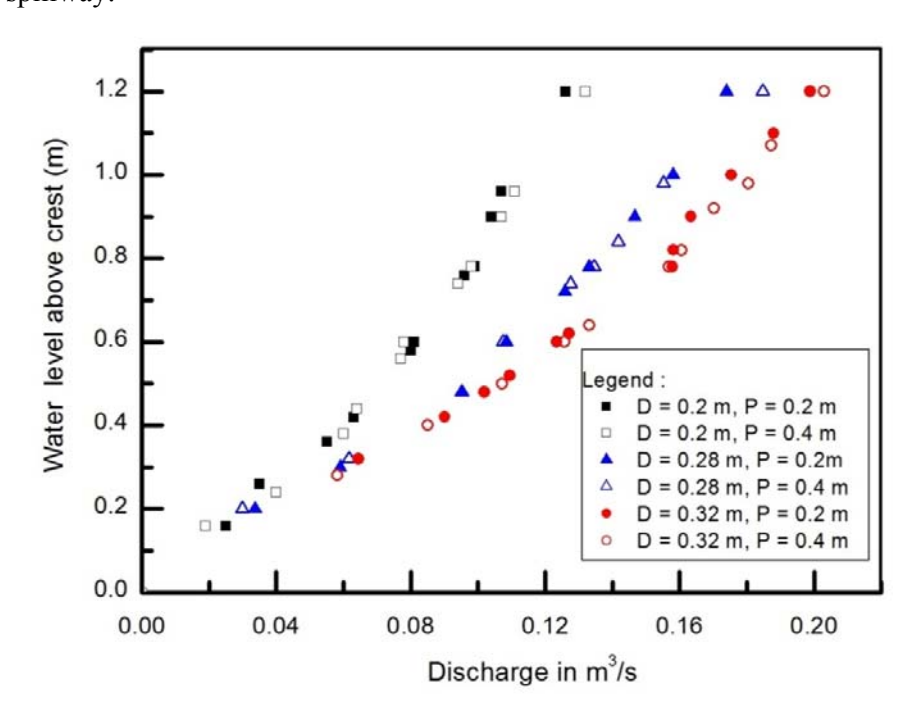


Fig. 4.16 Effect of P on discharging capacity

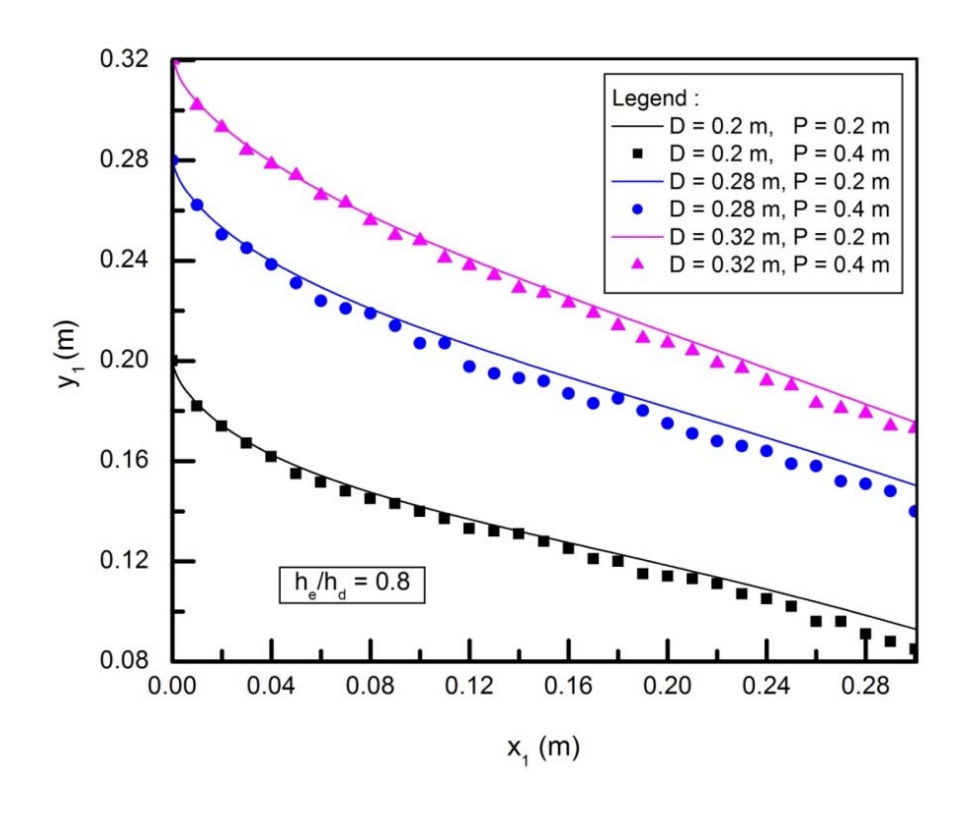
In orifice spillway, the flow is considered as a free and orifice flow when water level is below and above the height of orifice opening respectively. In case of an overflow spillway for free flow, the height 'P' of spillway above the stream bed affects the discharge coefficient (USACE, 1990). In overflow spillway, an increase in the height 'P', the coefficient of discharge C<sub>d</sub> increases. However, from Figure 4.16, it can be seen that for lower water levels above the crest (h<sub>e</sub> up to 0.4 m) i.e. in free flow regime; the discharge is almost same with variation of P value. It is also insignificant of height of orifice opening. However, as the water level above the crest increases, there is increase in discharge with increase in height of orifice opening. Hence, the height of orifice 'D' and head above the crest 'h<sub>cl</sub>' are governing parameters in deciding the discharging capacity of an orifice spillway. Nevertheless, it is seen that discharging capacity is independent of the height of spillway above the river bed 'P' in free as well as orifice regime, since the discharge is same for various water level above the crest for particular height of orifice.

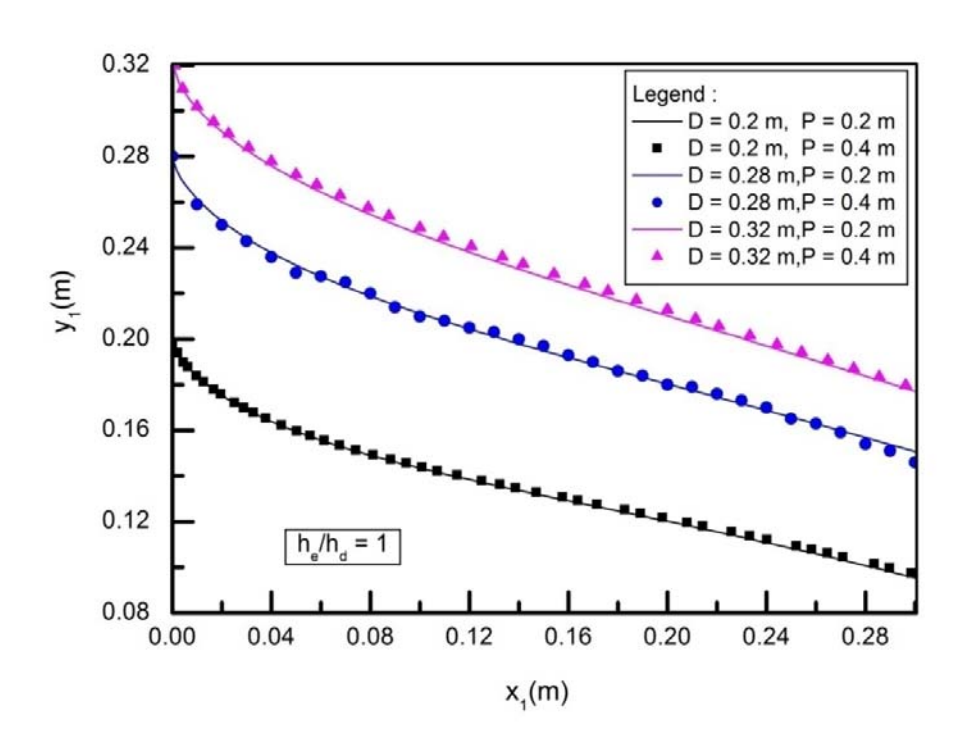
From Table 4.5, it can be seen that the coefficients of discharge were found to be in the range of 0.64 to 0.7. The  $C_d$  values were found to be more than the values obtained without providing solid bottom profile (as studied in set up 1). Similarly, the  $C_d$  values obtained in set up 2 were quite less than the values of 0.72 to 0.95 obtained with solid bottom and roof profiles for more than 22 physical model studies for different real life orifice spillway projects (Bhosekar et al. 2014). In this set up, roof profile was not introduced during the study. Hence, the results show the importance of roof profile in addition to other spillway components such as head and size of orifice opening, solid spillway bottom profile, shape of piers etc in deciding the discharging capacity of an orifice spillway. Hence, care should be taken in design of these components in case of orifice spillway.

#### 4.6.2 Upper nappe water surface profile

The results of upper nappe profiles obtained in the study may be useful in deriving an equation of roof profile of an orifice spillway. Hence, to study the effect of parameter P on roof profile is an essential step to carry out the present research. The resulted profiles were plotted considering the origin at the top of orifice opening for a particular case. Figures 4.17, 4.18 and 4.19 show the effect of 'P' on upper nappe profile for  $h_e/h_d = 0.8$ , 1.0 and 1.33 respectively.

Figures 4.17 to 4.19 show that upper nappe profiles measured for P=0.2 m matched well with the profiles obtained for P=0.4 m for all the cases. There is no change in the profile by changing the height of orifice spillway. Hence, it may be concluded that the effect of 'P' can be neglected in design of roof profile of an orifice spillway. In orifice spillway, the crest of spillway is kept as near to upstream river bed for flushing of sediment. In view of this, further studies on physical and numerical models mentioned in Table 4.4 were carried out for lowest height of spillway i.e. P=0.2 m.





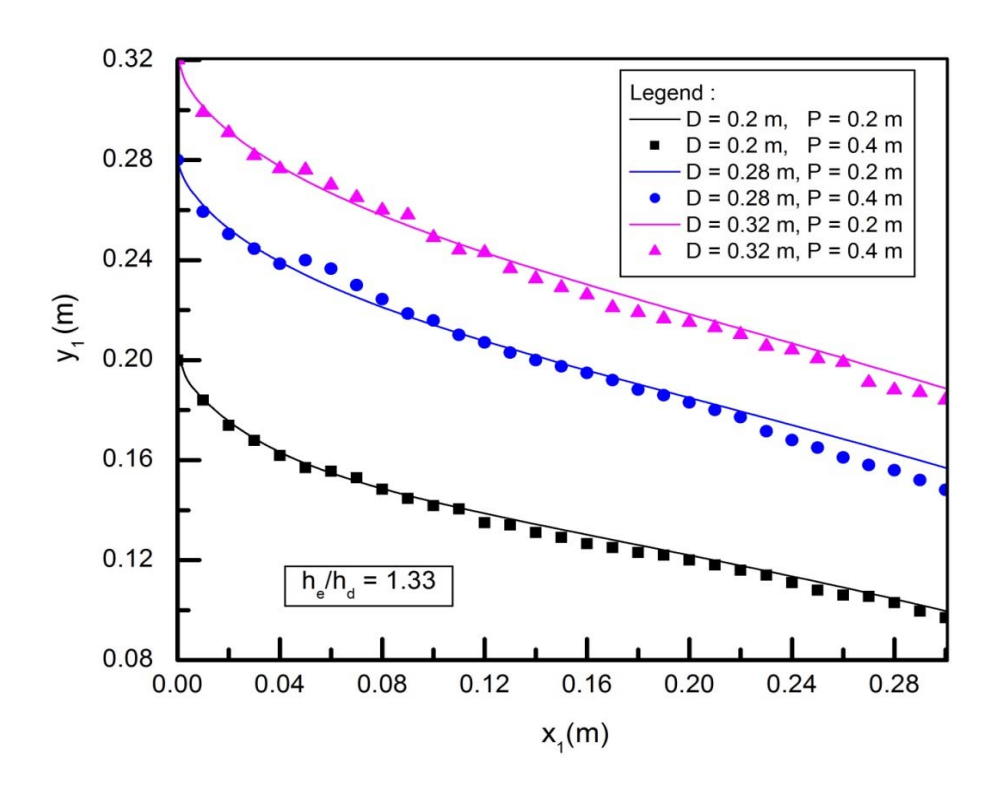


Fig. 4.19 Effect of P on upper nappe profiles for  $h_e/h_d = 1.33$ 

The physical model results obtained for spillway bottom profile designed for head of 0.8 m and numerical model results for spillway bottom profile designed for head of 0.6 m, 1.0 m and 1.4 m were combined for further analysis. The data in respect of upper nappe profile for various combinations of heads and height of orifice opening was analysed in detail. The upper nappe profile was computed throughout the length of spillway. However, the data up to the distance of 0.3 m were taken for the analysis as it covers the maximum length of roof profile adopted on most of the orifice spillway projects. Main objective of present set up is to design roof profile of an orifice spillway. Design head, operating head and height of orifice are essential hydraulic parameters in design of any components of orifice spillway. Hence, it is needed to study the effect of all these parameters on resulted pper nappe profile before deriving an equation of roof profile of an orifice spillway. The effect of each parameter has been studied in detail in following subsections. Even though, the studies were carried out for different  $h_{\rm e}/h_{\rm d}$  ratio, the results are discussed in detail for  $h_{\rm e}/h_{\rm d} = 1$  only, but the conclusions are derived based on analysis of all  $h_{\rm e}/h_{\rm d}$  ratios studies.

## 4.7 Effect of Design Head on Upper Nappe Profiles

Figure 4.20 shows effect of design head on the roof profile for different height of orifice opening. In the figure,  $x_1$  and  $y_1$  are horizontal and vertical coordinates of upper nappe profile from crest of spillway i.e at the origin (0,0) as shown in figure.

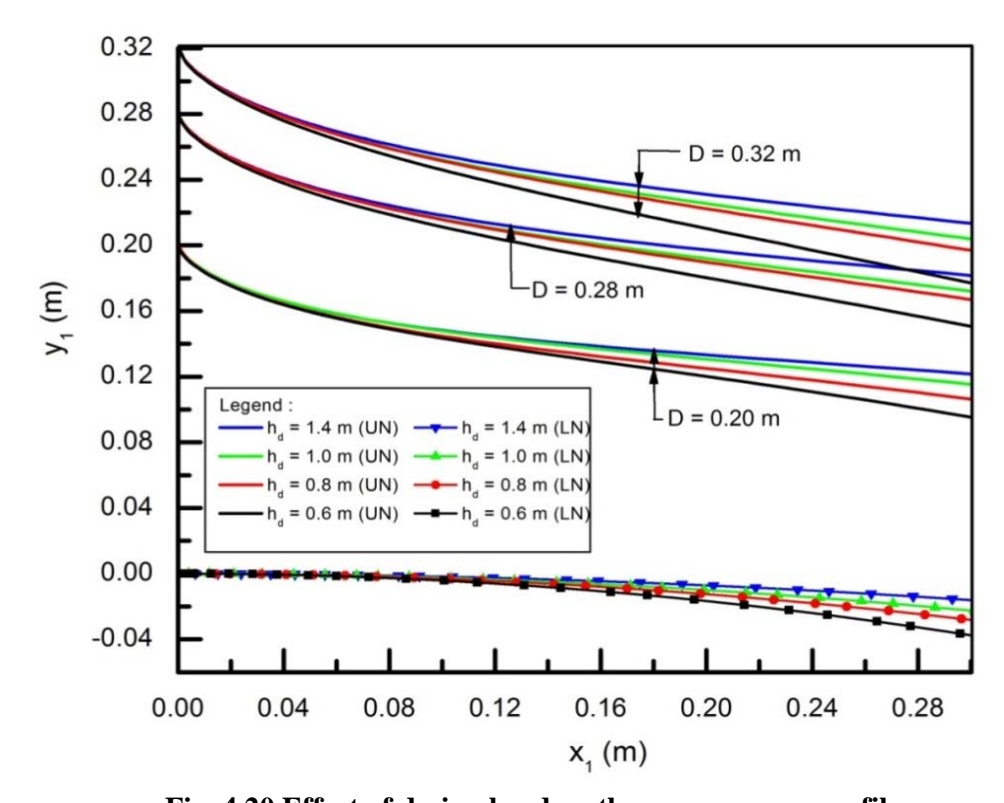


Fig. 4.20 Effect of design head on the upper nappe profiles

It is found from Figure 4.20 that for a given 'D', the upper nappe profiles diverge as the jet travels further downstream for various heads. The profile becomes flat for higher design head i.e 1.4 m as compared to low design head i.e 0.6 m. Hence, design head is found to be an important hydraulic parameter in design of the roof profile as there is a variation in upper nappe profile with the change in design head.

# 4.8 Effect of Operating Head on Upper Nappe Profiles

Figure 4.19 shows effect of operating head on the upper nappe profiles for different height of orifice opening. The origin for plotting the data was considered at the top of orifice opening.

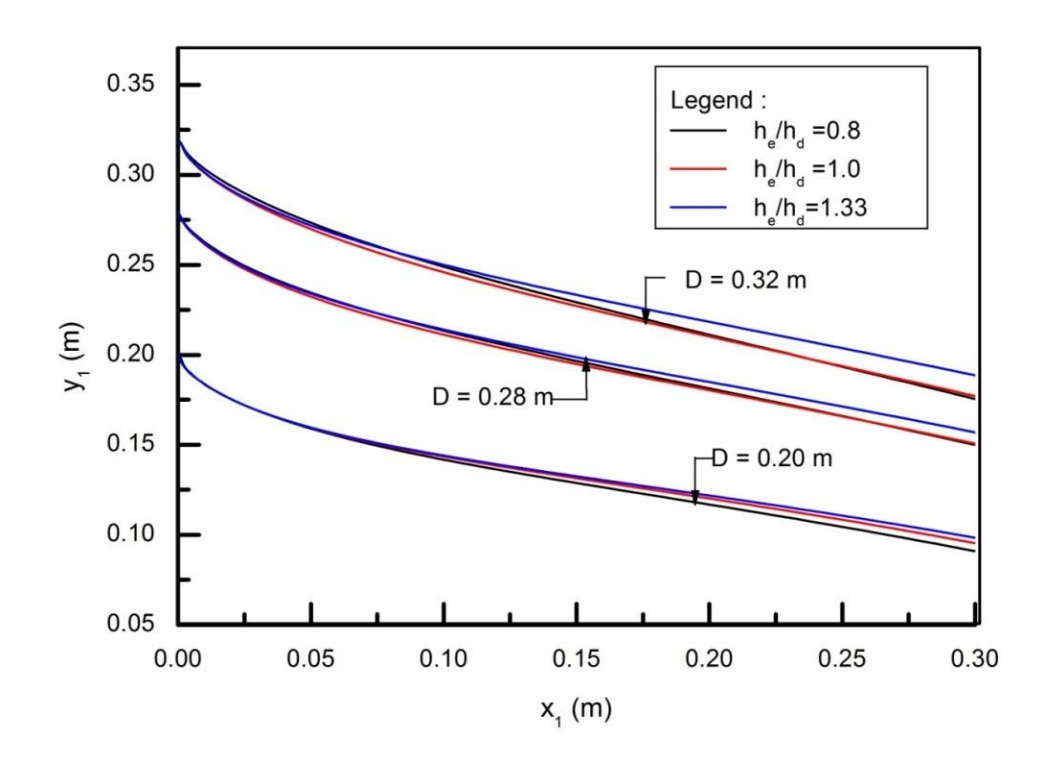
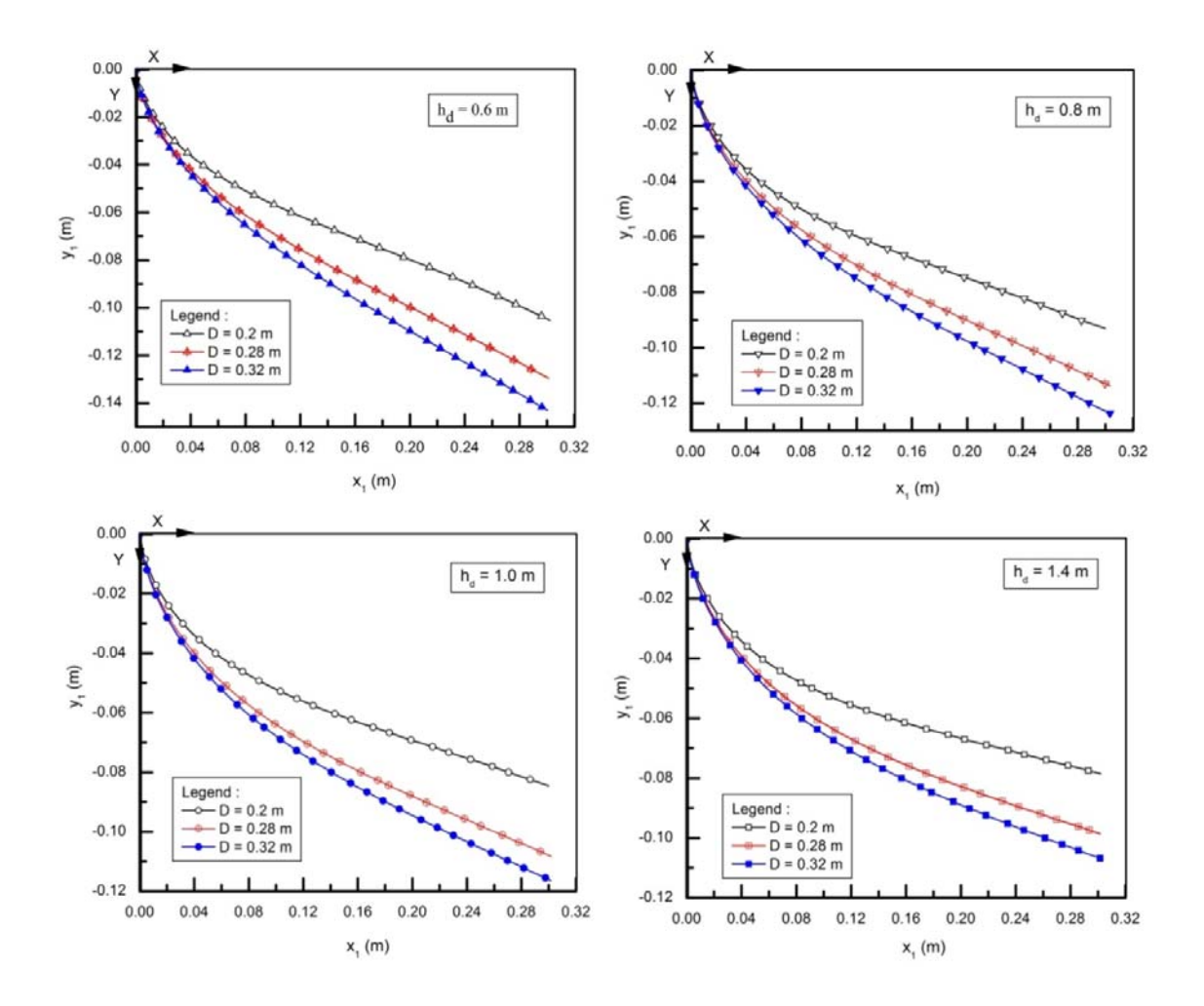


Fig. 4.21 Effect of operating head on the upper nappe profiles

Figure 4.21 indicates that there is a little variation in upper nappe profile with change in operating head for a particular height of orifice opening. The profiles obtained for design head and less than design head are closely matched for all the heights of orifice. However, there was a little bit variation in the profiles computed for more than design head i.e.  $h_e/h_d = 1.33$  beyond the distance of 0.15 m. The deviation in the values was more for large height of orifice opening. The variation in terms of maximum % error between these profiles was calculated as 6 % which is in the acceptable limit. It is to be noted here that the dam in actual operates at design head or less than design head. However, operation of spillway more than design head is a very rare event. Hence, effect of  $h_e$  can be neglected in design of roof profile of an orifice spillway.

# 4.9 Effect of Height of Orifice on Upper Nappe Profiles

Figure 4.22 shows effect of height of orifice opening (D) on the roof profile. The origin for plotting the profiles was considered same i.e. 0,0 to study the effect of D.



It was seen from Figure 4.22 that, for a particular design head (h<sub>d</sub>), as the height of orifice opening (D) increases the profile becomes steeper and steeper. Because, as D increases the mass of water passing through the orifice increases resulting in increased weight and steeper jet under influence of gravity. Hence, height of orifice is a governing parameter in design of roof profile.

Based on the above results,  $h_d$  and D are found to be the governing parameters in design of roof profile of an orifice spillway, whereas there was insignificant effect of parameters P and  $h_e$  on the roof profile.

# 4.10 Development of an Equation for Roof Profile of an Orifice Spillway

Physical and numerical model studies were carried out for height of orifice of 0.2 m, 0.28 m and 0.32 m with the different design heads. In addition to these heights of orifice (D), numerical simulations were also carried out for additional heights of orifice (D) of 0.4 m, 0.5 m and 0.6 m for  $h_e/h_d=1$  to generate more data for derivation of an equation for roof profile. The data was analysed for four different design heads ( $h_d$ ) of 0.6 m, 0.8 m, 1.0 m and 1.4 m. In all 3 numbers of physical and 17 numbers of numerical model results were used in deriving an equation for design of roof profile of an orifice spillway. The data of upper nappe profile for ratio of  $h_e/h_d=1$  were compiled. Figure 4.23 shows the closer view of the roof profile that shows all the parameters which should be considered in design of roof profile.

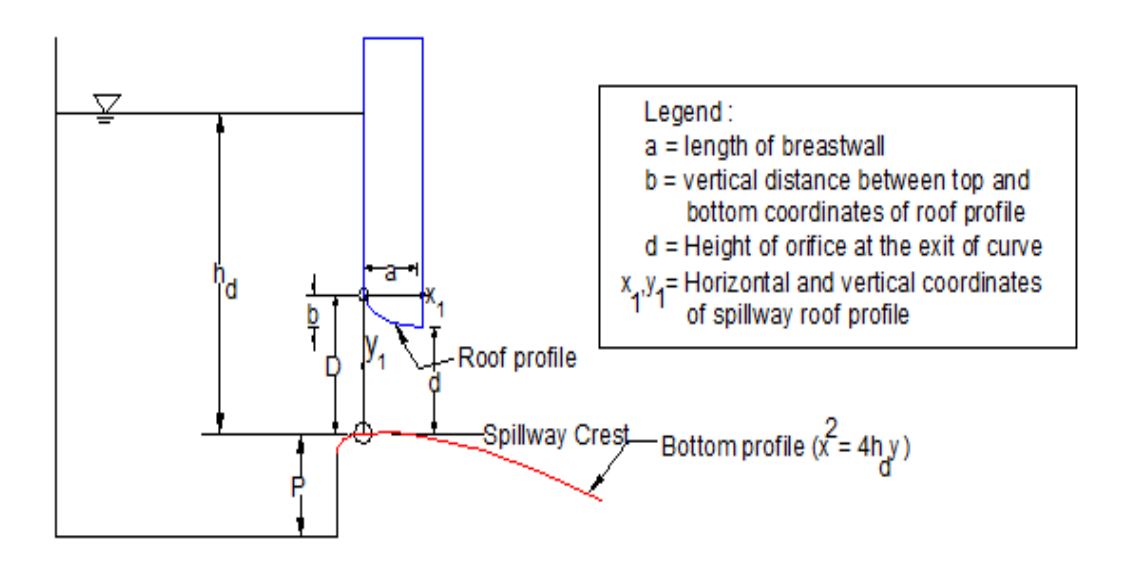


Fig. 4.23 Closer view of the roof profile

The height of curve 'b' plays a significant role in fixing the roof profile as it sharpens or flattens the profile with respect to b/d ratio for a particular height of orifice opening 'd'. While analysing the experimental data for about 22 major orifice spillways (Bhosekar et al. 2014), it was reported that the value of 'b' is in the range of 0.1 to 0.4 times of height of orifice opening at the exit of curve (d). In view of this, all the data was divided into the four categories i.e.b/d = 0.1, 0.2, 0.3 and 0.4. Height of orifice at the exit (d) is an important parameter in fixing the length of roof profile 'a' and calculation of discharging capacity of an orifice spillway. As the height of orifice at the entrance (D) is known, the height of orifice at the exit 'd' can be fixed using the relation D = 1.1 to 1.4d (Refer Figure 4.23). As the studies

were carried out for different D, with different categories of b/d ratios, number of sets for different heights of orifice at the exit of curve (d) could be generated. Total 84 numbers of sets were used to derive an equation of roof profile. Various forms of equations were tried using multiple regression analysis and checked in respect of R<sup>2</sup> value. However, the form of Eq. (4.4) with R<sup>2</sup> value of 0.976 was found suitable, which can be expressed as follows:

$$x_1 = a(\frac{y_1}{h})^m \tag{4.4}$$

$$x_{1} = a(\frac{y_{1}}{b})^{m}$$

$$a = A * (d) * (\frac{h_{d}}{d})^{B}$$
(4.4)

In Equation (4.4),  $x_1$  and  $y_1$  are the horizontal and vertical coordinates of the roof profile considering origin (0, 0) at the top of the orifice opening. The length of roof profile 'a' varies from project to project and no specific guidelines are available for fixing it based on hydraulic considerations. Hence, an attempt has been made to fix the length of roof profile 'a' in terms of 'd' and 'h<sub>d</sub>' as expressed in Equation (4.5). A, B and m in Equations (4.4) and (4.5) are coefficients obtained from regression analysis. The coefficients A, B and m and their variation with respect to b/d ratio are given in Figure 4.24.

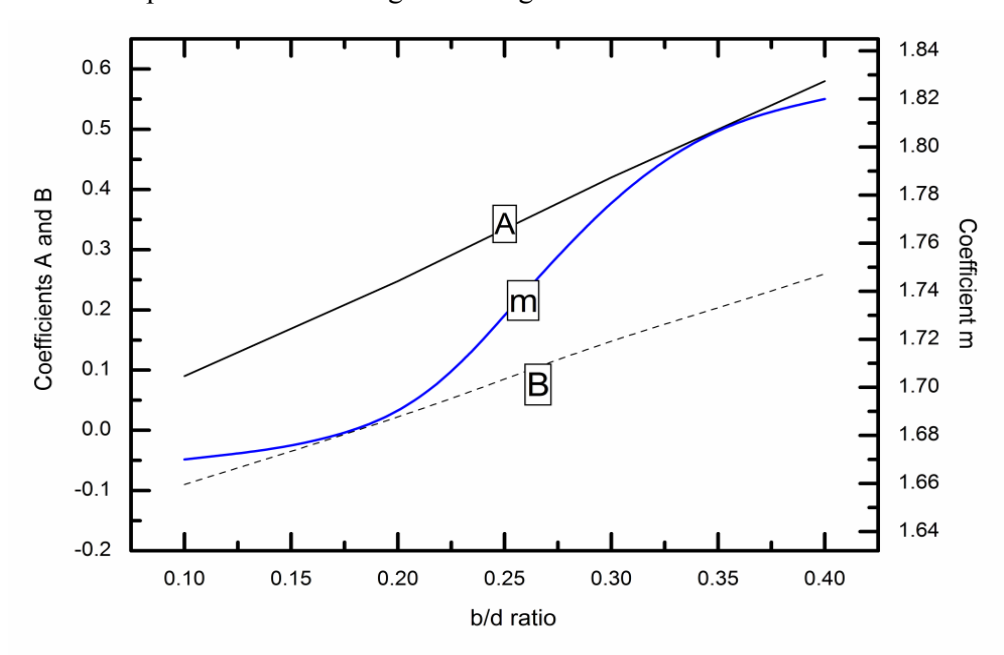


Fig. 4.24 Plot for coefficients 'A' and 'B' and 'm'

Equations (4.4) and (4.5) are valid for the following ranges of h<sub>d</sub>, d, h<sub>e</sub>/h<sub>d</sub> and b/d ratio

 $0.6 \text{ m} \le h_d \le 1.4 \text{m}$  (30 m to 70 m in prototype)

 $0.2 \text{ m} \le d \le 0.4 \text{ m}$  (10 m to 20 m in prototype)

 $0.8 \le h_e/h_d \le 1.33$ 

 $0.1 \le b/d \le 0.4$ 

In prototype, height of an orifice (d) should be selected in such a way that maximum design discharge estimated for the project should pass through the specified height of orifice with available gorge width. The value of 'b' generally varies between 0.1 d to 0.4 d (Deolalikar et al., 2008). As the value of 'b' increases, the length of roof profile also increases. This results in increase in discharging capacity. Thus, for a particular design head and height of orifice (d), the maximum discharging capacity can be achieved by designing the roof profile corresponding to b/d ratio of 0.4. This is because, the roof profile with b = 0.4 d is wider and steeper which guides the flow to a greater extent as compared to the profiles generated by b/d ratios varying from 0.1 to 0.3.

# 4.11 Verification of the Proposed Equation

In the present case, an equation was derived based on the data for  $h_e/h_d=1.0$ . However, the data of upper nappe profile for  $h_e/h_d=0.8$  and 1.33 and b/d ratio of 0.3 obtained from numerical model were used for verification of an equation. These numerical model results have not been used in derivation of the equation. The minimum and maximum range of head and height of orifice i.e.  $h_d=0.6$  and 1.4 m and D=0.2 m and 0.32 m were selected. The height of orifice at the exit of curve (d) was fixed corresponding to b/d ratio of 0.3 for a particular D. The values related to its configurations are given as input to Eqs. (4.4) and (4.5) to find the equation of roof profile. Figures 4.25 and 4.26 show the computed and estimated values of upper nappe water surface profile for  $h_e/h_d=0.8$  and 1.33 respectively.

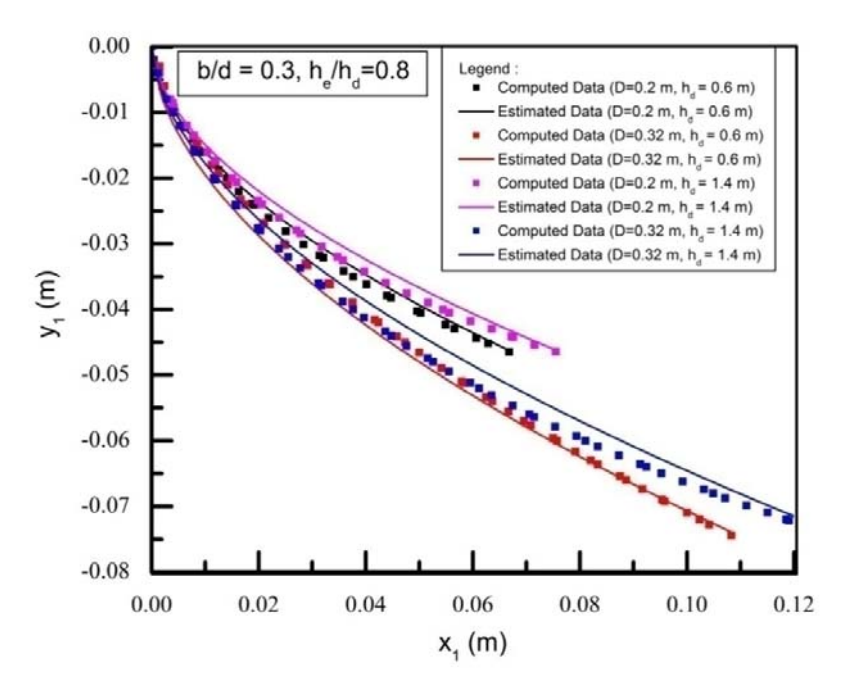


Fig. 4.25 Computed and estimated values of upper nappe profiles for  $h_e/h_d=0.8$ 

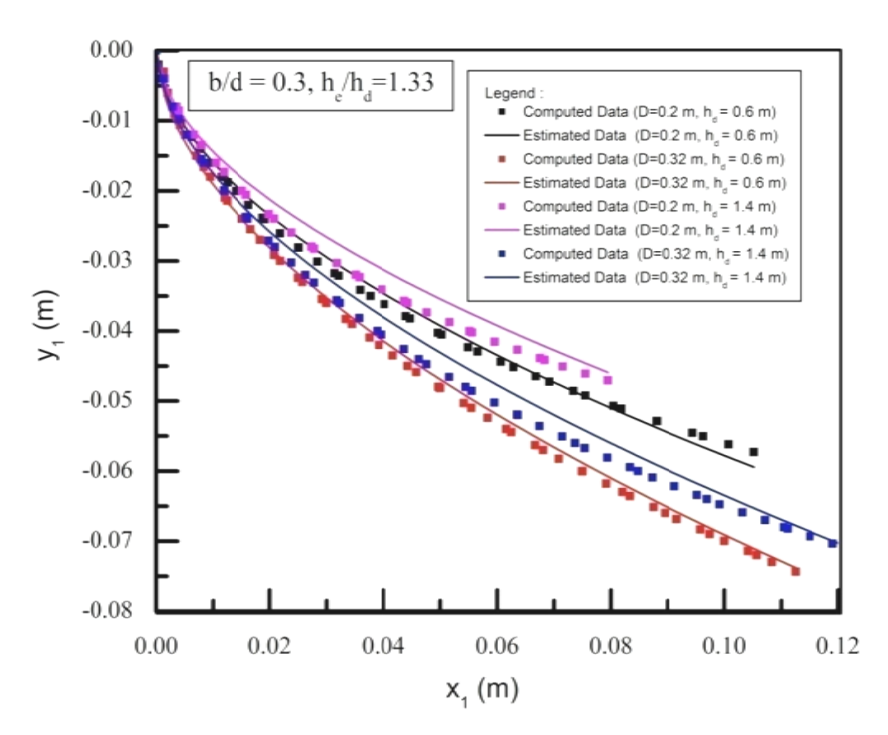


Fig. 4.26 Computed and estimated values of upper nappe profiles for  $h_e/h_d = 1.33$ 

Figures 4.25 and 4.26 show a good match and agreement between the computed and estimated upper nappe water surface profile (roof profile) values for entire range of D and  $h_d$ . There was a small variation in values at the middle of the curves. It is to be noted here that the computed data is for  $h_e/h_d = 0.8$ . However, estimated data using Eqs. (4.4) and (4.5) is for  $h_e/h_d = 1$ . The maximum % error between computed and estimated values was 7%, and  $R^2$  is 0.999, which is in the acceptable range. Hence, it is worth mentioning here that the Eqs. (4.4) and (4.5) can be valid for  $h_e/h_d$  range of 0.8 to 1.33. This verification confirms the applicability of the developed equation in design of basic roof profile of an orifice spillway for various ranges of D and  $h_d$ .

# 4.12 Validation of the Proposed Equation

In order to validate the equation for general and global applicability three prototype case studies have been used. These case studies are real life orifice spillways whose roof profile have been developed by trial and error method using physical model studies conducted at CWPRS, Pune. The roof profiles of orifice spillway were designed for a head ( $h_d$ ) of 0.67 m, 0.5 m and 0.72 m with the corresponding height of orifice (D) of 0.42 m, 0.30 m and 0.40 m for case study-1, case study-2 and case study-3 respectively. The parameters such as coefficient of discharge, pressures over bottom and roof profile and water surface profiles were used for validation of proposed Equation 4.4. The results obtained from the study have been discussed below.

## **4.12.1** Comparison of roof profiles

The modified roof profiles of all three case studies along with their original elliptical profile were compared with the roof profile designed using the Equation (4.4) proposed in the present study. The comparison of the profiles of all the case studies is shown in Figure 4.27. While plotting the Figures, the bottom coordinate of roof profile is kept constant for a particular case study to maintain height of orifice (d) same.

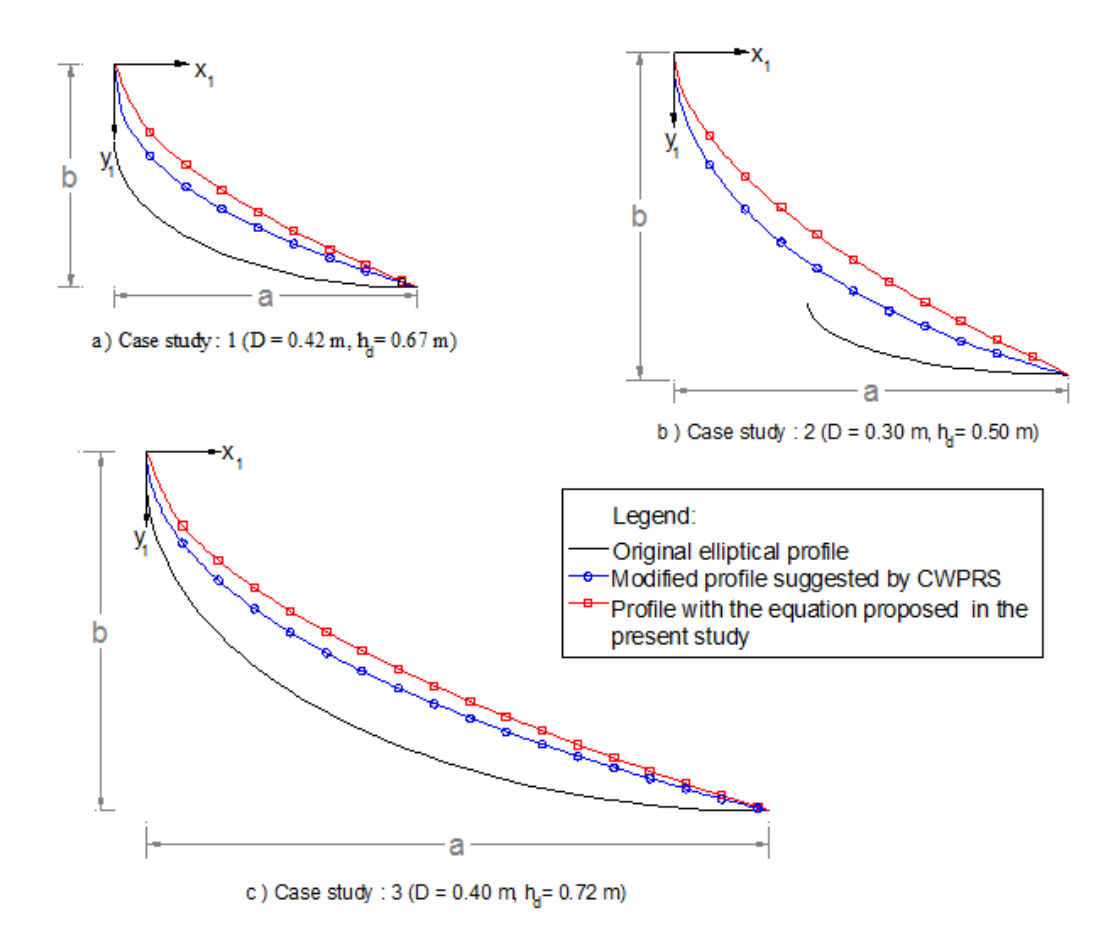
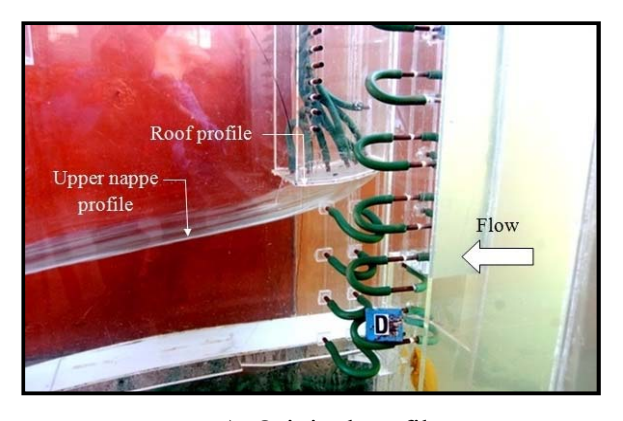


Figure 4.27 indicates that the roof profile designed with Equation (4.4) proposed in the present study is far away from original elliptical profile and closer to the profile modified based on physical model studies after a number of trials for each specific case. It is also to be noted that, the length of the breastwall 'a' in case study-2 was very small in original design and flow separation occurred on the profile. Hence the profile was modified that results in increase in b/d ratio and increase in the length of the profile. It results in maximum

discharging capacity of spillway. The comparison shows that large number of trial and error could have been avoided if the Equation (4.4) was available earlier at design stage.

#### 4.12.2 Flow conditions

Physical model studies indicated that the flow through orifice did not follow the original elliptical profile in all three cases. Flow separation occurred along the roof profile resulting in inadequate discharging capacity. Hence, the profiles were modified by trial and error based on the physical model results to maximize the discharging capacity. Figure 4.28 a and 4.28 b show the flow in the vicinity of roof profile for original profile and profile modified based on model studies respectively for case study - 3. The flow conditions in the vicinity of roof profile were also visualized in numerical model by creating a phase diagram of water and air along centreline of the spillway. Figure 4.29 show the simulation of flow in the vicinity of roof profile for case study 3.



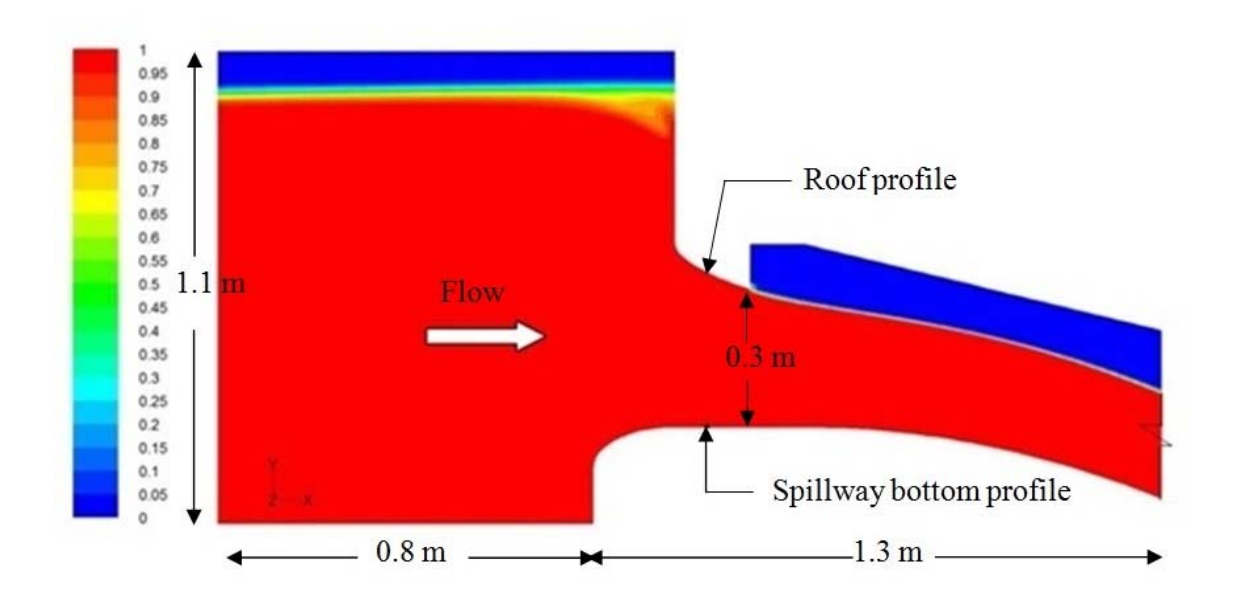


a) Original profile

b) Modified profile

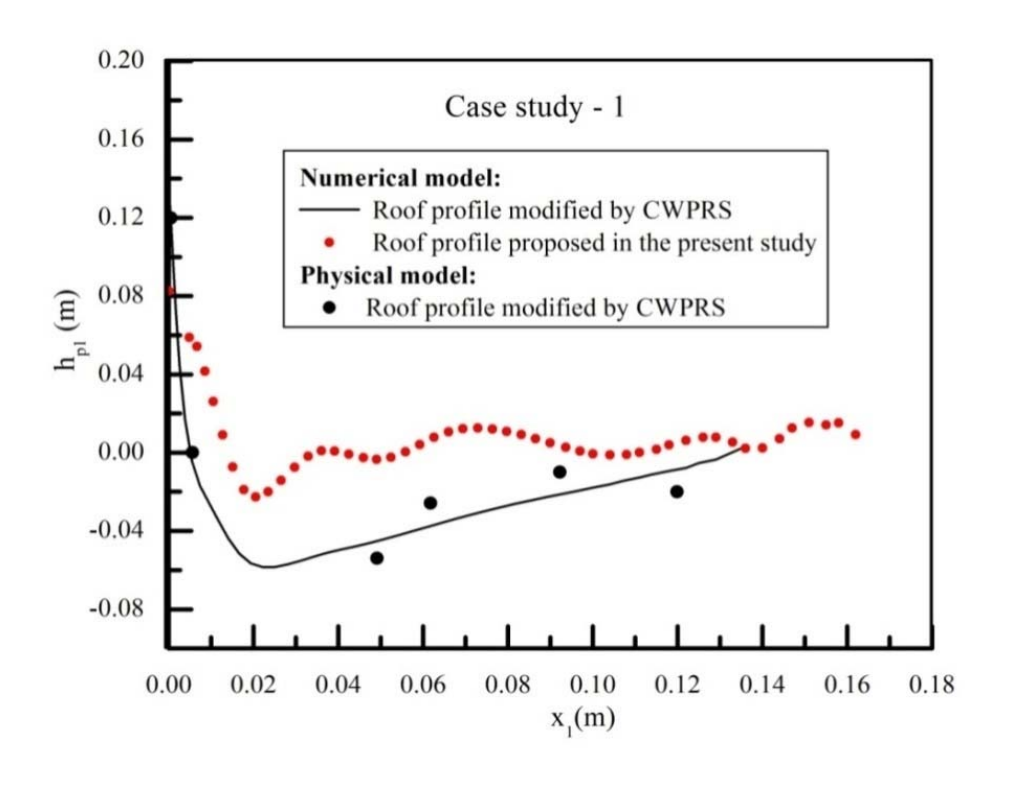
Fig. 4.28 Flow condition in the vicinity of original and modified design of roof profile for case study - 3

Figure 4.28 a show separation of flow below the roof profile resulting in reduced coefficient of discharge of 0.68. However, it can be seen from Figures 4.28 b that the flow adheres the modified roof profile resulting an increased  $C_d$  of about 0.77 for case study 3. These Figures show the importance of design of roof profile in deciding the discharging capacity of an orifice spillway. During the physical model studies, the end coordinates of roof profile was kept constant so that height of orifice remains constant and modified the roof profile as per the water surface profile measured below the roof profile results in change in b/d ratio. It is seen from the Figures 4.29 that flow conditions are well simulated in numerical models. Flow adheres the roof profile of orifice spillway same as observed in physical model. No separation is found on the roof profile.



# 4.12.3 Comparison of pressures on roof profile

Design of roof profile of orifice spillway should be such as to get maximum discharging capacity and the profile should not experience excessive negative pressures. In view of this, the equation proposed in the present study was validated in terms of coefficient of discharge, and pressures on the bottom and roof profile of an orifice spillway using numerical model studies. Numerical model simulations were run for all three prototype case studies with profile modified based on physical model studies and profile designed with the equation proposed from the present study. Figures 4.30, 4.31 and 4.32 show the comparison of pressures on the roof profiles for case study - 1, case study - 2 and case study - 3 respectively. In these Figures ' $x_1$ ' is the horizontal distance of pressure taps located on the centreline of roof profile measured from the origin (0, 0) at the top of orifice opening and ' $h_{p1}$ ' is the calculated pressure in m of water. Physical model results were also plotted in these figures for comparison.



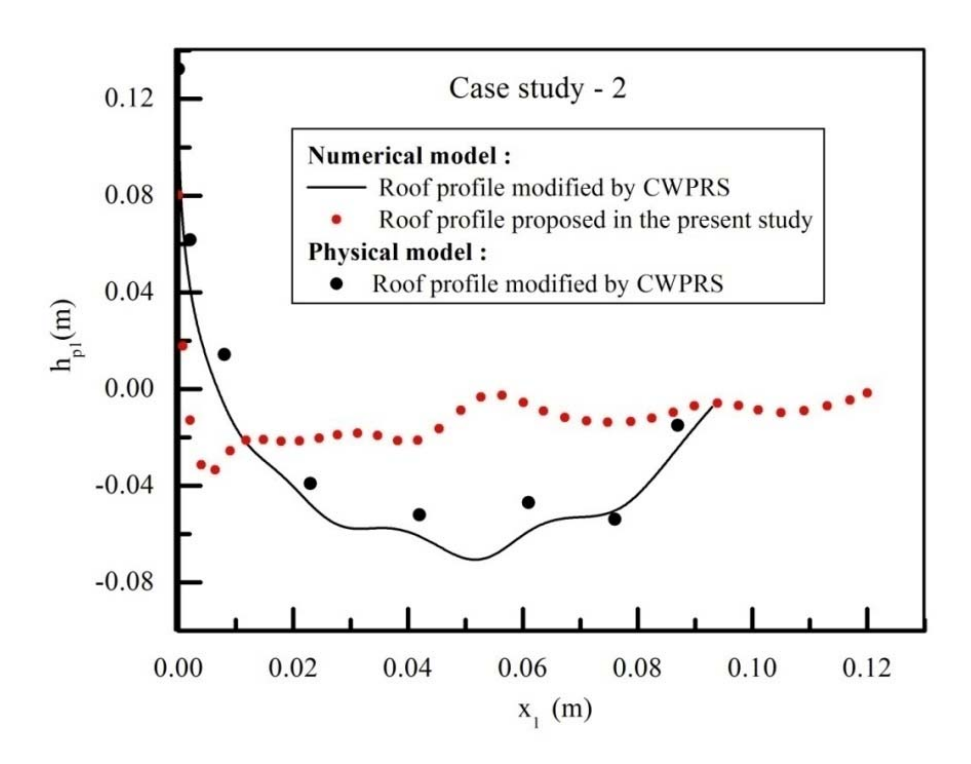


Fig. 4.31 Validation of proposed equation in respect of pressures on roof profile of orifice spillway for case study - 2

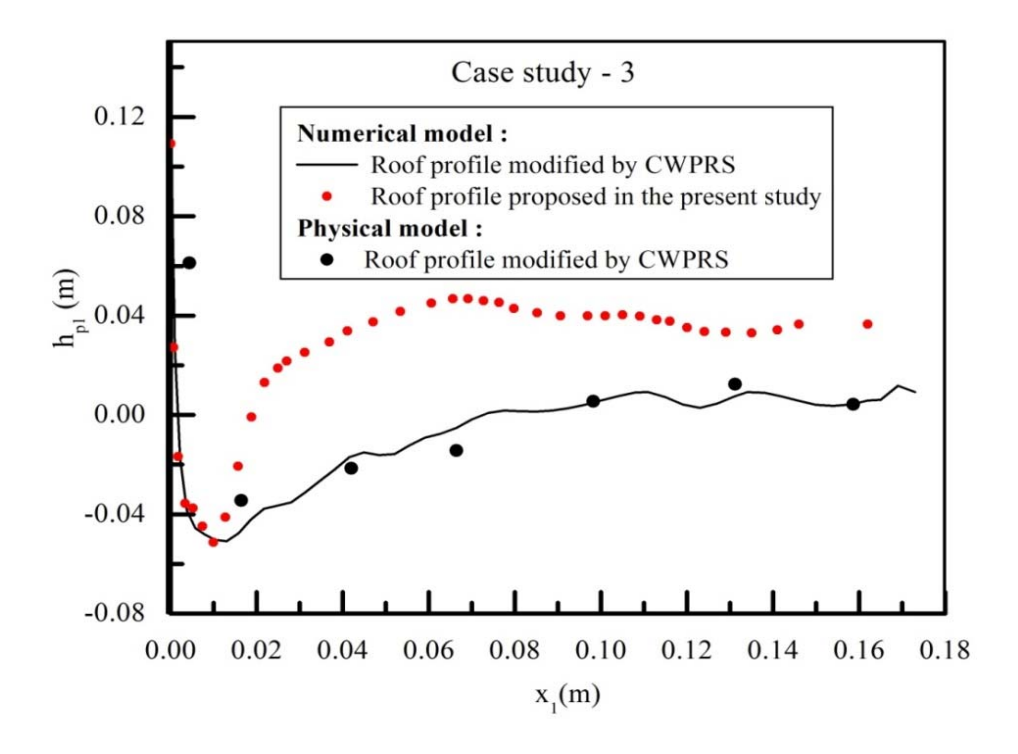


Fig. 4.32 Validation of proposed equation in respect of pressures on roof profile of orifice spillway for case study - 3

Numerical model results were found to be in good agreement with physical model for all the case studies as shown in Figures 4.30 to 4.32. It can be seen in Figure 4.30 that negative pressures were observed throughout the length of roof profile studied for case - 1. However, the roof profile of the proposed equation results in positive pressures, except the negative pressure in the initial region with a small magnitude of 0.02 m of water. Figure 4.31 shows that negative pressures were observed on both the profiles. However, negative pressures observed on the proposed equation profile were less as compared to pressures on the profile studied for specific case. It is observed from Figure 4.32 that pressures were negative with the same magnitude in the initial region. However, after a certain distance, pressures were positive on the roof profile designed using Equation 4.4. In all the three cases, it is observed that the roof profile is better with the proposed Equation 4.4.

# 4.12.4 Comparison of pressures on spillway bottom profile

The pressures on spillway bottom profile were observed with the roof profile studied for specific case and profile with proposed equation in present study. In both the cases the spillway bottom profile is kept same as designed in specific case study. Figures 4.33, 4.34 and 4.35 show pressures on spillway bottom surface for case study -1, case study -2 and case

study - 3 respectively. In the Figures, 'x' is the horizontal distance along the spillway bottom profile considered spillway crest as (0, 0) and 'h<sub>p</sub>' is the pressure in m of water.

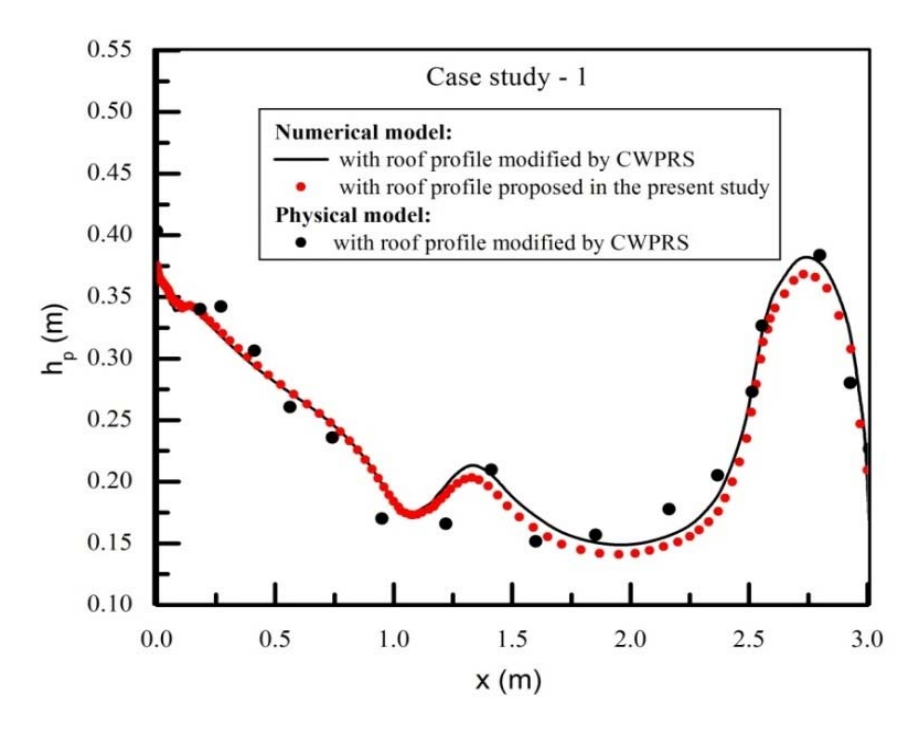
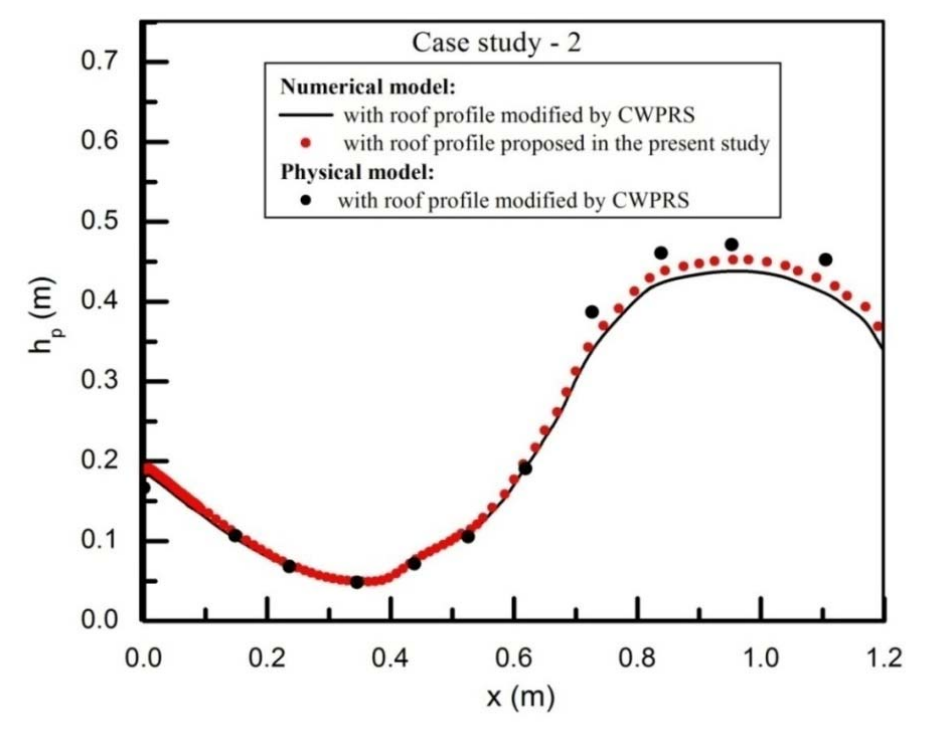


Fig. 4.33 Validation of proposed equation in respect of pressures on spillway bottom profile of orifice spillway for case study-1



rig. 4.54 vanuation of proposed equation in respect of pressures on spillway bottom profile of orifice spillway for case study - 2

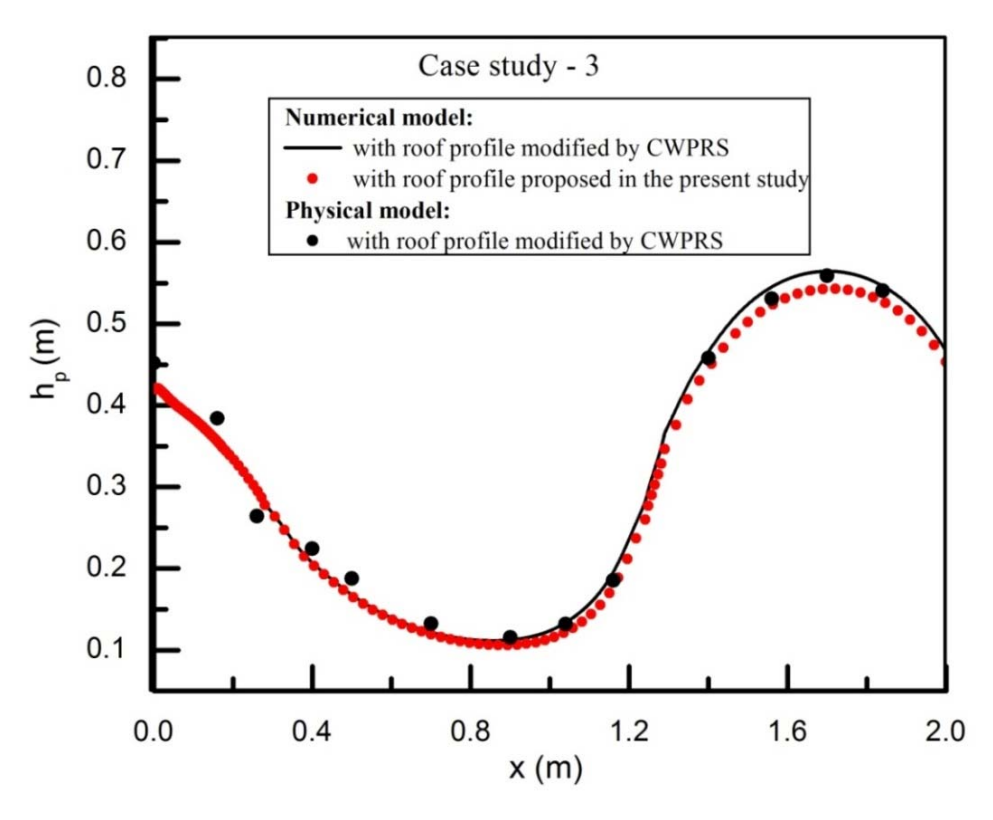


Fig. 4.35 Validation of proposed equation in respect of pressures on spillway bottom profile of orifice spillway for case study - 3

Physical and numerical model results were found in good agreement for all the case studies. It can be seen from the Figures that positive pressures were observed throughout the length of spillway for all the three cases. Hence, the pressures are found to be acceptable. However, Figures 4.33 to 4.35 show that there is insignificant effect on pressures on bottom profile with change in roof profile of orifice spillway.

## 4.12.5 Comparison of discharge

The proposed roof profile was also checked in terms of discharge through orifice spillway and coefficient of discharge,  $C_d$  as shown in Table 4.6. From the Table 4.6, it is observed that  $C_d$  value calculated with the proposed profile was less by about 4% as compared to the  $C_d$  calculated for specific case study 1 and 3. The  $C_d$  for case study 2 was increased by 5% with the profile designed using the proposed equation. However, it is important that the pressures on roof profile for a particular case study were improved and there may be no fear of cavitation failure for all the cases. Hence, it is concluded that the performance of roof profile designed with the proposed equation (4.4) was found to be more satisfactory in respect of pressures than observed on the roof profile modified by trial and error for specific case study.

Table 4.6 Comparison of discharge and coefficient of discharge calculated for different case studies

Case study	Profile studied f	for specific case	Profile proposed in the present study		
	Q in m <sup>3</sup> /s	$C_d$	Q in m <sup>3</sup> /s	$C_d$	
Case study-1	0.182	0.78	0.175	0.75	
Case study-2	0.094 0.84		0.098	0.88	
Case study-3	0.126	0.78	0.121	0.75	

Based on the verification and validation of proposed equation, it can be concluded that the proposed equation can be used as a guideline for designing the roof profile of an orifice spillway at the initial design stage.

# 4.13 Application of the Proposed Equation

Roof profile plays an important role in deciding the discharging capacity of an orifice spillway. The design of roof profile of most of the orifice spillway projects in India have been finalised so far based on trial and error method carried out on physical model studies. However, the proposed equation is a step forward in this regard and would be useful to the engineers to design the roof profile at the initial stage. The equation would be helpful in designing a roof profile that results in achieving maximum discharging capacity of the spillway. It would also be useful to design engineers to fix the length of roof profile as per hydraulic and structural requirements. The equation would also play a very important role in making the design of an orifice spillway hydraulically and economically efficient. The equation would be applicable for the design heads varying from 30 m to 70 m and heights of orifice varying from 10 m to 20 m.

# **Solution** Chapter 5 Design guidelines and non dimensional plots

## 5.1 Introduction

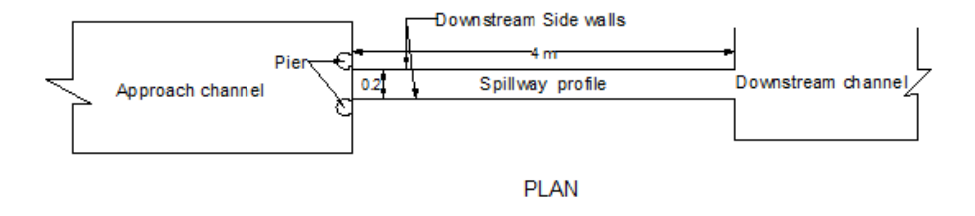
The main aim of the present study is to evolve basic guidelines for design of bottom and roof profiles of an orifice spillway. Therefore, the studies were carried out from very basic theory of orifice flow. In set up 1, flow through a sharp edged large orifice was investigated in terms of coefficient of discharge and lower and upper nappe water surface profiles. The results were compared with available literature. Based on the comparison of results of lower nappe profile, the bottom profile of orifice spillway was finalized with an equation  $x^2 = 4h_dy$ . In set up 2, solid bottom profile of spillway having an equation  $x^2 = 4h_dy$ was fixed at the downstream of the sharp edged orifice. Spillway profiles were designed for different heads i.e. 0.6 m, 0.8 m, 1.0 m and 1.4 m. Physical and numerical model studies were carried out for various combinations of heights of orifice and operating heads. The results were analysed in respect of coefficient of discharge, velocity, upper nappe water surface profiles and pressures over spillway bottom profiles. Based on the results of upper nappe profiles, an equation was derived to design the roof profile of an orifice spillway. The developed equation was verified and validated by comparing the results with the present study considered for the derivation of the equation. It was also verified with data pertaining to several orifice spillway projects studied in CWPRS.

In the present set up i.e in experimental set up-3, solid roof profile designed with the proposed equation was fixed on the roof of orifice opening. The bottom and roof profiles were designed for different heights of orifice 'd' and design heads (h<sub>d</sub>). Based on previous data (Deolalikar et. al., 2008 and Bhosekar et al., 2014) on orifice spillways, the range of height of orifice was selected as 0.20 m to 0.40 m and head in the range of 0.6 m to 1.4 m for the present research. Physical and numerical model studies were carried out to check the performance of orifice spillway for various operating heads and heights of orifice. Experiments were conducted on the spillway bottom and roof profiles designed with a head of 0.8 m in physical model. However, numerical simulations were carried out for spillway bottom and roof profiles designed with a head of 0.6 m, 0.8 m, 1.0 m and 1.4 m. The results obtained from the studies are discussed in subsequent sections. Based on physical and numerical model results, guidelines have been provided for design of an orifice spillway in respect of different hydraulic parameters.

# 5.2 Experimental Set Up 3

In the set up-3, the studies through orifice were carried out by providing the solid bottom and roof profile at the downstream of orifice opening. The design of spillway bottom profile was finalized based on the studies carried out on the set up-1 of sharp edged large orifice. The design of roof profile of spillway was finalized based on the studies carried out on the set up 2 i.e. orifice with solid bottom profile. The other spillway components such as pier and upstream spillway profile were also incorporated in the physical model. The side walls were provided at the downstream of orifice on both the sides, which will represent pier and training wall in prototype structure. Figure 5.1 shows the plan and section of physical model for experimental set up 3. Figure 5.2 and Figure 5.3 show a side view and upstream view of physical model. The geometry at the downstream portion of the profile after the crest was kept same as in the previous set ups. As shown in Figure 5.1, the geometry of bottom profile consists of three segments. The first segment is defined by the equation  $x^2 = 4h_dy$ , considering origin (0, 0) at spillway crest. The spillway bottom profile was designed for a head of 0.8 m. The second segment is a straight line and the third segment is a circular arc of a ski jump bucket to guide the flow towards downstream channel. The arrangement of approach channel and downstream channel was also kept same as in the previous studies. The width of span/ orifice was considered as 0.2 m, as the width is of the order of 10 m in the prototype adopted in most of the projects. The model was constructed in transparent Perspex sheet to visualize the flow conditions through the spillway.

In addition to other spillway components, the roof profile was incorporated during the experiments. The roof profile was designed as per the equation 4.4 derived in Chapter 4. In the equation  $x_1$  and  $y_1$  are horizontal and vertical coordinates of roof profile considering origin (0, 0) at the top of roof profile, from where the curve starts. The roof profile was fabricated in 6 mm and 12 mm thick transparent Perspex sheet. The structure was fixed at the bottom of the vertical wall (breastwall) as shown in Figure 5.1. Figure 5.4 shows close up view of roof profile. Height of orifice at the exit (d) is an important parameter in fixing the roof profile (length and height) and calculation of discharging capacity of an orifice spillway. Hence, it is used for analysis of flow through orifice spillway in the present set up 3. The length of roof profile/ breastwall i.e. 'a' was determined using equation 4.4 derived in Chapter 4. The height of curve 'b' was selected as 0.4 d, where d is the height of orifice at the exit. The coefficients A, B and m in the above equations were selected as 0.58, 0.26 and 1.82 respectively for b/d ratio of 0.4. The design head, h<sub>d</sub> was considered as 0.8 m. The roof profiles designed for a height of orifice, d of 0.20 m, 0.24 m, 0.28 m, 0.32 m and 0.36 m were studied in the physical model. The Reynolds numbers calculated for a combination of minimum and maximum range of head and height of orifice was calculated as 5.6 x10<sup>5</sup> and 1.8 x10<sup>6</sup> respectively which was found above the value suggested (Re > 10<sup>5</sup>) by many researchers to ensure turbulent flow conditions in the model (USBR, 1980, Pfister and Chanson, 2014). Thus, the scale effect due to viscous damping is not present.



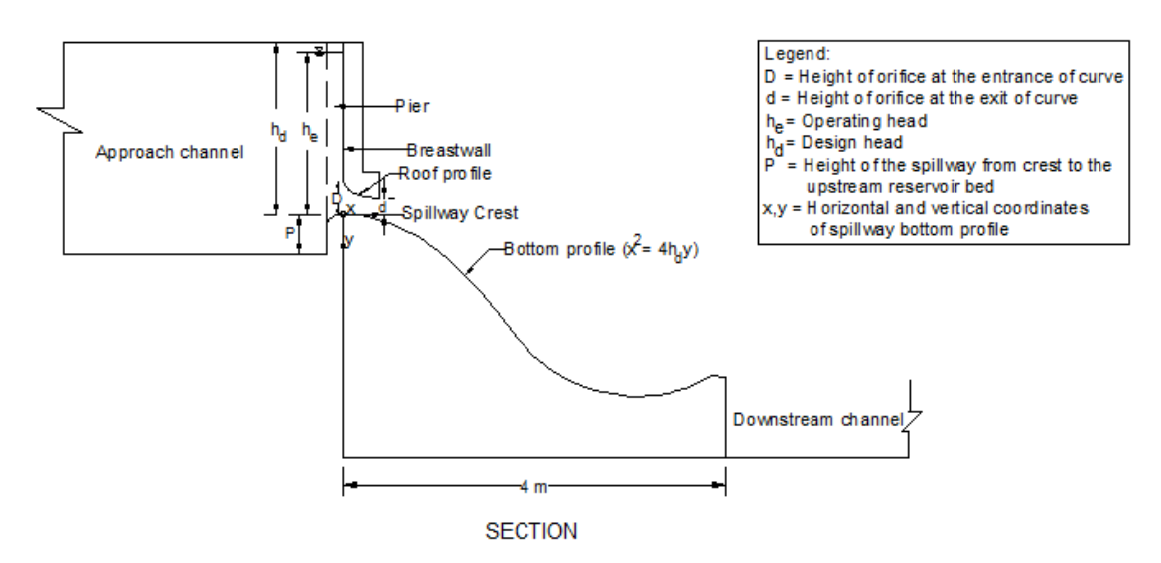


Fig. 5.1 Plan and section of physical model set up 3



Fig. 5.2 Side view of physical model showing bottom and roof profile for experimental set up 3

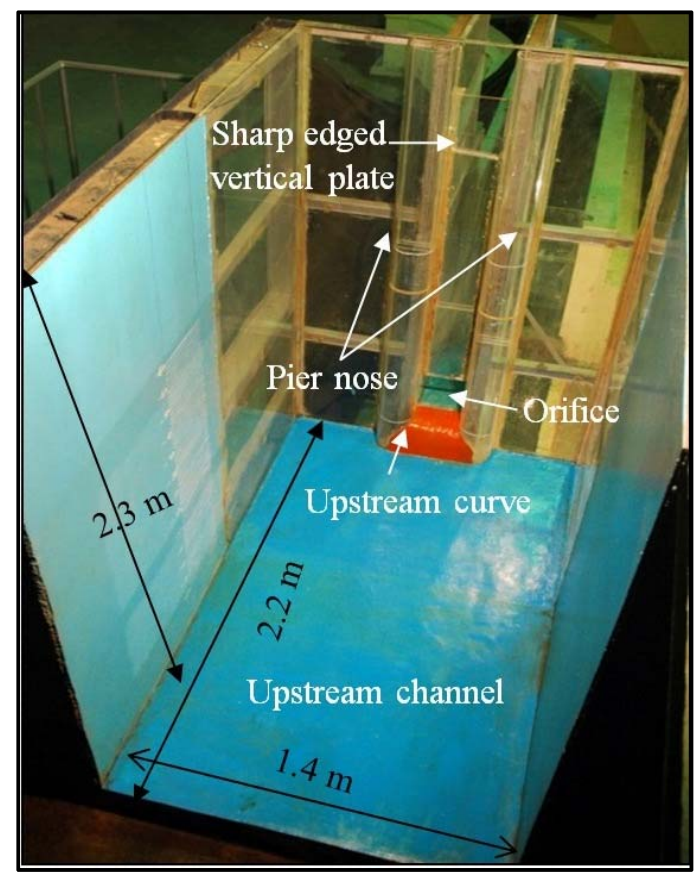
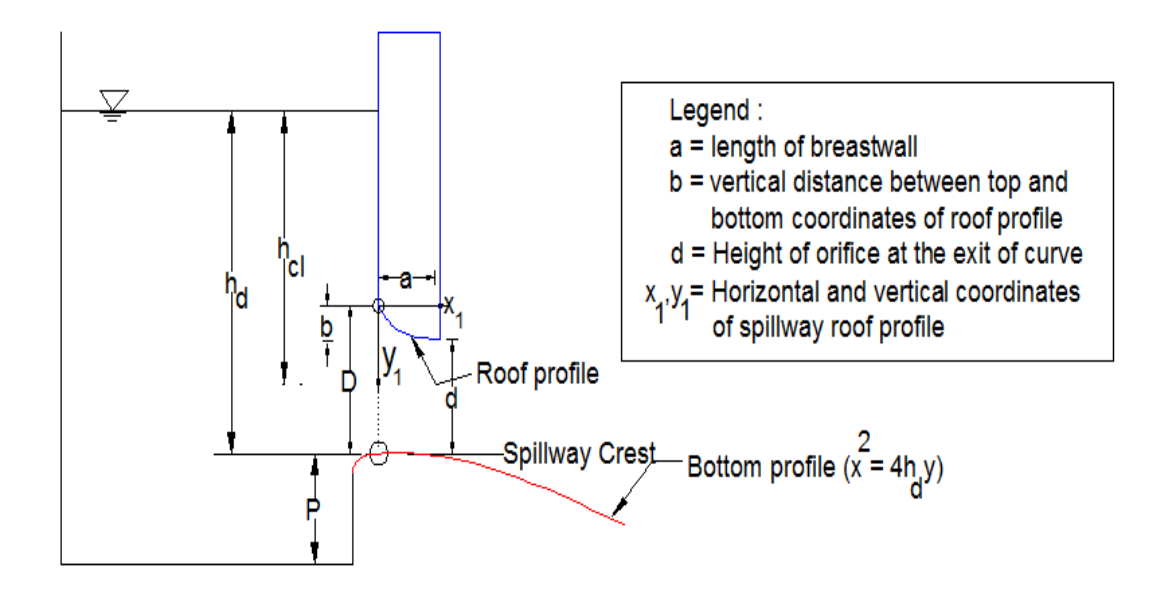


Fig. 5.3 Upstream view of physical model



## 5.2.1 Studies carried out on physical model

Physical model studies were carried out for design head ( $h_e/h_d=1$ ), head less than design head ( $h_e/h_d=0.8$ ) and head more than design head ( $h_e/h_d=1.33$ ) conditions. Experiments were conducted for five different heights of orifice openings viz. 0.20 m, 0.24 m, 0.28 m, 0.32 m and 0.36 m. The numerical simulations were carried out for different spillway profiles designed for the heads 0.6 m, 0.8 m, 1.0 m and 1.4 m. The heights of orifice were selected as 0.2 m, 0.24 m, 0.28 m, 0.32 m, 0.36 m and 0.4 m. The studies carried out in Chapter 4 indicated that there was no significant effect of height of spillway from the upstream reservoir bed (P) on different hydraulic parameters in assessing the performance of orifice spillway. However, height of spillway was selected as P=0.2 m in the present set up as the crest of orifice spillways are provided as near the river bed as possible to flush out the sediment. In orifice spillway, the total head required over the crest is up to 1.5 to 2 times the height of orifice (D) for change of regime from free flow to orifice flow. In view of this, height of orifice and operating heads were selected accordingly by ensuring orifice flow condition. Table 5.1 shows the list of experiments conducted on physical model for the setup 3.

Table 5.1 List of experiments conducted on physical model for set up-3

Sr. No.	d (m)	$h_d(m)$	$h_e/h_d$
1	0.20	0.8	0.8
2	0.24	0.8	0.8
3	0.28	0.8	0.8
4	0.32	0.8	0.8
5	0.20	0.8	1
6	0.24	0.8	1
7	0.28	0.8	1
8	0.32	0.8	1
9	0.36	0.8	1
10	0.20	0.8	1.33
11	0.24	0.8	1.33
12	0.28	0.8	1.33
13	0.32	0.8	1.33
14	0.36	0.8	1.33
	Total number	of studies =	14

The studies were carried out for assessing the performance of orifice spillway in terms of coefficient of discharge, pressure distribution on spillway bottom and roof profiles and water surface profile along centreline of spillway.

#### 5.2.2 Measurement set up

Various measurements like water discharge, pressure profile along bottom and roof profiles, water surface profile along centreline of spillway were carried out for assessing the performance of orifice spillway. Following instrumentations were used on the model:

- 1. Hook gauges and Rehbock plate to measure the water discharge
- 2. Piezometers over spillway bottom and roof profile for observing the pressures
- 3. Endevo made piezoresistive electronic transducer for measurement of hydrodynamic pressures with PC based data acquisition system
- 4. Pointer gauge for observing water surface profile along centreline of spillway
- 5. Photography for analysis of flow conditions through the spillway

The discharge was calculated by measuring the depth of flow over Rehbock plate. Stilling gauge wells were connected to the measurement channels 1.5 m upstream of the Rehbock plates. Hook gauges were used for measurement of head of water flowing over the Rehbock plates in the stilling wells. The piezometers were 4 mm in diameter and connected with the manometer for pressure measurements. The piezometers were located at the centre of spillway width along spillway bottom and roof profile for measuring the pressures using manometer. The piezometers were flushed with the spillway surface to avoid errors in measurements. Endevco make Miniature Piezoresistive electronic transducer with +5 PSI has been used on roof profile for measurement of hydrodynamic pressures coupled with PC based data acquisition system. The diameter of the sensing diaphragm of the transducer was 4 mm. The transducer was connected through signal conditioner with PC based data acquisition system containing A/D card and data acquisition software. The sampling rate was 100 samples per second with an accuracy of 0.1% in analog to digital conversion. Figure 5.5 shows arrangement of the transducers on roof profile of orifice spillway along with PC based data acquisition system. Pointer gauge of length 1.5 m with graduation of 1 mm on it was used for measurement of water surface profiles. Vernier scale with accuracy measurement of 1/10<sup>th</sup> mm was fitted on it for accurate measurement. Water surface measurements were taken at an interval of 1 cm along spillway profile.

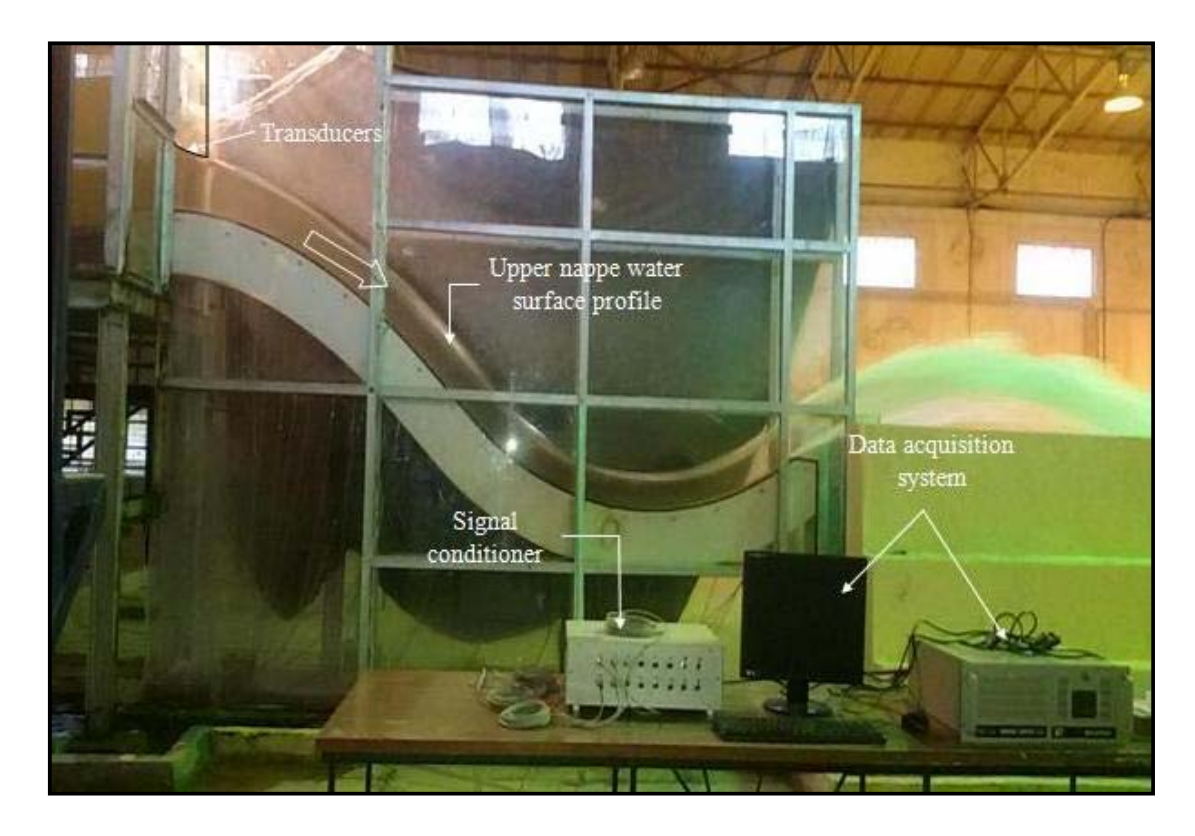


Fig. 5.4 Arrangement of the transducers on roof profile of orifice spillway in physical model (set up 3)

### **5.3 Numerical Model**

Computational Fluid Dynamics module of the FLUENT version 6.3.26 was used for the numerical simulations. The geometry of the model was created in GAMBIT software. The geometry of the present set up consists of upstream tank, piers, upstream curve and spillway roof and bottom profile and downstream channel. The spillway channel consists of three segments i.e. parabolic profile, slope and circular bucket. The domain extent was 2.4 m upstream and 6.4 m downstream from orifice opening. The domain height above the water surface was considered as 0.20 m to capture the air-water interface phenomena. The crest of the orifice spillway was kept 0.20 m above the bed of the approach channel to fulfil the criteria of flushing required.

#### 5.3.1 Grid size and boundary conditions

Selection of grid size and boundary conditions can have a major impact on the accuracy of results. The grid size 0.004 m was used for the study. This grid size was used throughout the area of the orifice. Coarser mesh was generated in regions of less interest. Figure 5.6 shows grid generation along centreline of orifice spillway. As the flow passes

through orifice, it suddenly changes from subcritical to supercritical state. Similarly, the flow become pressurized below the roof profile and again moves as a free surface flow once it leaves the roof profile. In view of this, the grid was made dense in the vicinity of roof profile to capture the transition state of flow accurately. Figure 5.7 shows closer view of grid generation in the vicinity of roof profile.

The pressure inlet boundary condition with turbulence intensity and viscosity ratio as 1% was used at domain inlet through which the water enters in the tank. The turbulence intensity was considered as 1% as the flow was supposed to enter the reservoir with minimum turbulence as is expected in a large reservoir. The upstream head in the tank was maintained at the domain inlet. The pressure inlet boundary condition was also defined at the top of the upstream tank and spillway. Pressure outlet boundary condition with turbulence intensity 10% and viscosity ratio 10% was used at domain outlet (FLUENT, 2006). The wall boundary with no slip condition was defined at the bottom and side of the upstream tank and spillway channel. All the boundary conditions defined to the domain are shown in Figure 5.6.

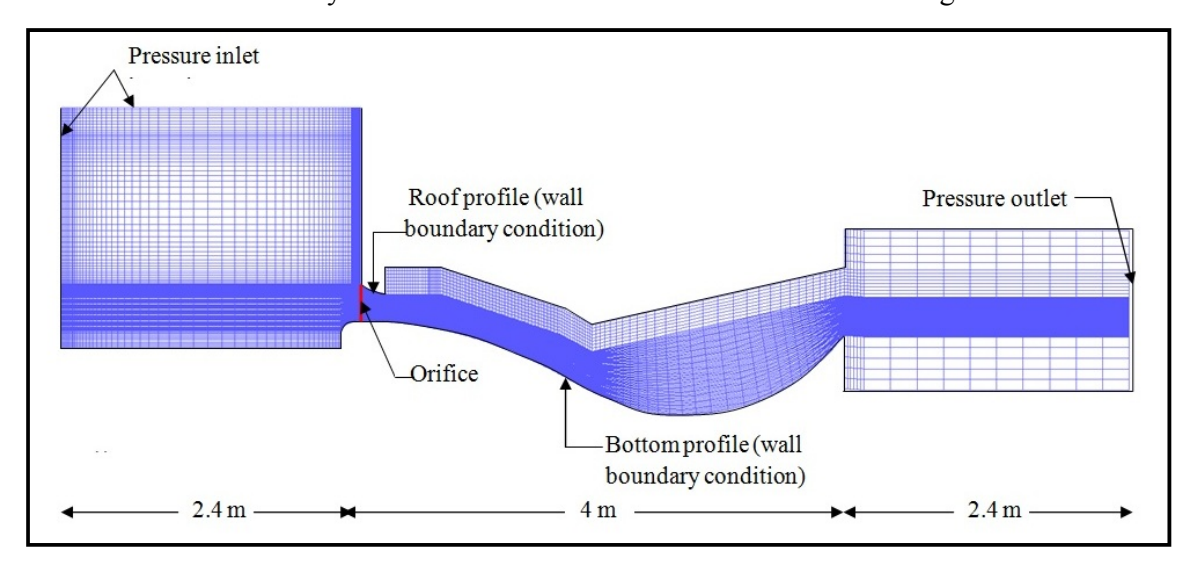


Fig. 5.5 Grid generation and boundary conditions of domain

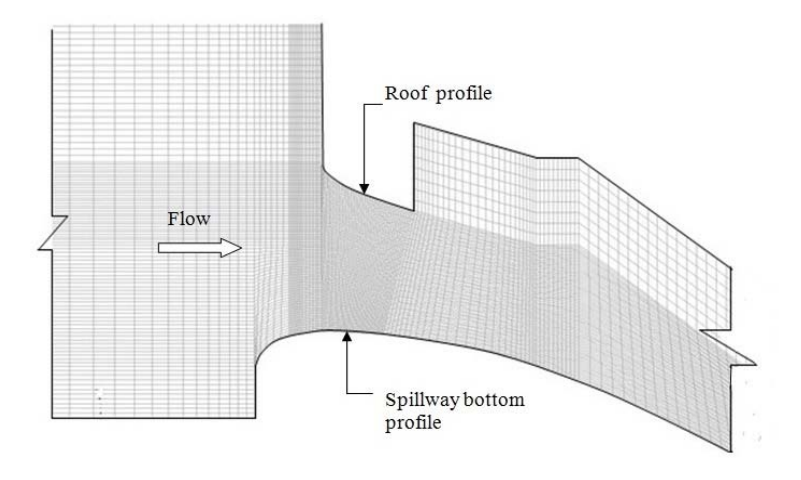


Fig. 5.6 Closer view showing grid generation in the vicinity of roof profile

#### 5.3.2 Studies carried out on numerical model

The numerical simulations were carried out for different spillway profiles designed for the heads 0.6 m, 0.8 m, 1.0 m and 1.4 m. The heights of orifice were selected as 0.2 m, 0.24 m, 0.28 m, 0.32 m, 0.36 m and 0.4 m. Studies were carried out for the design head ( $h_e/h_d = 1$ ), head less than design head ( $h_e/h_d = 0.8$ ) and head more than design head ( $h_e/h_d = 1.33$ ). Table 5.2 shows the list of simulations carried out on numerical model set up 3. In the Table 5.2, 'd' is height of orifice at exit of roof profile, ' $h_d$ ' is the design head for which spillway profiles are designed and ' $h_e$ ' is the operating head. Total 63 numbers of simulations were carried out on numerical model set up 3. Simulations were carried out only for those heights of orifice where orifice flow is fully developed (marked  $\sqrt{}$  in Table 6.2 are full orifice flow).

Table 5.2 List of simulations carried out on numerical model set up 3

C. N.	d :	1. /1.	Design head, h <sub>d</sub>					
Sr. No.	d in m	h <sub>e</sub> /h <sub>d</sub>	0.6 m	0.8 m	1.0 m	1.4 m		
1	0.20	0.8			V	$\sqrt{}$		
2	0.24	0.8			V	$\sqrt{}$		
3	0.28	0.8	-	1	V	V		
4	0.32	0.8	-	1	V	V		
5	0.36	0.8	-	-	V	V		
6	0.40	0.8	-	-	V	$\sqrt{}$		
7	0.20	1	V	1	V	V		
8	0.24	1	V	1	V	V		
9	0.28	1	V	√	V	V		
10	0.32	1		V	V	$\sqrt{}$		
11	0.36	1	-	1	V	$\sqrt{}$		
12	0.40	1	-	-	V			
13	0.20	1.33	V	√	V	$\sqrt{}$		
14	0.24	1.33	V	1	V	$\sqrt{}$		
15	0.28	1.33	V	1	V	$\sqrt{}$		
16	0.32	1.33			V	$\sqrt{}$		
17	0.36	1.33			V	$\sqrt{}$		
18	0.40	1.33		V	V	V		
	To	otal numbe	er of studio	es = 63	•			
Note:	- represents t	hat the flow	v is not full	v develop	ed orifice	flow		

Table 5.2 shows the list of simulations carried out on numerical model set up 3. In the Table 5.2, 'd' is height of orifice at exit of roof profile, 'h<sub>d</sub>' is the design head for which spillway profiles are designed and 'h<sub>e</sub>' is the operating head. Total 63 numbers of simulations were carried out on numerical model set up 3. Simulations were carried out only for those

heights of orifice where orifice flow is fully developed (marked  $\sqrt{}$  in Table 5.2 are full orifice flow).

The set up 3 of numerical model was same as the set up 1 and 2. Numerical model developed for this set up 3was verified in terms of grid convergence and turbulence model. The grid size of 0.004 m and Realizable k-ɛ turbulence model with Modified High Resolution Interface Capturing (HRIC) scheme was found to be suitable in analysing the flow over the spillway in respect all the parameters.

#### **5.3.3** Validation of numerical model

Validation of CFD code is an essential element of the code development process. In present work, large numbers of simulations were proposed to carry out for basic research on orifice spillway. Hence, numerical model was first validated by comparing the results with physical model in terms of discharge, pressures on bottom and roof profile and water surface profile. Total 14 numbers of studies carried out in physical model were used for validation of numerical model. Table 5.3 shows the comparison of discharge between physical and numerical model and corresponding calculated % error.

Table 5.3 Comparison of discharges between physical and numerical model

Experiment				rge in m <sup>3</sup> /s	Error
No.	<b>d</b> (m)	h <sub>e</sub> /h <sub>d</sub>	Physical model	Numerical model	in %
1	0.20	0.8	0.118	0.114	3.4
2	0.24	0.8	0.140	0.135	3.6
3	0.28	0.8	0.158	0.156	1.3
4	0.32	0.8	0.170	0.171	0.5
5	0.20	1	0.140	0.140	0
6	0.24	1	0.155	0.156	0.6
7	0.28	1	0.180	0.181	0.5
8	0.32	1	0.207	0.204	1.4
9	0.36	1	0.235	0.230	2.1
10	0.20	1.33	0.160	0.159	0.6
11	0.24	1.33	0.193	0.191	1
12	0.28	1.33	0.230	0.221	3.9
13	0.32	1.33	0.258	0.250	3.1
14	0.36	1.33	0.283	0.282	0.4

The study indicated that discharges obtained in numerical model very well match with physical model for all heights of orifice opening. The percentage error was estimated to be 0 to 3.9 % and  $R^2$  value was calculated as 0.997 which is found to be in acceptable limit. Figure 5.8 and 5.9 shows a typical plot for comparison between physical and numerical model in respect of pressures on the roof profile ( $h_{p1}$ ) and bottom profile ( $h_{p}$ ) respectively. The results were plotted by taking the distance from the orifice at which the pressure tap are located on x axis and calculated pressures in m of water on y axis. Figure 5.10 shows water surface profile along centreline of orifice spillway.

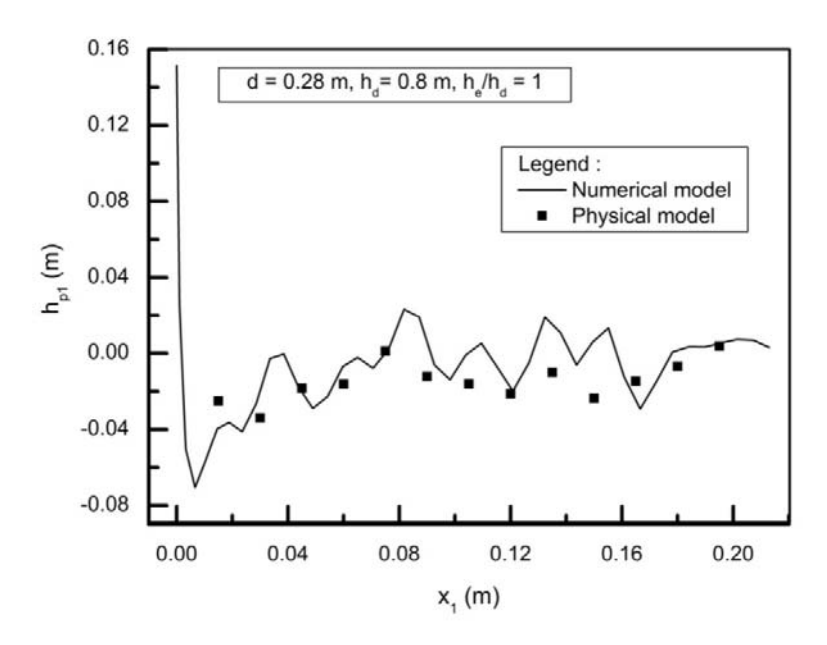


Fig. 5.7 Comparison of pressures on spillway roof profile between physical and numerical model studies

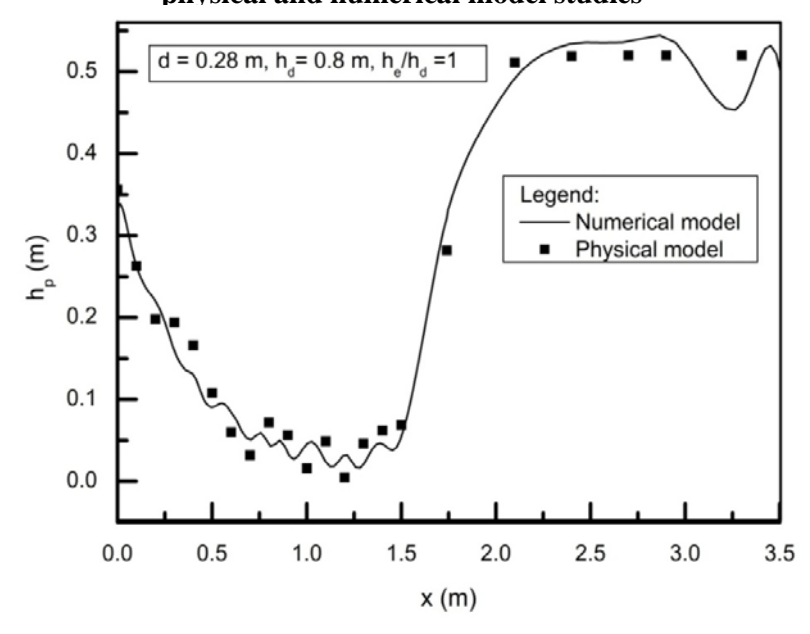


Fig. 5.8 Comparison of pressures on spillway bottom profile between physical and numerical model studies

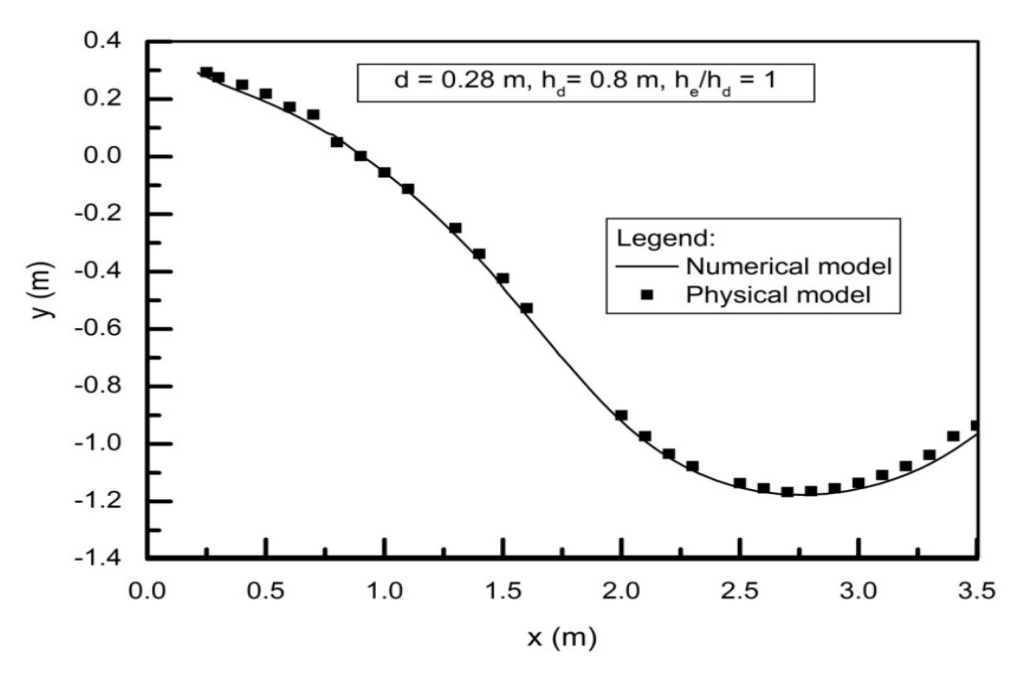


Fig. 5.9 Comparison of water surface profile between physical and numerical model

It can be seen from Figures 5.8 and 5.9 that the computed results in terms of pressures were in good agreement with those predicted by physical model. Similarly, the values of water surface profile computed in numerical model were also matching well with the values measured in physical model as shown in Figure 5.10. The Realizable k-ε turbulent model with Modified HRIC scheme could capture the pressures and water surface profile throughout the length of spillway accurately. The results were also analysed by calculating R<sup>2</sup>, % error and root mean square error for all the ranges of d and h<sub>e</sub>/h<sub>d</sub> ratios as shown in Table 5.4. All the parameters were found to be in acceptable range.

Table 5.4 indicates that the maximum R<sup>2</sup> value in respect of pressures on roof and bottom profile was calculated as 0.95 and 1 respectively. Minimum and maximum % errors were calculated as 0.02 and 0.24 with respect to the pressures on roof profile. However, minimum and maximum % errors were calculated as 0 and 0.15 with respect to the pressures on spillway bottom profile. Similarly, the maximum root mean square errors were calculated as 0.03 m and 0.1 m in respect of pressures on roof and bottom profile respectively. All these parameters were found in acceptable limits for the range of parameters studied indicating that the roof profile and bottom profile equations developed in the present study is a good choice to start for the design of orifice spillway. Table 5.4 also indicates that the R<sup>2</sup> value, maximum % error and root mean square error (RMSE) for water surface profile were calculated as 0.99, 7% and 0.12 m respectively, which were found to be acceptable. The results obtained seem promising for an application of numerical models in modeling the spillway flows. Hence, studies mentioned in Table 5.2 were carried out using numerical model for further analysis of flow.

Table 5.4 Calculation of R<sup>2</sup>, RMSE and average % error for validation of numerical model

Sr.			Pressures on roof profile			Press	sures on bot	tom profile	V	Vater surfac	e profiles
No.	<b>d</b> (m)	h <sub>e</sub> /h <sub>d</sub>	$\mathbb{R}^2$	RMSE (m)	Average % error	$\mathbb{R}^2$	RMSE (m)	Average % error	$\mathbb{R}^2$	RMSE (m)	Average % error
1	0.2	0.8	0.95	0.02	0.07	0.99	0.02	0.01	0.99	0.02	5.00
2	0.24	0.8	0.80	0.01	0.03	0.99	0.02	0.02	0.99	0.02	2.00
3	0.28	0.8	0.80	0.01	0.03	0.98	0.03	0.04	0.99	0.02	1.00
4	0.32	0.8	0.80	0.01	0.02	0.99	0.03	0.04	0.99	0.01	0.20
5	0.20	1	0.91	0.03	0.14	0.98	0.03	0.12	0.99	0.03	6.00
6	0.24	1	0.89	0.01	0.02	0.99	0.02	0.05	0.99	0.01	1.00
7	0.28	1	0.83	0.01	0.06	1.00	0.02	0.01	0.99	0.02	1.34
8	0.32	1	0.90	0.01	0.03	0.99	0.02	0.00	0.99	0.01	0.24
9	0.36	1	0.80	0.01	0.04	0.98	0.04	0.08	0.99	0.01	0.90
10	0.20	1.33	0.90	0.03	0.24	0.90	0.10	0.15	0.99	0.03	7.00
11	0.24	1.33	0.90	0.02	0.02	0.98	0.04	0.05	0.99	0.02	3.00
12	0.28	1.33	0.90	0.01	0.02	0.97	0.05	0.10	0.99	0.02	1.93
13	0.32	1.33	0.90	0.01	0.02	0.98	0.06	0.06	0.99	0.02	4.00
14	0.36	1.33	0.91	0.02	0.04	0.99	0.05	0.00	0.99	0.12	5.00

To visualize the flow conditions especially in the vicinity of roof profile is a very important step in assessing the performance of an orifice spillway. It was experienced from model studies conducted in CWPRS that flow through orifice spillway at the entrance does not follow elliptical profile recommended by United State Bureau of Reclamation on most of the orifice spillway projects. In such cases, flow separation takes place on the orifice roof profile for high operating heads resulting in reduced discharging capacity. Thus, the design of roof profile was finalised by trial and error method based on the results of specific case study. However, in the present research, the equation developed for the design of roof profile was finalised based on extensive experimentation on physical and numerical models. Equation was developed considering all practical design heads and heights of orifice. However, it is necessary to validate this equation by visualising the flow conditions near the roof profile. Flow conditions were observed in physical and numerical models for all the combinations of orifice spillway mentioned in Table 5.2. In numerical model, flow behaviour of orifice spillway was visualized by studying the phase diagrams generated during post processing of the results of numerical simulation. Figures 5.11 and 5.12 show a flow condition of orifice spillway observed in physical and numerical model respectively throughout the length of spillway. Figures 5.13 and 5.14 show a closer view showing the flow conditions in the vicinity of roof profile in physical and numerical model respectively.



Fig. 5.10 Flow conditions through orifice spillway in physical model

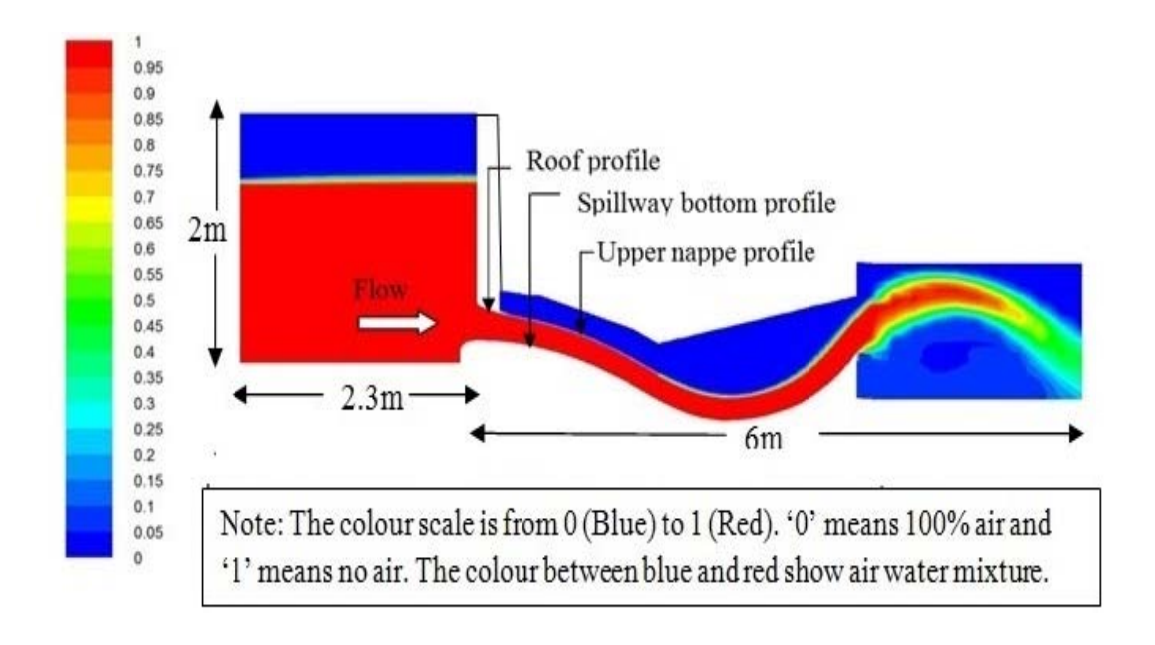
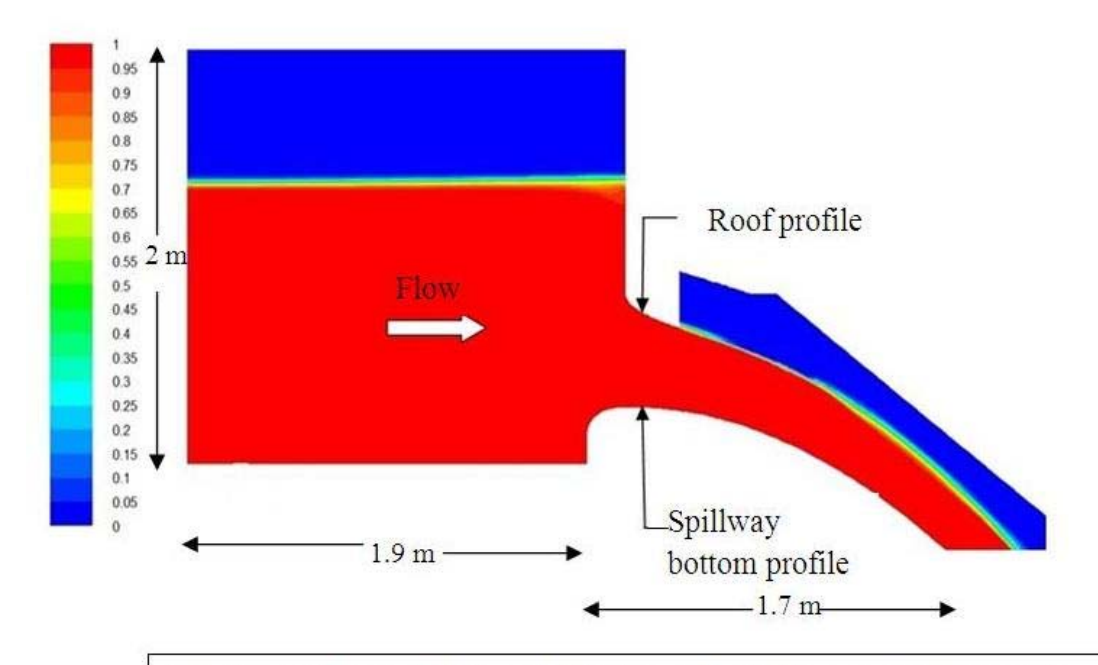


Fig. 5.11 Flow conditions through orifice spillway in numerical model



Fig. 5.12 Closer view showing flow conditions in the vicinity of roof profile in physical model



Note: The colour scale is from 0 (Blue) to 1 (Red). '0' means 100% air and '1' means no air. The colour between blue and red show air water mixture.

Fig. 5.13 Closer view showing flow conditions in the vicinity of roof profile in numerical model

It can be seen from Figures 5.11 to 5.14 that the flow condition is accurately simulated in numerical model as that of observed in physical model. Smooth flow conditions were observed throughout the length of spillway. The flow through orifice follows the path of roof profile that was designed with the proposed equation from the present study. No separation was found on bottom and roof profiles of orifice spillway. In addition to design head 0.8 m, the flow conditions were also observed in numerical model for the design heads of 0.6 m 1.0 m and 1.4 m and height of orifice varying from 0.2 m to 0.4 m. It was found that in all the cases flow adheres the roof profile resulting in maximum discharging capacity and acceptable pressure distribution on spillway surface.

# 5.4 Analysis of Results and Discussions

The studies were carried out for various combinations of spillway profiles designed with different heads, heights of orifice, design heads, less than design heads and greater than design heads as shown in Table 5.2. The simulations were carried out for those heights of orifice, 'd' at which orifice flow is fully developed. The data was combined and results were analysed in respect of coefficient of discharge, pressure distribution on spillway bottom and roof profile and water surface profile along centre line of spillway.

## 5.4.1 Discharging capacity of orifice spillway

Discharging capacity is one of the most important hydraulic parameters in design of spillway. The assessment of  $C_d$  is essential for the preliminary design of the spillway in order to provide sufficient waterway and to pass the probable maximum flood at the maximum reservoir water level. The coefficient of discharge  $(C_d)$  of an orifice spillway is influenced by number of parameters like head over the spillway crest, spillway bottom and roof profile, size of orifice opening, shape of pier etc. Assessment of the  $C_d$  is therefore difficult due to wide variation of these parameters from site to site. In the present research, systematic work has been carried out to study the effect of all these parameters on  $C_d$  values. Various combinations of spillway bottom and roof profile designed with different heads, head over the crest and heights of orifice (refer Table 5.2) were studied. The  $C_d$  was calculated using the following formula (BIS 6934: 1998):

$$Q = C_d * A * \sqrt{(2gh_{cl})}$$
 (5.1)

Where Q is the discharge through orifice in  $m^3/s$ , A is area of orifice in  $m^2$ , g is acceleration due to gravity in  $m/s^2$  and  $h_{cl}$  is centreline head in m ( $h_e$  –d/2).

The discharges passed through the orifice and corresponding coefficients of dischargefor the spillway profiles designed for a head ( $h_d$ ) of 0.6 m, 0.8 m, 1.0 m and 1.4 m are shown in Tables 5.5, 5.6, 5.7 and 5.8 respectively. In these tables, 'd' is height of orifice at the exit of the curve,  $h_d$  is design head,  $h_{cl}$  is centreline head,  $h_e$  is head at which the spillway is operated, Q is the discharge through orifice and  $C_d$  is corresponding coefficient of discharge.

Table 5.5 Discharges and corresponding C<sub>d</sub> for design head of 0.6 m

Sr. No.	d (m)	h <sub>d</sub> (m)	h <sub>e</sub> /h <sub>d</sub>	h <sub>cl</sub> (m)	$Q \text{ in } (m^3/s)$	$C_d$
1	0.2	0.6	0.8	0.38	0.094	0.861
2	0.24	0.6	0.8	0.36	0.106	0.831
3	0.2	0.6	1	0.50	0.112	0.894
4	0.24	0.6	1	0.48	0.131	0.889
5	0.28	0.6	1	0.46	0.153	0.909
6	0.32	0.6	1	0.44	0.166	0.883
7	0.2	0.6	1.33	0.70	0.136	0.919
8	0.24	0.6	1.33	0.68	0.159	0.908
9	0.28	0.6	1.33	0.66	0.189	0.939
10	0.32	0.6	1.33	0.64	0.205	0.905
11	0.36	0.6	1.33	0.62	0.235	0.937
12	0.4	0.6	1.33	0.60	0.251	0.916

Table 5.6 Discharges and corresponding  $C_{\text{d}}$  for design head of 0.8  $\mbox{m}$ 

Sr. No.	d (m)	h <sub>d</sub> (m)	h <sub>e</sub> /h <sub>d</sub>	h <sub>cl</sub> (m)	Q (m <sup>3</sup> /s)	$C_d$
1	0.2	0.8	0.8	0.54	0.114	0.876
2	0.24	0.8	0.8	0.52	0.135	0.881
3	0.28	0.8	0.8	0.50	0.156	0.889
4	0.32	0.8	0.8	0.48	0.170	0.866
7	0.2	0.8	1	0.70	0.135	0.911
8	0.24	0.8	1	0.68	0.156	0.890
9	0.28	0.8	1	0.66	0.181	0.898
10	0.32	0.8	1	0.64	0.204	0.900
11	0.36	0.8	1	0.62	0.230	0.916
13	0.2	0.8	1.33	0.96	0.159	0.914
14	0.24	0.8	1.33	0.94	0.191	0.925
15	0.28	0.8	1.33	0.92	0.221	0.927
16	0.32	0.8	1.33	0.90	0.250	0.928
17	0.36	0.8	1.33	0.88	0.282	0.940
18	0.4	0.8	1.33	0.86	0.309	0.938

Table 5.7 Discharges and corresponding  $C_{\text{d}}$  for design head of 1 m

Sr. No.	d (m)	h <sub>d</sub> (m)	h <sub>e</sub> /h <sub>d</sub>	h <sub>cl</sub> (m)	$Q (m^3/s)$	$C_d$
1	0.2	1	0.8	0.70	0.135	0.890
2	0.24	1	0.8	0.68	0.157	0.895
3	0.28	1	0.8	0.66	0.181	0.898
4	0.32	1	0.8	0.64	0.199	0.877
5	0.36	1	0.8	0.62	0.220	0.876
6	0.4	1	0.8	0.60	0.232	0.845
7	0.2	1	1	0.90	0.151	0.898
8	0.24	1	1	0.88	0.182	0.913
9	0.28	1	1	0.86	0.207	0.900
10	0.32	1	1	0.84	0.238	0.916
11	0.36	1	1	0.82	0.262	0.907
12	0.4	1	1	0.80	0.290	0.915
13	0.2	1	1.33	1.23	0.180	0.916
14	0.24	1	1.33	1.21	0.217	0.928
15	0.28	1	1.33	1.19	0.250	0.924
16	0.32	1	1.33	1.17	0.286	0.933
17	0.36	1	1.33	1.15	0.316	0.924
18	0.4	1	1.33	1.13	0.355	0.942

Table 5.8 Discharges and corresponding C<sub>d</sub> for design head of 1.4 m

Sr. No.	<b>d</b> (m)	$h_d(m)$	h <sub>e</sub> /h <sub>d</sub>	$h_{cl}(m)$	$Q (m^3/s)$	$C_d$
1	0.2	1.4	0.8	1.02	0.157	0.877
2	0.24	1.4	0.8	1.00	0.194	0.912
3	0.28	1.4	0.8	0.98	0.223	0.908
4	0.32	1.4	0.8	0.96	0.247	0.889
5	0.36	1.4	0.8	0.94	0.277	0.896
6	0.4	1.4	0.8	0.92	0.305	0.897
7	0.2	1.4	1	1.30	0.179	0.886
8	0.24	1.4	1	1.28	0.222	0.923
9	0.28	1.4	1	1.26	0.252	0.905
10	0.32	1.4	1	1.24	0.290	0.919
11	0.36	1.4	1	1.22	0.322	0.914
12	0.4	1.4	1	1.20	0.351	0.904
13	0.2	1.4	1.33	1.76	0.216	0.918
14	0.24	1.4	1.33	1.74	0.260	0.927
15	0.28	1.4	1.33	1.72	0.302	0.928
16	0.32	1.4	1.33	1.70	0.341	0.922
17	0.36	1.4	1.33	1.68	0.385	0.931
18	0.4	1.4	1.33	1.66	0.426	0.933

Tables 5.5 to 5.8 indicate that as the head over the crest increases, discharge through orifice also increases for a particular height of orifice opening. Similarly, there is increase in discharge with increase in height of orifice for a particular head over the crest. The coefficient of discharge was found in the range of 0.831 to 0.942. The  $C_d$  value was increased in the present set up 3 as compared to the sharp edged orifice with (set up 2) and without (set up 1) spillway bottom profile. This increase is due to provision of roof profile of orifice spillway which guided the flow and contributed in enhancing the discharging capacity of spillway. Thus, the study indicates the importance of roof profile in deciding the discharging capacity of orifice spillway. The coefficient of discharge was also substantially higher than  $C_d$  observed on most of orifice spillway projects reported by Bhosekar et al. (2014) as there is a large variation in various parameters on prototype. The better  $C_d$  values arrived in the present study are due to streamlined design of bottom and roof profiles for a given head and height of orifice. Hence, it can be concluded that in addition to d and  $h_d$ , bottom and roof profiles of orifice spillway are also important parameters which affect the discharging capacity of orifice spillway.

Tables 5.5 to 5.8 provide a large database of discharges and coefficient of discharge with variation of design head, operating head and various heights of orifice opening. This data would be useful to design engineers to decide the discharging capacity of orifice spillway at initial stage of design. However, as the data base was large, an attempt has been made to

develop an equation to estimate the  $C_d$  for an orifice spillway considering entire range of heads and heights of orifice studied. The equation developed for  $C_d$  is discussed in following subsections.

## 5.4.2 Effect of non-dimensional parameters on coefficient of discharge

Before deriving an equation, the effect of non-dimensional parameters on  $C_d$  has been studied. As per the dimensional analysis (discussed in Chapter 2),  $h_{cl}/h_d$  and  $h_{cl}/d$  are found to be the important parameters that decide  $C_d$  of orifice spillway. Hence, the  $C_d$  values were plotted in terms of non-dimensional parameters such as  $h_{cl}/h_d$  and  $h_{cl}/d$  for entire range of design heads, operating heads and heights of orifice studied. However, a typical non dimensional plot between the estimated  $C_d$  and  $h_{cl}/h_d$  is shown in Figure 5.15. Similarly a typical non dimensional plot between the estimated  $C_d$  and  $h_{cl}/d$  is shown in Figure 5.16.

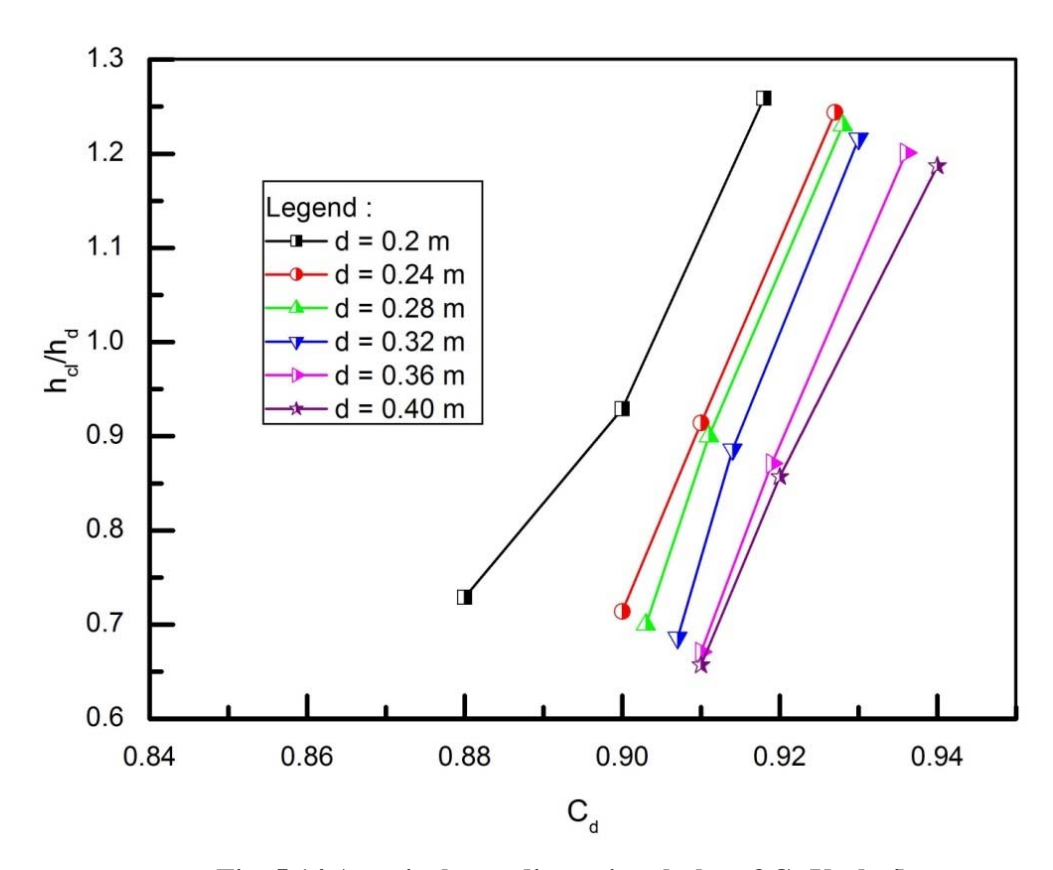


Fig. 5.14 A typical non-dimensional plot of C<sub>d</sub> Vs h<sub>cl</sub>/h<sub>d</sub>

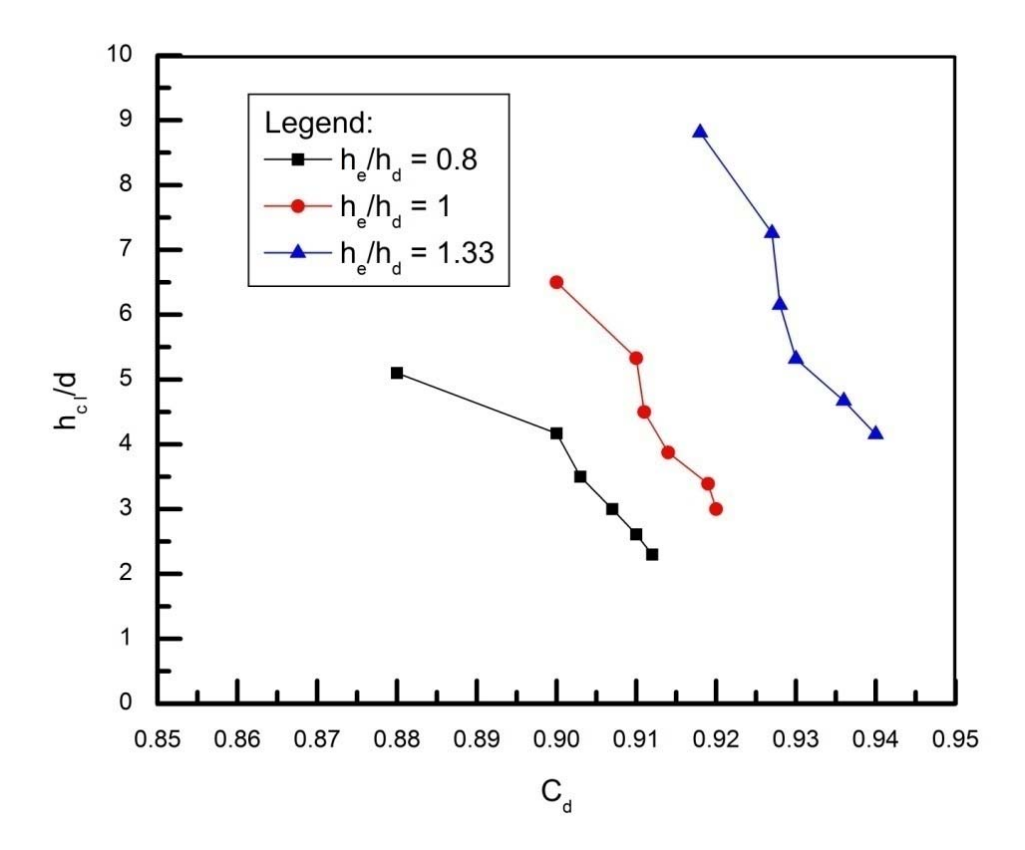


Figure 5.15 shows that for a particular height of orifice (d), the  $C_d$  increases with increase in  $h_{cl}/h_d$  ratio. However, for a particular head over the crest, as  $h_{cl}/d$  decreases, there is increase in  $C_d$  value as shown in Figure 5.16. Hence, the  $h_{cl}/d$ , and  $h_{cl}/h_d$  are found to be some of the governing non dimensional parameters in deriving an equation for  $C_d$  of an orifice spillway. Since the width of orifice has not been varied, the analysis in respect of  $h_{cl}/d$  is beyond the scope of the present study. The height of crest of spillway from the upstream reservoir bed (P) is found to be an insignificant parameter in determining the discharging capacity of orifice spillway. Hence, it can be neglected in deriving an equation of  $C_d$  of an orifice spillway.

# 5.4.3 Derivation of an equation to estimate $C_d$ of an orifice spillway

The present study identified the role of important parameters in determining the discharging capacity of an orifice spillway. The results of numerical models (63 complete sets of simulations) were used to develop an equation to estimate C<sub>d</sub> value. Various forms of equations were tried using multiple regression analysis. However, the form of Eq. (5.2) was found to be more suitable.

$$C_d = a * \left(\frac{h_{cl}}{d}\right)^b * \left(\frac{h_{cl}}{h_d}\right)^c$$
(5.2)

Where a, b and c are regression coefficients obtained while fitting the equation.

The range of design heads selected in the research is very high. Hence, the coefficients in equation 5.2 were derived for individual design head separately as shown in Table 5.9.

Table 5.9 Regression coefficients for estimating  $C_d$  of an orifice spillway

h <sub>d</sub> (m)	a	b	c	$\mathbb{R}^2$
0.6	0.958	-0.0578	0.139	0.94
0.8	0.964	-0.0477	0.122	0.95
1	0.959	-0.0353	0.101	0.95
1.4	0.980	-0.0409	0.093	0.92

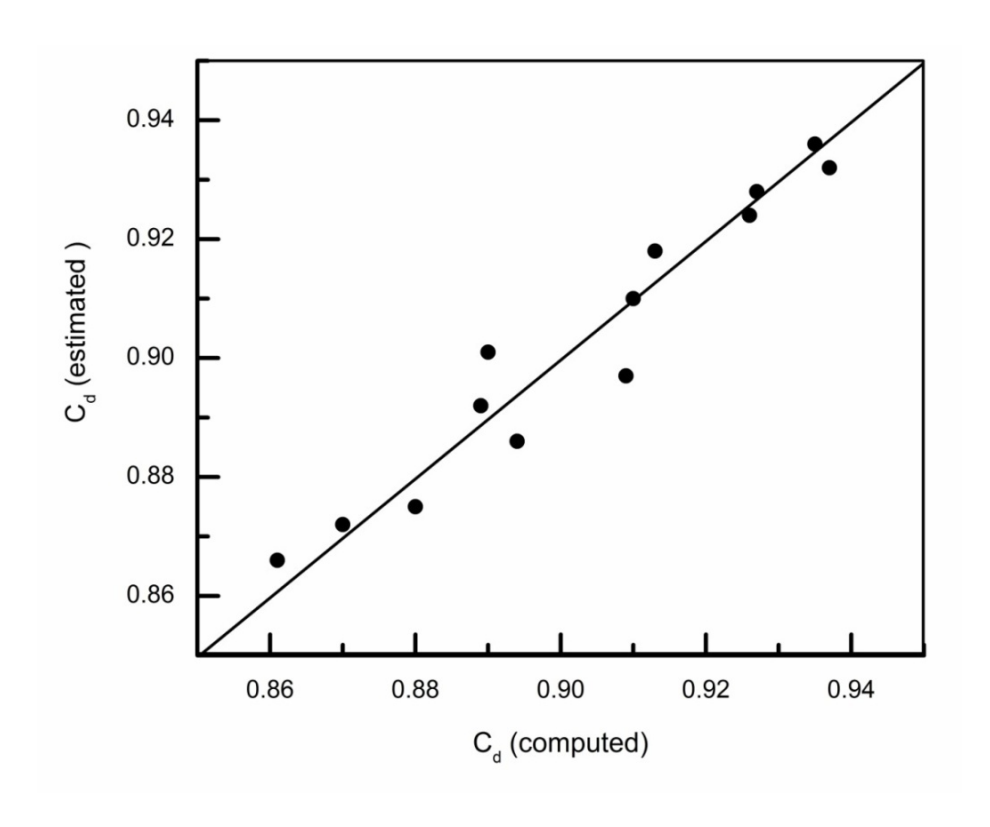
The data for all the design heads was also combined and following equation was developed.

$$C_d = 0.933 * \left(\frac{h_{cl}}{d}\right)^{-0.0131} * \left(\frac{h_{cl}}{h_d}\right)^{0.0834}$$
(5.3)

Equations 5.2 and 5.3 are developed from the present research based on properly designed bottom and roof profile (derived and explained in Chapter 4) for various heads and heights of orifice. The  $C_d$  values for all the combinations of hydraulic parameters mentioned in Tables 5.5 to 5.8 were estimated using equation 5.2 with coefficients corresponding to particular design head from Table 5.9. The estimated values were compared with computed values using equation 5.1. Figures 5.17 and 5.18 show comparison of estimated values (equation 5.2) and computed value (equation 5.1) of  $C_d$  for lower and upper range of heads i.e. 0.6 m and 1.4 m respectively.

Figure 5.17 and 5.18 reveals that the estimated  $C_d$  has a maximum error of  $\pm$  0.9 and 1.2 % for design head of 0.6 m and 1.4 m respectively. Thus, the comparison shows a satisfactory prediction of  $C_d$  through the orifice spillway using proposed formula. However, the derived equations 5.2 and 5.3 to estimate  $C_d$  are valid for the following ranges of d,  $h_d$  and b/d ratio:

$$\begin{array}{l} 0.2 \ m \leq d \leq 0.4 \ m \\ 0.6 \ m \leq h_d \leq 1.4 \ m \\ 0.8 \leq h_e/h_d \leq 1.33 \ m \\ b = 0.4 \ d \end{array}$$



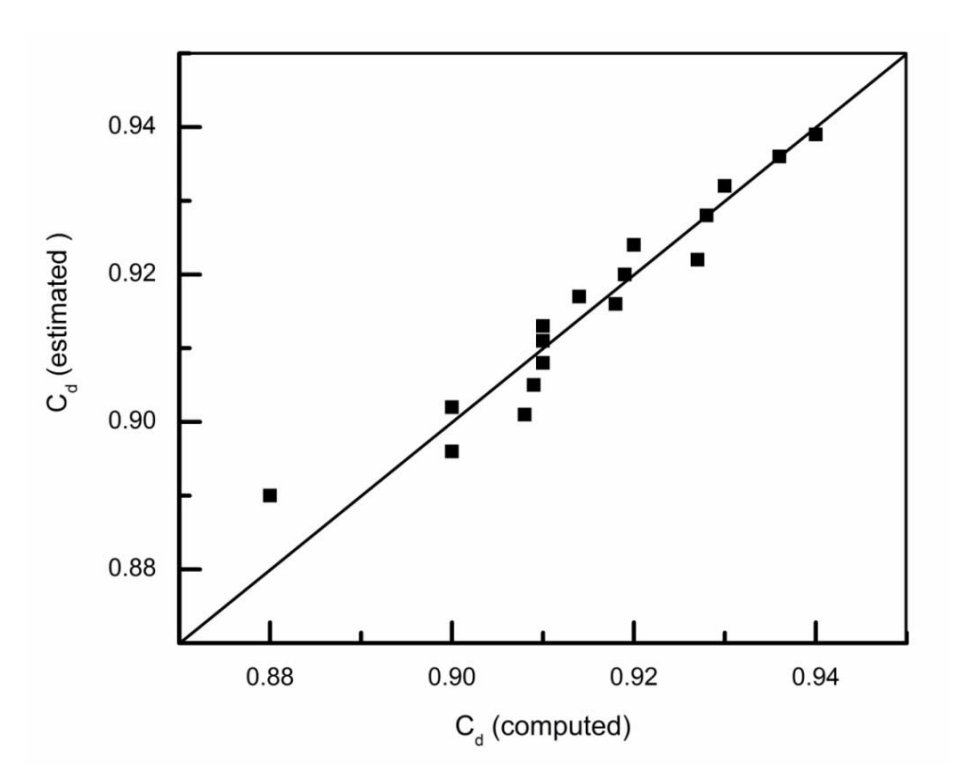


Fig. 5.17 Comparison of estimated and computed  $C_{\rm d}\,\text{for}$  a design head of 1.4 m

The proposed equations 5.2 and 5.3 to estimate  $C_d$  would be useful for design engineers to determine the discharging capacity of orifice spillway at the initial design stage. It is valid for the design heads varying from 30 m to 70 m and heights of orifice varying from 10 m to 20 m in prototype. The equations 5.2 and 5.3 would be applicable only for the design of bottom profile in the form of an equation  $x^2 = 4h_{dy}$  and roof profile derived using equations 4.4 and 4.5. The validations of the proposed equations are discussed in the next sections.

# 5.4.4 Validation of proposed equation with the results reported in literature

In order to validate the developed  $C_d$  equation for unknown inputs (parameters not used in the present study) equation has been validated with the measured  $C_d$  of 22 real life orifice spillway projects reported by Bhosekar et al. (2014). All the physical model studies of these projects are carried out at CWPRS, Pune, India. The  $C_d$  of those entire real life orifice spillway projects have been obtained by carrying out the trial and error process on the design of bottom and roof profiles. The  $C_d$  values for all the case studies were calculated using equation 5.1. Theses  $C_d$  values were compared with estimated  $C_d$  values using equation 5.3 for the validation. The comparison is shown in Table 5.10. In these case studies, the head and height of orifice varies from project to project. Hence, the equation 5.3 developed for the entire range of heads and height of orifice was used to estimate the  $C_d$  value for all the projects.

Table 5.10 Observed and estimated  $C_d$  of orifice spillways

					Coefficient of	discharge
Sr. No.	Name of Project	d (m)	h <sub>d</sub> (m)	h <sub>cl</sub> (m)	Observed from Physical model studies (Calculated using equation 5.1	Estimated from the present study (using equation 5.3)
1.	Chamera – I, India	12.8	32.5	28.6	0.84	0.91
2.	Chamera – III, India	16.5	37	28.75	0.78	0.91
3.	Dhauliganga, India	10	41.5	36.5	0.80	0.91
4.	Kurichu, Bhutan	14	28	20.6	0.83	0.90
5.	NathpaJhakri, India	8.5	37.5	33.25	0.88	0.91
6.	Nimobazgo, India	9	23.5	14.7	0.84	0.89
7.	Pandoh, India	13.5	21.64	15.34	0.71	0.91
8.	Parbati – II, India	9	33	11.31	0.77	0.85
9.	Parbati – III, India	14	32	24.85	0.74	0.91
10.	Sewa – II, India	10.8	29.5	15.5	0.76	0.88
11.	Subansiri Lower, India	14.7	60	42.05	0.80	0.89
12.	Tala, Bhutan	13.15	43	38.425	0.89	0.91
13.	Teesta – V, India	12	40.72	27.2	0.76	0.89
14.	Uri-II, India	11.4	24	10.91	0.81	0.87
15.	Myntdu, India	12	30.5	20.3	0.78	0.90
16.	Kotlibhel Stage-II, India	22	36	18.7	0.77	0.89
17.	Pare, India	14	29.15	23.215	0.80	0.91
18.	Punatsangchhu - I, Bhutan	15	36	28.5	0.80	0.91
19.	Punatsangchhu - II, Bhutan	13.2	46	37.4	0.85	0.90
20.	Mangdechhu, Bhutan	16	45	31	0.82	0.90
21.	Teesta-IV, India	14.5	39	31.75	0.84	0.91
22.	Kishanganga, India	9.5	20	15.25	0.77	0.91

Hydraulic model studies conducted at CWPRS for number of projects during the last two decades have contributed in evolving and improving design of orifice spillway (Deolalikar et al., 2008). Large range of design heads and heights of orifice was covered for

assessing the performance of various orifice spillway projects in India and Bhutan as shown in Table 5.10. The design head and height of orifice varies in the range 9 m to 22 m and 20 m to 60 m respectively. The C<sub>d</sub> of orifice spillway is influenced by various parameters. Roof profile played a very important role in enhancing C<sub>d</sub> value of orifice spillway in some of the important hydroelectric projects such as Punatsangchhu-I, Mangdechhu, Kishanganga, Pare and Teesta-IV. The C<sub>d</sub> value was found to be in the range of 0.77 to 0.84. It was observed that in all these cases water surface profile was not following the roof profile that resulted in inadequate discharging capacity. Hence, profiles were modified by trial and error method based on physical model results that resulted in improving C<sub>d</sub> value. The coefficient of discharge is seen to be high for Tala, NathphaJhakri and Punatsanghchhu- I projects. In all these cases the length of roof profile (breastwall thickness) was more than usual length of 6-7 m (Bhosekar et al., 2014). In Tala and Punatsanghchhu projects, various alternatives of roof profile were studied on physical model. It was observed from these studies that entry and exit angle of roof profile also influenced the C<sub>d</sub> value in addition to larger and steeper profile. In NathphaJhakri project, bell mouth entrance leads to smooth entry of flow had resulted in achieving higher C<sub>d</sub> of 0.88. For Subansiri project, three alternative spillway profiles viz.  $x^2$ =195y, 220 y and 250 y were studied (Bhosekar et al., 2014). The  $C_d$  is seen to be more for steeper profile of spillway ( $x^2=195$  y).

The C<sub>d</sub> reported by CWPRS through physical model studies for all the projects were found to be in the range of 0.71 to 0.89. The C<sub>d</sub> value with the proposed equation was found to be 10 % more than the one observed on individual physical model study reported by CWPRS. Because, in the present research, the design of bottom and roof profiles of orifice spillway have been finalised considering the effect of h<sub>d</sub>, d and various other parameters. However, the profiles for all 22 case studies listed in Table 5.10 were not standardized. However, the profiles were finalised by trial and error method. Hence, the present study shows that it is important to design the bottom and roof profile properly to achieve a higher discharging capacity of an orifice spillway. It is also concluded that the proposed C<sub>d</sub> equations (equation 5.2 and 5.3) are much better equations in finalising the profiles of an orifice spillway and can be a better guideline during the initial design stage.

# 5.4.5 Pressures on spillway bottom profile and corresponding cavitation index

Cavitation is the most complex hydrodynamic phenomenon and can cause serious damage to the spillway surface and is governed by pressures, velocities and duration of spillway operation. The inception of cavitation damage can be assessed by the cavitation index. In an orifice spillway, when flow passes from orifice opening, it changes from subcritical to supercritical state. At the orifice opening, velocity of flow is low. However, velocity increases as the flow accelerate to the downstream side. Velocity increases as the head over the crest increases. Present study covered a large range of design heads i.e. 30 m to

70 m in prototype to assess the performance of orifice spillway in respect of pressures on spillway bottom profile. Hence, there may be possibility of cavitation damage on spillway surface especially for high design heads. Therefore, it is felt necessary to study the cavitation phenomena by analysing the pressure distribution on spillway profiles for various configurations of spillway. Pressures were measured on the spillway bottom surface along centre line of spillway for all h<sub>e</sub>/h<sub>d</sub> ratios and different heights of orifice opening. Velocity on spillway bottom profile was calculated throughout the length of spillway to calculate the cavitation index. Pressures obtained in models were scaled up to prototype dimensions to calculate cavitation index. Cavitation index was calculated using the following formula:

$$\sigma = \frac{P_0 - P_v}{v_o^2 / 2g} \tag{5.4}$$

where,  $\sigma$  = cavitation index,

 $P_0$  = reference pressure head in m of water,

 $P_v$  = vapour pressure of water,

 $v_o$ = reference velocity in m/s

g = acceleration due to gravity in m/s<sup>2</sup>

The results were non dimesionalized with design head  $h_d$  in the form of  $x/h_d$  and  $h_p/h_d$ . The non-dimensional plots for pressure distribution were developed by considering  $x/h_d$  on x axis and  $h_p/h_d$  on y axis, where x is the distance from the orifice at which the pressure taps are located,  $h_p$  is calculated pressures in m of water and  $h_d$  is the design head for which spillway bottom profiles are designed. Similarly, corresponding cavitation index was plotted by taking non dimensional factor  $x/h_d$  on x axis and cavitation index on y axis.

The pressures and cavitation indices have been computed for less than design head ( $h_e/h_d = 0.8$ ), design head ( $h_e/h_d = 1$ ) and greater than design head ( $h_e/h_d = 1.33$ ) conditions. Figures 5.19 and 5.20 show the pressure distribution and corresponding cavitation index on the spillway bottom profiles designed for the heads 0.6 m & 0.8 m and 1.0 m & 1.4 m respectively for the spillway operated at less than design head condition. Figures 5.21 and 5.22 show the pressure distribution and corresponding cavitation index on the spillway profiles designed for the heads 0.6 m & 0.8 m and 1.0 m & 1.4 m respectively for the spillway operated at design head condition. Figures 5.23 and 5.24 show the pressure distribution and corresponding cavitation index for the spillway profiles designed for the heads 0.6 m & 0.8 m and 1.0 m & 1.4 m respectively for spillway operated at head greater than design head condition. In all the Figures, variation in pressure on spillway bottom profile with change in height of orifice opening and corresponding cavitation index was observed. The studies were carried out for heights of orifice of 0.2 m, 0.24 m, 0.28 m, 0.32 m, 0.36 m and 0.4 m.

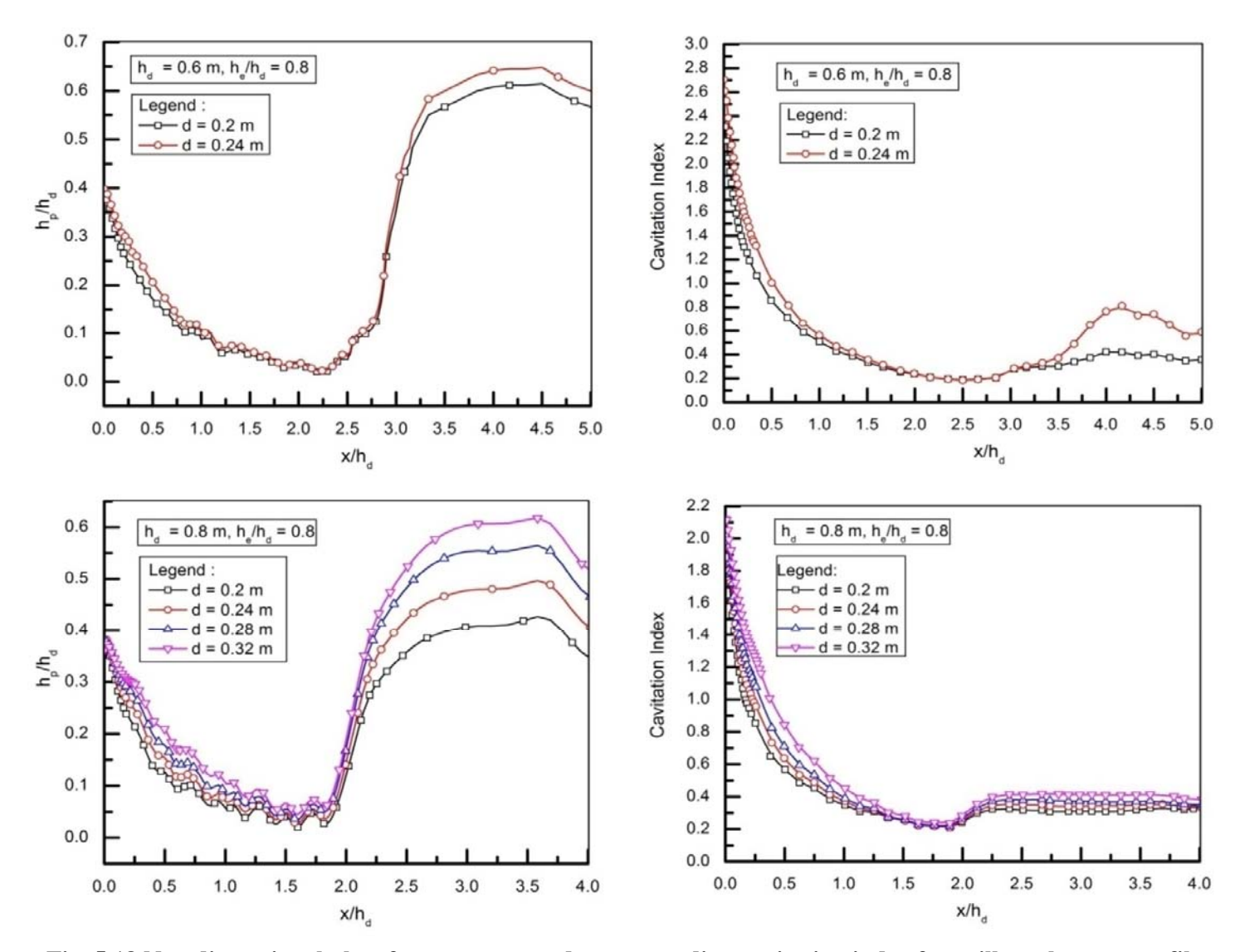


Fig. 5.18 Non dimensional plots for pressures and corresponding cavitation index for spillway bottom profiles designed for the heads 0.6 m and 0.8 m for  $h_e/h_d=0.8$ 

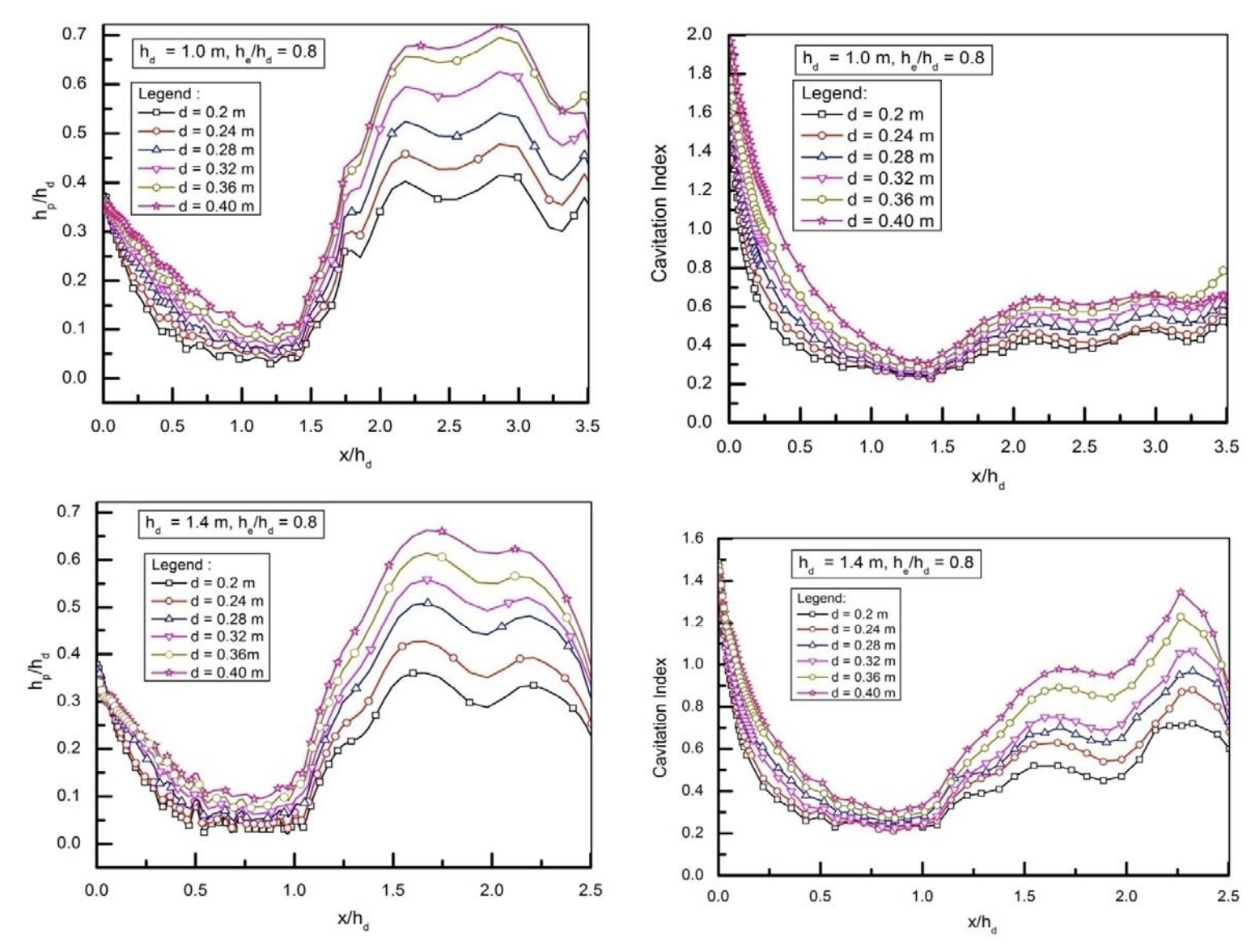
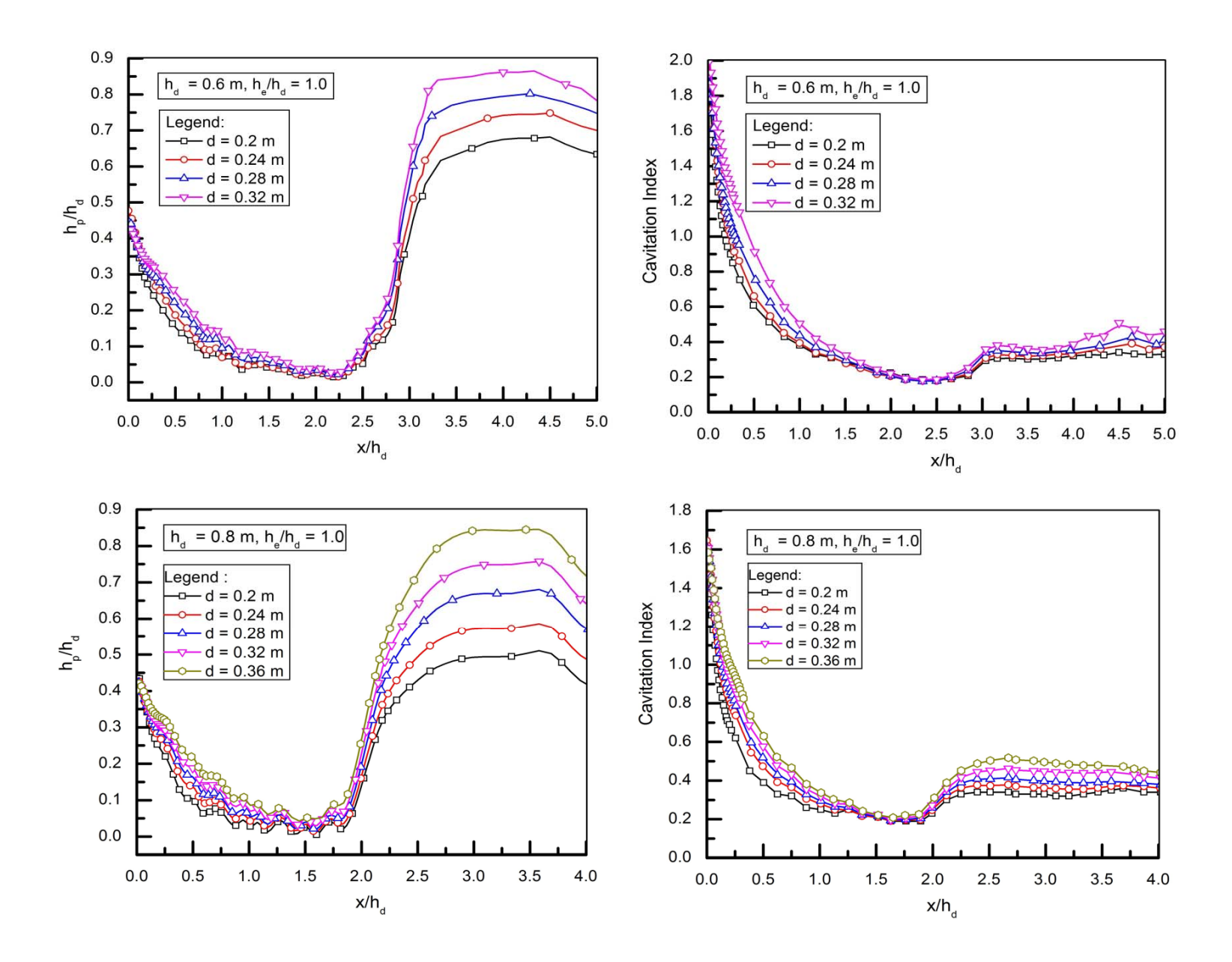
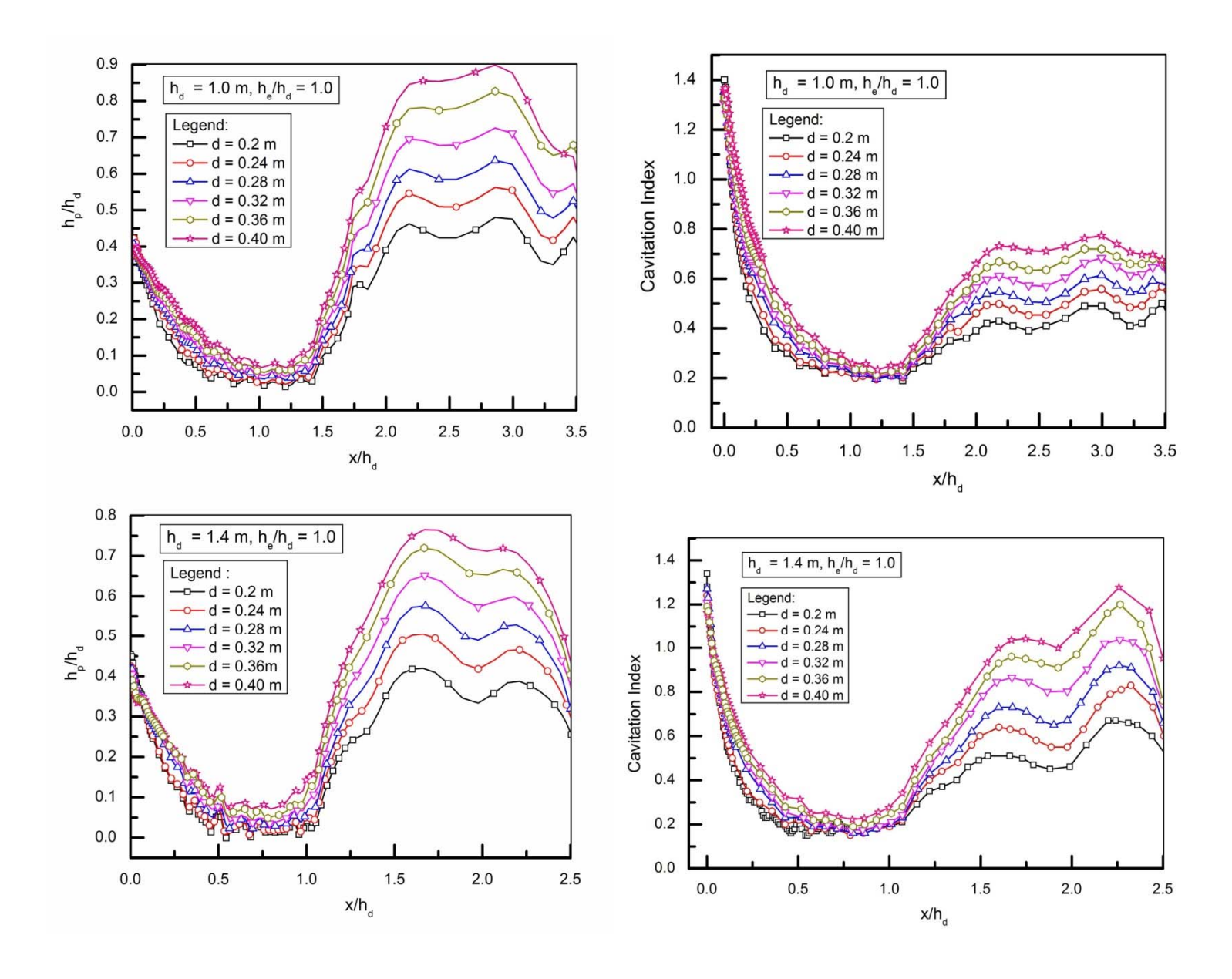
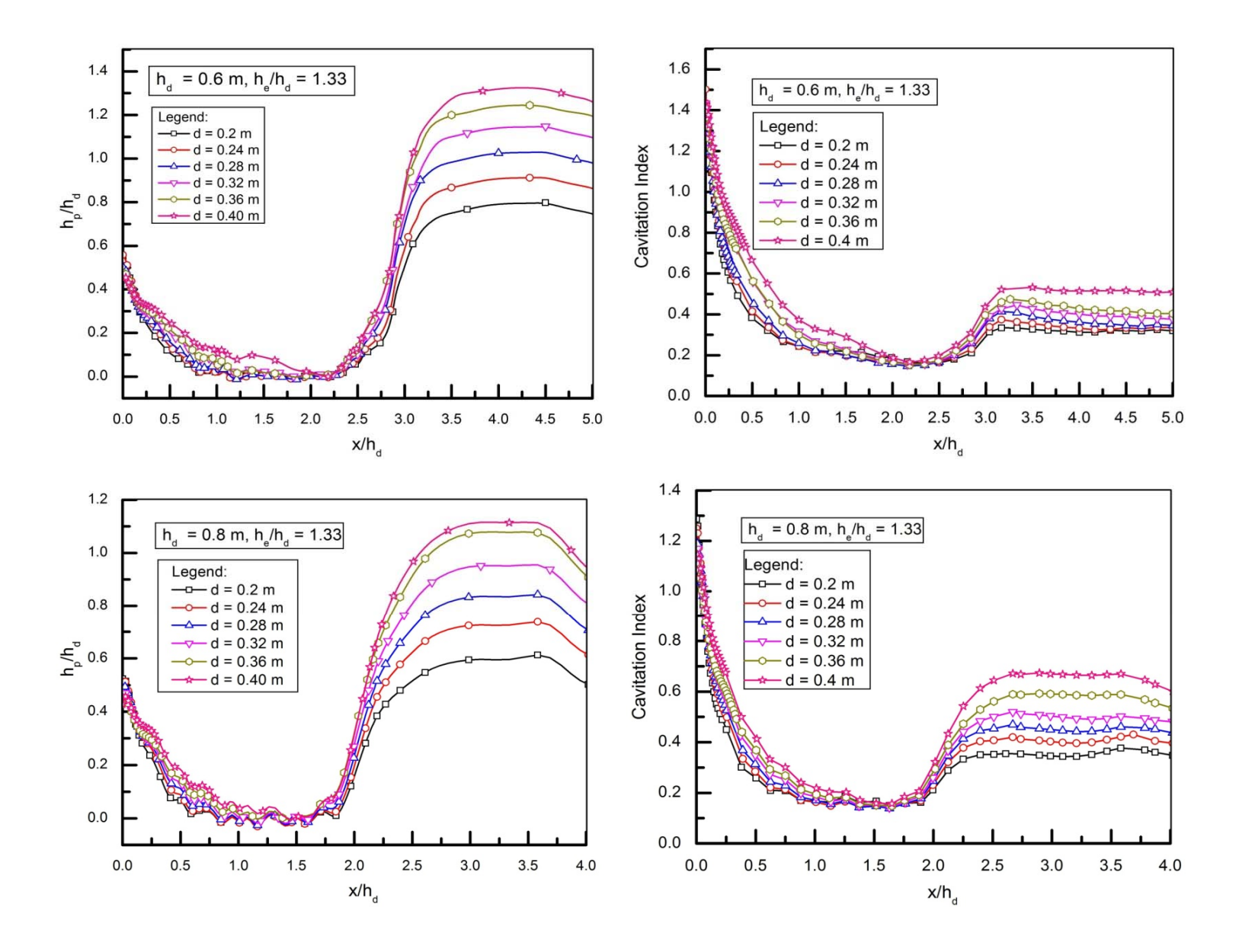
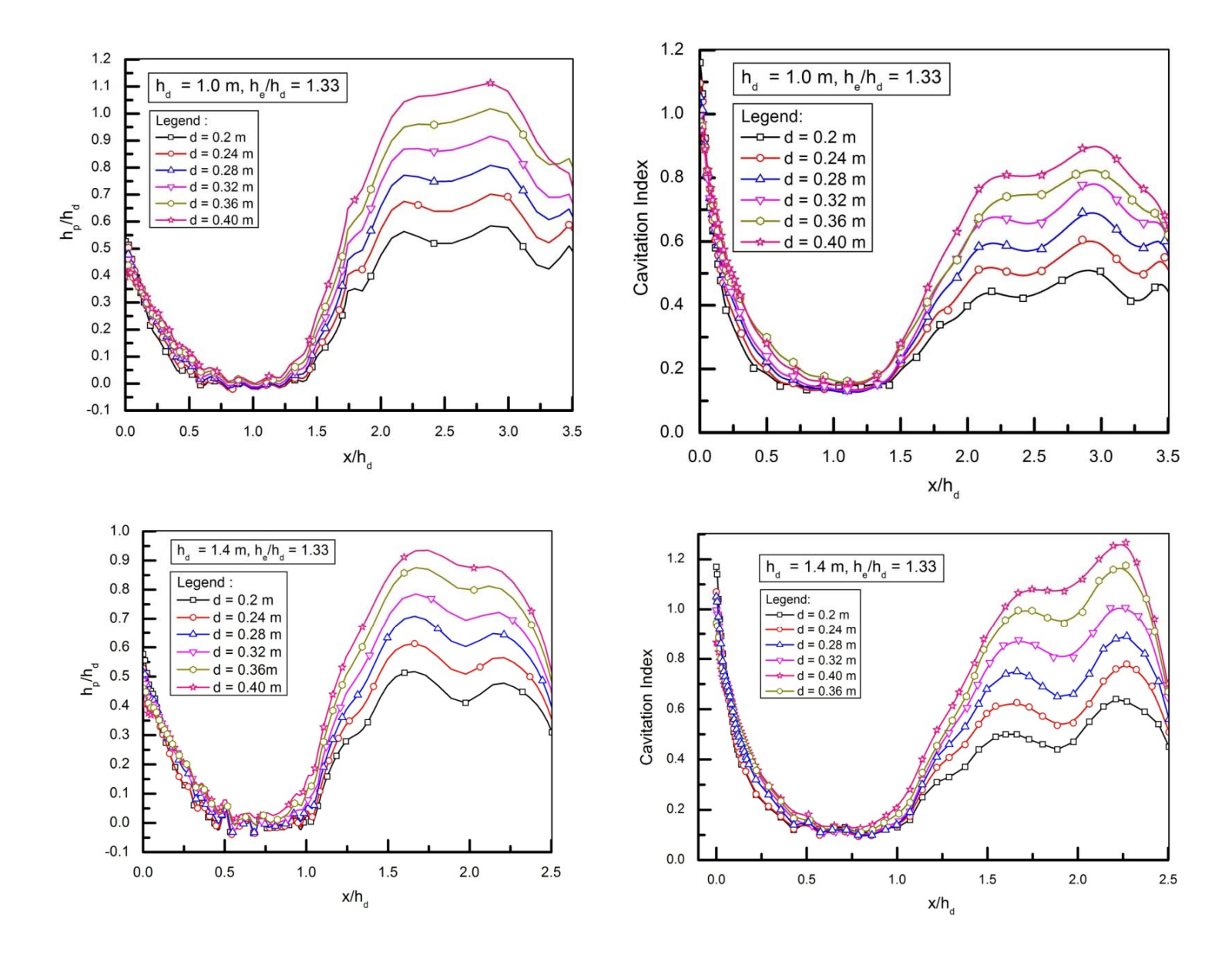


Fig. 5.19 Non dimensional plots for pressures and corresponding cavitation index for spillway bottom profiles designed for the heads 1 m and 1.4 m for  $h_e/h_d=0.8$ 









The studies indicated that as the orifice height (d) increases, the pressures on the spillway surface also increases resulting in increased cavitation index for the spillway bottom profile designed for a particular head and at a particular operating condition. Figures 5.19 and 5.20 show positive pressures throughout the length of spillway for all the combinations. The minimum and maximum range of cavitation index ( $\sigma$ ) works out to be 0.2 to 2.7 and 0.21 to 2.12 for the design heads of 0.6 m and 0.8 m respectively as shown in Figure 5.19. Similarly the range of  $\sigma$  works out to be 0.21 to 2 and 0.22 to 1.5 for the design heads of 1 m and 1.4 m respectively as shown in Figure 5.20. The cavitation indices calculated throughout the length of spillway are greater than critical cavitation index of 0.2 (Falvey, 1990). Hence, the design of spillway bottom profile having an equation  $x^2 = 4h_dy$  is found to be safe for all the design heads and heights of orifices at spillway operating at less than design head ( $h_e/h_d = 0.8$ ) condition.

The cavitation index over the spillway surface was also calculated for all heights of orifice at the spillway operating at design head ( $h_e/h_d=1$ ). The results are shown in Figures 5.21 and 5.22. The minimum and maximum range of cavitation index ( $\sigma$ ) works out to be 0.2 to 2.0 and 0.2 to 1.65 for the design heads 0.6 m and 0.8 m respectively as shown in Figure 5.21. Similarly the range of  $\sigma$  works out to be 0.20 to 1.4 and 0.18 to 1.34 for the design heads 1 m and 1.4 m respectively as shown in Figure 5.22. The cavitation indices calculated on most parts of the spillway surface are greater than critical cavitation index of 0.2 (Falvey, 1990). Hence, the design of spillway bottom profile having an equation  $x^2 = 4h_dy$  is found to be safe for all the design heads and heights of orifices at spillway operating at design head condition. However, it was observed that for high design head i.e. 1.4 m, cavitation index on some part of spillway surface was found to be around 0.18 which is marginally below critical cavitation index of 0.2, hence can be accepted.

Figures 5.23 and 5.24 show the pressure and cavitation index profiles for the head more than design head ( $h_e/h_d = 1.33$ ). The Figures indicate that the minimum cavitation index calculated for the spillway bottom profile designed for head of 0.6 m, 0.8 m, 1.0 m and 1.4 m are 0.14, 0.13, 0.13 and 0.1 respectively. Cavitation indices worked out to be minimum when the spillway is operated at greater than design head. This is because, as the head over the crest increases, velocity also increases which results in reduction in the pressures on the surface. It was also observed that for a particular spillway bottom profile, cavitation index works out to be minimum for smaller height of orifice. The discharge through orifice decreases with decrease in height of orifice. With increase in discharge and height of orifice, the pressures increase thereby increasing the cavitation index and the zone of susceptibility shrinks. Figures 5.23 and 5.24 indicate the zone where spillway surface is susceptible to cavitation damage. Cavitation damage on spillway surface starts at a horizontal distance of about 0.86 m, 0.62 m, 0.5 m and 0.4 m for spillway profile designed for a head of 0.6 m, 0.8 m, 1.0 m and 1.4 m respectively for height of orifice opening as 0.2 m. The starting point of cavitation damage increases with increase in height of orifice for a particular spillway profile. This means that the spillway profile designed for head of 0.6 m and operated at greater than design head would be susceptible to cavitation damage at distance of about 0.86 m, 0.9 m, 0.92 m, 0.98 m,

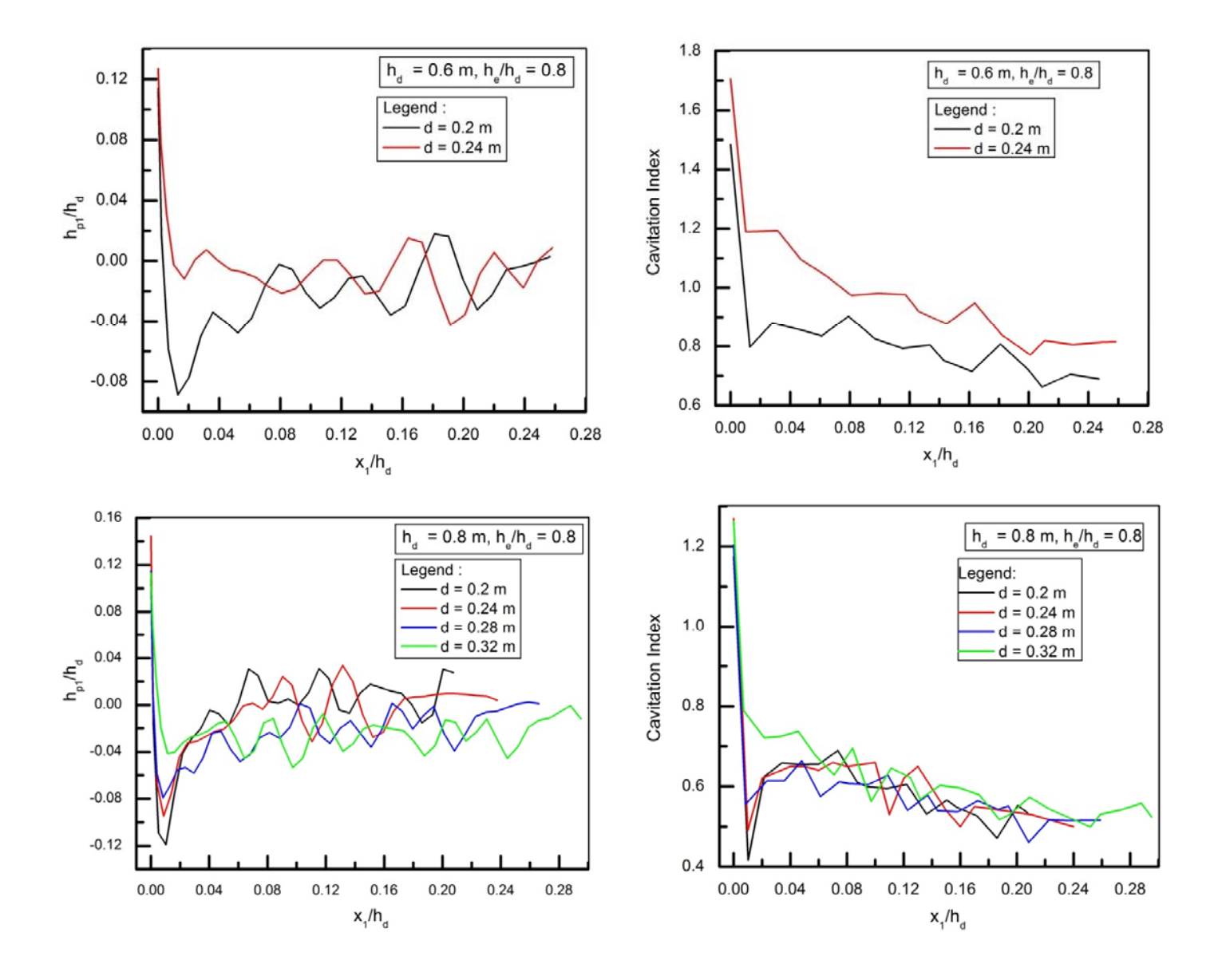
1.04 m and 1.16 m for height of orifice of 0.2 m, 0.24 m, 0.28 m, 0.32 m, 0.36 m and 0.4 m respectively. The spillway operating for head greater than design head will rarely occur in the prototype as rise in water level up to 30% more than the design head is likely to happen only in exceptional hydrological events.

## 5.4.6 Pressures on spillway roof profile and corresponding cavitation index

Roof profiles in the present study were designed using proposed equations 4.4 and 4.5 (mentioned in Chapter 4). Equations were developed based on extensive experimentation on physical model and numerical model simulations so as to achieve maximum discharging capacity with acceptable pressure distribution on roof profile. In view of this, the design of roof profile with proposed equation was checked in respect of pressures distribution on the surface for various combinations of spillway profiles designed with different heads, heights of orifice and various spillway operating conditions.

The results were non dimesionalized with respect to  $h_d$  in the form of  $x_1/h_d$  and  $h_{p1}/h_d$ . The non-dimensional plots for pressure distribution were developed by considering  $x_1/h_d$  on x axis and  $h_{p1}/h_d$  on y axis, where  $x_1$  is the distance from the orifice at which the pressure taps are located along the roof profile,  $h_{p1}$  is calculated pressures in m of water and  $h_d$  is the design head for which spillway roof profilesare designed. Similarly, corresponding cavitation indices have been calculated and plotted withnon dimensional factor  $x_1/h_d$  on x axis and cavitation index value on y axis.

Figures 5.25 and 5.26 show the pressure distribution and corresponding cavitation index on the spillway roof profile designed for head of 0.6 m & 0.8 m and 1.0 m & 1.4 m respectively for spillway operated at less than design head condition ( $h_e/h_d=0.8$ ). Figures 5.27 and 5.28 show the pressure distribution and corresponding cavitation index on the spillway roof profile designed with head of 0.6 m & 0.8 m and 1.0 m & 1.4 m respectively for spillway operated at design head condition ( $h_e/h_d=1$ ). Figures 5.29 and 5.30 show the pressure distribution and corresponding cavitation index on the spillway bottom profile designed with head of 0.6 m & 0.8 m and 1.0 m & 1.4 m respectively for spillway operated at greater than design head condition ( $h_e/h_d=1.33$ ).



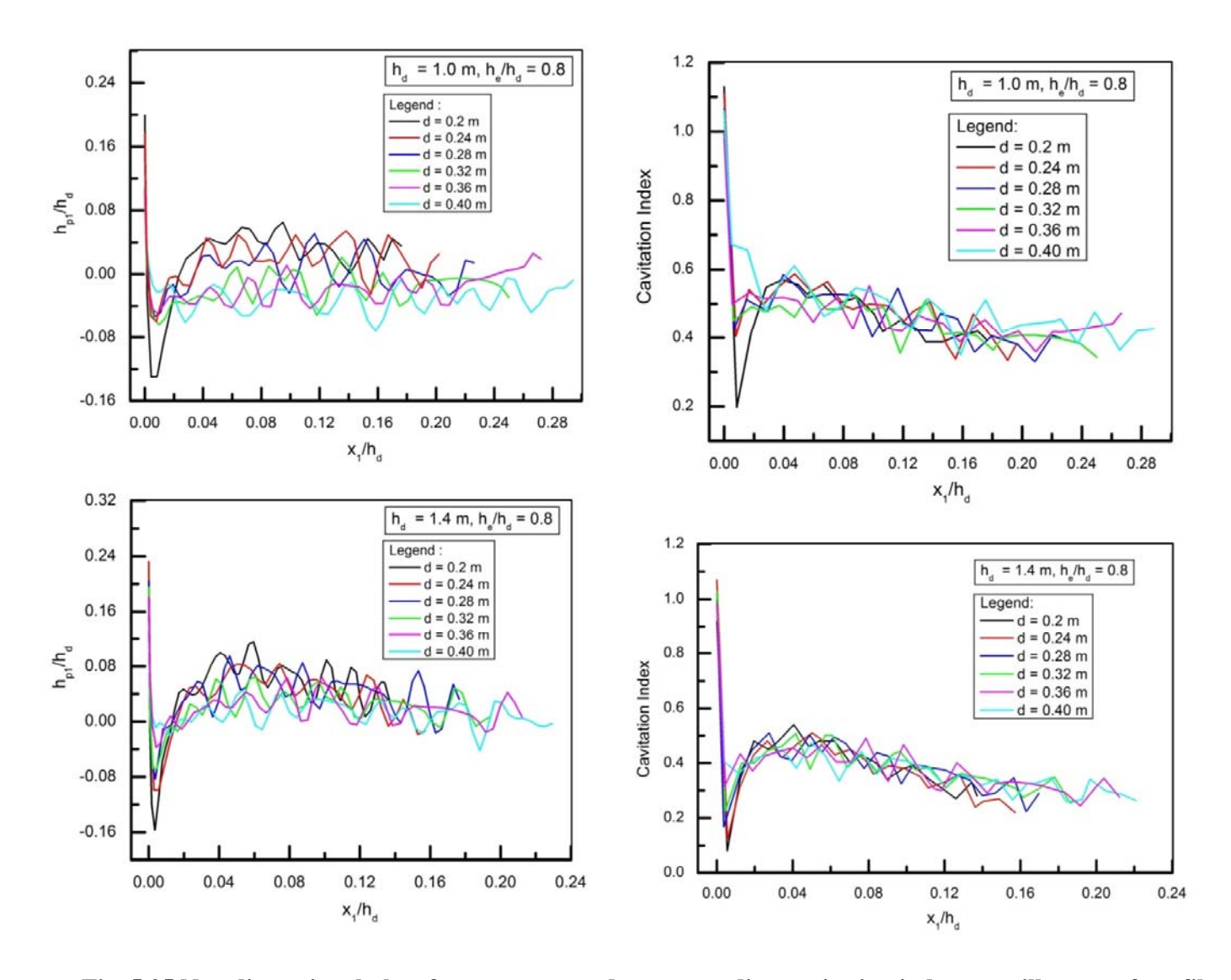
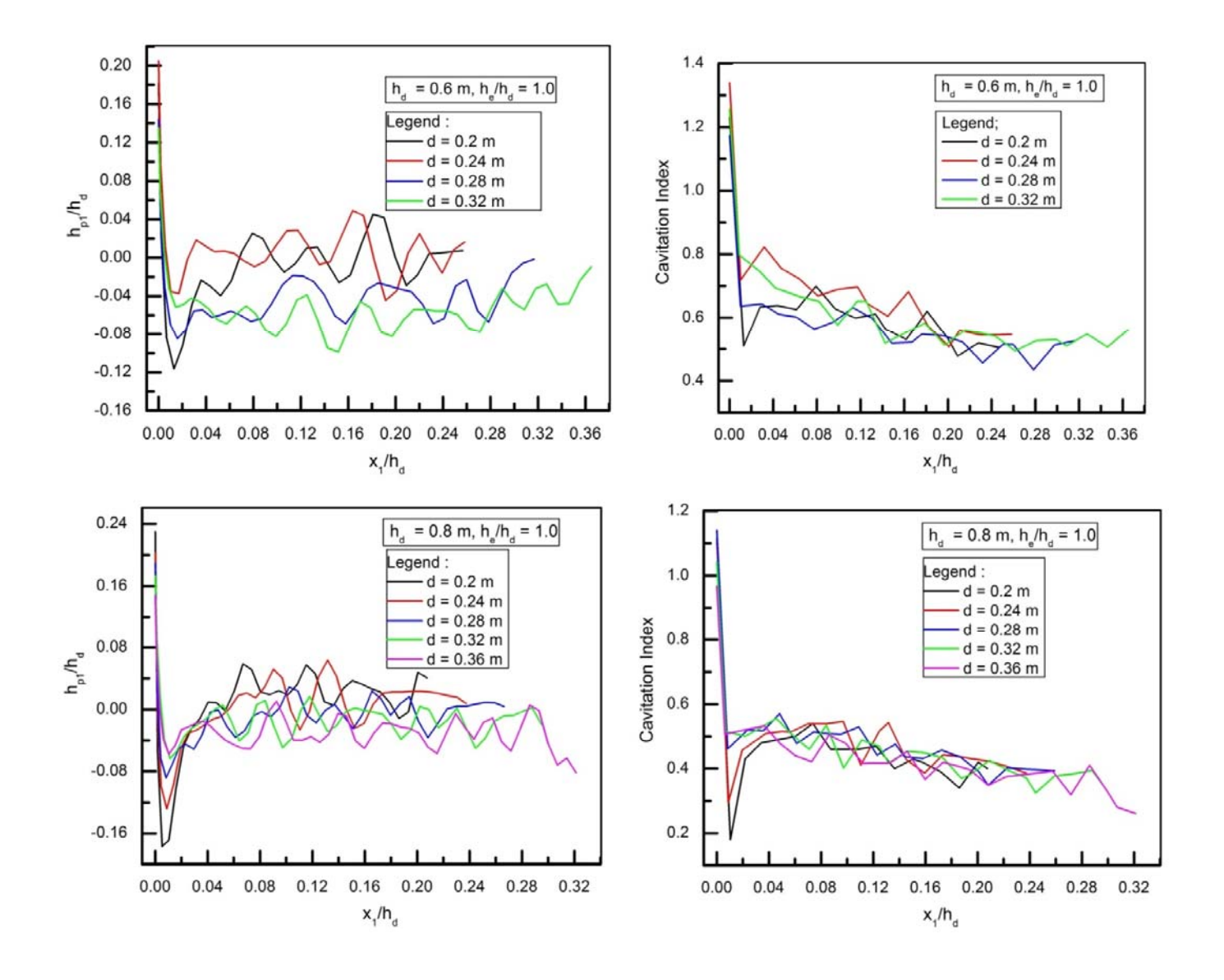
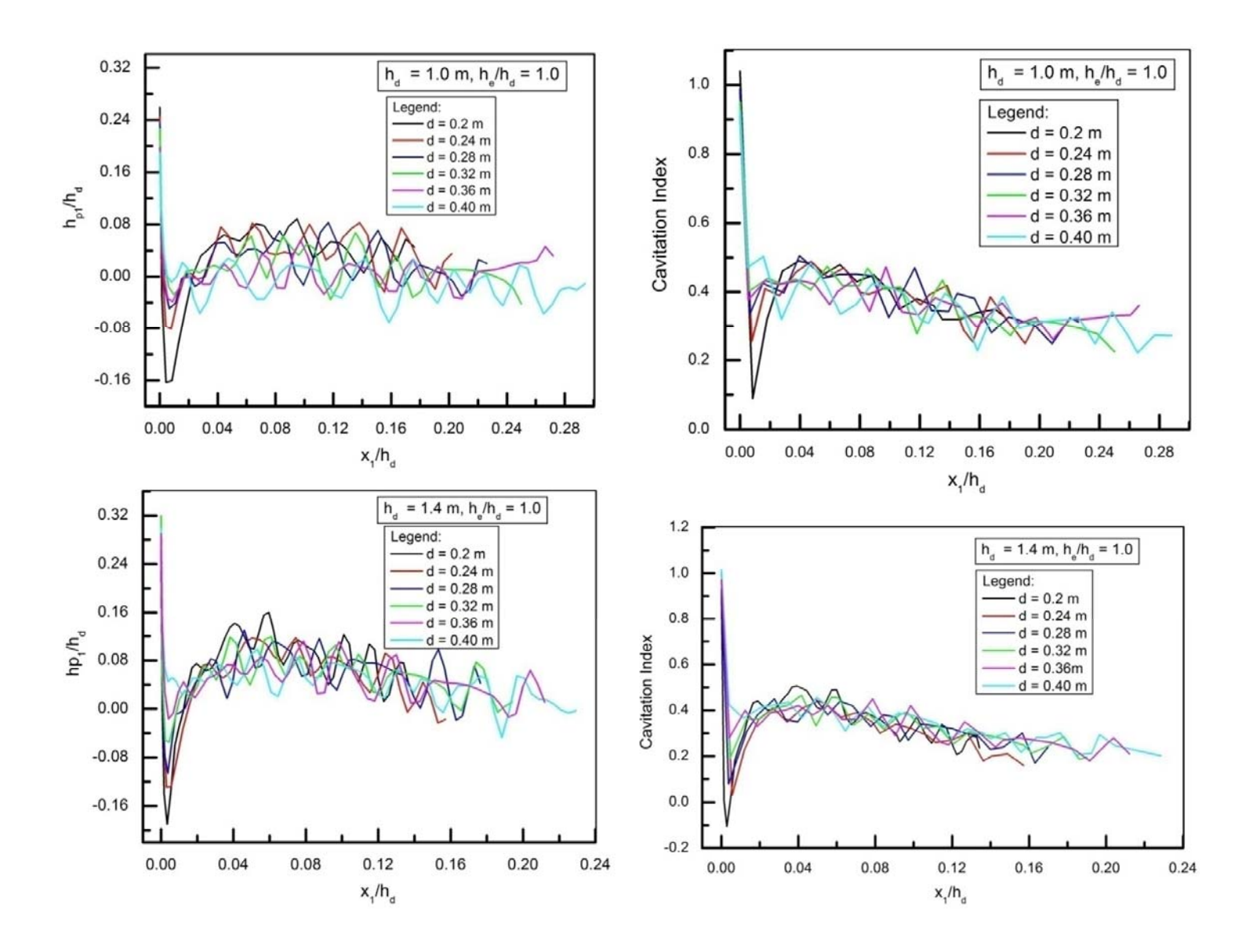
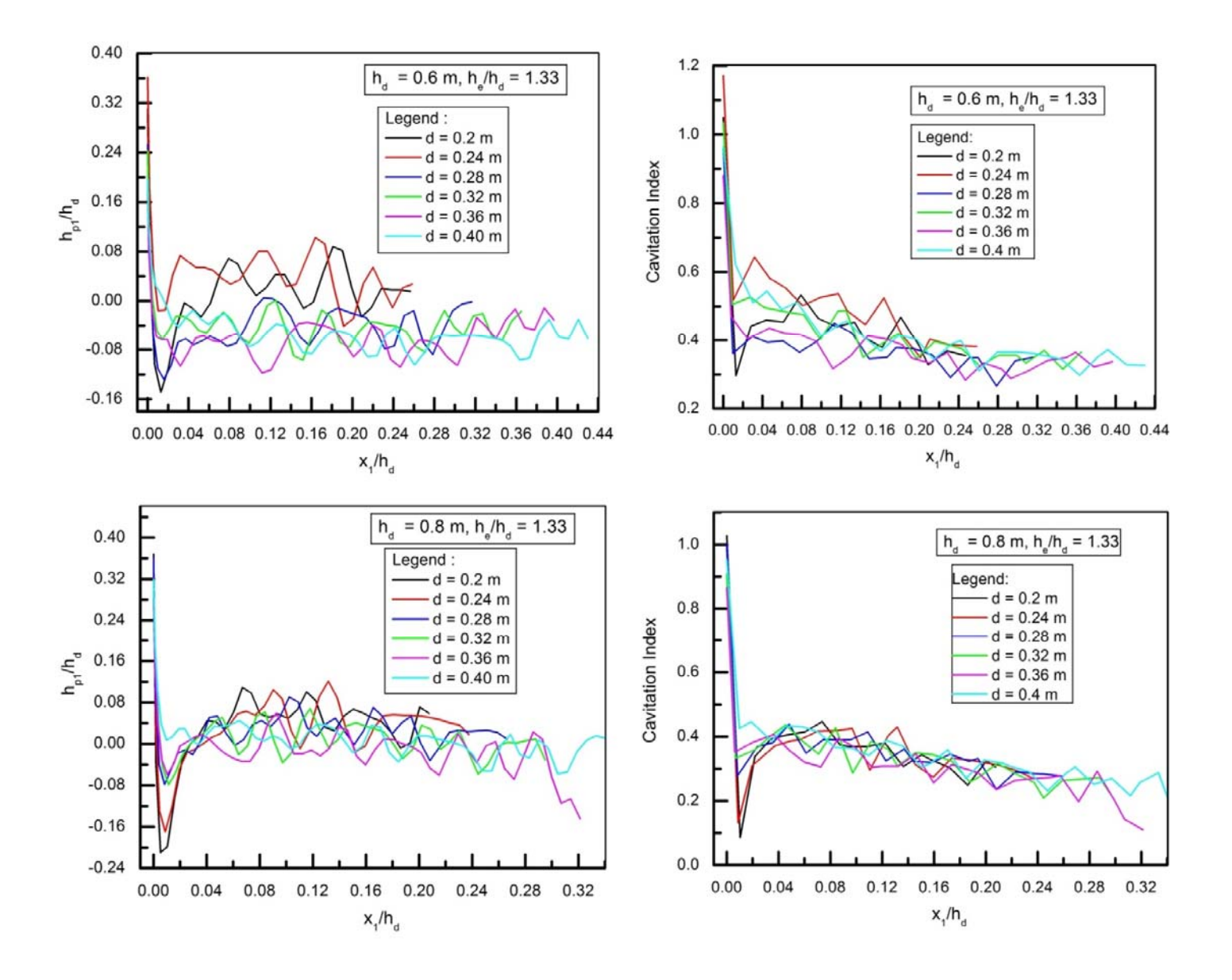
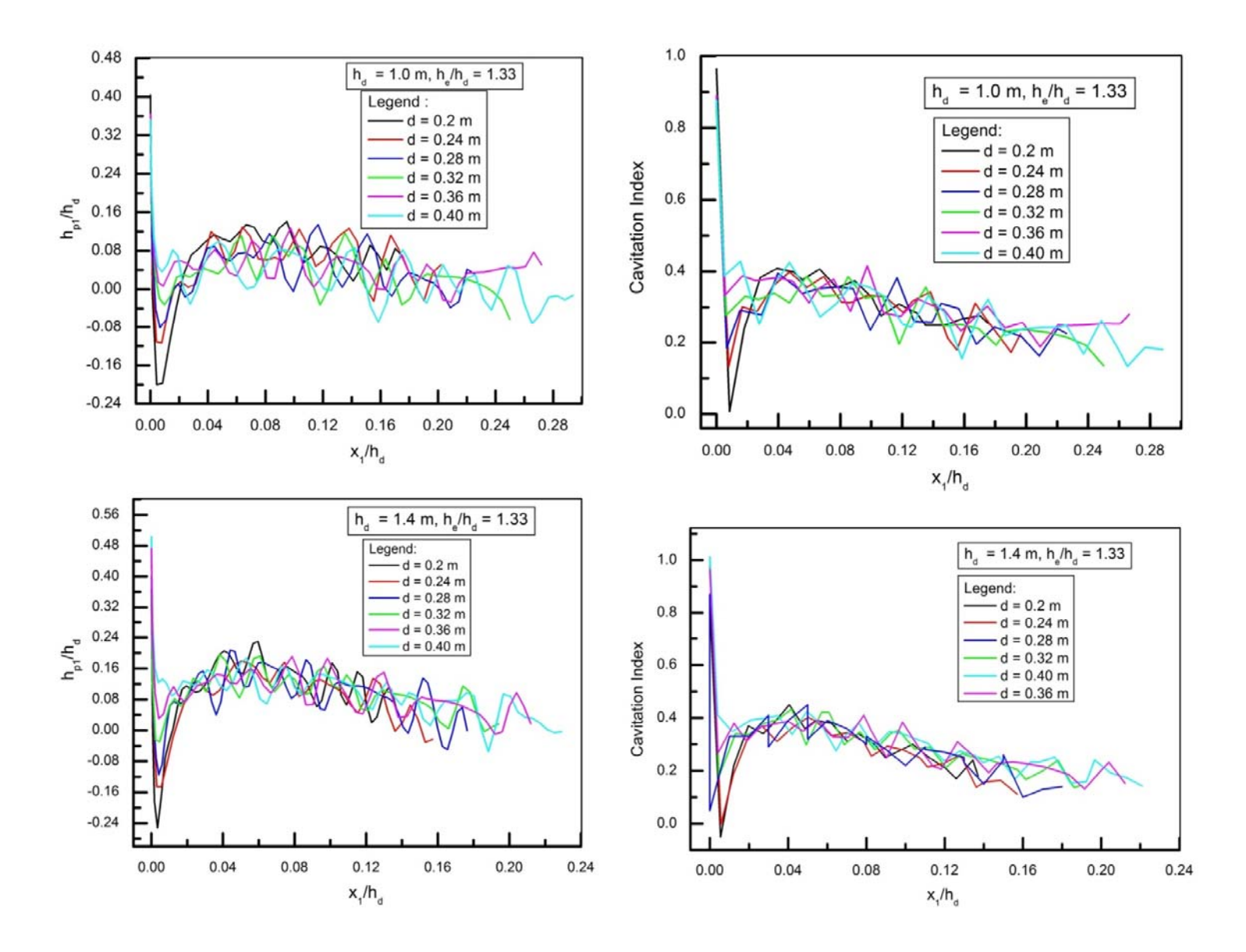


Fig. 5.25 Non dimensional plots for pressures and corresponding cavitation index on spillway roof profiles designed for the heads 1 m and 1.4 m for  $h_e/h_d=0.8$ 









As the flow passes through orifice, it suddenly changes its subcritical state to supercritical state. Below the roof profile the flow acts as a pressurized flow. Once it leaves the roof profile, the flow behaves as a free surface flow. Due to this transition of flow regime, it is very complicated task to capture the pressures on roof profile. There is a sudden drop in pressure near the entrance of orifice due to rapid change in velocity. After this, the flow stabilizes and starts following the path of roof profile and thus results in increased pressure over the surface.

Figures 5.25 to 5.30 show pressure distribution on roof profile for various conditions in respect of different heights of orifice. It was found that as the height of orifice increases for a particular operating head, the mass of water passing through the orifice increases resulting in increased weight and steeper jet under influence of gravity. This results in increase in pressures on spillway bottom surface. However, at the same time, there is reduction in pressures on roof profile. Hence, the pressures for small height of orifice opening i.e. of 0.2 m are more than the pressures for larger height of orifice i.e. 0.4 m for the particular design head. Thus, a reverse trend of the pressure profile is observed on spillway roof profile as compared to the pressures on bottom profile. This means that as the height of orifice increases, due to increase in discharge, the pressures on spillway bottom profile increase as shown in Figures 5.19 to 5.24.

The main aim of observing the pressures on roof profile is to check the profile in respect of susceptibility of profile due to cavitation damage. Hence, in view of this, pressures and corresponding cavitation indices were calculated for all the combinations of design heads, operating heads, and heights of orifice. For the spillway operating at less than design head i.e.  $h_e/h_d=0.8$ , the minimum and maximum pressures on the roof profile with respect to design head 0.6 m, 0.8 m, 1.0 m and 1.4 m were observed in the range of -0.04 to 0.01, -0.06 to 0.03, 0.06 to 0.05 and -0.04 to 0.08 respectively for the entire length of roof profile except in the small part of initial region. The corresponding cavitation indices work out to be 0.7 to 1, 0.47 to 0.7, 0.36 to 0.61 and 0.3 to 0.55 as shown in Figures 5.25 and 5.26. The values are found more than critical cavitation index of 0.2 (Falvey, 1990). Hence, the design of roof profile proposed in the present study was found to be safe for spillway operating at less than design head condition.

For the spillway operating at design head i.e.  $h_e/h_d = 1$ , the minimum and maximum pressures on the roof profile with respect to design head 0.6 m, 0.8 m, 1.0 m and 1.4 m were observed in the range of -0.1 to 0.04, -0.06 to 0.06, -0.06 to 0.08 and -0.02 to 0.15 respectively for the entire length of roof profile except in the small part of initial region. The minimum and maximum range of corresponding cavitation indices work out to be 0.46 to 0.7, 0.3 to 0.58, 0.22 to 0.5 and 0.2 to 0.51 respectively as shown in Figures 5.27 and 5.28. The values are found to be more than critical cavitation index of 0.2 (Falvey, 1990). Hence the design of roof profile proposed in the present study was found to be safe for spillway operating at design head condition.

For the spillway operating at head greater than design head i.e.  $h_c/h_d = 1.33$ , the minimum and maximum pressures on the roof profile with respect to design head 0.6 m, 0.8 m, 1.0 m and 1.4 m were observed in the range of -0.12 to 0.08, -0.06 to 0.11, -0.07 to 0.15 and -0.06 to 0.24 respectively for the entire length of roof profile except in the small part of initial region, as shown in Figures 5.29 and 5.30. The minimum and maximum range of corresponding cavitation indices work out to be 0.26 to 0.63, 0.2 to 0.46, 0.2 to 0.42 and 0.2 to 0.46. The values are found more than critical cavitation index of 0.2 (Falvey, 1990). Hence, the design of roof profile was found to be safe for the roof profile of spillway operating at greater than design head. It was also observed from the above Figures 5.29 and 5.30 that negative pressures occur in the initial region of the roof profile for entire range of 'd' and  $h_d$ . However, the cavitation indices for the heads of 1 m and 1.4 m for smaller heights of orifices viz. 0.2 m, 0.24 m and 0.28 m, were observed below the critical cavitation index. Hence, there may be a possibility of cavitation damage in this region for these heads. It may be mentioned here that such a condition will rarely occur in the prototype as rise in water level up to 30% more than the design head is likely to happen only in exceptional hydrological events.

The pressure profiles indicated that the flow is extremely unstable in the vicinity of roof profile of the spillway as compared to the bottom profile. Hence, large fluctuations were observed in the pressure on roof profile of the orifice spillway as shown in Figures 6.25 to 6.30 especially for smaller d values. To study this phenomenon in more details it was found necessary to install electronic pressure transducers on the physical model to record the hydrodynamic pressures on the roof profile. The analysis of results of pressure transducers is presented in the following section.

## 5.4.7 Hydrodynamic pressures on spillway roof profile

The pressures on spillway roof profile were also measured by installing 5 PSI Endevco make Miniature Piezoresistive electronic transducers. The Piezoresistive type pressure transducers were calibrated using 15 cm diameter vertical PVC pipe. During calibration, transducers were fixed to the vertical pipe at the bottom for static head in the range of 0 to 3.3 m. Output voltage generated by pressure transducer was directly proportional to the water head in calibration pipe. Table 5.11 shows the pressure and voltage generated during calibration. After this calibration, the transducers were used on physical model set up for measurement of pressures.

Table 5.11 Static pressures in pipe, pressures using DAS set up and voltage generated during calibration of pressure transducers

Hydraulic static pressure in pipe (m of water column)	Pressure using DAS set up ( m of water column)	Output voltage (volts)	
0.00	-0.01	-0.01	
0.15	0.14	0.15	
0.30	0.28	0.23	
0.45	0.44	0.36	
0.60	0.57	0.48	
0.75	0.72	0.60	
0.90	0.88	0.73	
1.05	1.02	0.85	
1.20	1.19	0.99	
1.35	1.34	1.11	
1.50	1.49	1.24	
1.65	1.63	1.36	
1.80	1.77	1.48	
1.95	1.93	1.61	
2.10	2.07	1.73	
2.40	2.37	1.98	
2.70	2.65	2.22	
3.00	2.97	2.48	
3.30	3.26	2.72	

The transducers were connected through signal conditioner with PC based data acquisition system containing A/D card and data acquisition software. Transducers were fixed at five locations viz  $b_1$ ,  $b_2$ ,  $b_3$ ,  $b_4$  and  $b_5$  along the roof profile of orifice spillway as shown in Figure 5.31. Point  $b_1$  is located near the entrance of roof profile, whereas point  $b_5$  is located at exit. Data was acquired with a frequency of 0.01 Hz (100 samples per second) for a duration of 1200 seconds. The data was acquired for a typical set up of experiment viz. spillway bottom profile designed for 0.8 m, height of orifice varying for 0.2 m, 0.24 m, 0.28 m, 0.32 m and 0.36 m and spillway operating for  $h_e/h_d = 0.8$ , 1.0 and 1.33. Figures 5.32, 5.33, 5.34, 5.35 and 5.36 show typical time series for locations  $b_1$ ,  $b_2$ ,  $b_3$ ,  $b_4$  and  $b_5$  respectively for height of orifice of 0.28 m and  $h_e/h_d = 1$ . The average pressure measured using piezometer has also been plotted on the Figures 5.32 to 5.36. The average pressures obtained from the time series of transducer and Piezometer matched very well.

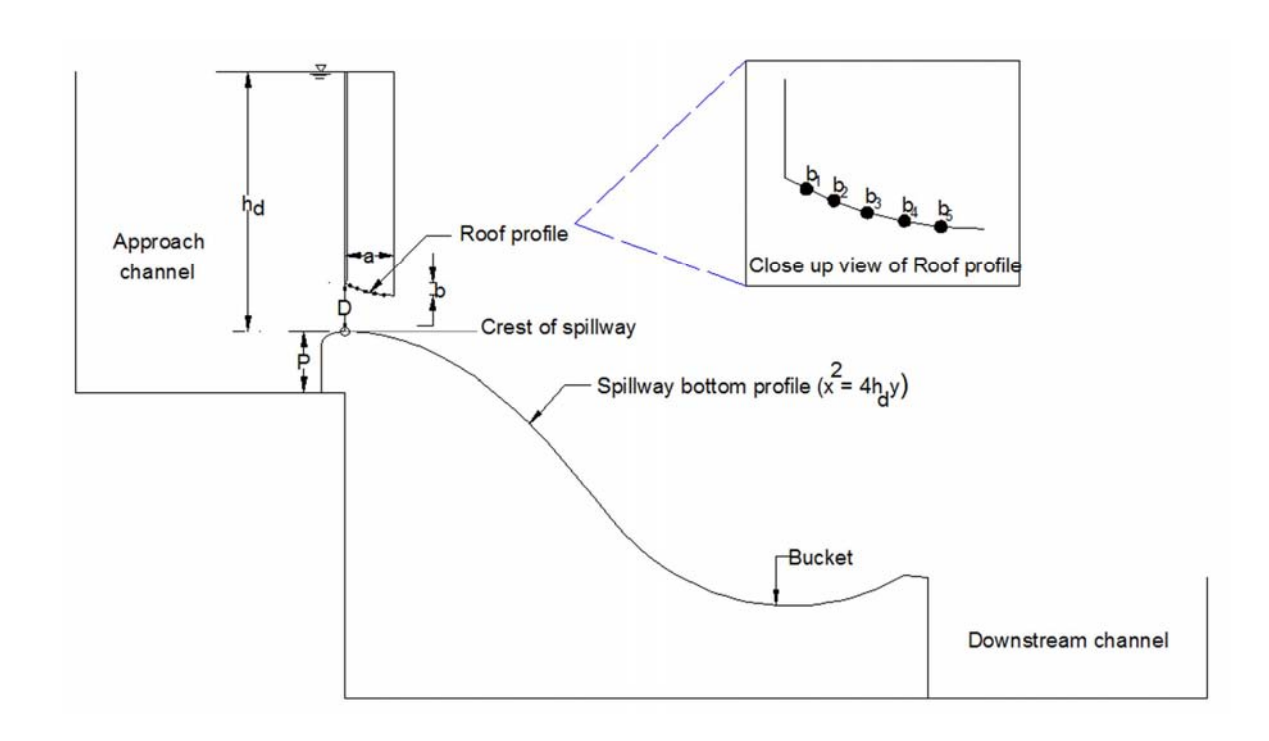
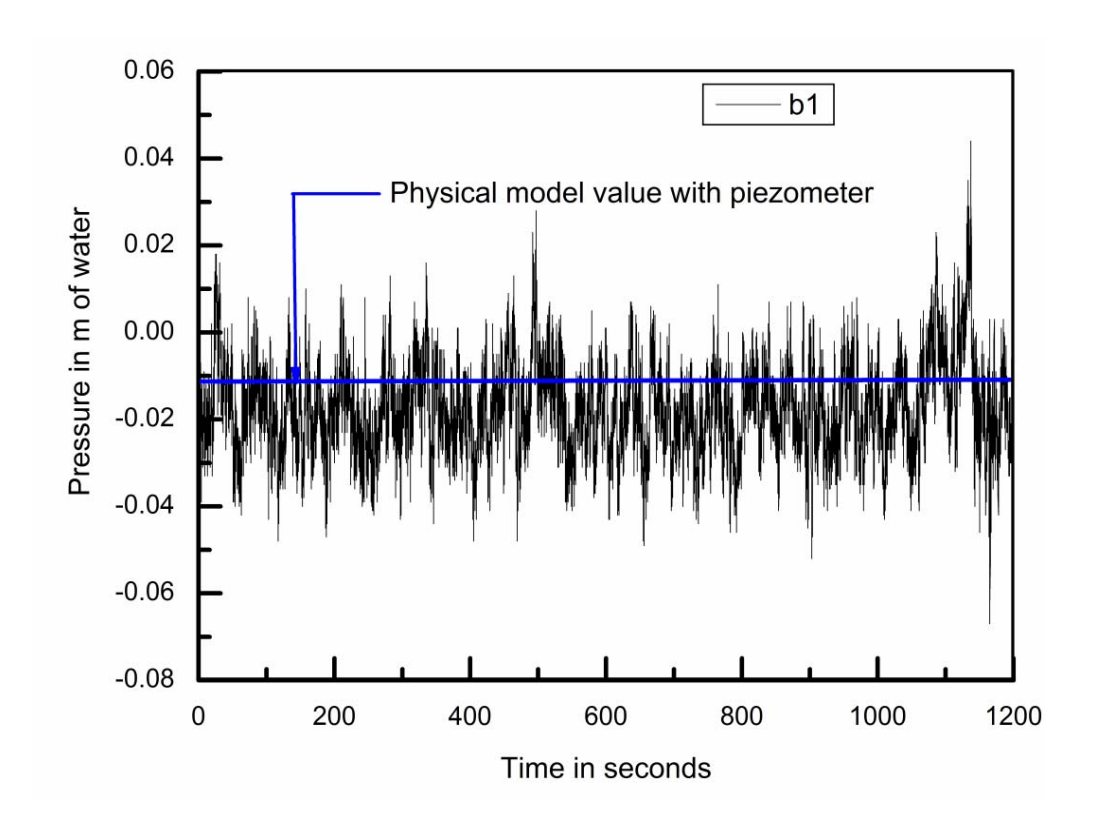


Fig. 5.30 Location of transducers along spillway roof profile in the physical model



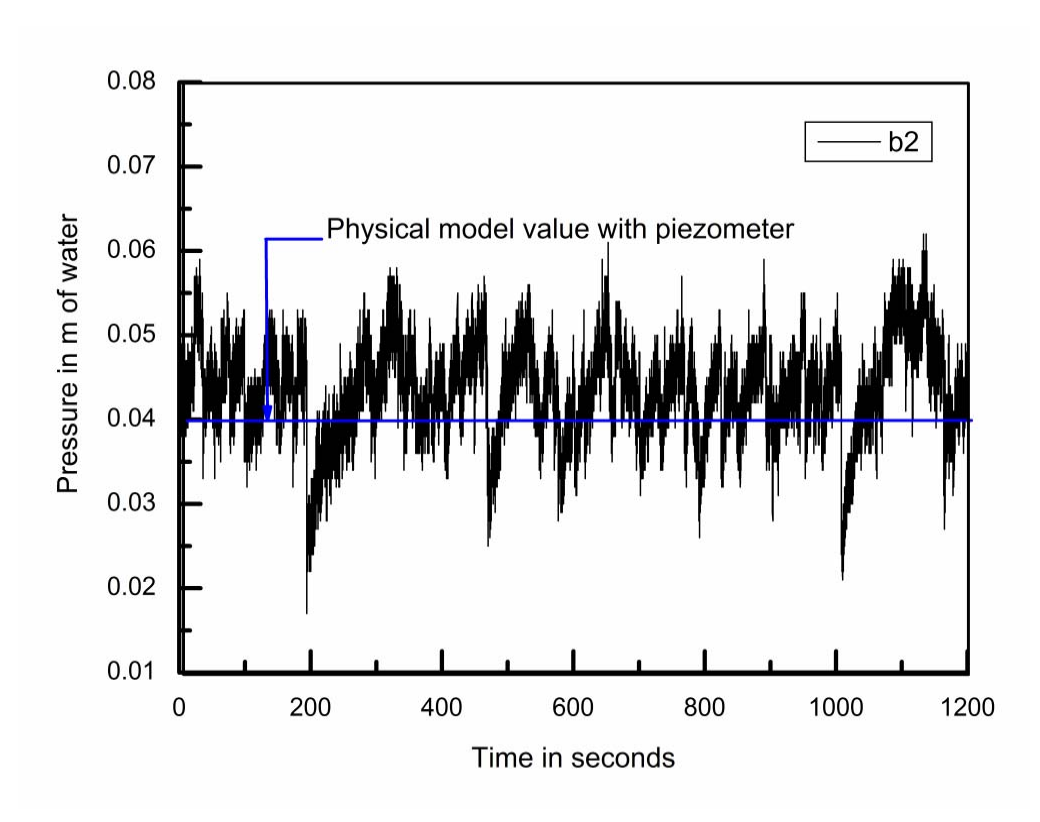


Fig. 5.32 Time series plot of pressure variation at point b<sub>2</sub> on roof profile

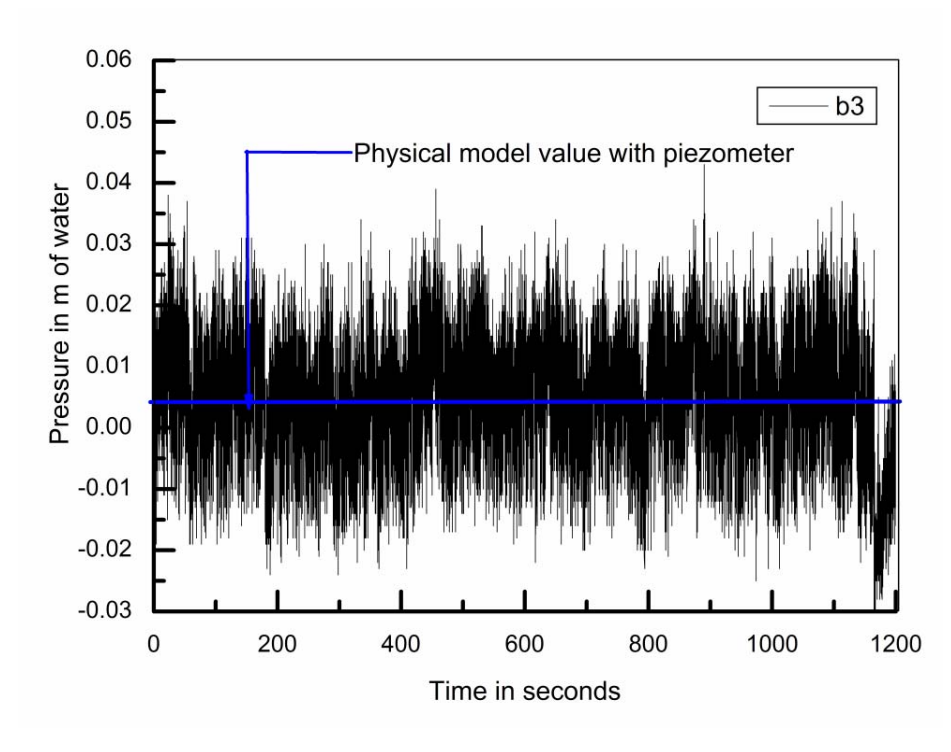


Fig. 5.33 Time series plot of pressure variation at point b<sub>3</sub> on roof profile

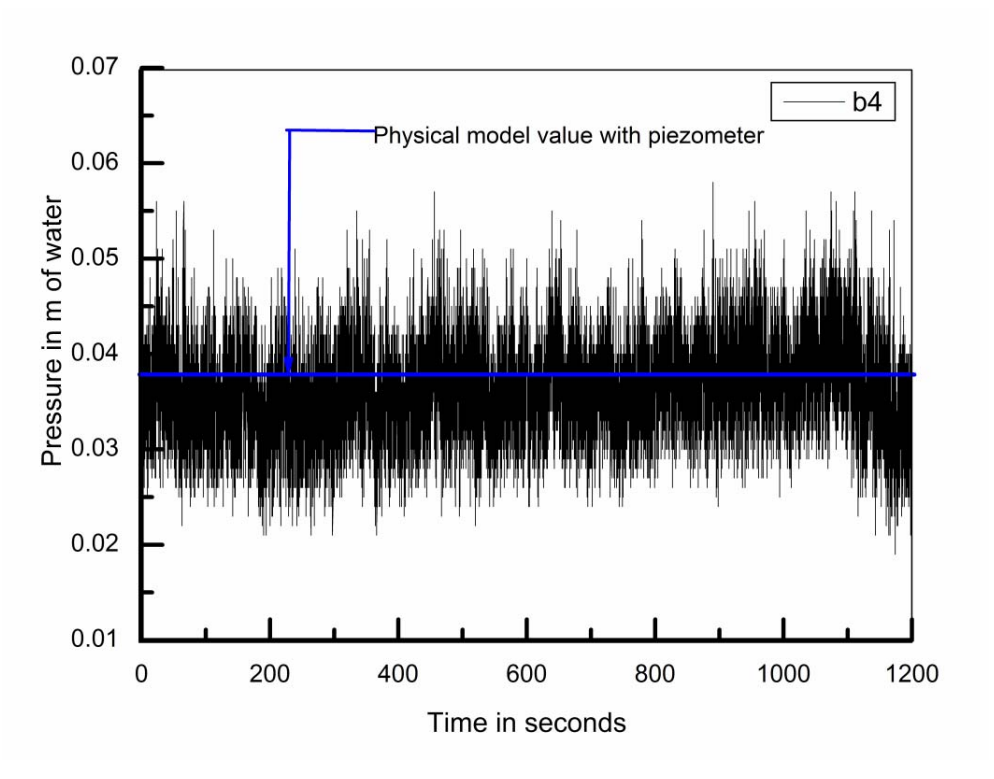


Fig. 5.34 Time series plot of pressure variation at point b<sub>4</sub> on roof profile

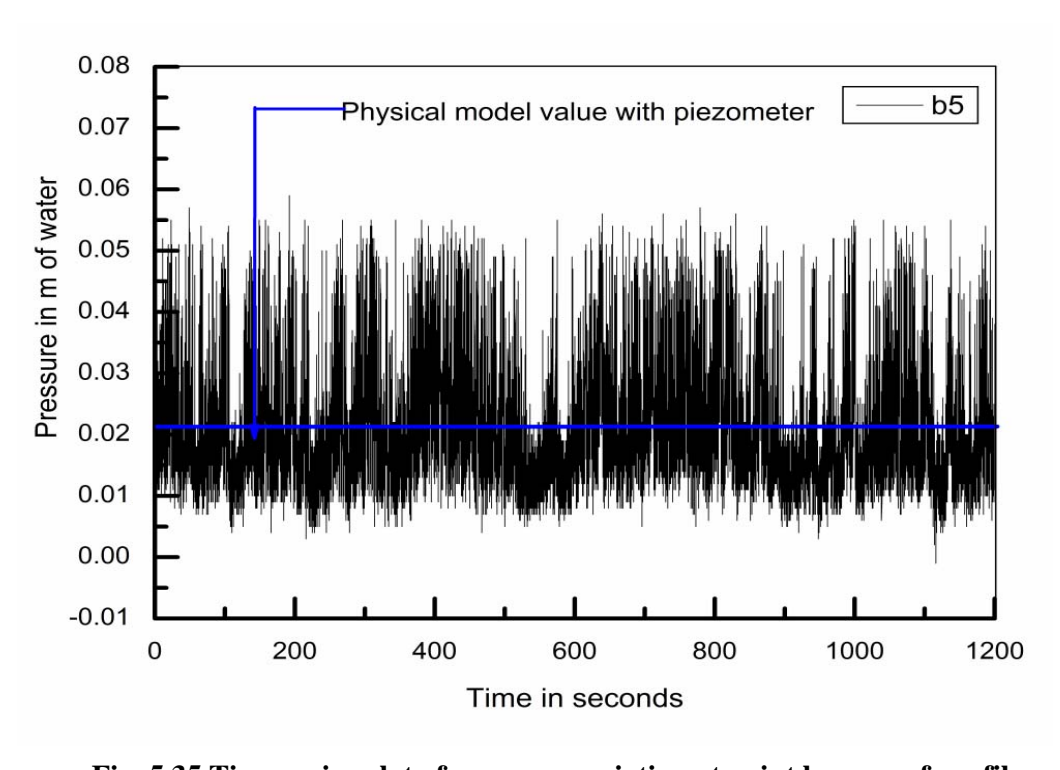


Fig. 5.35 Time series plot of pressure variation at point b<sub>5</sub> on roof profile

The time series data was analysed for calculation of statistical parameters such as minimum, maximum, mean and RMSE values and is shown in Table 5.12.

Table 5.12 Statistics of pressures on roof profile measured using transducers

Sr. No.	Location of transducers	Minimum pressure in m of water head	Maximum pressure in m of water head	Mean pressure in m of water head	RMSE (m)	% time (negative )
1	b <sub>1</sub>	-0.04	0.04	-0.02	0.02	90.95
2	$b_2$	0.02	0.06	0.04	0.04	0
3	b <sub>3</sub>	-0.04	0.05	0.01	0.01	27.21
4	b <sub>4</sub>	0.04	0.07	0.04	0.01	0
5	b <sub>5</sub>	0.02	0.06	0.02	0.02	0

The pressure at point b<sub>1</sub> was observed as -0.01m in physical model. However, minimum and maximum values of pressures were observed as -0.04 m to 0.04 m using transducers on physical model. The negative pressures were observed for longer duration at point b<sub>1</sub> i.e. 90.95 % of time. The maximum negative pressure of 0.04 was observed 4 to 5 % of time as shown in Figure 5.37. The cavitation index corresponding to maximum negative value of 0.04 was calculated as 0.38. Pressures at points b<sub>2</sub>, b<sub>3</sub>, b<sub>4</sub> and b<sub>5</sub> were positive and hence found to be acceptable. Design of roof profile is found to be safe in respect of susceptibility of cavitation damage to the surface. Thus, time series analysis of hydrodynamic pressures was found to be useful to find out the variation in pressure with respect to time at a particular point in time domain.

100 Cumulative Probability (Percentage of Time) 80 60 40 20 -0.04 -0.06 -0.02 -0.080 0.02 0.04 0.06 Pressure(Metre)

Fig. 5.36 Cumulative probability distribution of pressure at point  $b_1$  with respect to occurance in % of time

### **5.4.7.1** Impact of vibration on roof profile (Resonance study)

While designing structures in flowing fluid, it is desirable and sometimes even a prerequisite to pay attention to the possible occurrence of vibrations. Special attention for dynamic behaviour is particularly necessary when dealing with a new type of design. Hydraulic structures can fail in test either by applying very heavy load or by applying small load frequently. Therefore, it is required to do the frequency analysis of the time record data of pressures. The power spectral density function (PSD) analysis of the time domain data is shown in Figure 5.38. The PSD shows the strength of the variations (energy) as a function of frequency.

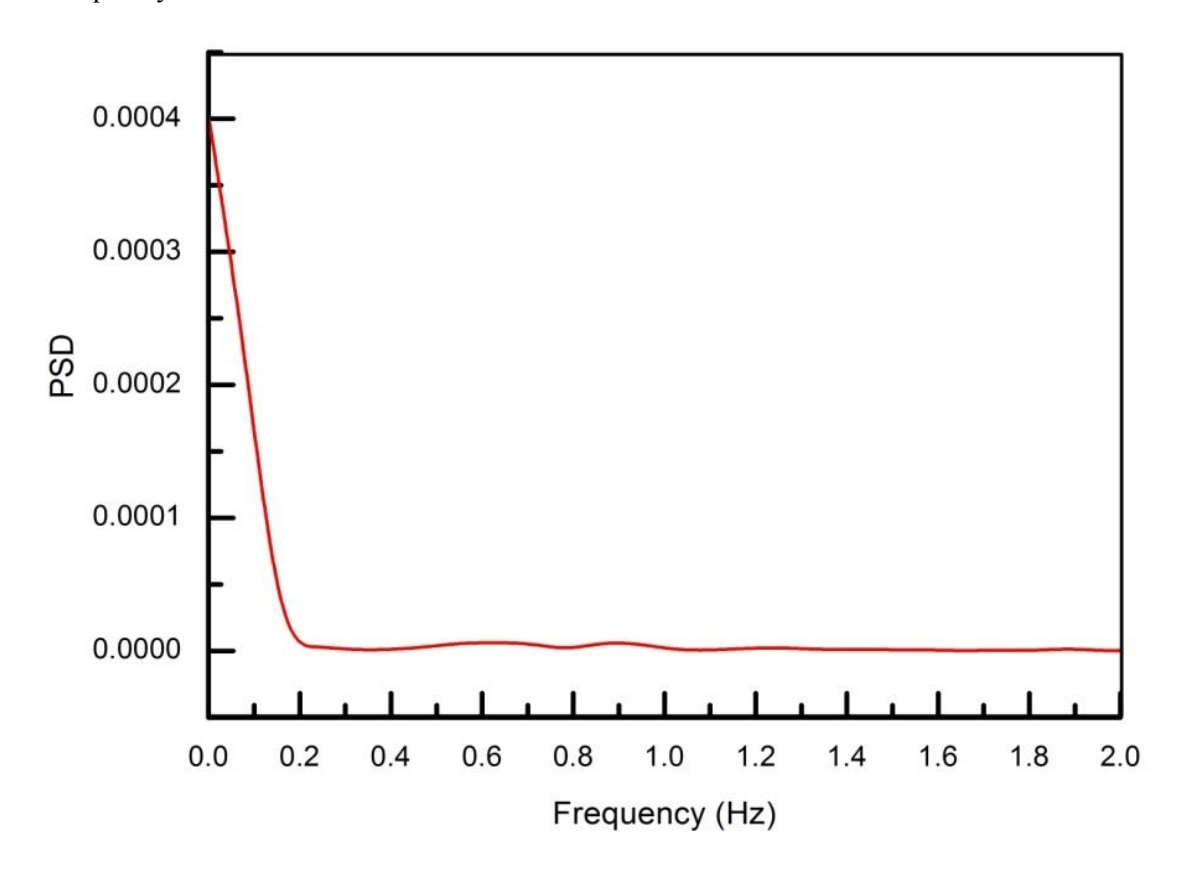


Fig. 5.37 Typical plot for power spectral density

It is observed that the pressure fluctuations are very strong at low frequencies between 0 and 0.2 Hz. The energy content at frequencies above 0.2 is zero. The natural frequency of the breastwall was calculated by using a following formula (Weaver and Johnston, 1987).

$$f = \frac{1}{2\pi} \sqrt{\frac{k}{m}} \tag{5.5}$$

In the equation 5.5, 'k' is stiffness, 'm' is mass and 'f' is a natural frequency. The natural frequency of the breast wall works out to be 11.5 Hz. Thus, it can be seen that the natural frequency of the structure and the forcing frequency of the flow are far apart. Hence, there is no possibility of failure of the breast wall due to resonance.

#### 5.4.8 Water surface profiles along centreline of spillway

Water surface profiles computed along spillway profile are used to determine the height of training wall and to fix the position of trunnion of the gate. These measurements are very important for the designer. Figures 5.39, 5.40, 5.41 and 5.42 show the water surface profiles computed along centre line of spillway for spillway profiles designed for heads of 0.6 m, 0.8 m, 1.0 m and 1.4 m respectively. Once the flow passes through the orifice, there is no significant change in depth of flow with change in spillway operating condition i.e.  $h_e/h_d = 0.8$ , 1 and 1.33. However, there is increase in depth of flow with increase in height of orifice opening. Hence, water surface profiles computed for  $h_e/h_d = 1$  has been analysed and presented for different heights of orifice openings.

Non-dimensional plots are developed by considering  $x/h_d$  on x axis and  $y/h_d$  on y axis. In the Figures, x and y are the horizontal and vertical coordinates of water surface profile,  $h_d$  is the design head for which spillway bottom profile is designed and 'd' is height of orifice. The profiles were plotted by considering origin at the tip of roof profile (end of roof profile curve) for a particular height of orifice opening.

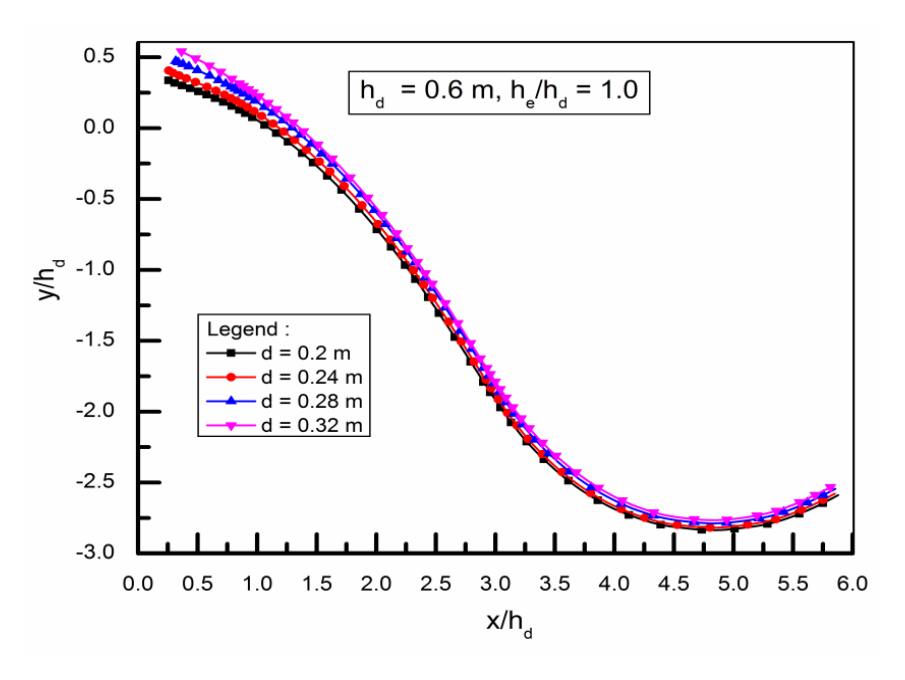


Fig. 5.38 Non dimensional plots for water surface profiles along orifice spillway bottom profile designed for head 0.6 m

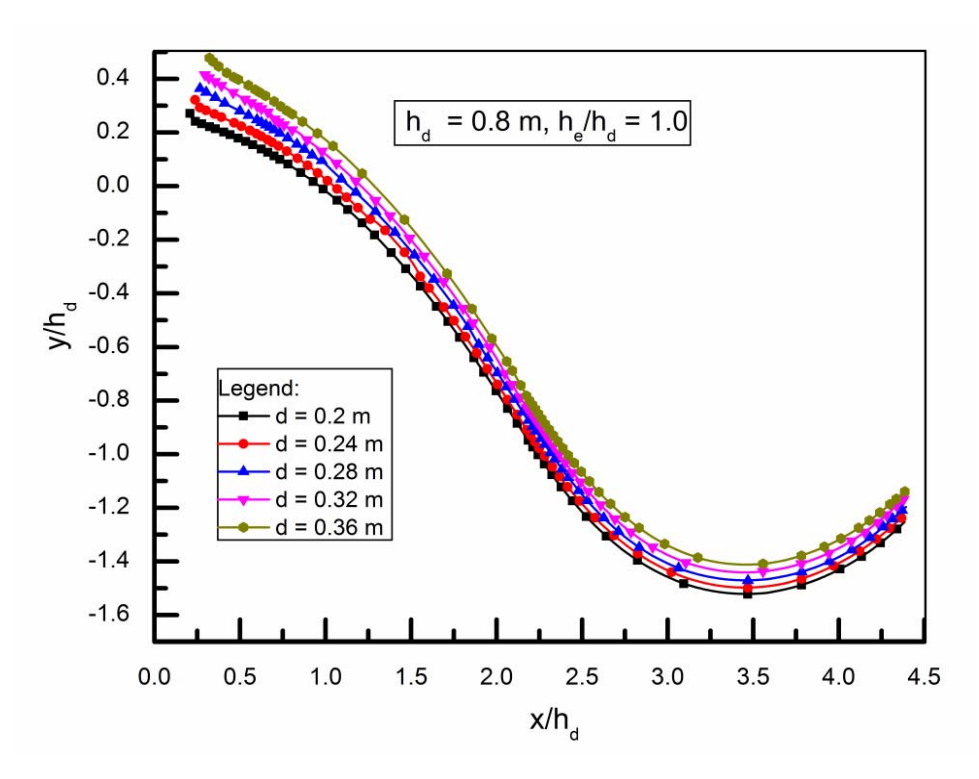


Fig. 5.39 Non dimensional plots for water surface profiles along orifice spillway bottom profile designed for head 0.8 m

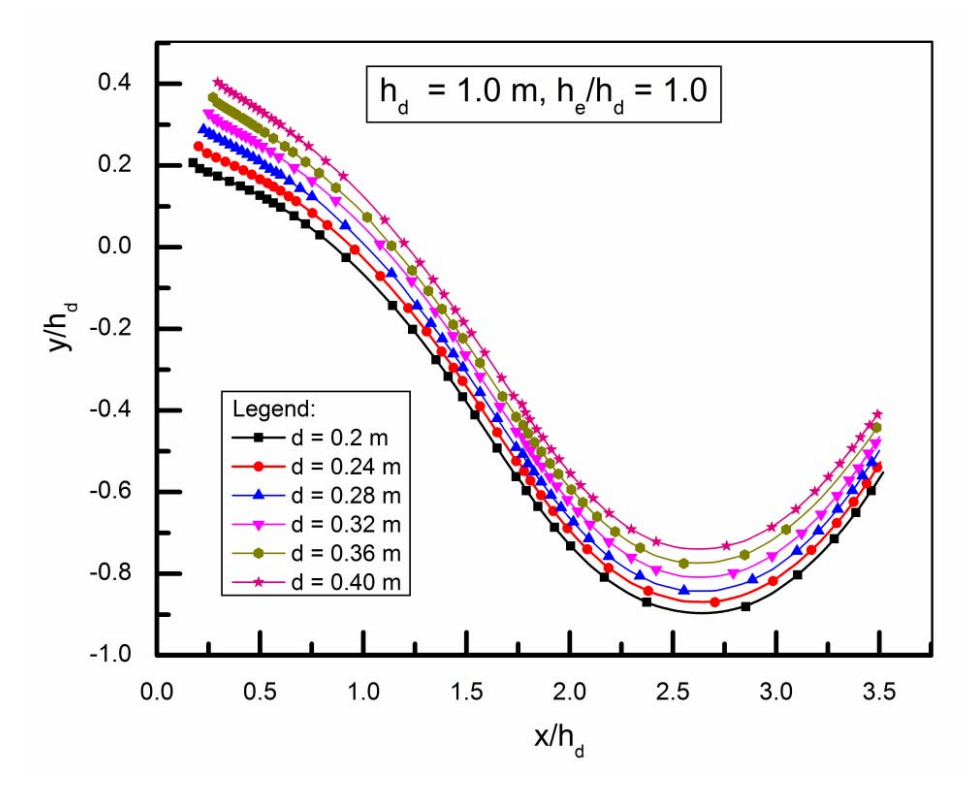


Fig.5.40 Non dimensional plots for water surface profiles along spillway bottom profile designed for head 1 m

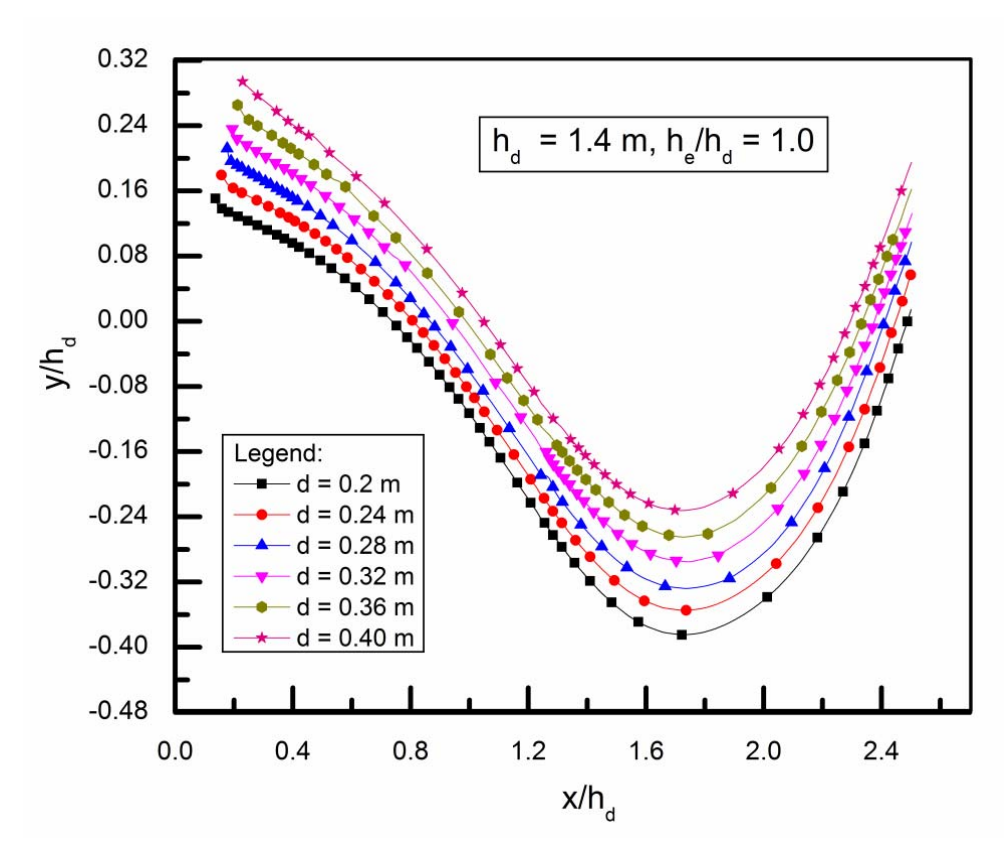


Fig. 5.41 Non dimensional plots for water surface profiles along spillway bottom profile designed for head 1.4 m

Systematic study was carried out to compute the water surface profiles throughout the length of spillway. The study provides a large data set of water surface profile for various configurations of spillway. These large data base may be useful for design engineers while designing the height of training wall and location of gate trunnion at early stage of design of an orifice spillway.

# Chapter 6

# Studies for Assessing the Effect of Various Hydraulic Parameters on Orifice Spillway using Numerical Model Studies

### **6.1 Introduction**

The parameters such as design head (h<sub>d</sub>), head over the crest (h<sub>e</sub>), width (w) and height of orifice (d), bottom and roof profiles, height of spillway from upstream reservoir bed (P) are important parameters to be considered while designing an orifice spillway. All the above parameters affect the performance of orifice spillway in respect of discharging capacity and pressures on bottom and roof profiles of spillway. Hence, care should be taken while selecting these parameters in design of an orifice spillway.

In the present study, design of bottom and roof profiles of spillway has been standardized with respect to different heads and heights of orifice. Studies were conducted for assessing coefficient of discharge, pressure and water surface profile along centre line of spillway. During the studies, height of spillway crest from the bed of the upstream reservoir (P) and width of orifice (w) were kept as 0.2 m. However, these parameters may vary from project to project. Hence, there is a need to check the performance of orifice spillway with variation of P and w of orifice opening. The spillway bottom profile was provided in the form of an equation  $x^2 = kh_dy$ . The value of k was considered as 4 for the study. However, the k value varies between 3 and 4 as discussed in Chapter 4. Hence, it is needed to study the performance of orifice spillway with variation of k value also. Roof profiles were designed corresponding to the coefficients derived for b/d = 0.4. However, equation for roof profile was derived for b/d ratio of 0.1, 0.2, 0.3 and 0.4. Hence there is also a need to check the performance of orifice spillway with variation of b/d ratio.

Numerical model studies were carried out to study the effect of P, w, k and b/d ratio on the performance of orifice spillway in terms of discharge, pressures and water surface profiles. Out of 63 combinations mentioned in Table 5.2, the spillway profiles designed for a head of 1 m and height of orifice opening of 0.24 m is randomly selected for the study. The results are discussed in the following sections.

# **6.2** Effect of Height of Crest of Spillway from the Bed of the Upstream Reservoir (P)

Three heights of spillway i.e P = 0.2 m, P = 0.4 m and P = 0.8 m were chosen for the study. The discharges through orifice spillway were estimated as 0.182 m<sup>3</sup>/s, 0.180 m<sup>3</sup>/s and 0.179 m<sup>3</sup>/s for P = 0.2 m, 0.4 m and 0.8 m respectively. The discharge computed for heights of spillway of 0.4 m and 0.8 m was found to be 1.1 % and 1.6 % less than the discharge obtained for P = 0.2 m. This can be considered as a very small difference. Hence, it can be concluded that the effect of 'P' upto the height of 0.8 m can be neglected while determining the discharging capacity of an orifice spillway. The effect of parameter 'P' was also studied in respect of pressures and water surface profiles. Figures 6.1, 6.2 and 6.3 show the effect of 'P' on pressures on spillway roof and bottom profile and water surface profile along centreline of spillway respectively.

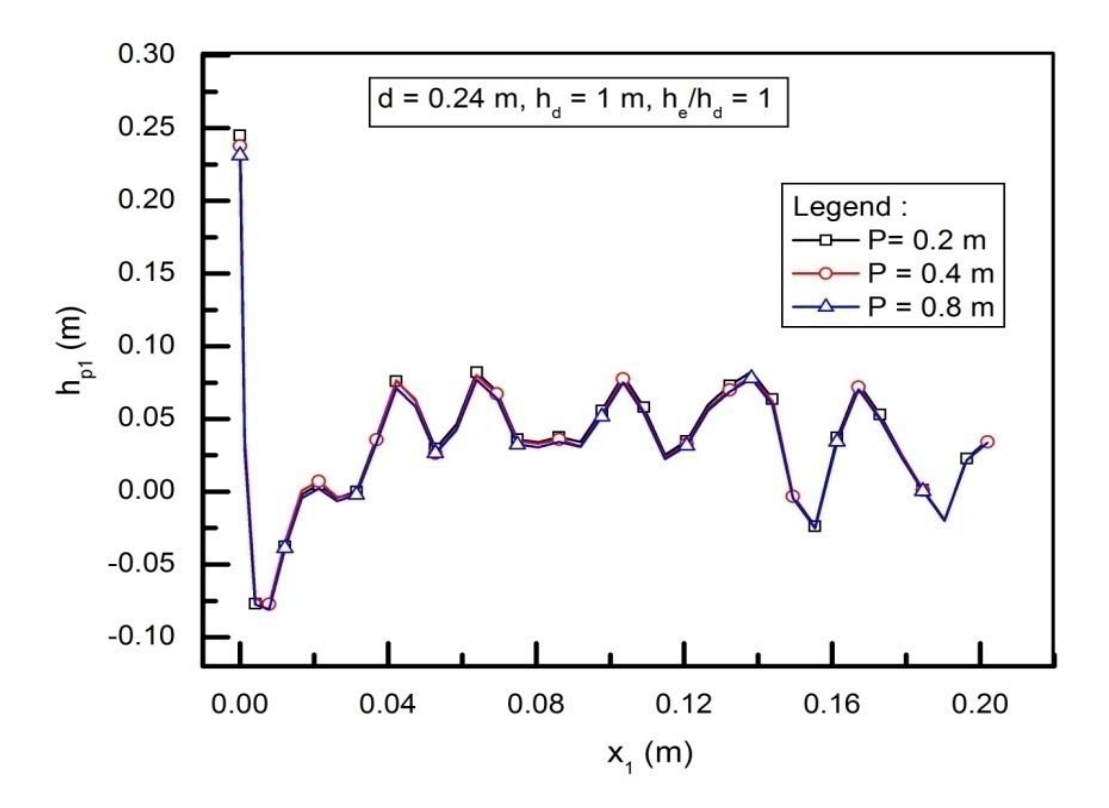
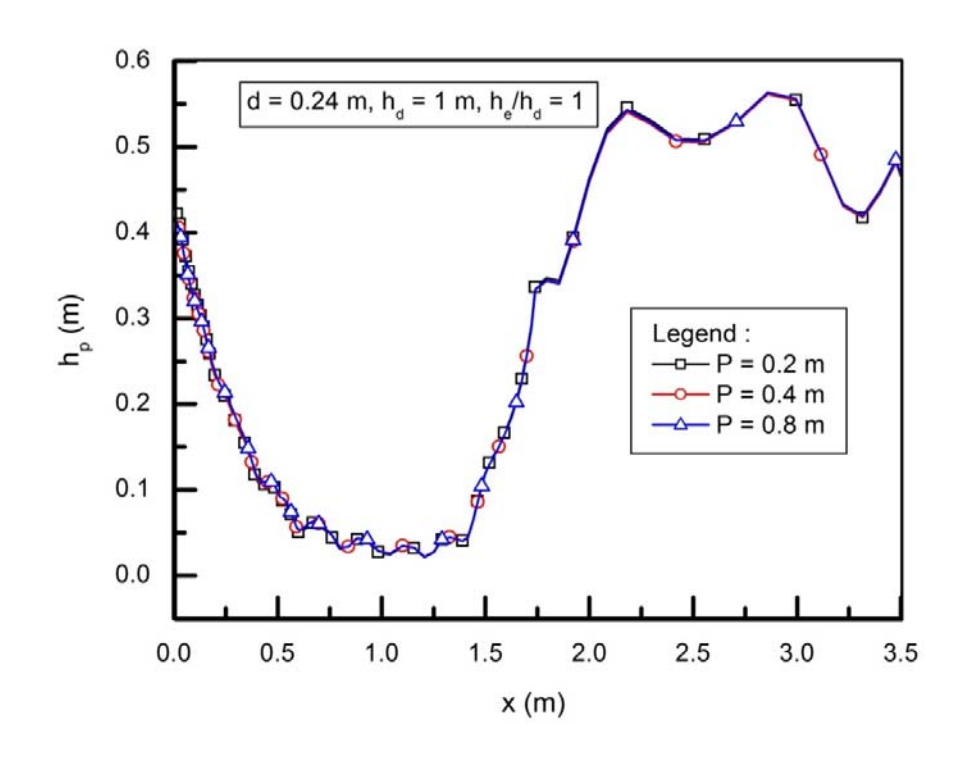


Fig. 6.1 Effect of 'P' on the pressures on spillway roof profile



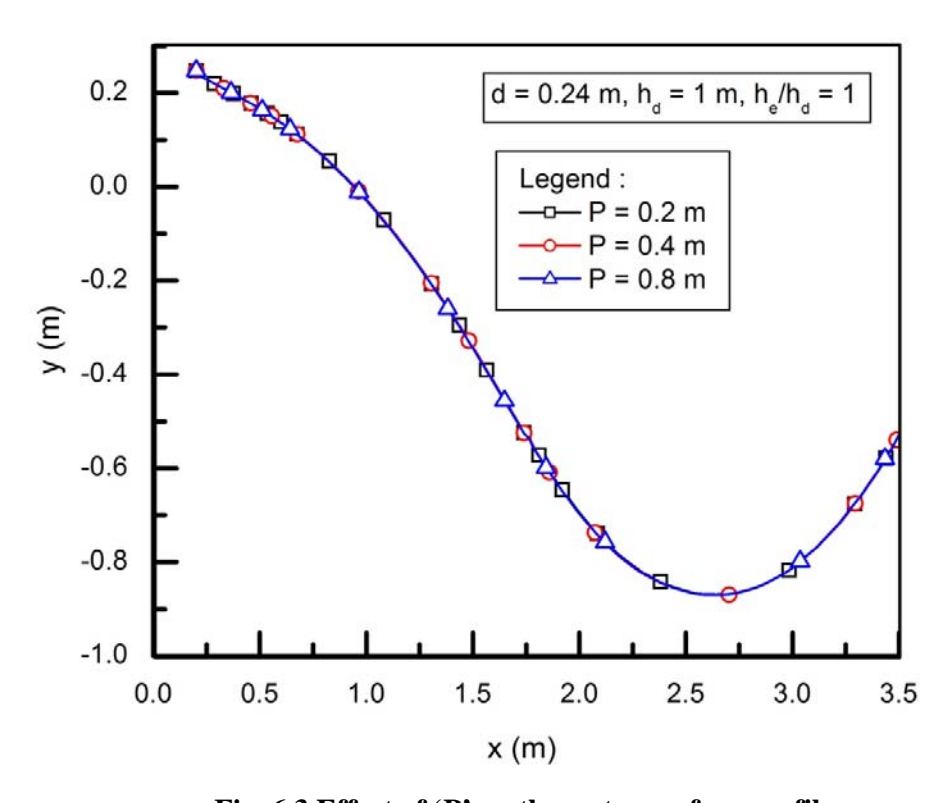
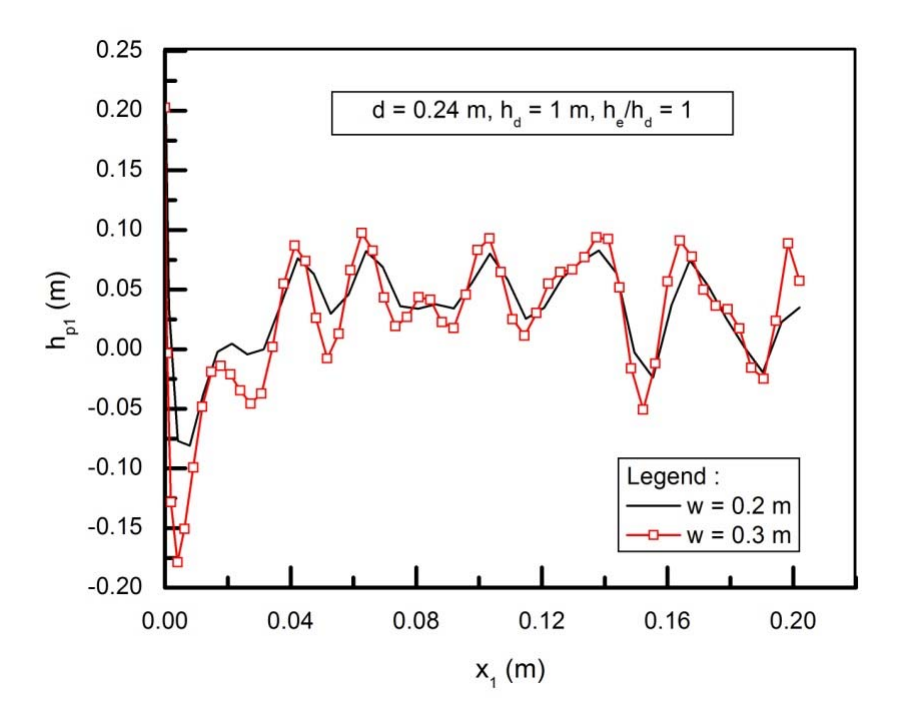


Fig. 6.3 Effect of 'P' on the water surface profile

Figures 6.1 to 6.3 indicate that there is no significant effect of P on pressures on the roof and bottom profile of orifice spillway. Similarly, there is no variation in centre line water surface profile with change in height of spillway as shown in Figure 6.3. Thus, it is concluded that the performance of orifice spillway for the proposed design of bottom and roof profile is found to be satisfactory from P = 0.2 m to 0.8 m. However, in real life larger P is not desirable and crest of the orifice spillway should be kept as near to the upstream reservoir bed as possible for effective flushing of sediments.

# 6.3 Effect of Width of Orifice (w)

The width of orifice/span 'w' was selected as 0.3 m to study the effect of change in width of spillway span on various important parameters of orifice spillway. The results computed from w = 0.3 m were compared with the results obtained for w = 0.2 m. Discharge has increased with increase in width of span. However, the coefficient of discharges were calculated as 0.91 and 0.93 for w = 0.2 and 0.3 m respectively. Thus, even though the discharge has increased due to increase in width, there is marginal increase in the coefficient of discharge. Figures 6.4, 6.5 and 6.6 show the effect of 'w' on pressures on the roof profile, pressures on bottom profile and water profile along centreline of spillway.



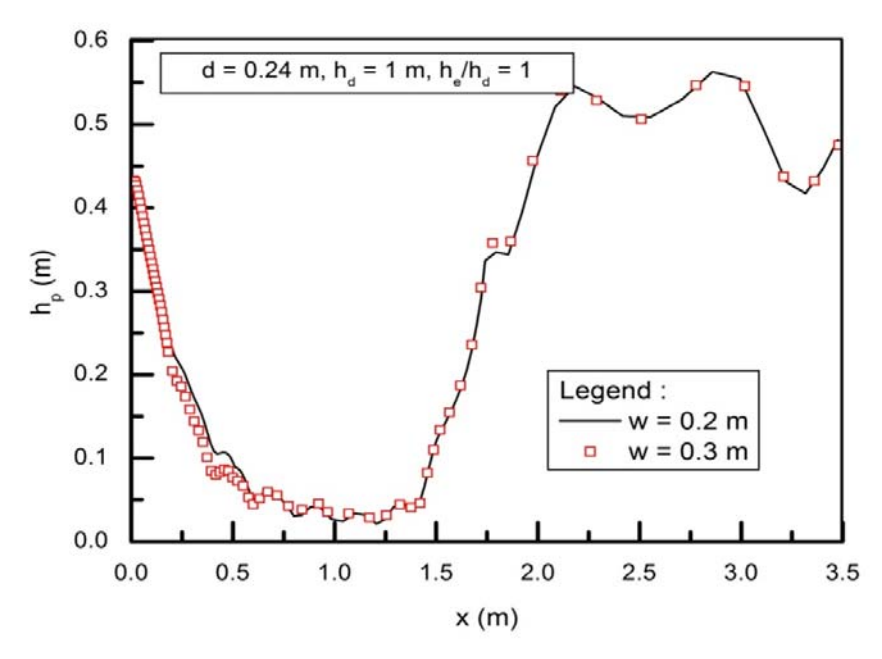


Fig. 6.5 Effect of 'w' on the pressures on spillway bottom profile

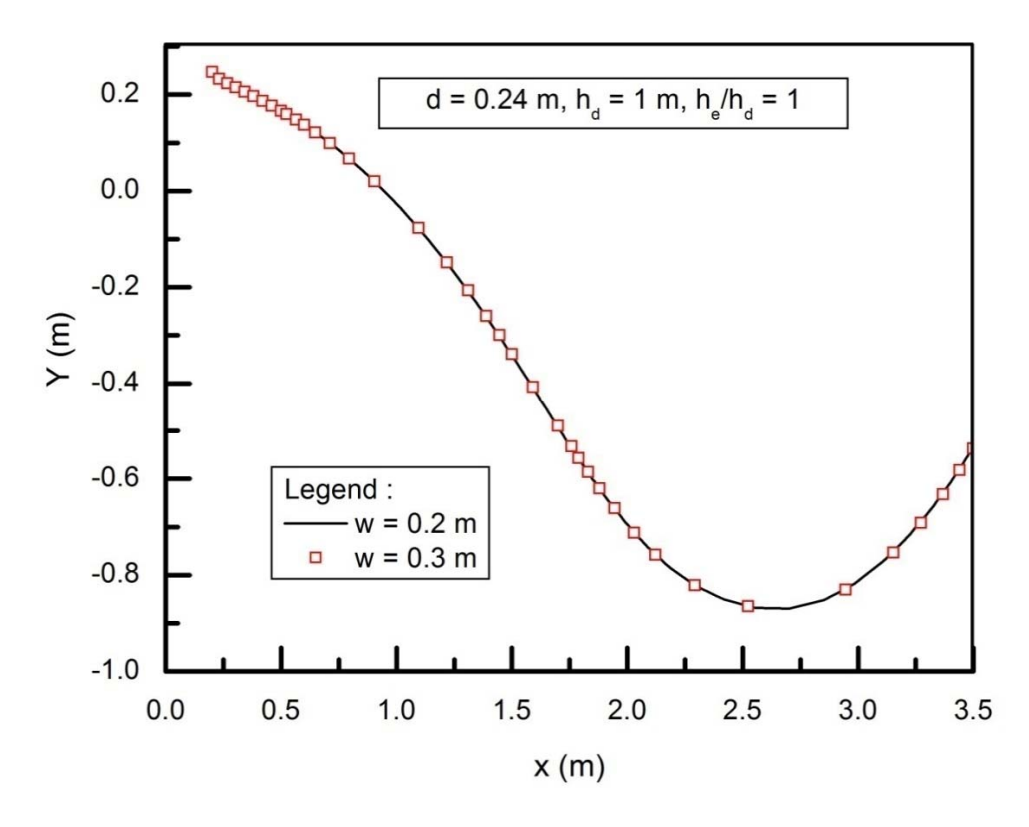


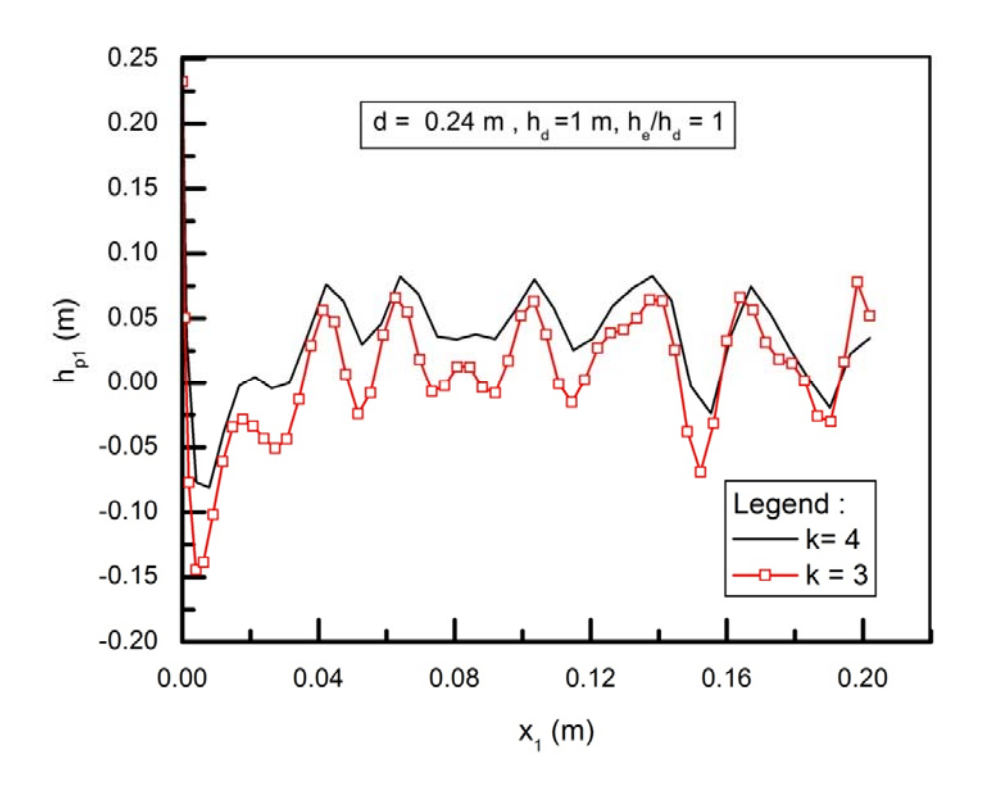
Fig. 6.6 Effect of 'w' on the water surface profile along centerline of spillway

Figure 6.4 indicates that due to increase in discharge by increasing the width of orifice, pressures on roof profile vary marginally. In the initial region, there is a sudden drop in pressure due to change of flow regime from free to pressurized flow. The magnitude of negative pressure is increased with increase in discharge for w = 0.3 m. However, the pressures on most of the part of roof profile were found positive. The cavitation index corresponding to minimum pressure of magnitude 0.17 was found to be 0.1 which is quite below the critical cavitation index of 0.2. Hence, there is a further need to study the roof profile with variation of orifice width. Minimum and maximum % difference was found to be 0.03 % to 0.68 % respectively. However, R<sup>2</sup> and root mean square error was calculated as 0.9 and 0.03 m respectively. Hence, the performance of roof profile was sound to be satisfactory throughout the length except the initial region of roof profile.

Figure 6.5 shows the effect of width on pressures on spillway bottom profile. Positive pressures were observed on the spillway bottom profile for w = 0.3 m. It is observed that there is a little variation in pressures with change in width of orifice. Minimum and maximum % difference was found to be 0.39 % to 0.28 % respectively. However,  $R^2$  and root mean square error was calculated as 0.99 and 0.014 m respectively. Hence, the pressures on bottom profile of spillway are found to acceptable for w = 0.3 m. Figure 6.6 indicates that there is no change in water surface profile with change in width of orifice indicating that width of orifice does not play a role in water surface profile.

# 6.4 Effect of factor 'k' while designing spillway bottom profile

The spillway bottom profile is generally provided in the form of  $x^2 = kh_dy$ . The value of k changes the slope of the profile. The studies in the present research work have been carried out for k = 4. However, an alternative study was carried out for k = 3 to investigate its effect on discharging capacity and pressures on spillway bottom and roof profiles. It is seen that the profile becomes flatter for k = 4 than k = 3. The studies indicated that the discharge through orifice is increased from 0.182 m³/s to 0.188 m³/s for spillway bottom profile with k = 3. Discharge was increased by about 3 % due to the steep profile. Figures 6.7, 6.8 and 6.9 show the effect of 'k' on pressures on roof profile, pressures over the bottom profile and water profile along centreline of spillway.



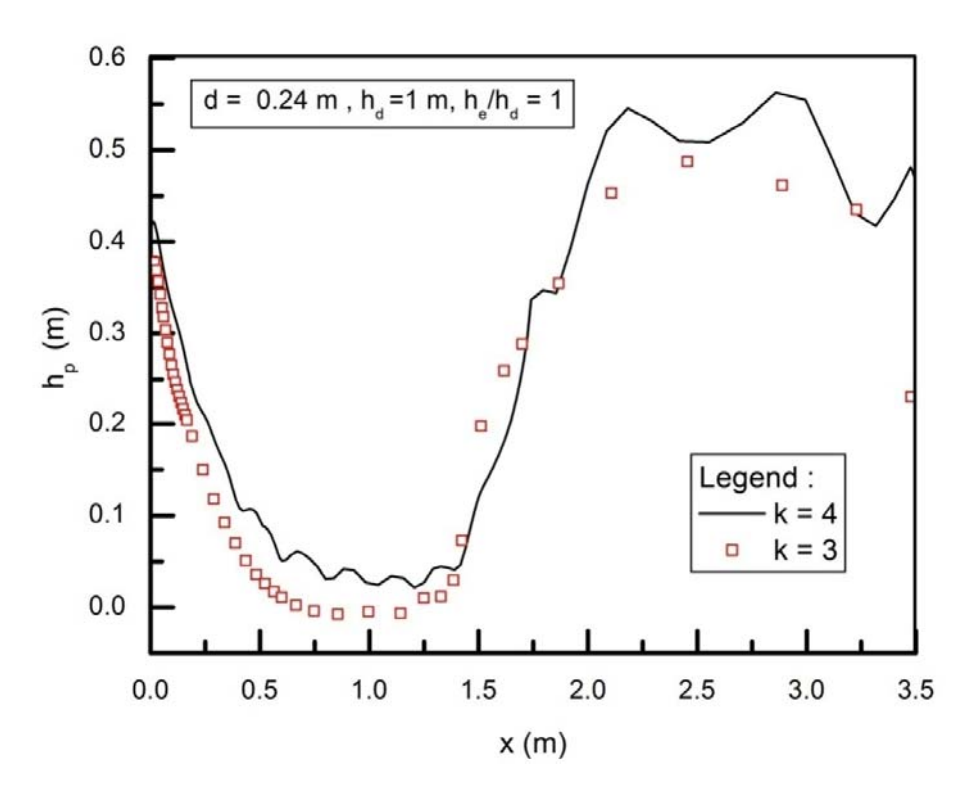
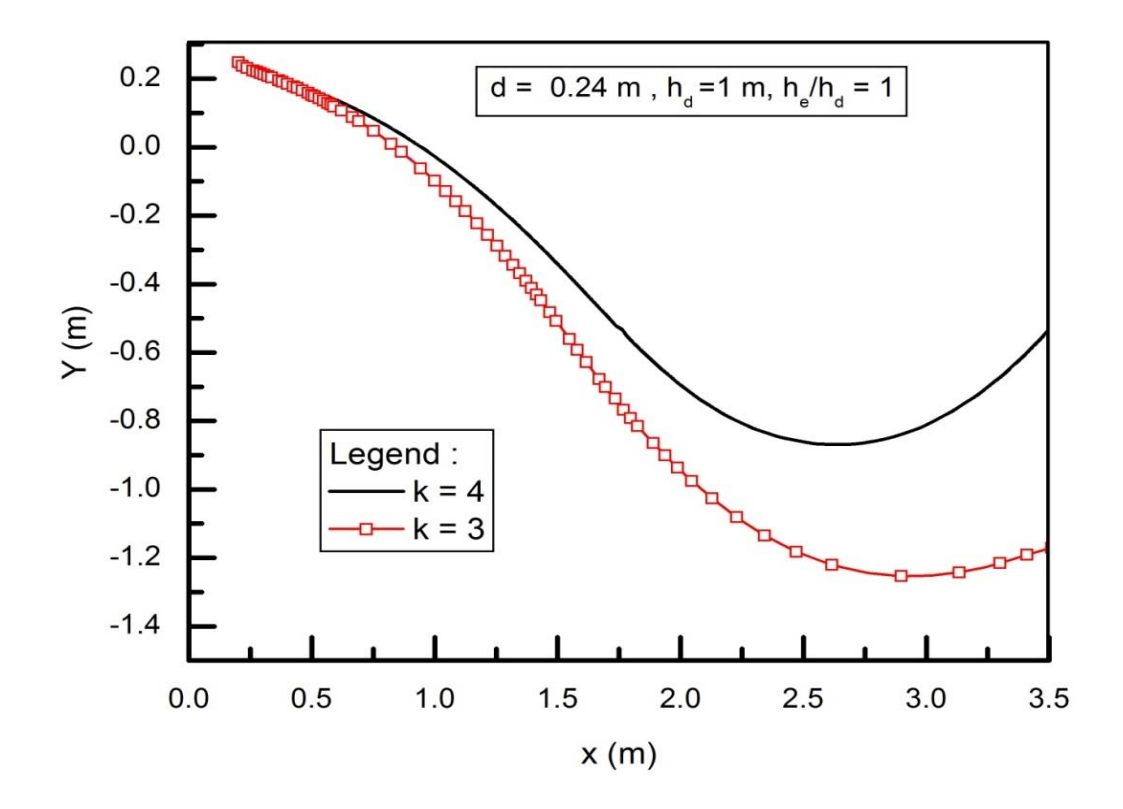


Fig. 6.9 Effect of 'k' on the pressures on spillway bottom profile



It was found that as the bottom profile becomes steep with k=3, discharge through orifice spillway increases. Hence, due to steeper spillway bottom profile, the jet of water also becomes steeper. This results in decrease in pressures on the roof profile as shown in Figure 6.8. Negative pressure of magnitude 0.14 was observed at the initial region. Beyond this point, there are positive pressures on roof profile throughout the length of roof profile. The cavitation index corresponding to negative pressure was found to be 0.14 which is less than critical cavitation index of 0.2. Hence, there may the possibility of cavitation damage upto the distance of about 0.04 m from crest of spillway. It was observed that there is a variation in pressures on roof profile with change in spillway bottom profile. Minimum and maximum percentage difference was found to be -0.53 and 0.98 respectively. However,  $R^2$  and root mean square error was calculated as 0.91 and 0.04 m respectively. The values are found in acceptable limit. However, the performance of spillway bottom profile with k=4 are found to be more satisfactory than k=3.

From Figure 6.9, it can be seen that the pressures on spillway bottom profile with k = 3 were minimum than the pressures obtained for k = 4. Due to steeper profile with k = 3, the velocity over the spillway surface increases that results in decrease in pressure values. However, positive pressures were observed on spillway bottom profiles for k = 3 and 4. Figure 6.10 shows the comparison of water surface profile with spillway bottom profiles with k = 3 and 4. The depth of flow on the spillway surface will be helpful for determining the

height of training walls adjacent to the structures. In this case height of training wall was more for flatter profile i.e k = 4 than k = 3.

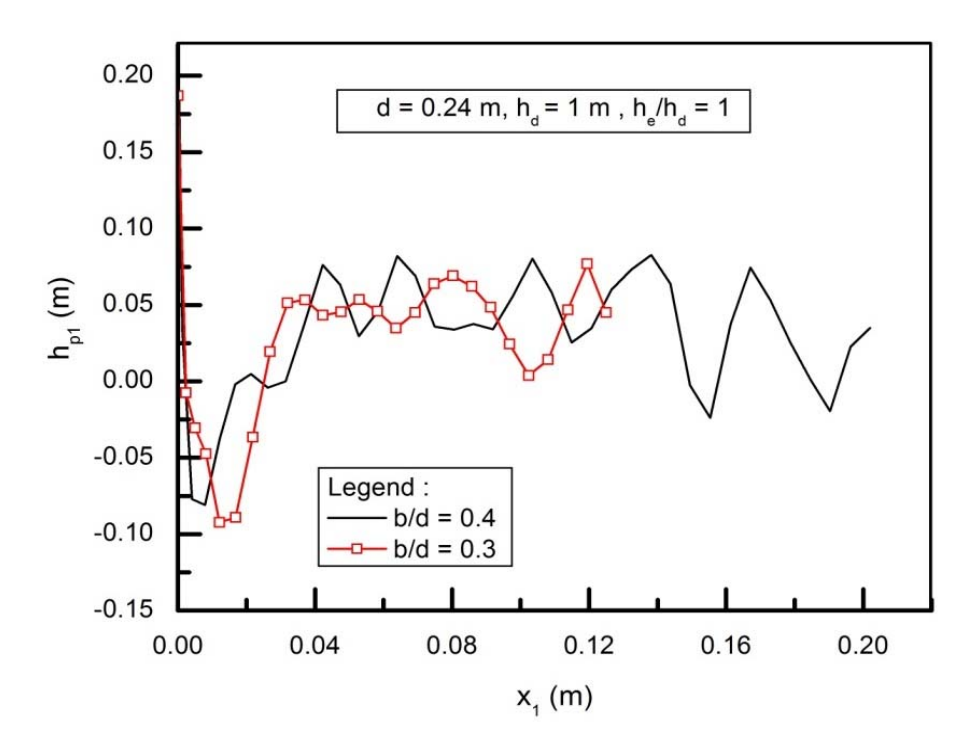
# 6.5 Effect of b/d Ratio while Designing Roof Profile

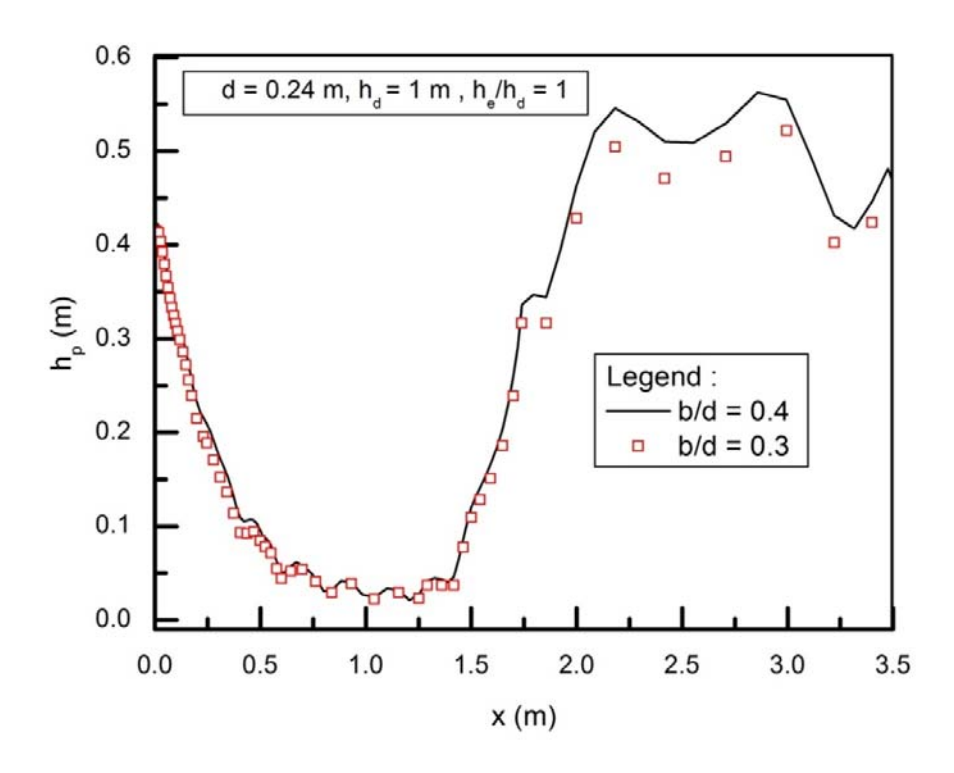
The selection of height of roof profile i.e. b is generally decided based on height of orifice (d). The data for more than 22 orifice spillway projects studied in CWPRS was analysed and the height of roof profile in the form of b/d ratio was compiled. It was found that b/d variesfrom 0.1 to 0.4. It was also experienced from the model studies that b/d ratio affects the design of roof profile thereby affecting the discharging capacity of orifice spillway. The present research work was carried out only for the roof profile designed for b/d = 0.4. Hence, additional studies were also carried out by changing the roof profile in terms of b/d = 0.3 and keeping the bottom profile in the form of an equation  $x^2 = 4h_dy$ .

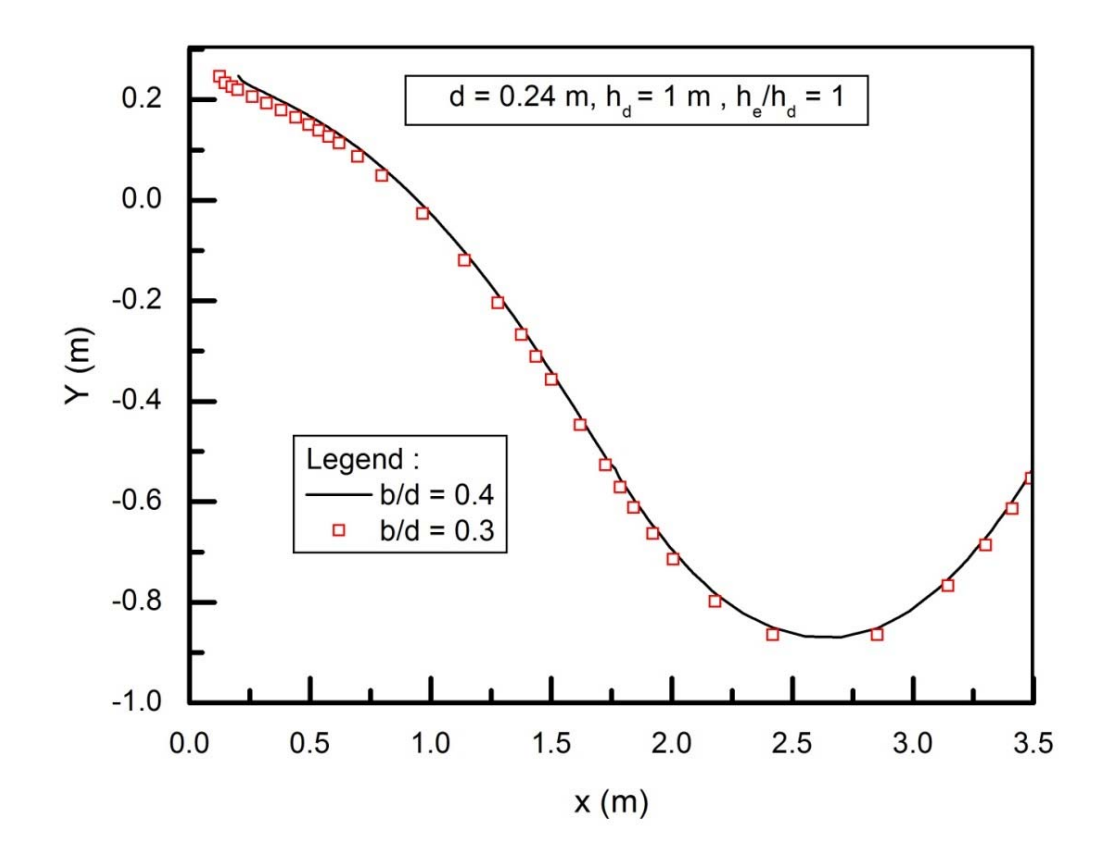
Figures 6.11 and 6.12 show the effect of b/d ratio on the pressures over roof and bottom profile of spillway respectively. Figure 6.13 shows the effect of b/d ratio on the water surface profile along centreline of spillway. The length of roof profile depends on height of orifice, head and b/d ratio as discussed in Chapter 4. The length of breastwall increases with increase in b/d ratio. Hence, in Figure 6.11 length of the roof profile is about 0.21 m for b/d ratio of 0.4 which is more than 0.13 m for b/d ratio of 0.3. Due to extended roof profile, the discharge through orifice spillway also increased for a particular head over the crest and spillway bottom profile designed with specific head. It was observed from the studies that the discharges of 0.168 m³/s and 0.182 m³/s could pass through orifice spillway for the roof profile designed for b/d ratio of 0.3 and 0.4 respectively at design head of 1 m. Hence, there is about 8 % increase in discharge in increasing the b/d ratio from 0.3 to 0.4. The corresponding coefficients of discharges were calculated as 0.84 and 0.91. The results show that increase in b/d ratio results in increase in coefficient of discharge. Hence, it can be concluded that design of roof profile play an important role in determining the discharging capacity of an orifice spillway.

Figure 6.11 shows that there is marginal change in pressures on roof profile with increase in b/d ratio. After the distance of about 0.03 m, positive pressures were observed throughout the length of roof profile. The cavitation index for negative pressure was calculated as 0.20, which is equal to critical cavitation index of 0.2 (Falvey, 1990). Hence, the design of roof profile was found to be safe for both b/d ratios. Minimum and maximum % difference was found to be and -0.49 to 0.55 % respectively. However, R²and root mean square error was calculated as 0.81 and 0.04m respectively. Figures 6.12 and 6.13 indicate that there is miniscule change in pressures on spillway bottom profile and water surface profile along centreline of spillway by changing the roof profile with different b/d ratio.

From the study, it can be concluded that the roof profile developed from the proposed equation was found to be safe in respect of all the above parameters with variation of b/d ratiofrom 0.4 to 0.3. However, it is designer choice to select the roof profile in such a way so as to make the structure economically efficient.







## **6.6 Performance of Orifice Spillway for Gated Condition**

The performance of orifice spillway was checked in terms of different important hydraulic parameters for spillway operating at free flow condition. Studies were carried out for all practical design heads, heights of orifice and properly designed bottom and roof profiles of orifice spillway. Orifice spillways are also operated at gated conditions to maintain high reservoir water level. Hence, there is a need to study the performance of orifice spillway at spillway operating at gated conditions. The case with the spillway profiles designed for a head of 1 m and height of orifice opening of 0.24 m was randomly selected for the study. Numerical model was used to simulate the flow through orifice spillway at gated operation of spillway. Gate opening was reduced by 25%, 50% and 75% of the full height of orifice. The corresponding opening sizes are 0.06 m, 0.12 m and 0.18 m respectively. During the simulations, height of water above the crest was kept as same i.e. design head of 1 m. Results were analysed in the form of pressures distribution on spillway bottom and roof profile of

orifice spillway. Figures 6.14 and 6.15 show the pressures on the roof and bottom profile of orifice spillway respectively for gated as well as ungated operation of orifice spillway.

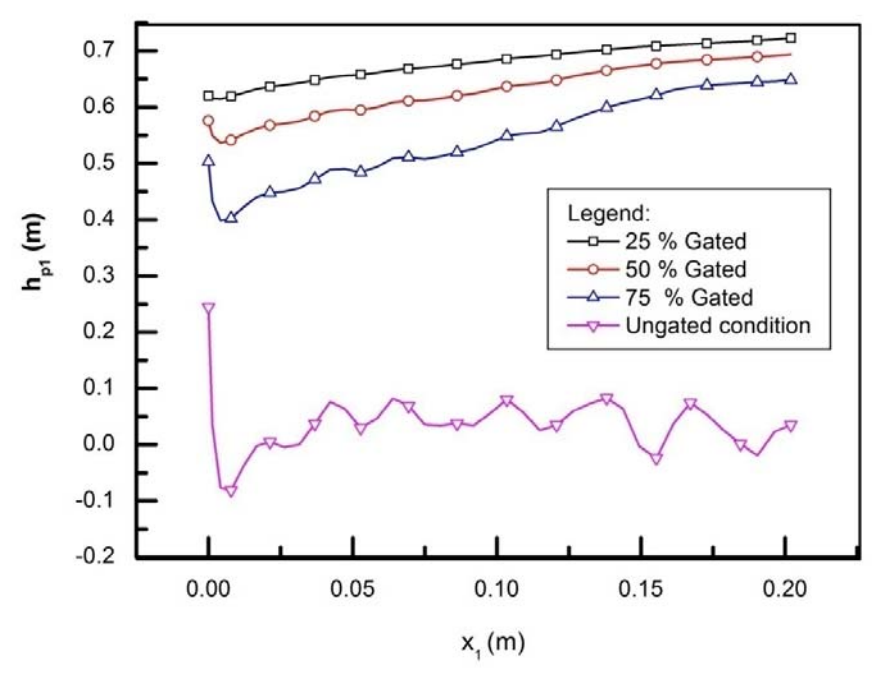


Fig. 6.14 Pressures on roof profile for gated and ungated operation of orifice spillway

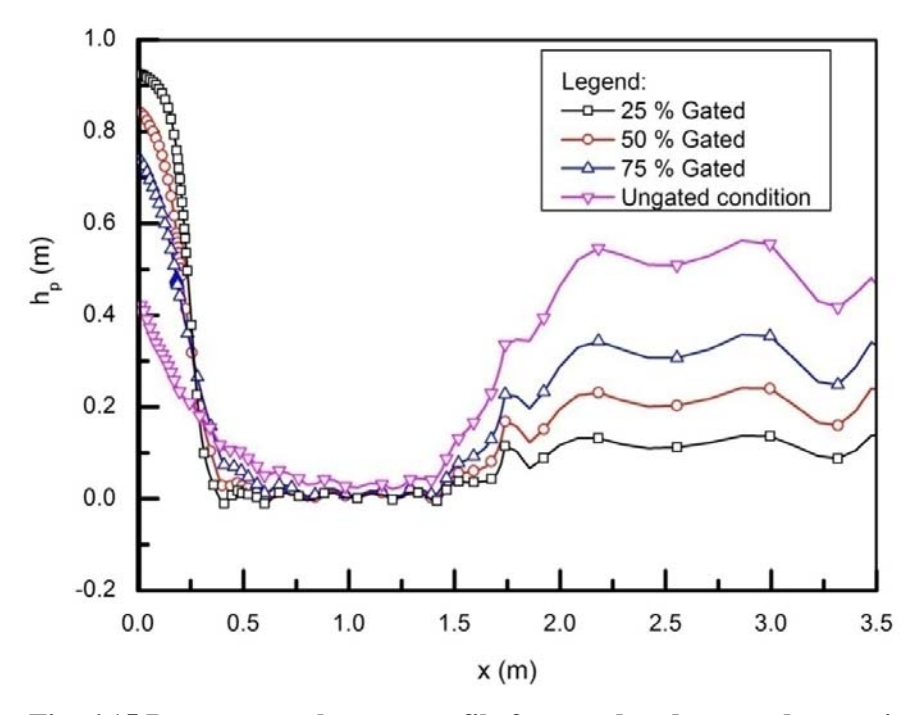


Fig. 6.15 Pressures on bottom profile for gated and ungated operation of orifice spillway

In gated condition, flow is pressurized below roof profile that results in positive pressures on the spillway bottom and roof profile. Figure 6.14 shows positive pressures throughout the length of roof profile. Hence, the design of roof profile is found to be safe in terms of cavitation damage at gated operation of spillway. When the flow passess through gate opening it suddenly changes from pressurized to free surface flow. The velocity of flow goes on decreasing with increase in gate opening for a particular head over the crest. This results in increase in pressures on the spillway bottom profile. Figure 6.15 show that the pressures over the bottom profile computed for small gate opening (25%) are lower than that of the higher gate opening (75% or ungated). When flow passes through gate opening, some negative pressures were observed on spillway bottom profile at few locations just downstream of gate lip for lower gate opening of 0.06 m (25% gate opening). However, corresponding cavitation index works out to be 0.2 which is equal to critical cavitation index. Hence, design of bottom profile can be considered as safe for small gate operation of spillway for this case. Flow was visualised in numerical model by creating phase diagram of air and water throughout the length of domain as shown in Figure 6.16. In this Figure, blue colour shows air and red colour shows water in the domain. However, colour between 0 and 1 gives air-water interface.

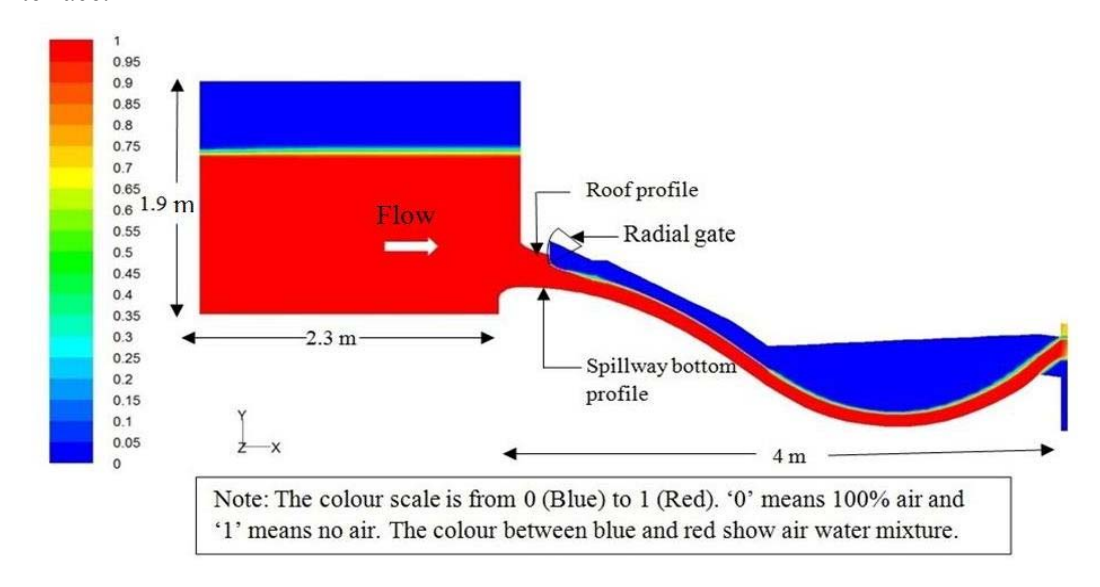


Fig. 6.16 Simulation of flow for 75 % gated operation of orifice spillway

Figure 6.16 shows that there is no separation of flow on bottom and roof profile of orifice spillway. Smooth flow conditions were observed throughout the length of spillway. Numerical model was also used to visualize the pressure and velocity field in the vicinity of gate opening. Figures 6.17 and 6.18 show contour plots for pressures and velocity vectors respectively in the vicinity of roof profile for 75 % gated operation of spillway. The units of pressure and velocity shown in the figures are m and m/s respectively.

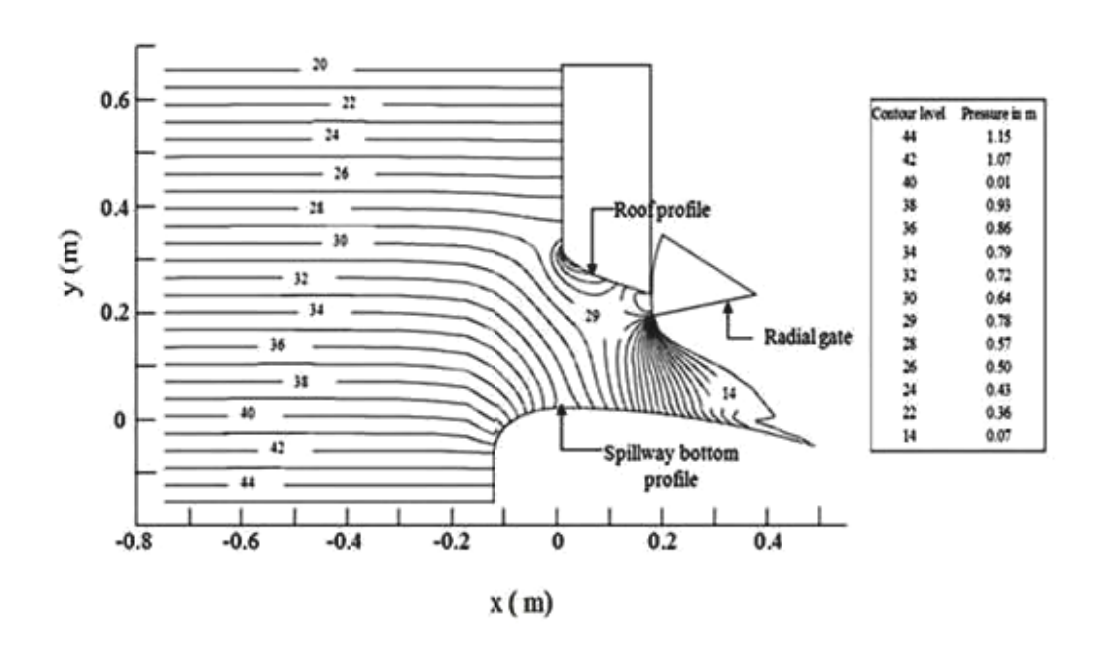


Fig. 6.17 Contour plot showing pressures in the vicinity of roof profile for 75 % gated operation of orifice spillway

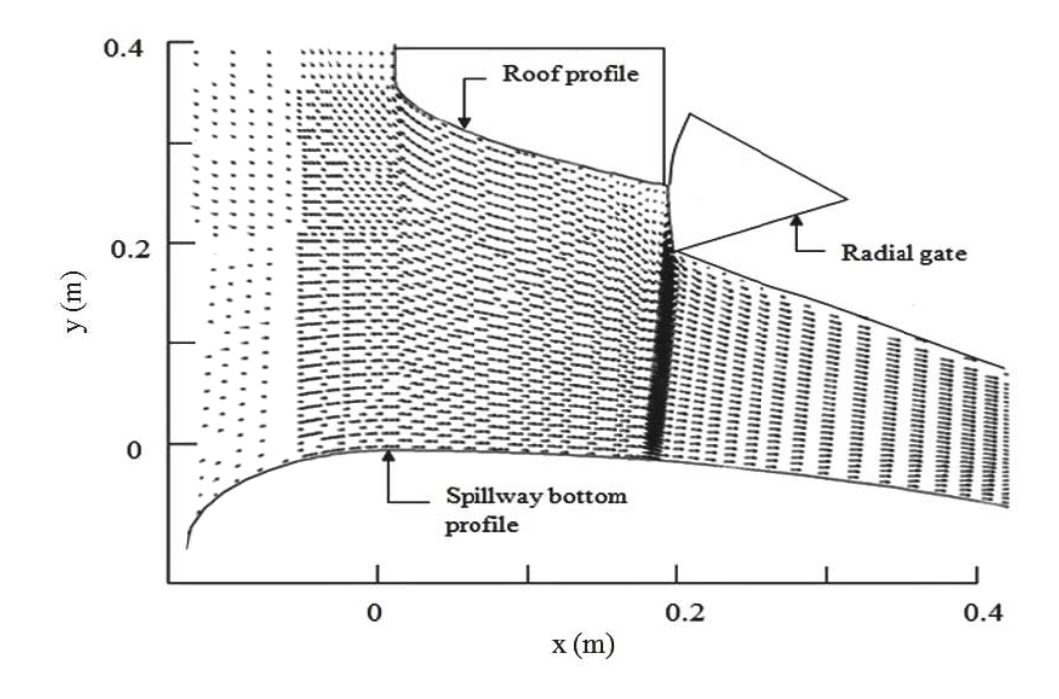


Fig. 6.18 Velocity vectors in the vicinity of roof profile for 75 % gated operation of orifice spillway

It can be seen from Figure 6.17 that there are positive pressures over spillway bottom and roof profile of orifice spillway for gated operation of spillway. When flow exits through

the gate opening, it attains maximum velocity due to supercritical flow on surface. The horizontal component of velocity is high and the flow has a tendency to separate from the spillway bottom profile. This results in low pressures over spillway bottom profile as shown in Figure 6.17. Velocity is found to be minimum below the roof profile due to pressurized flow in this region. It was also observed that bottom and roof profile were guiding the streamlines entering into the orifice as shown in Figure 6.18. The results prove the capability of numerical model in visualising the flow conditions through orifice spillway at gated operation of spillway.

## **Chapter 7**

## **Summary and Conclusions**

### 7.1 Summary

Dams, reservoirs and canal networks are some of the important hydraulic structures used to reduce the problem of spatial and temporal water availability. One of the most important and primary component of a dam is its surplus spillways. They are used to pass surplus as well as flood water safely from upstream to downstream of the dam. Recently, attention is focused on developing run-of-the-river schemes in cascades with suitable sediment disposal arrangement instead of large storage dams on the rivers, in order to minimize the deposition of silt in the reservoir. Thus, apart from safe disposal of flood from upstream to downstream of dams, the sediments entering into the reservoir should also be flushed to the downstream.

Nowadays, orifice spillways in the form of breastwall/sluice are becoming popular due to their ability to flush the sediment out of the reservoir especially for a run-of-the-river scheme in addition to regulating the flood discharge. However, no systematic guidelines have been reported for design of an orifice spillway especially in respect of bottom and roof profile of an orifice spillway. The discharging capacity, pressure distribution on spillway bottom profile, pressure distribution on spillway roof profile and water surface profile along spillway profile are some of the essential parameters to be studied while assessing the performance of orifice spillway. The U. S. Army Corps of Engineers (USACE, 1990) have provided the guidelines for design of overflow spillway. Unlike overflow spillway, the design of orifice spillway has not been evolved with respect to its different hydraulic parameters. The main objective of the present research work is to conduct basic research to develop hydraulic equation for the design of roof and bottom profiles of an orifice spillway. It is also aimed to provide design guidelines in respect of all hydraulic parameters of an orifice spillway for

various combinations of design heads and orifice sizes. It is also aimed to develop non dimensional plots for basic design of an orifice spillway.

Physical model studies are being used extensively to understand the complexity of spillway flows. The physical model study includes systematic examination of each feature of the original design. It also examines the necessity of any modification from operational point of view, possible reduction in cost of construction as well as reduction in maintenance cost. In the present study, experiments were carried out on basic physical model constructed at Central Water and Power Research Station (CWPRS), Pune, India. Today, with the help of high-performance computers and more efficient Computational fluid dynamics (CFD) codes, the behaviour of hydraulic structures can be investigated numerically in reasonable time and cost. The CFD software FLUENT version 6.3.26 was used to simulate the flow through orifice spillway. The numerical model has been verified and validated in terms of grid convergence and turbulence model by comparing the results with physical model. The numerical model was also validated in respect of discharge, pressures and water surface profiles for the configurations of spillway with the measured values. The grid convergence study was also carried out based on the guidelines given by American Society of Mechanical Engineers (ASME). The Grid Convergence Index (GCI) method used herein is an acceptable and recommended method that has been evaluated over several hundred CFD cases.

In the present study, total 226 numbers of experiments and simulations were carried out on physical and numerical models. The studies were carried out for three experimental set up:

- In the first set up, the flow through a sharp edged orifice was investigated for various heads and heights of orifice. Based on the study, the bottom profile of an orifice spillway was finalized in the form of  $x^2 = 4h_dy$ . The studies also indicated a need for further work to develop the equation for design of roof profile.
- In second set up, the flow through an orifice was investigated with solid spillway bottom profile in the form of an equation  $x^2 = 4h_dy$ . The roof profile was not introduced during the studies. The studies were carried out at various spillway operating conditions for different heads and heights of orifice openings. The observed data from set up 2 was analyzed in respect of discharge through orifice, pressures over spillway bottom profile and upper nappe profile to check the performance of orifice spillway. The effect of height of orifice, head and height of spillway from upstream reservoir bed

- was also studied. Based on upper nappe profile observed in this set up, an equation was developed to design the roof profile of an orifice spillway.
- In the third set up, flow through an orifice spillway was investigated with solid spillway bottom and roof profile. The studies were carried out at various spillway operating conditions for different combinations of heads and heights of orifice. Based on the study, guidelines were provided to design the bottom and roof profile of an orifice spillway in respect of discharging capacity, pressure and water surface profiles along the spillway.

#### 7.2 Conclusions

The major conclusions emanated from present study are given in the following sections.

## 7.2.1 Conclusion from physical and numerical model studies of sharp edged large orifice (set up-1)

Physical and numerical model studies were carried out to investigate the flow through sharp edged large orifice for heads in the range of 0.5 m to 0.8 m and the height of orifice at the entrance (D) in the range of 0.2 m to 0.4 m. Total 60 numbers of studies were carried out on physical and numerical models. The conclusions are listed below:

- 1. Physical and numerical model results were found to be in good agreement. Therefore, it is inferred that CFD can be used as a complementary tool to physical model for modelling the orifice type of flows.
- 2. Generally, the equation of bottom profile of the orifice spillway is taken as  $x^2 = kh_dy$ . From the present study it is found that
  - The 'k' value is in the range of 3 to 4.
  - The corresponding values for coefficient of velocity (C<sub>v</sub>) are found to be in the range of 0.89 to 1.0.
  - Coefficient of discharge was found in the range of 0.61 to 0.65, which corroborate well with the existing literature on sharp edged orifice.

- 3. Studies indicated that there is large difference in upper nappe profiles computed from the present study using physical & numerical models and available literature. Hence, it can be concluded that the upper nappe profile computed from the sharp edged large orifice flow cannot be directly used as a roof profile of an orifice spillway. It is also concluded that the solid spillway bottom profile is found to be a governing parameter in designing the roof profile of orifice spillway.
- 4. Based on the comparison between physical model, numerical model and available literature the spillway bottom profile confirming to an equation  $x^2 = kh_dy$  with 'k' as 4 was finalized for the initial design. However, it was felt that the bottom profile with k value varying between 3 (steep slope) and 4 (flat slope) should also be checked in terms of coefficient of discharge and pressure distribution over the spillway surface.

# 7.2.2 Conclusion from physical and numerical model studies with solid spillway bottom profile without roof profile (set up 2)

Physical and numerical model studies were carried out for the spillway bottom profile designed for head 0.6 m, 0.8 m, 1.0 m and 1.4 m and height of orifice openings of 0.2 m, 0.28 m and 0.32 m. About 66 numbers of studies were conducted for various combinations of heads and heights of orifice. Based on physical and numerical model results, following conclusions are drawn.

- 1. The effect of height of spillway, 'P' was found to be insignificant on coefficient of discharge, pressures over the profiles and upper nappe profile of orifice spillway. Hence, it is concluded that the effect of parameter 'P' can be neglected in design of roof profile of orifice spillway. However, design head 'h<sub>d</sub>' and height of orifice 'd' are found to be the governing parameters for the design.
- 2. Based on upper nappe water surface profile data, following equation has been developed and proposed for the design of roof profile of an orifice spillway:

$$x_1 = a(\frac{y_1}{b})^m$$

where 
$$a = A*(d)*(\frac{h_d}{d})^B$$
 (7.1)

- 3. The proposed equation 7.1 was verified with the data of present study which has not been used in deriving the equation. The agreement between computed and estimated values was found to be good. The maximum % error between computed and estimated values was 7%, and R<sup>2</sup> is 0.999, which is in the acceptable range.
- 4. Roof profile designed with equation 7.1 was also compared with the profile modified by trial and error method on physical model results for existing case studies of orifice spillway. The comparison shows that large number of trial and error could have been avoided if the equation 7.1 was available earlier at design stage.
- 5. The proposed equation 7.1 was also found to be more efficient in respect of coefficient of discharge and pressures over the roof profiles for a particular case study.
- 6. The equation proposed in the present study would be useful for the design engineers at initial stage of design of orifice spillway. The equation would be useful to make the structure economically and hydraulically efficient.

# 7.2.3 Conclusion from physical and numerical model studies with solid spillway bottom and roof profiles (set up 3)

Physical and numerical model studies were carried out for the spillway bottom profile designed with an equation  $x^2 = 4h_dy$  and roof profile designed with proposed equation 7.1 from present research work. The studies were carried out for design heads 0.6 m, 0.8 m, 1.0 m and 1.4 m and heights of orifice openings 0.2 m, 0.24 m, 0.28 m, 0.32 m, 0.36 m and 0.4 m for spillway operating at design head ( $h_e/h_d = 1$ ), less than design head ( $h_e/h_d = 0.8$ ) and greater than design head ( $h_e/h_d = 1.33$ ). In total 76 numbers of experiments were conducted for various combinations of heads and heights of orifice. The performance of orifice spillway was assessed in terms of discharging capacity, pressure distribution on spillway bottom and

roof profile and water surface profile. The following conclusions are drawn from the present study:

- 1. The numerical model of orifice spillway was verified in terms of grid convergence and different turbulence models. A grid size of 0.004 m and Realizable k-ε turbulence model was found to be suitable for modelling the flow through an orifice spillway.
- 2. Coefficient of discharge (C<sub>d</sub>) was found to be in the range of 0.831 to 0.942. The C<sub>d</sub> value has increased in the present case in comparison with that of sharp edged orifice with and without spillway bottom profile. It may be concluded that roof profile is an important component that governs the discharging capacity of the orifice spillway.
- 3. Based on the results, the following equation has been developed to estimate coefficient of discharge of an orifice spillway.

$$C_d = a * \left(\frac{h_{cl}}{d}\right)^b * \left(\frac{h_{cl}}{h_d}\right)^c$$
(7.2)

- 4. The estimated C<sub>d</sub> values using equation 7.2 were compared with the C<sub>d</sub> values computed from present research study. The estimated and computed results were found in good agreement with maximum 1.2 % of error.
- 5. The coefficient of discharge estimated from the proposed equation 7.2 was compared with  $C_d$  observed on the physical model for 22 orifice spillway projects. The  $C_d$  value with equation 7.2 was found to be better than the one observed on respective physical model. Hence, it can be concluded that the design of bottom profile with equation  $x^2 = 4h_dy$  and roof profile deigned with equation 7.1 is optimum to achieve maximum discharging capacity of an orifice spillway.
- 6. Positive pressures were observed on spillway bottom surface designed with head of 0.6 m, 0.8 m, 1.0 m and 1.4 m for entire range of heights of orifice while spillway operating at design head ( $h_e/h_d = 1$ ) and less than design head ( $h_e/h_d = 0.8$ ). The corresponding cavitation indices were found to be greater than critical cavitation

index. Thus, it may be concluded that design of spillway bottom profile having an equation  $x^2 = 4h_d y$  is found to be safe.

- 7. The design of spillway roof profile with the proposed equation i.e. equation 7.1 is also found to be safe for all the combinations of heads and heights of orifice for spillway operating at design head and less than design head condition.
- 8. Negative pressures were observed on some part of spillway bottom and roof profile designed for entire range of heads and heights of orifice for spillway operating at greater than design head ( $h_e/h_d=1.33$ ). The corresponding cavitation indices worked out to be less than critical cavitation index. It may be mentioned here that such a condition will rarely occur in the prototype as rise in water level up to 30% more than the design head is likely to happen only in exceptional hydrological events.
- 9. It may be concluded that the water surface profiles measured along centerline of spillway would be useful to design engineers at initial design stage of an orifice spillway. It may also be concluded that these would be useful to determine height of training wall and to fix the position of trunnion of the gate for corresponding height of orifice and design head for which spillway bottom profile is designed.
- 10. It may be concluded that the flow through orifice followed the path of roof profile that was designed using the proposed equation. The flow was touching the roof profile for design head varying from 0.6 m to 1.4 m and height of orifice varying from 0.2 m to 0.4 m that resulted in sufficient discharging capacity of orifice spillway.
- 11. The performance of orifice spillway for the proposed design of bottom and roof profile is found to be satisfactory for P = 0.2 m to 0.8 m in respect of discharging capacity and pressure distribution on the spillway surfaces. However, in real life larger P is not desirable and crest of the orifice spillway should be kept as near to the upstream reservoir bed as possible for effective flushing of sediments.
- 12. The performance of orifice spillway for the proposed design of bottom and roof profile is found to be satisfactory for w = 0.2 m and 0.3 m in respect of coefficient of

discharge and pressure distribution on spillway bottom profile. However, pressures on the roof profile were found satisfactory throughout the length except in the initial region of roof profile for w = 0.3 m.

- 13. The coefficient of discharge was found to be increased for the steep spillway bottom profile with k = 3 than k = 4. However, the performance of spillway bottom profile with k = 4 are found to be more satisfactory than k = 3 in respect of presures on spilway bottom and roof profiles.
- 14. The increase in b/d ratio results in increase in coefficient of discharge. Hence, it can be concluded that design of roof profile with variation of roof profile play an important role in determining the discharging capacity of an orifice spillway. The design of roof and bottom profile proposed in the present research was found to be safe for b/d ratio 0.3 and 0.4 in respect of pressures.
- 15. The studies indicated that the design of roof and bottom profile plays a very important role in assessing the performance of orifice spillway in respect of discharging capacity and pressure distribution on the spillway surfaces.
- 16. It may also be concluded that the performance of orifice spillway was also found to be satisfactory in respect of pressures over bottom and roof profile for spillway operated at gated condition for a specific design head and height of orifice.

### 7.3 Limitation of the Present Study

The limitations of the present studies are as follows:

- 1. Physical and numerical model studies were carried out for constant width of orifice/span.
- 2. Numerical model studies were carried out for scaled dimensions of physical model and not for the prototype dimensions.

3. The shape of pier, size of pier nose and upstream spillway profile were kept constant throughout the physical and numerical model studies.

#### 7.4 Research Contributions from the Present Studies

The major research contributions from the present study are as follows:

- 1. Developed an equation for design of the roof profile of an orifice spillway considering all practical design heads and heights of orifice.
- Developed an equation for estimating the coefficient of discharge of an orifice spillway. The equation gives importance of bottom and roof profile proposed in the present research for achieving the maximum discharging capacity of an orifice spillway.
- 3. Developed non dimensional plots that provide the guidelines in terms of pressures on the roof profile, pressures on bottom profile and water surface profiles for various combinations of design heads, operating heads, heights of orifice and different spillway operating conditions.
- 4. Based on the verification and validation studies, it was concluded that numerical model can be used as a complementary tool to physical model for modelling the flow through orifice spillway.

### 7.5 Scope for Further Studies

Considering the work carried out on orifice spillways, certain aspects require further investigations as follows:

- 1. Extending the applications of physical and numerical model to assess the performance of orifice spillway using k value 3 and 3.5 in the design of spillway bottom profile and using b/d ratio between 0.2 and 0.4 for design of the roof profile.
- 2. Extending the applications of physical and numerical model to investigate the effect of shape of pier on orifice flow.
- 3. Extending the applications of physical and numerical model to investigate the effect of width of orifice/span on orifice flow

### REFERENCES

Bansal, R. K. (2010). A Textbook of fluid mechanics and hydraulic machines. ISBN: 9788131808153, ed. 9, Laxmi Publications (P) Ltd., New Delhi.

Bazin (1888). Report on open channel hydraulics, McGraw-Hill Book Co. (1987) USA.

Bhajantri, M. R. (2007). "Numerical investigations on hydrodynamic characteristics of spillway flows". Ph.D. Thesis, Indian Institute of Technology Bombay, Mumbai.

Bhajantri, M. R., Eldho, T. I. and Deolalikar, P. B. (2007). "Numerical modelling of turbulent flow through spillway with gated operation". International Journal for Numerical Methods in Engineering, Vol. 72 (2), pp. 221-243.

Bhajantri, M. R., Eldho, T. I. and Deolalikar, P. B. (2008). "Numerical investigation of the effects of sluice spillway roof profiles on the hydraulic characteristics". International Journal for Numerical Methods in Fluids, Vol. 57(7), pp. 839-859.

Bhosekar, V. V. (2011). "Physical and numerical model studies for aerator on orifice spillway". Ph.D. thesis, Indian Institute of Technology Bombay, Mumbai.

Bhosekar, V. V., Jothiprakash V. and Deolalikar, P. B. (2012). "Orifice spillway aerator: hydraulic design". Journal of Hydraulic Engineering, ASCE, 138 (6), pp. 563–572.

Bhosekar, V. V., Patnaik, S. R., Gadge, P. P. and Gupta, I. D. (2014). "Discharge characteristics of orifice spillway". International Journal of Dam Engineering, XXIV(1), pp. 5-18.

BIS (6934 : 1998). "Hydraulic design of high ogee overflow spillways - Recommendations". Bureau of Indian Standards code, New Delhi, India.

BIS (6934 : 2010). "Draft Indian Standard. Hydraulic design of high ogee overflow and orifice spillways-Recommendations". Bureau of Indian Standard WRD 9 (570), New Delhi, India.

Boes, R. M. and Minor, H. E. (2002). "Hydraulic design of stepped spillways for RCC dams". Journal of Hydropower and Dams, 9 (3), pp.87-91.

Broadhead, B. L., Rearden, B. T., Hopper, C. M., Wagschal, J. J. and Parks, C. V. (2004). "Sensitivity and uncertainty-based criticality safety validation techniques". Nuclear Science and Engineering, 146 (3), pp. 340–366.

Bryant, D. B., Khan, A. A. and Aziz, N. M. (2008). "Investigation of flow upstream of orifices". Journal of Hydraulic Engineering, 134 (1), pp. 98-104.

Cederstrom, M., Hammer, L., Johansson, N. and Yang, J. (2000). "Modelling of spillway discharge capacity with computational fluid dynamics (CFD)". Proceedings of the 20<sup>th</sup> International Congress, International committee on Large Dams, Beijing.

Chamani, M. and Rajaratnam, N. (1999). "Characteristics of skimming flow over stepped spillways". Journal of Hydraulic Engineering, 125(4), pp. 361-368.

Chanel, P. G. and Doering, J. C. (2007). "An evaluation of computational fluid dynamics for spillway modelling". 16<sup>th</sup> Australian Fluid Mechanics Congress, 2-7 December 2007, pp. 1201-1206.

Chanson, H. (1999). "The hydraulics of open channel flow". Arnold, 338 Euston Road, London NW1 3BH, UK.

Chanson, M., Aoki, S. and Maruyama, M. (2002). "Unsteady two dimensional orifice flow: a large size experimental investigation". Journal of Hydraulic Research, IAHR, 40 (1), pp. 63–71.

Chen, Q., Dai, G. and Liu, H. (2002). "Volume of fluid model for turbulence numerical simulation of stepped spillway overflow". Journal of Hydraulics Engineering, ASCE, 128 (7), pp. 683-688.

Cheng, X., Chen, Y. and Luo, L. (2006). "Numerical simulation of air-water two-phase flow over stepped spillway". Science in China series E: Technological science, 49 (6), pp. 674-684.

CW&PRS (1991). "Hydraulic model studies for Ranganadi dam spillway, Arunachal Pradesh". Tech. Rep. 2932, Central Water and Power Research Station, Pune, India.

CW&PRS (2000). "Hydraulic model studies for Tala Dam Spillway, Bhutan". Tech. Rep. 3700, Central Water and Power Research Station, Pune, India.

CW&PRS (2005). "Hydraulic model studies for spillway and power intake of Chamera H. E. project, stage - III, Himachal Pradesh". Tech. Rep. 4254, Central Water and Power Research Station, Pune, India.

CW&PRS (2014). "Hydraulic model studies for Punatsangchhu H. E. Project, Stage-1, Bhutan". Tech. Rep. 5237, Central Water and Power Research Station, Pune, India.

Daneshfaraz, R., Kaya, B., Sadeghfam, S. and Sadeghi, H. (2014). "Simulation of flow over ogee and stepped spillways and comparison of finite volume and finite element methods". Journal of Water Resource and Hydraulic Engineering, 3 (2), pp. 37-47.

Dargahi, B. (2006). "Experimental study and 3D numerical simulations for a free-overflow spillway". Journal of Hydraulic Engineering, ASCE, 132 (9), pp.899-907.

Darvas, L. A. (1971). "Discussion on performance and design of labyrinth weir". Journal of Hydraulic Division, ASCE, 97(8), pp.1246-1251.

Deolalikar, P. B., Bhosekar, V. V. and Pethe P.C. (2008). "Research into factors which influence hydraulic design of breastwall/sluice spillways". Technical Memorandum, Central Water and Power Research Station, Pune, India.

Deng, J., Xu, W., Lei, J. and Diao, M. (2005). "Numerical simulation of hydraulic characteristics of high head spillway tunnel". Journal of Hydraulic Engineering, ASCE, 36 (10), pp.1209-1212.

Eca, L., Hoekstra, M. and Roache, P. J. (2007). "Verification of calculations: an overview of the 2<sup>nd</sup> Lisbon workshop". Second workshop on CFD uncertainty analysis, AIAA Computational Fluid Dynamics Conference, Miami, FL, Jun., AIAA Paper No. 2007-4089.

Falvey, H. T. (1990). "Cavitation in chutes and spillways". Engineering Monograph No. 42, USBR publication, Denver, CO.

Ferziger, J. H. and Peric, M. (1996). "Further discussion of numerical errors in CFD". International Journal for Numerical Methods in Fluids, 23, pp. 1263–1274.

FLUENT (2006). Version 6.3.26. Documentation Manual and User's guide. Lebanon, NH: Fluent Inc.

Freitas, C. J. (1993). Journal of fluids engineering editorial policy statement on the control of numerical accuracy. Journal of Fluids Engineering-Transactions of the ASME, 115 (3), pp. 339-340.

Gambit (2007). Version 2.4. Command reference guide, FLUENT.

Gill, M. A. (1987). "Flow through side slots". Journal of Environmental Engineering, 113 (5), pp.1047–1057.

Gunter, A., Stuck, J., Werth, S., Doll, P., Verzano, K. and Merz, B. (2007). "A global analysis of temporal and spatial variations in continental water storage". Water Resources Research, 43, W05416, pp. 1-19.

Hay, N. and Taylor, G. (1970). "Performance and design of labyrinth weirs". Journal of Hydraulic Engineering, ASCE, 96(11), pp. 2337-2357.

Higgs, J. A. (1997). "Folsom dam spillway vortices computational fluid dynamics model study". Memorandum Report, USBR.

Hinds, J. (1926). "Side channel spillways-Hydraulic theory, economic factors and experimental determination of losses". Transaction, ASCE, 89.

Hirt, C. W. and Nichols, B. D. (1981). "Volume of fluid (VOF) method for the dynamics of free boundaries". Journal of Computational Physics 39, pp. 201-225.

Ho, H., Boyes, K., Donohoo, S. and Cooper, B. (2003). "Numerical flow analysis for spillways". Proc, 43<sup>rd</sup> ANCOLD Conf., Hobart, Tasmania, pp. 24-29.

Hu, C., Wei, Y. and Zheng, Z. (1990). "Study of configurations of overflow dams with breastwall". Proceedings of 7<sup>th</sup> Congress APD-IAHR, November, Beijing, pp. 209-214.

Hussain, A., Ahmad, Z. and Asawa, G. L. (2010). "Discharge characteristics of sharp-crested circular side orifices in open channels". Journal of Flow Measurement and Instrumentation, 21 (3), pp. 418–424.

Hussain, A., Ahmad, Z. and Asawa, G. L. (2011). "Flow through sharp-crested rectangular side orifices under free flow condition in open channels". Journal of Agricultural Water Management, 98 (10), pp.1536-1544.

Hussain, S., Hussain, A. and Ahmad, Z. (2014). "Discharge characteristics of orifice spillway under oblique approach flow". Flow Measurement and Instrumentation, 39, pp. 9-18.

Jeon, Y. and Sheen, D. (2005). "Analysis of a cell boundary element method". Advances in Computational Mathematics, 22 (2005), pp. 201-222.

Johnson, M. C. and Savage, B. M. (2006). "Physical and numerical comparison of flow over ogee spillway in the presence of tailwater". Journal of Hydraulic Engineering, ASCE, 132 (12), pp. 1353-1357.

Jothiprakash, V., Bhosekar, V. V. and Deolalikar, P. B. (2015). "Flow characteristics of orifice spillway aerator: Numerical model studies". ISH Journal of Hydraulic Engineering, 21(2), pp. 216-230.

Judd, H. and King, R. S. (1908). "Some experiments on the frictionless orifice". Engr. News, 56 (13), pp. 326-330.

Keller, R. J. and Rastogi, A. K. (1977). "Design chart for prediction critical point on spillways". Journal of Hydraulic Division, ASCE, 103(12), pp.1417–1429.

Khatsuria, R. M. (2004). "Hydraulics of spillway and energy dissipators". Marcel Dekker publication, New York, NY.

Kim, D. G. and Jae, H. P. (2005). "Analysis of flow structure over ogee-spillway in consideration of scale and roughness effects by using CFD model". KSCE, Journal of Civil Engineering, 9 (2), pp.161-169.

Kjellesrig, H. M. (1996). "Numerical modelling of flow over spillway". Hydroinformatics' 96, Balkema, Rotterdam.

Khodashenas, S. R., Roshan, R., Sarkardeh, H. and Azamathulla, H. M. (2010). "Vortex study at orifice spillways of Karun III Dam". Dam Engineering, 21(2), pp. 131-142.

Knight, A. (1989). "Design of efficient side channel spillway". Journal of Hydraulic Engineering, ASCE, 115 (9), pp. 1275-1289.

Li. S., Cain, S., Wosnik, M., Miller, C., Kocahan, H. and Wyckoff, R. (2011). "Numerical modelling of probable maximum flood flowing through a system of spillways". Journal of Hydraulic Engineering, ASCE, 137(1), pp. 66-74.

Lienhard (V), J. H. and Lienhard (IV), J. H. (1984). "Velocity coefficients for free jets from sharp-edged orifices". Journal of Fluids Engineering, 106, pp. 13-17.

Mao, Y., Chao, W., Yunliang, C. and Qin, Z. (2006). "Case study of a S-shaped spillway using physical and numerical models". Journal of Hydraulic Engineering, ASCE, 132 (9), pp. 892-898.

Margeirsson, B. (2007). "Computational modelling of flow over a spillway". Master's Thesis. Department of Applied Mechanics. Chalmers University of Technology Gothenburg, Sweden.

Montes, J. S. (1997). "Irrotational flow and real fluid effects under planar sluice gates". Journal of Hydraulic Engineering, 123(3), pp. 219–232.

Murphy, T. E. (1973). "Spillway crest design". Misc. Paper H-73-5, U. S. Army Corps of Engineers Waterways Experiment Station, Vicksburg, Mississippi.

Nguyen, C., Wang, L. and Tang, H. (2015). "The effect of curved bed on the discharge equation in a spillway with a breastwall". Journal of Hydrodynamics, 27 (3), pp. 311-318.

Nguyen, C. and Wang, L. (2015). "Physical and numerical model of flow through the spillways with a breastwall". Journal of Civil Engineering, KSCE, 19 (7), pp. 2317-2324.

Nisar, Z., Sarwar, M. K. and Nabi, G. (2015). "Hydraulic performance assessment of an orifice spillways using CFD modelling". Sci. Int.(Lahore), 27 (2), pp. 1303-1308.

Novak, P., Guinot, V. Jeffrey, A. and Reeve, D. E. (2010). "Hydraulic modelling - an introduction". Principles, methods and applications. Spon press, Abingdon, UK.

Olsen, N. R. and Kjellesvig, H. M. (1998). "3-D Numerical flow modelling for estimation of spillway capacity". Journal of Hydraulic Research, IAHR, 36(5), pp. 775-784.

Oscar, C. (2009). "Hydraulics of developing chute flow". Journal of Hydraulic Research, IAHR, 47 (2), pp. 185-194.

Pfister, M., Duarte, R., Muller, M. and De Cesare G. (2012). "Cavitation risk estimation at orifice spillway based on UVP and dynamic pressure measurements". 8<sup>th</sup> International

Symposium on Ultrasonic Doppler Methods for Fluid Mechanics and Fluid Engineering, Dresden, Germany, 137–140.

Pfister, M. and Hager, W. H. (2014). "History and significance of the Morton number in hydraulic engineering". Journal of Hydraulic Engineering 140(5), DOI:http://dx.doi.org/10.1061/(ASCE) HY.1943-7900.0000870.

Pfister, M. and Chanson, H. (2014). "Two-phase air-water flows: Scale effects in physical modelling". Journal of Hydrodynamics, 26(2), pp. 291-298.

Qian, Z., Hu, X., Huai, W. and Amador, A. (2009). "Numerical simulation and analysis of water flow over stepped spillway". Science in china series E: Technological Sciences, 52 (7), pp. 1958-1965.

Richardson, L. F. and Gaunt, J. A. (1927). "The deferred approach to the limit, Philos". Trans. R. Soc. London, Ser. A, 226, pp. 299–361.

Roache, P. J. (1993). Perspective: A Method for uniform reporting of grid refinement studies. Proceedings of Quantification of Uncertainty in Computation Fluid Dynamics, Edited by Celik, et al., ASME Fluids Engineering Division Spring Meeting, Washington, D.C., June 23–24, ASME Publ. No. FED-Vol. 158.

Roache, P. J. (1994). "Perspective: a method for uniform reporting of grid refinement studies". Journal of Fluid Engineering, 116 (3), pp. 405-413.

Roache, P. J. (1997). "Quantification of the uncertainty in computational fluid dynamics". Annual Review Fluid Mechanics, 29, pp.123-160.

Roache, P. J. (1998). "Verification of codes and calculations". AIAA 36, pp. 696-702.

Sartaj, M., Beirami, M. K. and Fooladgar, A., (2006). "Analysis of two-dimensional flow over standard ogee spillway using RNG turbulence model". 7<sup>th</sup> International Conference on Civil Engineering, Tehran, Iran, 8-10 May 2006.

Savage, B. M. and Johnson, M. C. (2001). "Flow over ogee spillway: physical and numerical model case study". Journal of Hydraulic Engineering, ASCE, 127 (8), pp. 640-649.

Senturk, F. (1994). "Hydraulics of dams and reservoirs". Water resources publications, Highland Ranch, Colorado, U.S.A.

Shammaa, Y., Zhu, D. Z. and Rajaratnam, N. (2005). "Flow upstream of orifices and sluice gates". Journal of Hydraulic Engineering, ASCE, 131(2), pp. 127-133.

Smith, G. D. (1985). "Numerical solution of partial differential equations: Finite difference methods". 3<sup>rd</sup> edition, Clarendon Press, Oxford.

Som, S. K and Biswas, G. (2004). Introduction to fluid mechanics and fluid machines. Second edition, Tata McGraw-Hill Publishing company limited, New Delhi.

Steven, A., Cohen, J. and Hugh, A. (2008). "Physical model study of wave action in New Thomsen Harbor, Sitka, Alaska". US Army Corps of Engineers.

Tadayon, R. and Ramamurthy, A. S. (2009). "Turbulence modelling of flow over circular spillways". Journal of Irrigation and Drainage Engineering, ASCE, 135 (4), pp. 493-498.

Tropea, C., Yarin, A. and Foss, J. (2007). Springer handbook of experimental fluid mechanics.

Unami, K., Kawachi, T., Babar, M. and Itagaki, H. (1999). "Two-dimensional numerical model of spillway flow". Journal of Hydraulic Engineering, ASCE, 125 (4), pp. 369-375.

US Army Engineer-Waterways Experiment station-Hydraulic design criteria - 1952 and subsequent editions.

USACE (1990). "Hydraulic design of spillways". U. S. Army Corps of Engineers. Engineer Manual 1110-2-1603.

USBR (1960). "Design of small dams". United States Bureau of Reclamation, A Water Resources Technical Publication.

USBR (1987). "Design of small dams". United States Bureau of Reclamation 3<sup>rd</sup> edition, US Govt. printing office, Washington D. C.

USBR (1980). "Hydraulic laboratory techniques". A Water Resources Technical Publication, U. S. Bureau of Reclamation, Denver, Colorado.

Versteeg, H. K. and Malalasekera, W. (1995). "An introduction to computational fluid dynamics - The finite volume method". Longmon Scientific & Technical, England, 1995.

Warnock, J. E. (1950). "Hydraulic similitude in Engineering Hydraulics", edited by H. Rouse New York: John Wiley & Sons. New York, pp 136-176.

Weaver, W. and Johnston, P. R. (1987). "Structural dynamics by finite elements". Prentice-hall, Inc., Englewood Clifts, New Jersey.

WES (1952). "Hydraulic design criteria". Waterways Experiment Station Vicksburg, USA.

WES Design Charts (1987). "Hydraulic design charts". Handbook published by Waterways Experiment Station, Vicksburg, Mississippi, USA.

Yang, J. and Johansson, N. (1998). "Determination of spillway discharge capacity – CFD modelling and experiment Verification". Proc. 3<sup>rd</sup> Int. Conf. on Advances in Hydroscience and Engineering Cottbus, Germany.

Zienkiewicz, O. C., and Taylor, R. L. (1991). "The finite element method- Vol. 2: Solid and fluid mechanics". McGraw-Hill, New York.

**ACKNOWLEDGEMENT** 

These guidelines are based on the work as part of the PhD research work carried out by Dr

Mrs P P Gadge, Sc B at CWPRS and IIT Bombay under the guidance of Dr Mrs V v

Bhosekar, Sc E as external supervisor. The authors wish to express deep sense of gratitude to

the research Supervisor, Prof. V. Jothiprakash, at IIT Bombay for his invaluable guidance and

encouragement throughout the course of this study. We are also thankful to Prof. T. I. Eldho

and Prof. Balaji, Members Research Review Panel, IIT Bombay for many valuable

suggestions, guidance and encouragement during the study. We would also like to thank the

authorities of IIT Bombay for providing access to CFD software FLUENT.

We are grateful to Dr M K Sinha, Director, CWPRS to encourage us to conduct this research

work. We are also thankful to MoWR, RD & GR for providing the funds for the research

work and creating the experimental facility.

Last but not the least, we are also thankful the design and site engineers of various project

authorities for discussions and providing ideas for the studies of orifice spillways of various

projects.

Dr. (Mrs.) V. V. Bhosekar

Dr (Mrs.) P P Gadge

199



To be a world-class centre of excellence in hydraulic engineering research and allied areas; which is responsive to changing global scenario, and need for sustaining and enhancing excellence in providing technological solutions for optimal and safe design of water resources structures.

#### **MISSION**

- To meet the country's need for basic & applied research in water resources, power sector and coastal engineering with world-class standards
- To develop competence in deployment of latest technologies by networking with the top institutions globally, to meet the future needs for development of water resources projects in the country effectively
- To disseminate information, build skills and knowledge for capacity-building and mass awareness for optimization of available water resources

### **MAJOR FUNCTIONS**

 Undertaking specific research studies relating to development of water resources, power and coastal projects · Consultancy and advisory services to Central and State Governments,

private sector and other countries

 Disseminating research findings and promoting/assisting research activities in other organizations concerned with water resources projects

 Contributions to Bureau of Indian Standards and International Standards Organization

• Carrying out basic and applied research to support the specific studies

 Contribution towards advancements in technology through participation in various committees at National and State Levels





**Central Water and Power Research** Khadakwasala, Sinhqad Road, Pune 411 024

Telephone: +91-20-24103200/ 24381801

Fax : +91-20-24381004 Web : www.cwprs.gov.in